

Abstract:

This aim of this study was twofold. The first aim was to assess the consequences of a hemi-section of the cervical cord in adult macaque monkeys. The aspects particularly investigated were the anatomical changes at cortical and spinal levels mainly, the behavioural consequences regarding manual dexterity and locomotion, and the functional organisation of the primary motor cortex. Second, the data obtained in control (untreated) animals have been compared with those in monkeys treated with an antibody directed against a myelinic protein inhibiting the growth of axons in the central nervous system of adult mammals called Nogo.

The motor cortex in the large sense, comprising the Primary motor cortex (M1), the Premotor cortex (PM), the supplementary motor area (SMA) and the cingulate motor area (CM) is responsible for the control of manual dexterity in primates and transmits its commands to the motoneurons of the spinal cord in the great majority through the corticospinal (CS) tract. A lesion of the CS tract at cervical level results in a dramatic impairment of manual dexterity and other motor functions for which the motoneurons are located caudally to the segmental level of the lesion.

In control monkeys, subjected to a partial hemisection aiming to interrupt the CS tract at C7-C8 level and receiving a control inactive treatment, the lesion resulted in a dramatic loss of manual dexterity immediately after the surgical lesion, dropping to a score of 0 in two manual dexterity tests that quantify the precision grip ability of the animals: the “Brinkman board” test and the “Drawer” test. The “Brinkman board” test consisted in a task requiring the monkey to retrieve 50 small pieces of food in wells randomly distributed on a Perspex board. The “Drawer” task consisted for the animal to fully open a drawer and to retrieve with the precision grip of the same hand a food reward inside the drawer. In the following weeks, a certain “spontaneous” functional recovery occurred for the “Brinkman board” test, rather based on a change of strategy in the shape of the precision grip of the affected left hand than a real recovery of the original function. No recovery was observed for the “Drawer” test. The more qualitative tests assessing the general locomotion using hands and/or feet showed a good level of functional recovery. The anatomical changes in the motor cortex were assessed by area measurement of the soma of the pyramidal cells located in M1 and SMA projecting to the spinal cord. This analysis showed a size decrease of the soma of these cells in the affected contralesional hemisphere compared to the ipsilesional hemisphere, whereas the total cell number was quite comparable. The cervical cord lesion thus produced a cell shrinkage of the axotomised CS cells rather than a cell loss. The

functional organisation of M1 was investigated with the intracortical microstimulation (ICMS) method and showed a dramatic decrease of the number of the cortical sites eliciting movements of the hand after the cervical lesion in the contralesional hemisphere, whereas the threshold of current needed remained roughly unchanged. The ICMS identified hand area of the contralesional M1 was transiently inactivated at the end of the period of recovery and resulted in the dramatic loss of the recovered manual dexterity of the affected hand in the “Brinkman board” test.

In treated monkeys subjected to a comparable cervical hemi-section, no evidence for a regeneration of the lesioned CS axons was observed caudally to the lesion site. However, the functional recovery of the precision grip ability (“Brinkman board” test) occurred more rapidly and to a greater extent than in the control monkey. There was also a significant recovery for the “Drawer” test. The other, qualitative behavioural tests showed a comparable level of recovery, compared to the control animals. The transient inactivation experiment showed a possible influence of the ipsilesional hemisphere in the enhanced recovery of function, in addition to the main contribution of the contralesional hemisphere.

We can conclude that a unilateral lesion of the CS resulted in the impairment of precision grip of the affected hand of adult primates. A treatment enhancing the regeneration and the compensatory sprouting of CNS axotomised fibres produced an improvement of the manual dexterity in treated monkeys, more rapidly and more extensively than in the control monkeys. The absence of axonal regeneration indicates that this improvement of function is rather due to a compensatory sprouting, at cortical and/or cervical levels, or to the recruitment of unaffected motor systems such the rubrospinal tract, reticulospinal tract or the propriospinal system.

Résumé :

Le but de cette étude est double. Le premier but était d'évaluer les conséquences d'une hémi-section de la moelle épinière cervicale chez le macaque adulte. Les aspects particulièrement approfondis étaient les suivants : les changements anatomiques au niveau cortical et spinal principalement, les conséquences sur la dextérité manuelle et sur la locomotion, ainsi que sur l'organisation fonctionnelle du cortex moteur primaire (M1). Deuxièmement, les données obtenues chez les singes contrôles (non traités) ont été comparées avec celles obtenues chez des singes traités avec un anticorps dirigé contre une protéine myélinique inhibant la croissance d'axones dans le système nerveux central des mammifères adultes et appelé Nogo.

Le cortex moteur comprenant dans son sens large le cortex moteur primaire (M1), le cortex prémoteur (PM), l'aire motrice supplémentaire (SMA) et le cortex cingulaire (CM) est responsable du control moteur de la dextérité manuelle chez les primates et transmet ses commandes aux motoneurones de la moelle épinière en grande partie par la voie corticospinale (CS). Une lésion de cette projection au niveau cervical résulte en une paralysie dramatique de la dextérité manuelle et d'autres fonctions motrices dont les motoneurones sont situés caudalement par rapport au niveau segmentaire de la lésion.

Chez les animaux contrôles, ayant subi une hémi-section partielle dont le but était d'interrompre la voie CS au niveau C7-C8 et bénéficiant d'un traitement contrôle inactif, la lésion a eu comme conséquence une perte dramatique de la dextérité manuelle immédiatement après la chirurgie, tombant à un score de 0 dans deux tests quantifiant la capacité de pince de précision des animaux : le test du « tableau de Brinkman » et le test du « Tiroir ». Le test du « tableau de Brinkman » consistait en une tâche demandant à l'animal de retirer 50 petits morceaux de nourriture dans des puits distribués au hasard dans un tableau de Perspex. Le test du « tiroir » consistait pour l'animal à complètement ouvrir un tiroir avec les doigts d'une main et retirer une récompense sous forme de nourriture à l'intérieur du tiroir avec la même main. Les semaines suivant la lésion virent une certaine récupération fonctionnelle « spontanée » quant au test du « tableau de Brinkman », plutôt due à un changement de stratégie dans la formation de la pince de précision de la main touchée qu'à une réelle récupération fonctionnelle de la fonction originale. Les changements anatomiques dans le cortex moteur ont été analysés en mesurant la surface du soma des cellules pyramidales situées dans M1 et SMA et projetant vers la moelle épinière. Cette analyse a démontré une réduction de la taille de ces cellules dans le cortex touché, contralésionnel, comparé au cortex ipsilésionnel, alors que le nombre total de cellules était

comparable entre les deux hémisphères. La lésion cervicale a résulté ainsi plutôt en un rétrécissement de la taille des corps cellulaires plutôt qu'en une mort cellulaire. L'organisation fonctionnelle de M1 a été analysée grâce à la méthode de la microstimulation intracorticale (ICMS) et a démontré une diminution marquée du nombre de sites corticaux à l'origine des mouvements de la main à la suite de la lésion cervicale dans l'hémisphère contralésionnel, alors que le seuil de courant efficace est resté inchangé. L'aire corticale de la main identifiée dans le cortex contralésionnel grâce à l'ICMS a été transitoirement inactivée à la fin de la période de récupération et a résulté en une perte dramatique de dextérité manuelle de la main affectée lors du test du « tableau de Brinkman ».

Chez les animaux traités ayant subi une héli-section cervicale comparable, aucune trace de régénération des axones lésés n'a été observée caudalement à la lésion. Cependant, la récupération fonctionnelle de la capacité de pince de précision testée grâce au « tableau de Brinkman » est apparue plus rapidement, et avec une plus grande envergure. Nous avons également observé une récupération significative lors du test du « tiroir ». Les autres tests comportementaux ont montré un niveau de récupération comparable à celui des animaux contrôles. L'expérience d'inactivation transitoire de M1 a montré une possible influence de l'hémisphère ipsilésionnel lors de la meilleure récupération fonctionnelle, en plus du rôle majeur joué par l'hémisphère contralésionnel.

Nous pouvons donc conclure qu'une lésion unilatérale de la projection CS a eu comme conséquence une paralysie de la pince de précision de la main affectée d'un primate adulte. Un traitement améliorant la régénération et le bourgeonnement axonal compensatoire de fibres nerveuses du CNS a entraîné une amélioration de la dextérité manuelle chez les animaux traités. L'absence de régénération axonale a indiqué que l'amélioration fonctionnelle était plutôt due à un bourgeonnement axonal compensatoire, au niveau cortical et/ou cervical, et/ou au recrutement de systèmes moteurs non touchés par la lésion, comme les tracts rubrospinaux, ou réticulospinaux, ou encore le système propriospinal.

1: General introduction	7
1.1: The lesioned CNS: overview and perspectives	8
1.2: General organisation of the central motor system	9
1.2.1: The corticospinal tract (CST):	10
1.2.2: Cortical areas	12
1.2.2.1: Anatomical organisation of the motor cortex	12
1.2.2.2: Properties of SMA: distinction between SMA proper and pre-SMA	14
1.2.2.3: Pyramidal neurones	16
1.2.2.4: Role of Motor cortex in motor behaviour in general and in manual dexterity in particular	17
1.2.2.5: Electrophysiological properties of M1 (output map of M1)	20
1.2.3: The rubrospinal pathway	21
1.2.4: Spinal cord	24
1.2.4.1 Corticospinal projections: convergence and divergence	26
1.2.3.4: Distribution of motoneurons in the cervical spinal cord	31
1.2.4.3: Corticomotoneuronal system	34
1.2.4.4: Propriospinal system	36
1.3: Lesions of the corticospinal (CS) system	41
1.3.1: General aspects: lesions of the CS system at different levels	41
1.3.2: Physiopathology of the spinal cord lesions	48
1.4: Functional recovery	51
1.4.1: General considerations	52
1.4.2: Cortical mechanisms involved in functional recovery: Plasticity	52
1.4.3: Other pathways involved	53
1.4.3.1: Rubrospinal pathway	53
1.4.3.2: Reticulospinal pathway	53
1.4.4: Role of Propriospinal neurones in functional recovery after spinal cord injury (SCI)	54
1.5: Regeneration in the central nervous system (CNS)	54
1.5.1: Introduction	54
1.5.2: Historical approach of CNS regeneration	58
1.5.3: Different approaches to CNS regeneration	59
1.5.3.1: Direct approach: Promote the regeneration	59
1.5.3.2: Indirect approach: suppression of the inhibitory growth environment	60
1.5.4: Regeneration in spinal cord	60
1.6: Nogo: a myelin associated growth inhibiting protein	62
1.6.1: Identification of Nogo as a possible growth inhibitory agent	62
1.6.2: Molecular structure of the different forms of Nogo.	64
1.6.3: Function of Nogo A	65
1.6.4: Blocking the activity of Nogo with a monoclonal antibody	66
1.6.5: Strategy developed to inactivate NOGO in situ and in vivo or how to delivery IN-1 with maximum efficacy	71
1.6.6: Improvement of motricity in rats treated with Anti-Nogo A antibody	72
1.7: Aim of the present thesis and methodological strategies	73
1.7.1: Goals	73
1.7.2: Brief survey of the methodological strategies	74
1.7.2.1 Behaviour	74
1.7.2.2: Role of the cortex in behavioural tasks: reversible pharmacological inactivation	74
1.7.3: Electrophysiology	75
1.7.4: Anatomy	75
1.7.5: Treatment	76

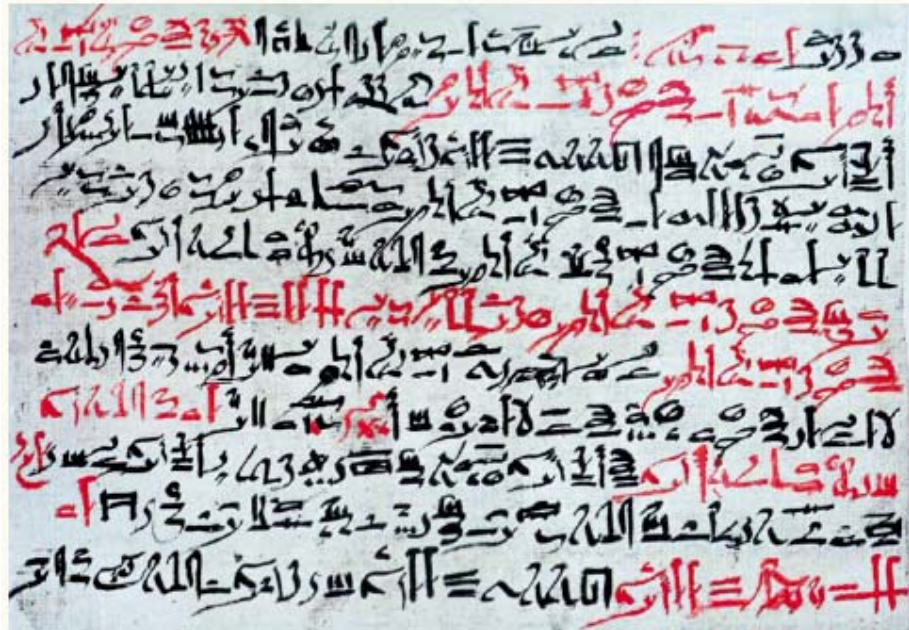


Fig. 1A: Roll papyrus manuscript of the first description of a cervical injury in man made in old Egypt. "If you examine a man with a neck injury ... and find he is without sensation in both arms and both legs, and unable to move them, and he is incontinent of urine ... it is due to the breaking of the spinal cord caused by dislocation of a cervical vertebra. This is a condition which cannot be treated." Edwin Smith Surgical Papyrus, Case 31. Thebes, c. 1550 BC. Taken from Breasted, J.H. (ed.) The Edwin Smith Surgical Papyrus © The University of Chicago Press, 1930

Spinal cord lesion at cervical level in primate: anatomical, behavioural and electrophysiological evaluation in control versus anti-Nogo treated monkeys

Or in other words: have we made some progress after 3550 years of research on spinal cord injury?

1: General introduction

The aim of this study was manifold: the first goal consisted in evaluating the manual dexterity of sub-human primates in quantitative and qualitative motor tasks before and after a spinal cord lesion at cervical level. This evaluation concerns two groups of lesioned monkeys: a control group and a group subjected to a treatment based on inactivation of an axon growth inhibitory myelinic protein called Nogo. A second aim was to evaluate the role played by the motor cortex in the control of the different behavioural tasks using electrophysiological approach and transient pharmacological inactivation. A third aim consisted in assessing the anatomical changes induced by the cervical lesion in motor centres such as motor cortex, red nucleus and the spinal cord itself.

Chapter 2 describes the different methods applied in this study to reach the above mentioned goals. The chapter 3 is dedicated to the behavioural and electrophysiological results obtained in two untreated animals with spinal cord lesion, together with anatomical data comparing the consequences of the cervical lesion with two intact animals. Chapter 4 exposes the general results obtained in the two animals that have been lesioned and treated with the Anti-Nogo antibody (see below). Chapter 5 will present a compilation of compared analysis of data obtained in treated versus untreated lesioned animals and the general discussion.

In this first section, I will present first a short history of the clinical assessment of spinal cord injured patients. The second part presents a survey of the organisation of the components of the motor system that are involved in the control of voluntary movements in primates, including the neural structures that are concerned by the lesion of the corticospinal tract and the rubrospinal tract. The third part of the Introduction will give a short review of the consequences of the lesions of the motor system in the CNS and the possible mechanisms underlying

functional recovery following such lesions. The fifth section of the Introduction presents a summary of the studies that led to the discovery and the application of the treatment used here (anti-Nogo) to enhance the functional recovery. The last part of the introduction presents shortly the strategy adopted to answer our questions.

1.1: The lesioned CNS: overview and perspectives

Spinal cord injuries in human patients (Data from the NIH):

Here is a short history of the spinal cord injury (SCI) in human patients and its treatment through ages: the first trace of a medical description of a patient suffering of SCI comes from Old Egypt in a papyrus roll manuscript. It describes the consequences of a cervical dislocation of the vertebrae, resulting in complete paralysis without any possible treatment resulting in any functional recovery (Fig. 1. A). The first treatment of SCI was applied in Greece by Hippocrates and consisted in external traction of the back to re-establish a normal curvature of the spine, decreasing the tensions in the internal rachis. The roman physician Galen made experiments on subhuman primates including spinal cord injury and the observed loss of function made him conclude that both sensory and motor functions depend on this extension of the central nervous system called spinal cord. Vesalius described in details for the first time in his anatomy text book published in 1543 the structure of the spinal cord and he introduced the nomenclature referring to different zones by its segments, cervical, thoracic, lumbar, sacral and coccygeal, that are still used nowadays. In the middle of the twentieth century, with the use of the X-rays, was established a standard procedure including reposition and fixation in place of the broken spine and tentative rehabilitation with physical exercises (physiotherapy). A recent procedure consisted of the immediate application of an anti-inflammatory treatment, applied shortly after the lesion, treatment that decreases the effect of the reaction of the body against the spinal trauma.

1.2: General organisation of the central motor system

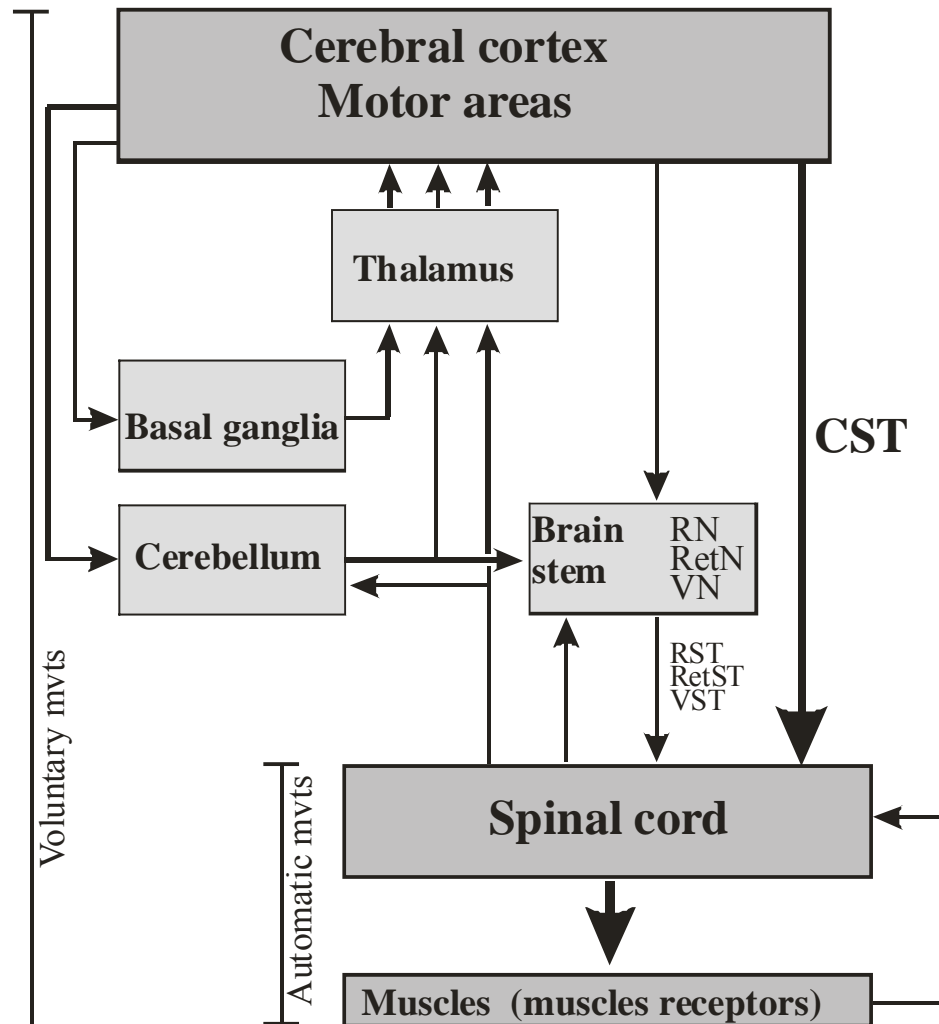


Fig. 1.1: Simplified diagram showing the hierarchical and parallel organisation of the motor system, with emphasis on the connections between motor centres and the spinal cord.

A summary of the main connections between the different motor centres controlling movement is presented in Fig. 1.1. This organisation chart shows that the major motor input to the spinal cord originates from the corticospinal tract (CST), in addition and in parallel to projections originating from sub-cortical structures such as the Red Nucleus (RST), the Reticular

Formation (RetST), the vestibular nuclei (VST), the tectum and many others (see (Holstege 91) for review in the cat).

1.2.1: The corticospinal tract (CST)

The origin, trajectory and termination of the CST are shown schematically in Fig. 1.2. This drawing exhibits the location of the CST at different levels along the corticospinal pathway involved in fine finger movements in primates. A more detailed representation of the CST is shown in Fig. 1.3, illustrating the crossed (lateral) and uncrossed (ventral) components. Note that the origin of the CST is not limited to the primary motor cortex. Furthermore, the two components of the CST address spatially distinct motoneuronal pools in the spinal cord.

Descending lateral corticospinal pathway

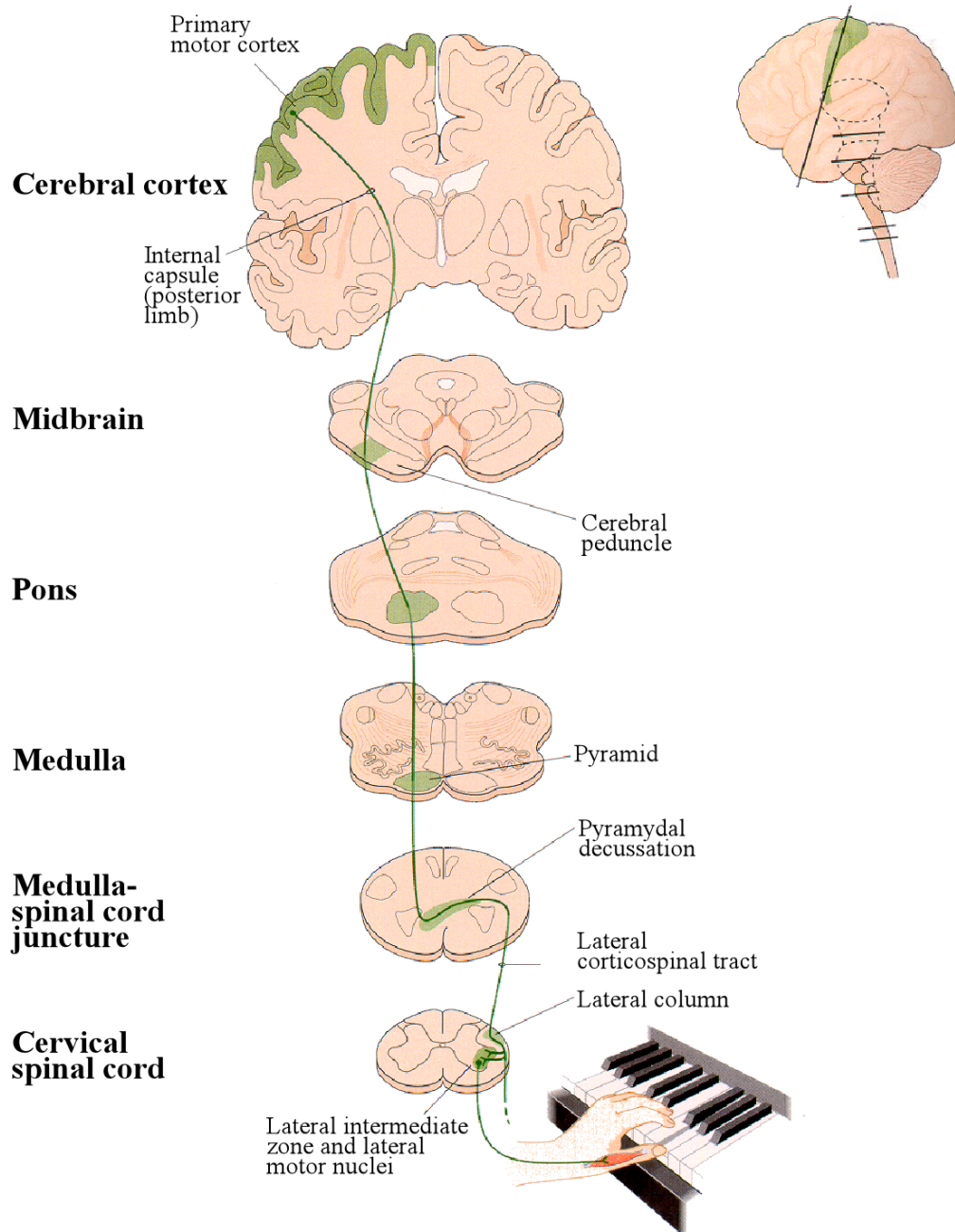


Fig. 1.2: Drawing showing the trajectory of the corticospinal tract (CST) on its way to the cervical spinal cord at different rostro-caudal levels. Only the main (crossed) components of the CST is shown here, which is believed to be involved in fine motor movements of distal muscles, like here controlling the fingers. The uncrossed component of the CST is not shown here.

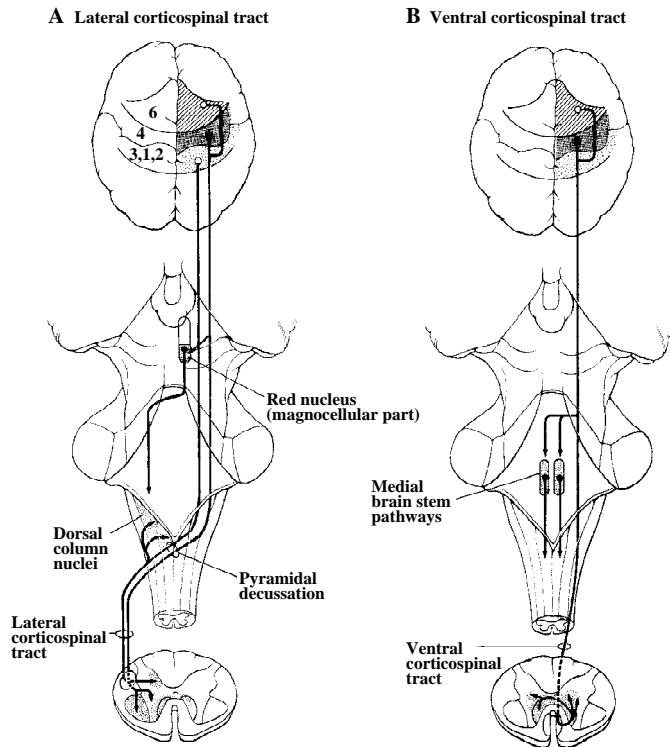


Fig. 1.3: Origin, trajectory and zone of termination of the two components (crossed, A; uncrossed, B) of the CST. The numbers correspond to the Brodman's cortical areas.

The lateral (crossed) CST contacts motoneurons located laterally, involved in the distal musculature, whereas the medial (uncrossed) CST reaches motoneurons located medially, involved in the control of axial and proximal muscles.

1.2.2: Cortical areas

1.2.2.1: Anatomical organisation of the motor cortex

The motor cortex (in the large sense) is divided in 4 main regions (Fig. 1.4):

- The primary motor cortex (M1), referred to also as area F1.

- The premotor cortex (PM), subdivided in a dorsal part (PMd) and a ventral part (PMv). PMd and PMv comprise each a rostral zone (PMd-r or area F7; PMv-r or area F5) and a caudal zone (PMd-c or area F2; PMv-c or area F4).
- The supplementary motor area (SMA), subdivided in a rostral part referred to as pre-SMA (or area F6) and a caudal part, corresponding to the SMA-proper (or area F3).
- The cingulate motor cortical areas (CMA), comprising 3 subareas (rostral, dorsal, ventral).

This parcellation is based on both anatomical and physiological criteria (Wiesendanger and Wiesendanger 85; Matelli et al 85; Wiesendanger 86; Luppino et al 90; Matelli et al 91; Kurata 91; Matsuzaka et al 92; Luppino et al 93; Tanji 94; Kurata and Hoffman 94; Kurata 94; Tanné et al 95; Picard and Strick 96; Matelli and Luppino 96; Caminiti et al 96; Passingham 96; Preuss et al 96; Rizzolatti et al 96; Shima and Tanji 98; Petit et al 98; Nakamura et al 98; Geyer et al 98; Clower and Alexander 98; Vorobiev et al 98; Nakamura et al 99; Ikeda et al 99; Deiber et al 99; Gabernet et al 99; Yazawa et al 00).

Voluntary movements take their origin in the motor cortex. The primary motor cortex (M1) or area 4 of Brodmann, where is located the majority of the frontal lobe corticospinal (CS) neurones (50%), is located in the precentral gyrus (Dum and Strick 91). It has been identified as the area where the lowest threshold of current of stimulation produces movements of the limbs. As compared to M1, electrical stimulation of the premotor areas can produce more complex movements of the limbs involving multiple joints, at usually higher threshold than in M1. Other motor cortical areas give rise to a CST projection to the spinal cord, such as SMA-proper, PMd-c (F2), PMv-c (F4), PMv-r (F5) and the 3 CMA sub-areas. Note that pre-SMA (F6) and PMd-r (F7) do not give rise to a CST projection (Fig. 1.4). The distribution of CS neurones is shown in Fig. 1.4, as derived from recent tracing studies (He et al 93; Galea and Darian-Smith 94; He et al 95; Dum and Strick 96).

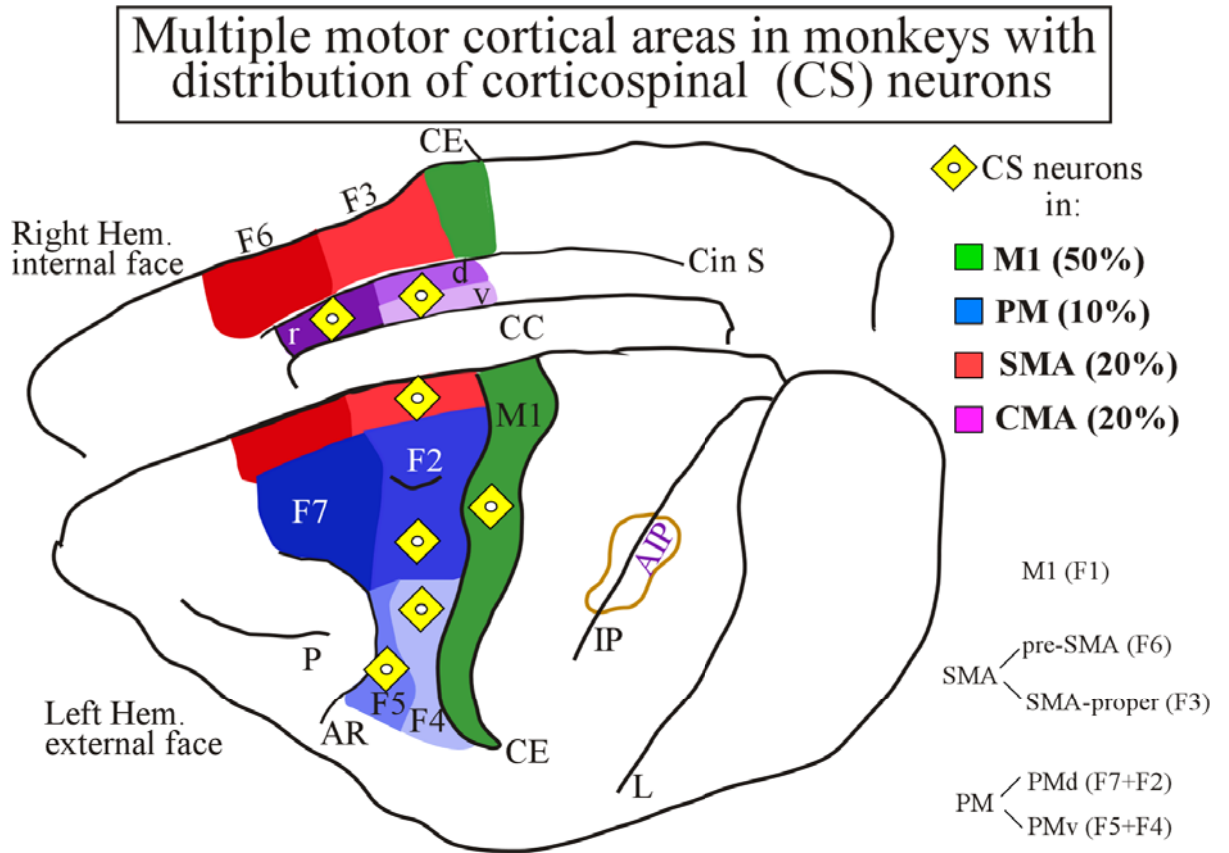


Fig. 1.4: Multiple motor cortical areas in the frontal lobe of macaque monkeys, with schematic distribution of corticospinal (CS) neurones. Note that pre-SMA (area F6) and the rostral part of the premotor cortex (area F7) do not contain CS neurones. In this figure, CS neurones located in the parietal lobe were not taken into account.

1.2.2.2: Properties of SMA: distinction between SMA proper and pre-SMA

The cortical area SMA projects to the grey matter of the spinal cord in primates. In a double labelling study, Rouiller and collaborators have observed close appositions between BDA anterogradely stained CS fibres from SMA and motoneurons retrogradely stained with Cholera toxin B subunit (Rouiller et al 96). In primates, both functional and anatomical data argue for a distinction between a rostral part (pre-SMA) and a caudal part (SMA-proper) of SMA. According to the numerous anatomical studies made on the corticospinal projections originating in the multiple motor areas, pre-SMA participates to cortical motor activity without directly projecting to the spinal cord, whereas SMA-proper directly projects to the spinal cord.

Differences between M1 and SMA-proper have been studied by Maier and colleagues (Maier et al 02), who investigated their participation to the supraspinal control of the motoneurone's activity. In their electrophysiological results, they observed that the volleys elicited by stimulation of M1 had larger amplitudes and faster conduction velocities than those elicited by stimulation applied to SMA-proper. The authors concluded that even if both regions M1 and SMA-proper project to the motoneurons of the spinal cord, M1 projections are more numerous and have more powerful excitatory effects than SMA-proper projections.

The functional differences between pre-SMA and SMA-proper have been investigated by Matsuzaka and collaborators (Matsuzaka et al 92) by recording neuronal activity in both areas. They observed that electrical stimulation in macaque monkeys in the caudal part (SMA-proper) elicited movements in the limbs or in the face, whereas stimulations in the rostral part (pre-SMA) infrequently elicited movements. The pharmacological transient inactivation of SMA resulted in the inability of the monkey to place its hands in the right position to start a bimanual or an unimanual specific task (Kermadi et al 97). Single unit recordings indicated that the activity of the neurones in pre-SMA were modulated in response to visual cue (Kermadi et al 98), whereas the activity in SMA-proper was modulated by passive movements of the limbs. In addition, the activity of pre-SMA neurones is involved in updating motor plans or during acquisition of new procedures of movements (Matsuzaka and Tanji 96; Shima et al 96; Nakamura et al 99). Anatomical tracing studies showed the existence of strong connections between SMA-proper and the ipsilateral M1, whereas there was no clear evidence for such connections between pre-SMA and M1 (Luppino et al 93). The pre-SMA region is more involved in the acquisition of new procedures of movement (Matsuzaka and Tanji 96; Shima et al 96), whereas the SMA-proper region is more involved in the control of well practiced voluntary movements.

1.2.2.3: Pyramidal neurones

The cortical areas 4 and 6 are devoid of granular layer IV at the light microscope. As seen above, they also contain the CS neurones of the frontal lobe, corresponding to long distance projecting pyramidal neurones in layer V. These neurones, the largest of which are referred to as ‘Betz’ cells, present a typical polarized morphology, with a large apical dendrite at the top that leaves the soma in the direction of the cortical surface. The cell body is vertically elongated. The axon leaves the base of the cell body to project downward in the white matter. Even though large pyramidal Betz cells are easily recognisable, the entire population of pyramidal cells present a great variety of size and shape. They can be specifically stained in layers III and V with the marker SMI-32, an antibody directed against neurofilaments of long projecting neurones (Figs. 1.5 and 1.6), nevertheless CS neurones are only located in layer V. The perikaryal size of Betz cells can reach the extraordinary dimension of 60 μm of diameter (Feldman 84).

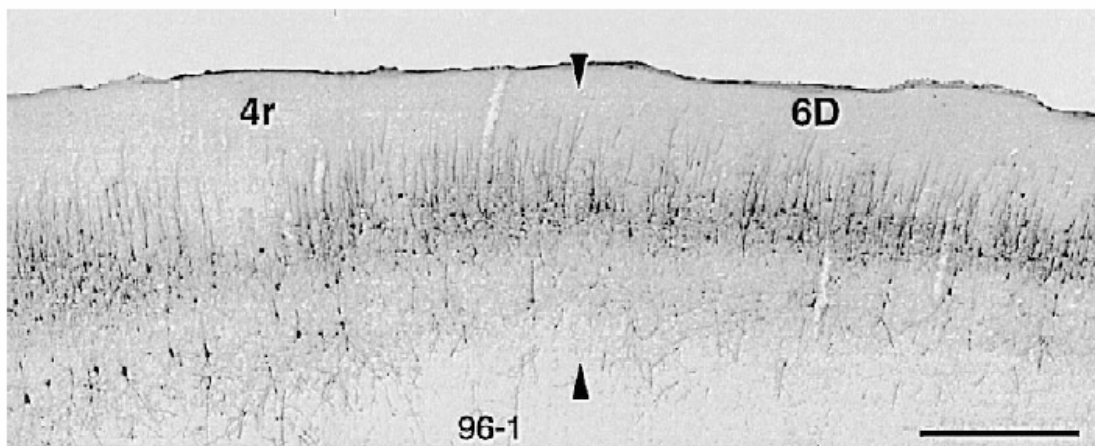


Fig. 1.5: Photomicrograph showing the border between Brodmann area 4 (M1) and area 6 (PM), as seen using the marker SMI-32 on a sagittal section of the macaque brain (adapted from Preuss et al 97).

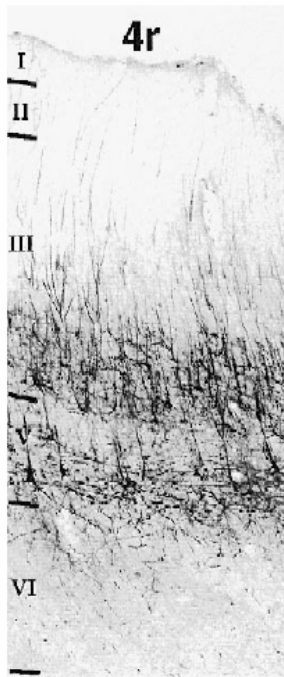


Fig. 1.6: Photomicrograph showing the distribution of pyramidal neurones in layer III and V of the primary motor cortex as seen in material stained for SMI-32 (adapted from Preuss et al 97a).

1.2.2.4: Role of Motor cortex in motor behaviour in general and in manual dexterity in particular

The first experimental approach of the role played by the cerebral cortex in the execution of movements was made in 1870, when Fritsch and Hitzig demonstrated that galvanic current applied over the motor cortex of a dog could evoke movements of the contralateral limb. Furthermore, lesion of the primary motor cortex (M1) affects dramatically the motor control, as described in details in chapter 1.3.

A part of the corticospinal tract projects monosynaptically to the motoneurons of the ventral horn of the spinal cord through the corticomotoneuronal system, strongly implicated in the finger movements in primates. An anatomical study (Bortoff and Strick 93) showed the intimate relationship between the properties of the corticospinal tract and the manual dexterity as reflected in the precision grip: they observed that in two distinct species of primate having the same anatomical capabilities of the hand to perform a precision grip, one performed the precision grip (cebus monkeys) whereas the other did not (squirrel monkey). Using injections of WGA-

HRP in the motor cortex to stain the CST projections, they analysed the corticospinal termination in the ventral horn (lamina IX) and observed that the percentage of stained CST fibres terminating in Lamina IX was much more prominent in the manual dexterous monkey spinal (cebus monkey) than in the less dexterous Squirrel monkey (Fig. 1.7).

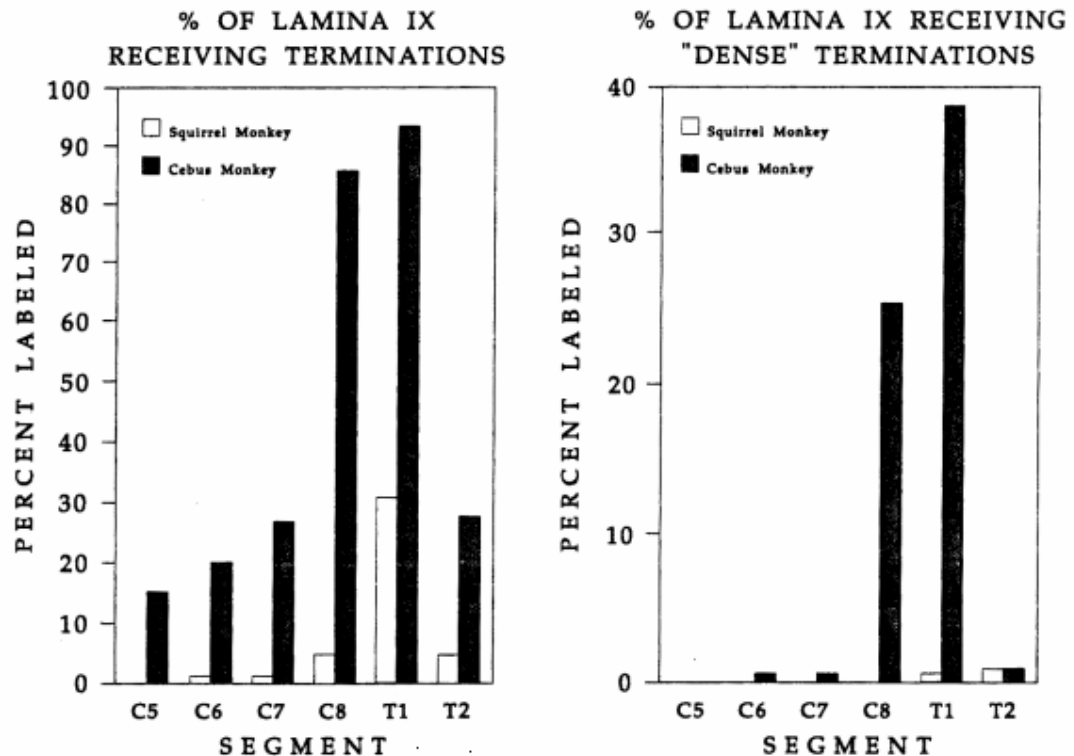


Fig. 1.7: Histogram showing the differences of the distribution of the corticospinal terminals in lamina IX in the grey matter of the spinal cord along the spinal segments. The density of terminals was correlated to the degree of independence of the movements of the fingers (adapted from Bortoff and Strick 93).

The great complexity of hand movements in primates reflects the activity taking origin in a large cortical network. Each motor cortical area receives and integrates a great amount of processed inputs, and their outcome is transferred to other motor centres, principally to M1, the main contributor to the CM system.

Organisation and distribution of the corticomotoneuronal cells in the motor cortex

Two aspects are to be taken in consideration: first, the area of M1 controlling the hand movement is relatively large in primates, in comparison to the size of the cortical area devoted to greater parts of the body like the leg or the arm; second, this area is stimulated with a lower threshold of current as compared to the neighbouring areas of M1. The complexity of the possible movements of the primate's hand is linked to the complexity of the organisation of the primary motor cortex: a multiple representation of the same group of muscle within M1, fact that leads to a convergence of signals to the alpha motoneurons of the spinal cord, resulting in a greater amount of complex and rapid mobilisation of the muscles of the hand.

The motor cortex influences the output of the motoneurons of the hand located in the cervical grey matter through two distinct mechanisms of activation: co-contraction and fractionation. These two mechanisms permit a large compound of various possibilities of modulation, resulting in the great complexity of finger movements.

Co-contraction is needed when two or more muscles are working together, in the stabilisation of the hand for example. Fractionation, in contrast, is needed when the hand is moving to shape a new grip in a reach and grasp task. These two principles seem to be opposite but are in fact co-working (Lemon 99).

The mechanism of fractionation has been studied in primates by Bennet and Lemon (Bennett and Lemon 96). They recorded in primate identified CM cells during a precision grip task and they investigated CM cells that produced post-spike facilitation in at least two different intrinsic hand muscles. CM cells were identified by spike-triggered averages of rectified EMG activity. The great majority of the cells increased their firing rate during the precision grip. CM cells were most active during periods of fractionation of EMG activity, with one muscle more active than the other. During such periods a given CM cell tended to be more active when the muscle in which it produced the strongest CM effect was contracting.

Another aspect of the complexity of the primary motor cortex in its role of controlling the independent finger movement has been investigated by Baker and colleagues (1998): they stimulated simultaneously M1 hand area of macaque monkeys using a single pulse ICMS technique and they recorded the rectified EMG activity of intrinsic hand muscles. They concluded that different areas within the hand area of M1 can interact to modulate the CS output and that a single ICMS pulse could activate a widespread portion of M1 (Baker et al 98).

M1 is source of access (50%) to the motoneurons of the spinal cord, although the non-primary motor cortical areas are in position to address the spinal motoneurons but in a lesser extent than M1 (Lemon 93). The involvement of the primary motor cortex in the ability to perform independent finger movement in precision grip task through the corticomotoneuronal cells has been widely investigated (Lawrence and Hopkins 76; Fetz et al 76; Wiesendanger 81; Porter 87; Maier et al 93; Bennett and Lemon 94; Nudo and Milliken 96). Each CM cell possesses a “muscle field” that is defined as a small group of muscle whose activity is directly correlated with the activity of the CM cell. This is particularly true for muscles involved in precision grip.

1.2.2.5: Electrophysiological properties of M1 (output map of M1)

To evaluate the functional organisation of the hand area in the primary motor cortex and its reorganisation after an interruption of the corticospinal tract, a suitable method has been first designed and used by Asanuma and colleagues (Asanuma and Sakata 67) when they mapped for the first time the motor cortex of the cat using intracortical microstimulation (ICMS). The strategy was to micro-stimulate restricted cortical territories, at several depths with microelectrodes and record the EMG activity, in order to establish the topographical representation in the cortex of the stimulated muscles. The intracortical microstimulation of the hand area of M1 in macaques produced EPSP in the corresponding motoneurons through the

corticomotoneuronal pathway, with a threshold of current of stimulation of around 10 μ A (Palmer and Fetz 85). Nudo and colleagues (Nudo and Milliken 96) used this technique in anaesthetised monkeys subjected to ischemic cortical lesion of M1 to derive a detailed map of the re-organised cortical representation of the distal movements. They obtained responses in the forelimbs with threshold of current of about 20 μ A. Several groups worked with the ICMS technique to define and map the functional role of the primary motor cortex of sub-human primates involved in hand movements (Kwan et al 78; Murphy et al 85; Lemon et al 87; Liu and Rouiller 99).

A new aspect of the role of the precentral cortex has been investigated with different parameters of intracortical microstimulation by Graziano and colleagues (Graziano et al 02). Using longer trains of stimuli (500ms), they observed in macaque monkeys that repetitive stimulations of one site in the precentral cortex elicited repetitively the same complex movement, like for example the reach and grasp movement followed by the bring to mouth movement. They concluded that focal sites of the motor cortex are not only organised to perform simple movements when stimulated as is commonly accepted but also complex and reproducible movements.

1.2.3: The rubrospinal pathway

The Red Nucleus (RN), located in the brain stem, is made of two distinct regions: the part containing a great amount of neurones called the Magnocellular part (RNm) and a part mainly made of fibres called the Parvocellular part (RNp). The functional relevance of the Red nucleus has been investigated in the monkey by Burman and colleagues (Burman et al 00) using a combination of retrograde staining of the rubral output and an anterograde staining of the corticorubral input. They injected the migrating markers in three different sites in the spinal cord: Fast Blue (FB) at cervical level on the left side, Rhodamine Latex Microspheres (RLM) in the contralateral grey matter at the same level and Diaminido Yellow dihydrochloride (DY) at

thoracal level on the right side. Their results showed that the rubrospinal neurones are distributed in RNm, but absent from RNp (Fig. 1.8). They also observed a few extra rubral neurones labelled with RLM in the reticular complex, dorsal to the red nucleus and in the periaqueductal grey matter. Holstege and colleagues showed the anatomical preferences of the rubrospinal fibres to terminate in the spinal region controlling distal muscles of the forelimb than in the region controlling proximal muscles (Holstege et al 88). These anatomical data are supported by extracellular recordings made in the RNm showing that these cells' activity is highly modulated during movements of distal joints (Miller et al 93; McKiernan et al 98).

Corticorubral input to the red nucleus of macaque monkeys

In the same paper, Burman and colleagues injected anterograde tracers in the macaque's M1, SMA and CMA. They found that the three injected cortical regions send projections to the ipsilateral RNp, whereas only M1 projects to the ipsilateral RNm.

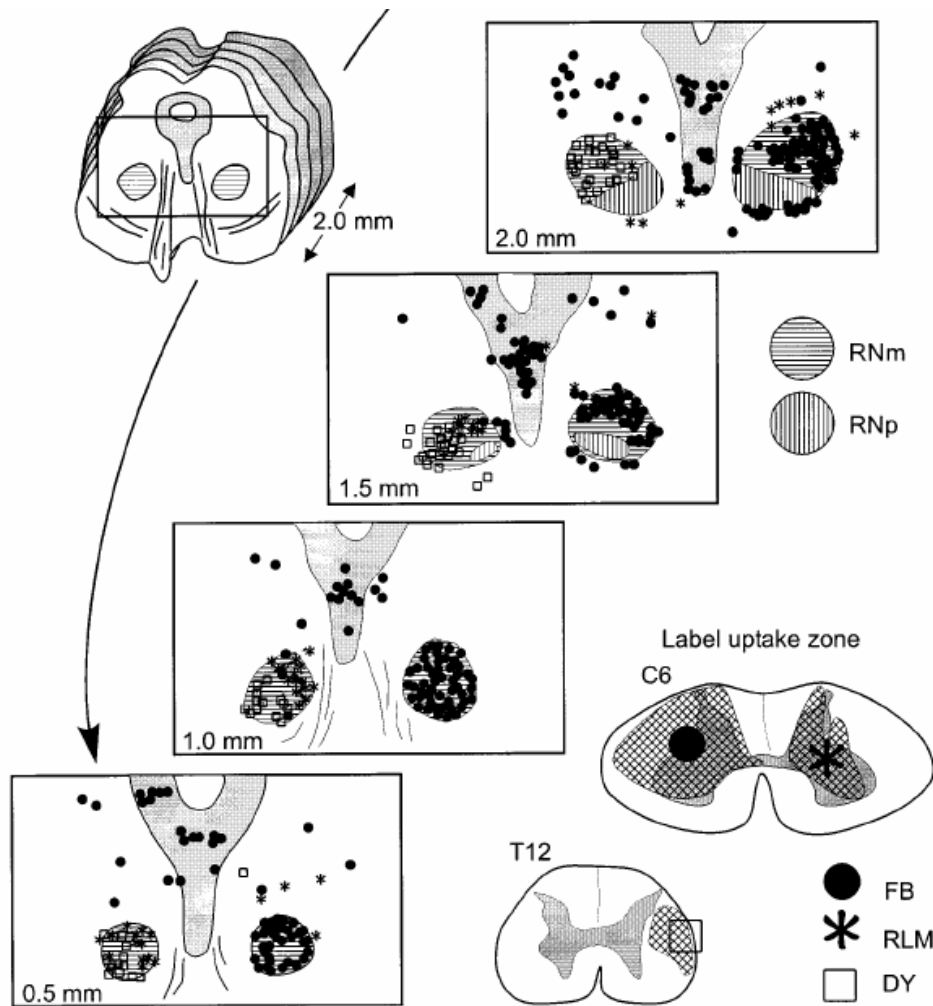


Fig. 1.8: This picture shows the distribution of neurones retrogradely stained in the red nucleus (RN) after injections of 3 distinct tracers in the spinal cord of macaque monkeys. In more details, one can see that rubrospinal neurones are not distributed homogeneously between the two main subdivisions of the red nucleus: most labelled neurones were in the pars magnocellularis RNm and very few, if any, in the pars parvocellularis RNp (adapted from Burman et al 00).

Lawrence and Kuypers (1968b) noticed in their pyramidal lesions in monkeys that the residual control of the hand after a bilateral pyramidotomy disappeared after an additional lesion affecting the RN or the rubrospinal projections. Electrophysiological studies showed that the effects of current stimulation of the RN with high amplitude of current are similar to those obtained with stimulation of M1 hand area with lower current amplitude in the cat (Ghez 75).

The Rubrospinal tract is known to play a certain role in the control of finger movements: in the studies made by Lawrence and Kuypers, a lesion of the pyramids was performed in macaque monkeys and the noticeable improvement of manual dexterity occurring in the recovery period was attributed to the remaining rubrospinal tract (Lawrence and Kuypers 68b). Other studies showed that the close electrophysiological relationship between motoneurons and CST or RST axons are very similar, both tracts establishing monosynaptic connections with the motoneurons (Phillips and Porter 77; Holstege et al 88).

Belhaj-Saïf and collaborators made electrophysiological studies using the technique of spike-triggered averaging (StA) in the red nucleus of macaque monkeys and EMG recordings in forelimb muscles. They analysed the influence (positive: facilitation or negative: suppression) of RNm on proximal versus distal muscles and flexor versus extensor muscles groups (Belhaj-Saïf and Cheney 00). They observed a functional reorganisation of the magnocellular part of the Red Nucleus consisting in a redistribution of the activity of rubro-motoneuronal cells on flexor-extensor muscles, and in the proximal-distal axis.

1.2.4: Spinal cord

The spinal cord is an important part of the central nervous system, bridging the brain and the periphery but also being able of integration and modulation of nervous signals; it is organised in mammals and subsequently in primate as follows: the grey matter, containing the soma of the neurones is located in the middle and is surrounded by the white matter that contains the different ascending and descending tracts. The grey matter has been divided in different zones following cytoarchitectonical criteria in Rexed regions or laminae, from I to XII (Fig. 1.9 C). These delimitations of the grey matter of the spinal cord have been first described in the cat and later adapted to the primates (Rexed 54; Nieuwenhuys et al 88).

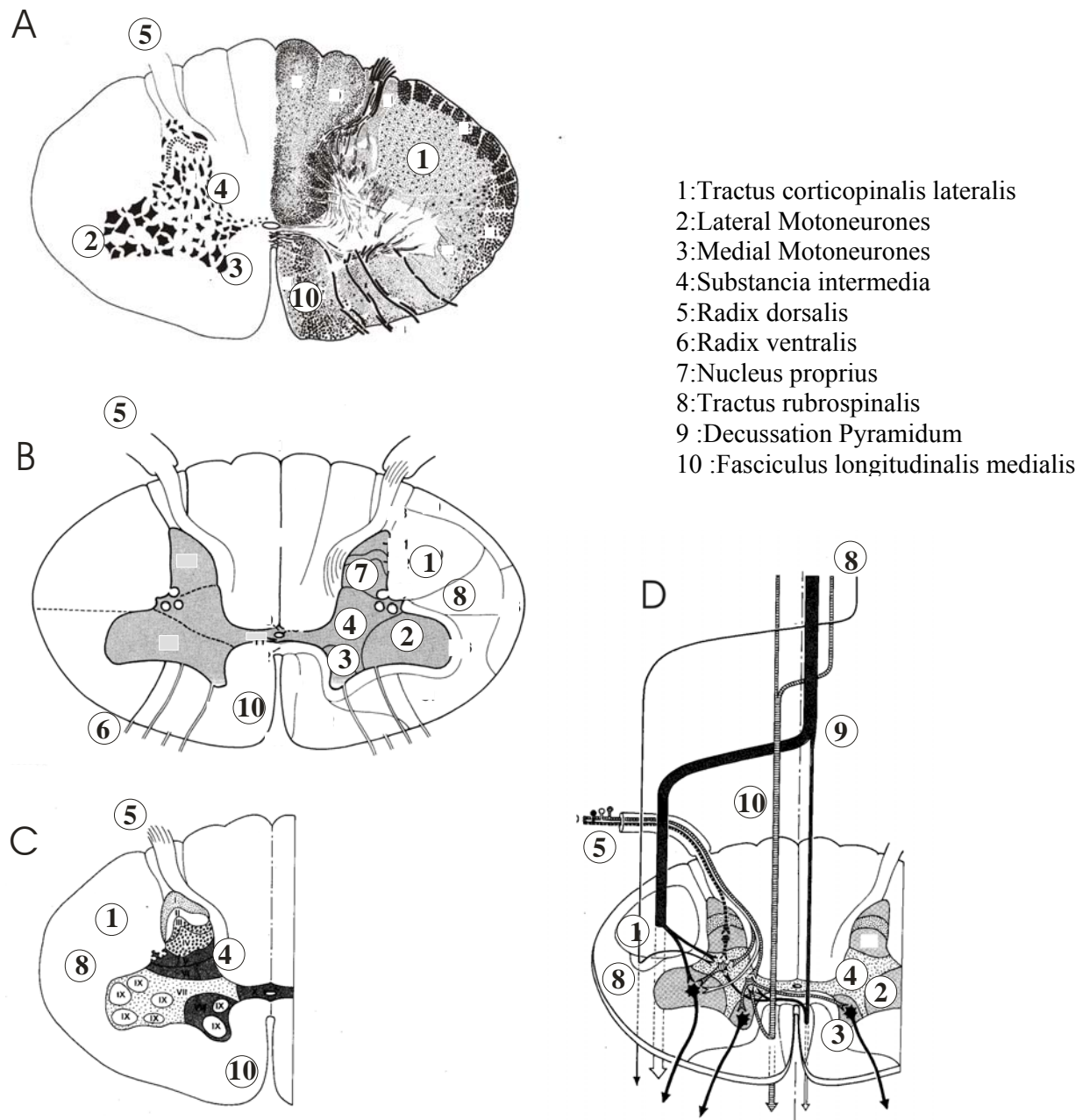


Fig. 1.9: Structure and organisation of cervical spinal cord in humans: sections through the spinal cord at low cervical level.

A: Cellular (left) and fibrous (right) organisation

B: Subdivisions of the grey and white matters in the spinal cord

C: Rexed's organisation of the grey matter of the spinal cord: the zone IX corresponds to location of the motoneurones in the ventral horn

D: Location of the descending tracts with emphasis on the dorsolateral funiculus containing the CST and the RST (adapted from Nieuwenhuys et al 88).

1.2.4.1 Corticospinal projections: convergence and divergence

The corticospinal tract has a distributed origin in multiple motor and premotor areas such as M1, PM, SMA-proper and CMA. It makes widespread spinal connections in several Rexed laminae, in the intermediate zone as well as in the ventral horn. Descending pathways from supraspinal structures are divided into the dorsolateral system, made of the corticospinal tract (CST) and the rubrospinal tract (RST), and into the ventromedial system including the vestibulospinal and the reticulospinal tracts. The axons of the CST terminate mainly in the intermediate zone of the grey matter of the spinal cord, a zone representing about 70 % of the entire zone of termination (Fig. 1.10).

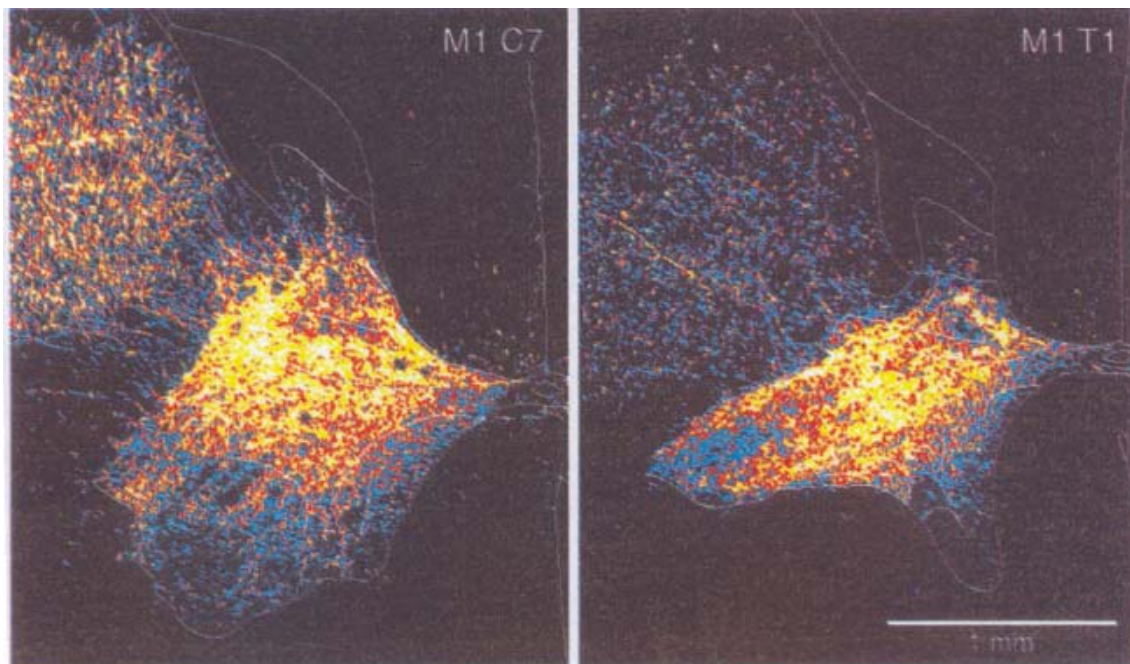


Fig. 1.10: Termination zones of the corticospinal projections in the grey matter of the spinal cord at cervical (C7) and thoracic (T1) levels in monkey. CS axons terminals were labelled as a result of WGA-HRP injection in the opposite M1. This figure shows the widespread of CS terminations not only in Rexed lamina IX but, even denser, in the intermediate zone, where interneurons are located (adapted from Dum and Strick 96).

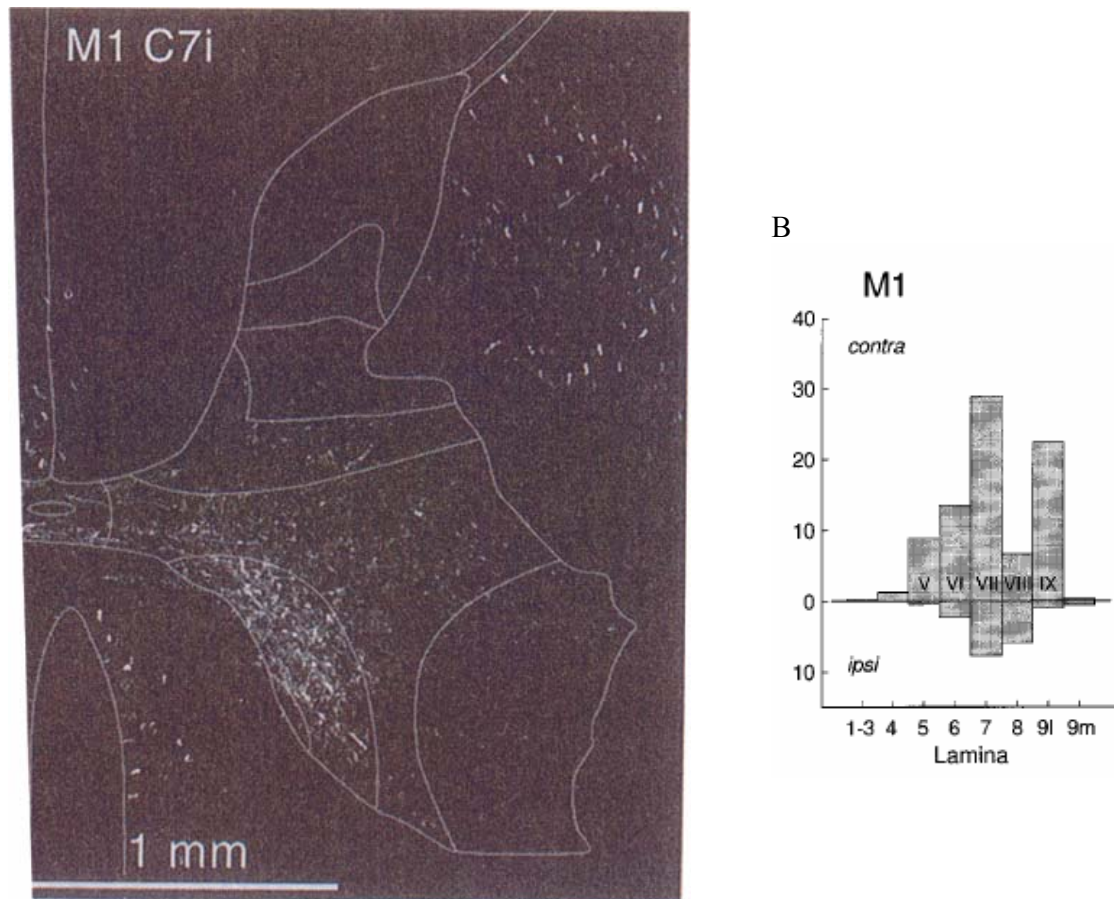


Fig. 1.11: A: Same data as in Fig. 1.10, but for the ipsilateral (uncrossed) CS projection. Photomicrograph shows the ipsilateral CS projections in monkey. One can see that the majority of the terminals are located in the medial part of the MN innervating the axial and proximal muscles, but a certain quantity of stained axons also reach the intermediate part, where interneurons and propriospinal neurones are located (adapted from Dum and Strick 96). B: Histogram showing the summary of the density of stained CST fibres coming from M1 and terminating in distinct laminae of the cervical spinal cord, for the crossed projections (bins towards top) and the uncrossed projections (towards bottom).

The density and localisation of axon terminals for the uncrossed corticospinal fibres are shown in Fig. 1.11: they are distributed rather homogeneously inside the dorsolateral funiculus, blended with the crossed CST fibres coming from the opposite hemisphere. The uncrossed CS axons terminate mainly in lamina VII (Fig. 1.11). In man, the cortical representation of ipsilateral muscles of the hand has been investigated by Wasserman and colleagues (1994). They recorded the motor evoked potentials of voluntary contracted ipsilateral muscles after

transcranial magnetic stimulation (TMS) and they recorded a certain number of sites over the motor cortex producing changes in the electrophysiological activity of ipsilateral first dorsal interosseus muscle when stimulated (Wassermann et al 94).

The cortical extent of a neurones' population converging to one motoneurone in the spinal cord of macaque monkeys has been studied using the electrophysiological method of microstimulation (Andersen et al 75). It resulted that the portion of motor cortex representing single motoneurone is relatively large: 5 to 12 mm². This finding led to the notion of inevitable overlapping. Later, several studies based on ICMS technique confirmed that M1 is not simply organised in parallel to the somatosensory cortex with limited and well separated somatotopically organised portions of cortex but rather in multiple overlapping clusters of neurones responsible for single motor joints forming a complex mosaic (Schieber 01). Recordings made from single M1 neurones showed neuronal activity in relationship with movements of different fingers in rhesus monkeys (Schieber and Hibbard 93). The recorded neurones were spread in the whole hand region of M1, without a significant indication of a close relationship between somatotopic function and spatial localisation. Further investigations about the distribution of M1 specialised neurones in independent finger movements made by Poliakov and Schieber (1999) showed that the recorded neurones can not be easily grouped, working rather in a large network (limited number of cluster) of elements in controlling independent finger movements (Poliakov and Schieber 99). These data are compatible with the anatomical data obtained by Shinoda and colleagues (Shinoda et al 81) when they injected HRP in a single corticospinal cell and they reconstructed in the spinal cord the multiple branches in the different Rexed laminae, showing the large number of collaterals in monkeys (Fig.1.12). These data illustrates the great possibilities of axonal collaterals and the principle of divergence (see also(Lemon 88)).

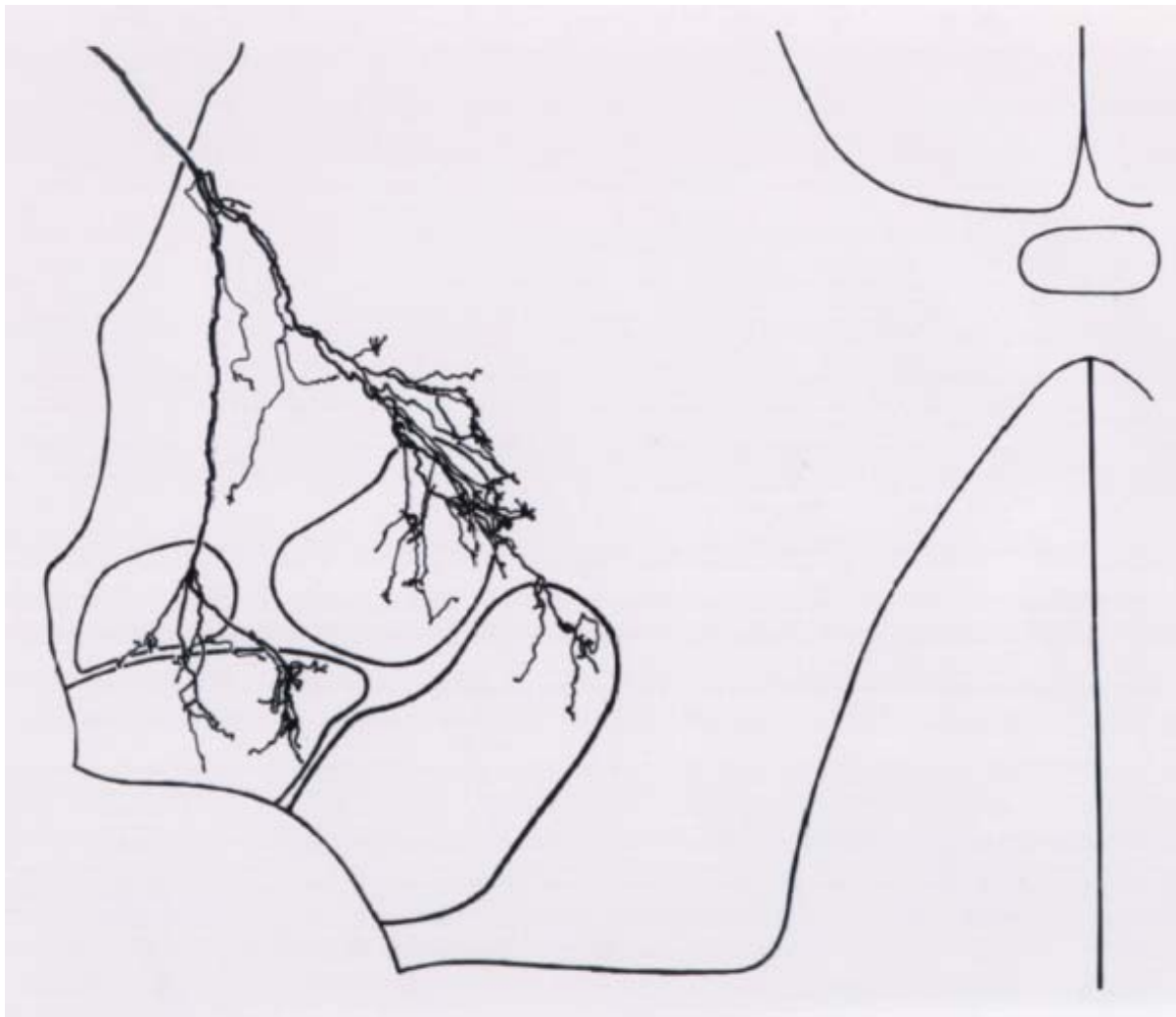


Fig. 1.12: Reconstruction of the terminal portion of an individual CS axon, intra-axonally filled with HRP. These data in monkey demonstrate that a single CS axon send collaterals making connections with several pools of motoneurons in the C7 segment (adapted from Shinoda et al 81).

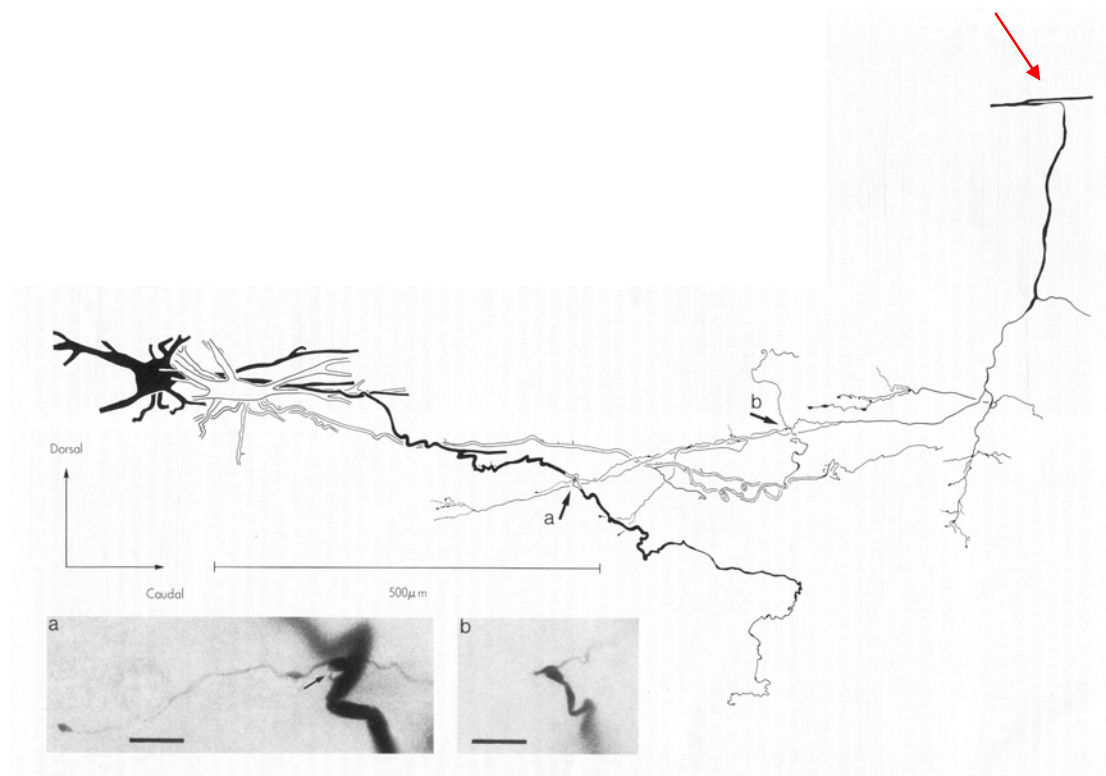


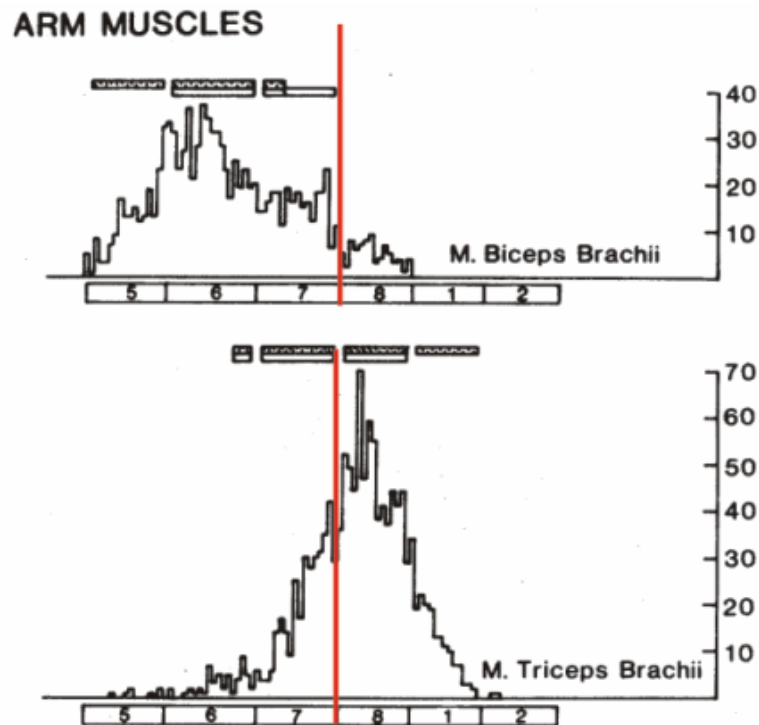
Fig. 1.13: Camera lucida reconstruction of collateral branches of a primate CM axon (red arrow) which establishes a synaptic contact with two distinct motoneurons. The photomicrographs a and b correspond to the synaptic contacts shown by the black arrows, (a) with the black motoneuron and (b) with the white motoneuron (adapted from Lawrence et al 85).

Using intracellular staining of the corticomotoneuronal system in primate, Lawrence and colleagues (1985) showed the divergence of contacts between the same corticomotoneuronal axon and few targets (two motoneurons are shown in Fig. 1.13). They injected HRP in corticospinal axons in the hand area of the precentral gyrus of rhesus monkey and in the nearby motoneurons in the cervical spinal cord in Lamina IX. The authors concluded to a relative specificity of contact to the motoneurons from one collateral of corticomotoneuronal axon (Lawrence et al 85).

1.2.3.4: Distribution of motoneurons in the cervical spinal cord

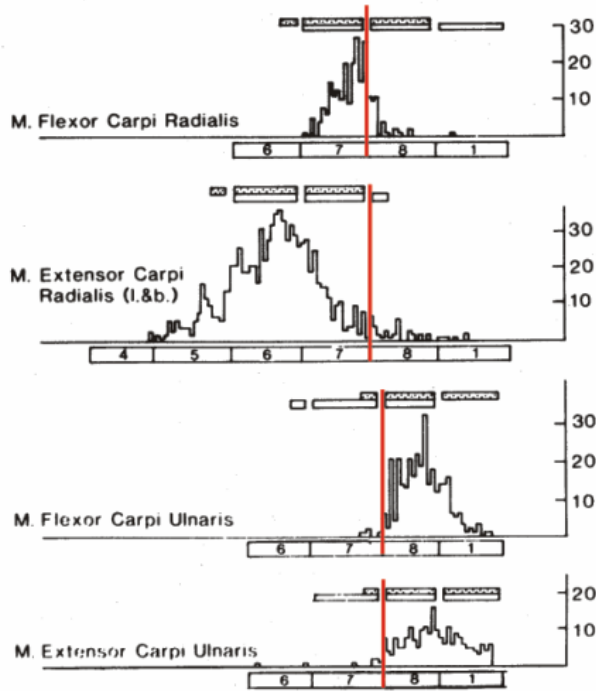
The longitudinal distribution of MNs in the ventral horn at cervical level has been studied by Jenny and Inukai (1983). The strategy used was to inject a retrograde tracer in the muscles and to evaluate their distribution in the spinal cord. They injected HRP in different muscular groups of the arm in 10 macaque monkeys and they evaluated the topographical organisation of the motoneurons in the ventral horn of the spinal cord segment after segment (Jenny and Inukai 83). As shown in Fig.1.14 (panels C and D), the vast majority of hand muscles are located in the spinal segments C8-T1. In the present study, the localisation of the hemi-section of the spinal cord on the rostro-caudal axis was chosen to be at the border between C7 and C8, in order to be between the population of MNs responsible for Biceps contraction (above the lesion) and the population of MNs controlling the triceps (below the lesion). Such lesion allowed the injured animal to move the arms (shoulder, elbow and wrist articulations), but resulted in a complete paresis of the fingers with loss of the precision grip.

A



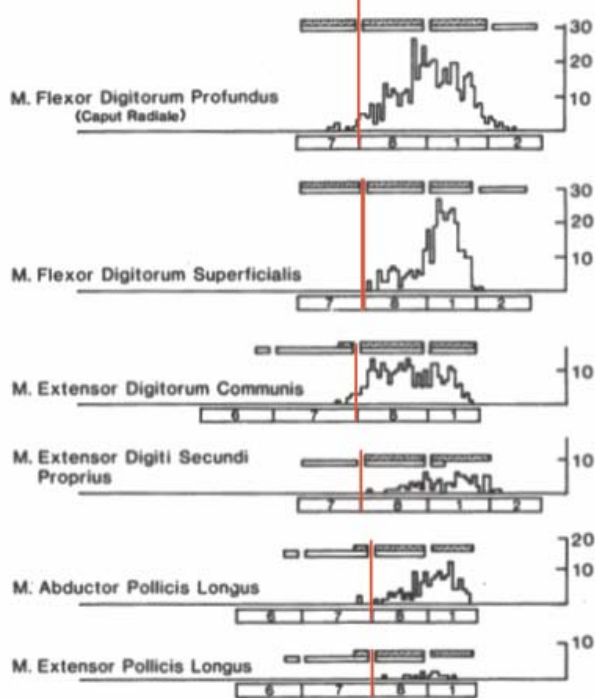
B

FOREARM MUSCLES (Wrist)



C

FOREARM MUSCLES (Hand)



D

HAND MUSCLES

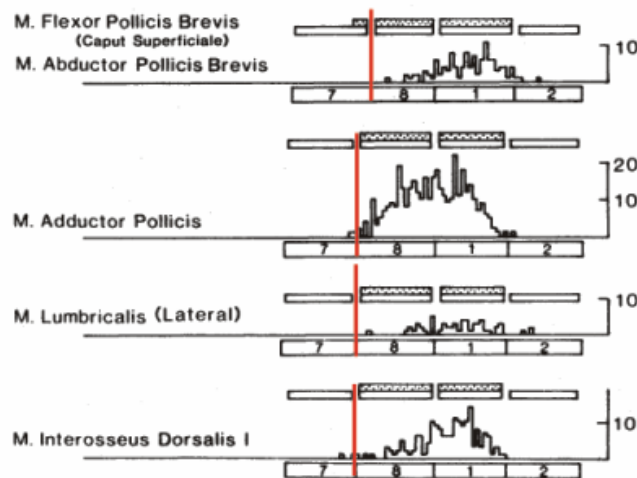


Fig. 1.14: Histograms representing the distribution of motoneurons along the ventral horn of the spinal cord at cervical (4-8) and thoracal levels (1-2). The orientation is the following: rostral is on the left and caudal is on the right. The red line indicates the level of spinal cord lesion in our model.

A: Location of motoneurons of the biceps and the triceps muscles in cervical spinal cord.

B: Same for forearm muscles involved in wrist movements.

C: Same for forearm muscles involved in hand movements. These muscles are directly involved in precision grip, as well as muscles in D.

D: Same for muscles intrinsic to the hand (adapted from Jenny et al. 1983).

The motoneurons (MNs) located in the ventral horn of the spinal cord receive excitatory and inhibitory inputs from different sources: from sensory afferents in the reflex pathways (directly or via local interneurons), from other spinal neurones of the propriospinal system and from supraspinal centres. The MN cell bodies are arranged in longitudinal clusters in the ventral horn. They are spatially distributed following two anatomical and functional principles: the proximal-distal rule and the flexor-extensor rule (Fig. 1.15).

1.2.4.3: Corticomotoneuronal system

In primate, a substantial part of CS axons (up to 75 % of upperlimb motoneurones) establish monosynaptic connections with spinal motoneurones, corresponding to the so-called corticomotoneuronal (CM) system, directly linking the motor cortex with the alpha motoneurones of the spinal cord (Lemon et al 98). In contrast, only little (Liang et al 91) or no evidence was found for the presence of CM system in other mammals (e.g. cat, rat). In particular, in an electrophysiological study (Alstermark et al 04), no monosynaptic CM EPSP was found as a result of pyramidal stimulation. Furthermore, a study based on electron microscopy (Yang and Lemon 03) showed that a combined labelling of the CS fibres, anterogradely stained in M1 with BDA and retrogradely stained in the muscles with cholera toxin subunit B (CTB) resulted in the observation of 8 close appositions between BDA labelled axons and CTB stained motoneurones in Rexed lamina IX using the light microscopy technique. The close appositions observed in light microscopy were not confirmed as being synapses in electron microscopy investigations. (Yang and Lemon 03). It is thus believed that the CM system is a speciality of primate which is, to some extent, correlated with manual dexterity.

Intracellular recordings showed that the minimal linkage in primate was monosynaptic, in opposite to other species that present a lower degree of independent finger movement. In that direction, the development of monosynaptic connections in primates correlates with manual dexterity, for example during precision grip ability. Lemon and collaborators compared quantitatively the distribution in M1 and SMA of corticospinal neurones supplying motor control to hand and finger muscles in macaque monkeys (Lemon et al 02; Maier et al 02). Their anatomical results based on anterograde tracing showed a greater density of corticospinal projections in M1 (81% of the motoneuronal area for hand and digit motoneurones) compared to the only 6% coming from SMA. In the same study, the electrophysiological data showed that stimulation in M1 and SMA could evoke direct and indirect responses recorded with EMG in

the hand and finger muscles. However M1 volleys were larger in amplitude and conducted with faster velocities, compared to volleys from SMA. In a double staining study of the corticospinal tract in primate, Rouiller and colleagues (1996) showed close appositions in the grey matter of the cervical cord between CST anterogradely stained and hand supplying motoneurons retrogradely stained. The injections site in the motor cortex were identified with intracortical microstimulation in M1 and SMA (Rouiller et al 96). These results suggest that the SMA can control hand movements in parallel to M1 following the same type of corticomotoneuronal connection, although the SMA projection appears to be less dense, slower and less potent (Maier et al 02).

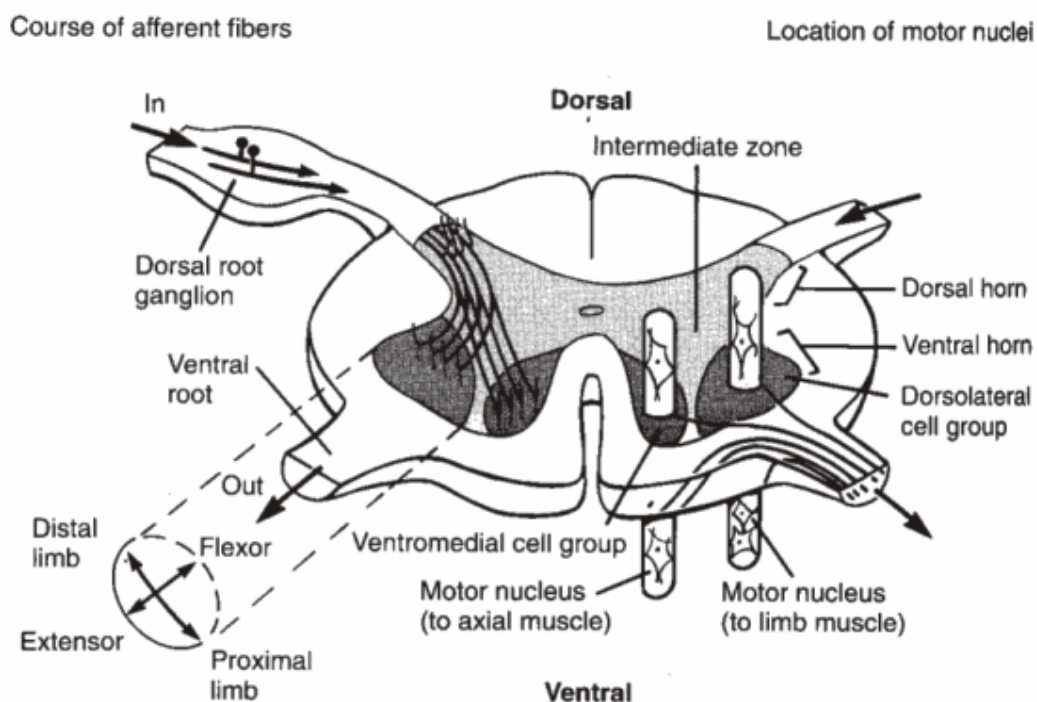


Fig. 1.15: Spatial distribution of the motoneurons (MNs) in the spinal cord at cervical level showing the extensor-flexor gradient and the proximal-distal gradient on the left side. The motoneurons devoted to the axial musculature are located medially and the motoneurons devoted to limb muscles are found more laterally within the dorsolateral group of MNs. There is also a medio-lateral gradient for proximal-distal MNs.

1.2.4.4: Propriospinal system

In the term propriospinal neurones are included all intrinsic spinal cord neurones which axons terminate in remote spinal cord segments. The term interneurone includes neurons that terminate in the same spinal segment whereas propriospinal neurones terminate in distant spinal segments. Corticospinal input to the hand motoneurons (C8-T1) could be relayed indirectly by the propriospinal pathway in higher mammals, located at C3-C4 level. Propriospinal neurones are neurones located in the grey mater of the spinal cord, in the intermediate region, giving rise to an axon, which contacts neurones located in other spinal segments. They are in that sense different from true local interneurons (e.g. Renshaw cells). Two categories of propriospinal neurones have been described: long propriospinal neurones whose axons are located in the ventromedial part of the spinal cord, whereas the short propriospinal neurones send their axons in the dorsolateral part, close to the grey matter (Fig. 1.16). The role played by the propriospinal system in the control of movement has been first described in the cat by Lundberg (1976), as a secondary indirect pathway to the motoneurons, located inside the cervical spinal cord (Illert and Tanaka 76). This system was later described as the C3-C4 propriospinal system and its important role in the control of forelimb movement in the cat is ubiquitously accepted (Illert et al 76a; Illert et al 76b).

In primates, the role played by the propriospinal system has been studied mainly in three groups of research, namely Pierrot-Deseilligny in France, Alstermark in Sweden and Lemon in England. The first study made by Lemon and collaborators in anaesthetised monkeys was based on the following strategy: measure the EPSPs in motoneurons after stimulation of the pyramids and define the proportion of monosynaptic connections coming from the corticomotoneuronal system and the proportion of disynaptic connections that could come from the propriospinal system (Maier et al 98). In addition, a unilateral section at C5 level affecting the dorsolateral funiculus thus interrupting the monosynaptic CS fibres was expected to emphasize the role

played by the propriospinal system. In contrast, only a few EPSPs with a disynaptic-type latency were observed in the intact animal (3%) and 14% of motoneurons had disynaptic-like EPSPs after the spinal cord lesion, which can be due to remaining direct CS fibres with somewhat longer latency (Maier et al 98). To answer this question, Alstermark and colleagues postulated that these negative results were due to stronger inhibitory control of the C3-C4 propriospinal system in the monkey than in the cat. In this direction, they added strychnine injections to block the glycinergic inhibition during the recording of motoneurone activity (Alstermark et al 99). The late disynaptic EPSPs observed in Lemon's experiments did not appear in the great majority of cases and the authors concluded to an inhibitory role of the C3-C4 propriospinal system in normal conditions, that could relay the corticospinal information in case of cervical lesion (Alstermark et al 99). As their first experiment was done under anaesthesia, a second study was conducted by Lemon and collaborators in awake or lightly sedated monkey, which was based on the recording of single motor units (SMU) after stimulation of the pyramidal tract. The results showed no evidence for a non-direct corticospinal excitation to upper limb motoneurons in macaque monkeys by non-monosynaptic pathway (Olivier et al 01).

In our model of spinal cord injury, considering the position and extent of the cervical lesion (see chapter 3) the short propriospinal neurones will probably have their axons interrupted, whereas the long propriospinal system is likely to be preserved.

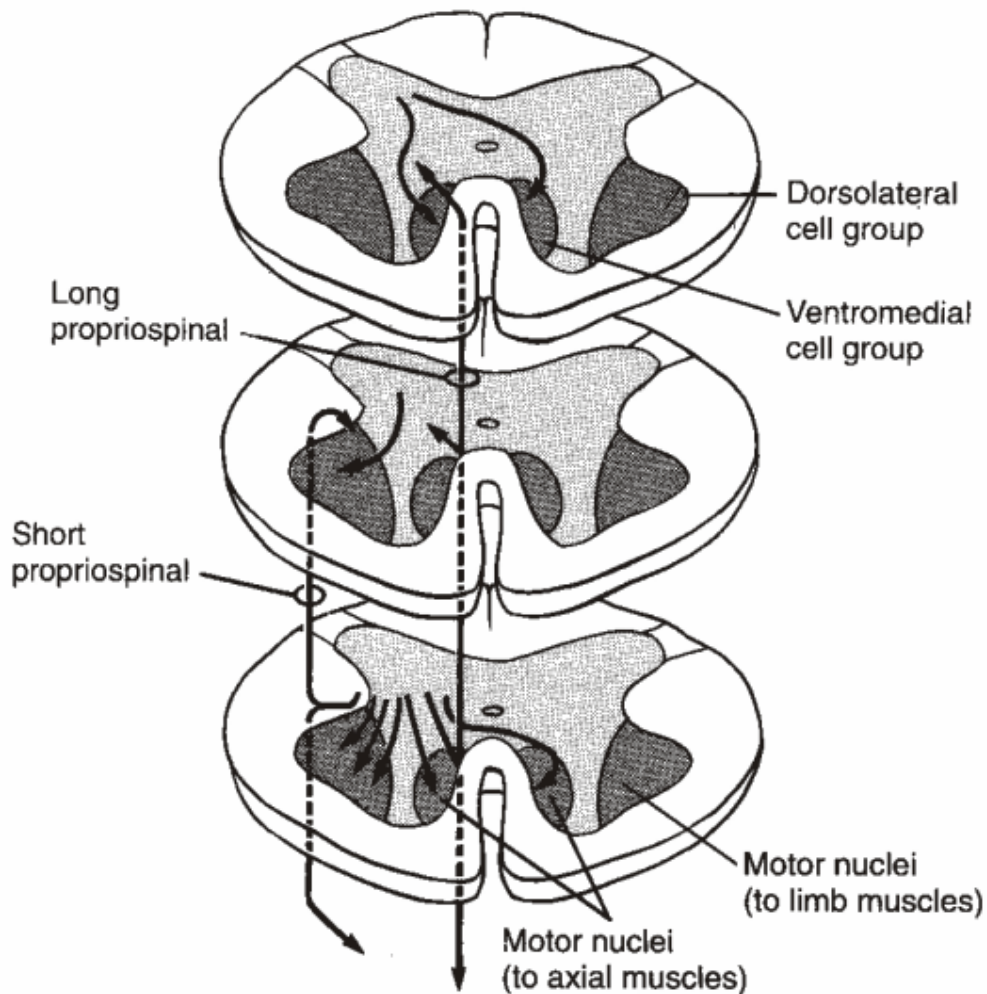


Fig. 1.16: Schematic representation of the propriospinal organisation in the cervical spinal cord of primate, subdivided into the long propriospinal system whose axons are ventro-medially located and the short propriospinal system located in the dorsolateral funiculus, close to the grey matter.

Another sort of cortical efferent that can influence indirectly the motoneurons are indirect projections through sub-cortical centres like thalamus, striatum, pons, lateral reticular nucleus (reticulospinal tract) which may modulate internal motor programs for execution by the corticomotoneuronal system.

1.2.4.5: Organisation of the ventromedial system

Reticulospinal and vestibulospinal tracts

The exact localisation of the reticulospinal tract in humans differs significantly according to different textbooks of anatomy. In humans, a great number of reticulospinal fibres terminate in the cervical enlargement, entering the grey matter in the anterior horn and in the zona intermedia (Fig. 1.17). The reticulospinal fibres descend bilaterally, mainly ipsilaterally in the cervical spinal cord, without forming a distinct tract, scattered in the anterior and the lateral funiculi (Nathan et al 96). This descending pathway sends numerous axon collaterals along its pathway along the spinal cord (Holstege and Kuypers 87). But the reticulospinal fibres influence motoneurons of the spinal cord responsible for axial or proximal musculature rather than distal movements.

The lateral vestibulospinal tract is located at cervical level 1 to 3 laterally to the anterior roots, whereas in the lower cervical segments it moves to the sulcomarginal angle. In the cat, the Phaseolus Vulgaris anterograde staining method was used to trace the pathway of reticulospinal fibres that descend from the reticular formation to the spinal cord ; (Matsuyama et al 93; Mori et al 96). The reticulospinal axons terminate in Rexed laminae VI to IX, in the region of the motoneurons.

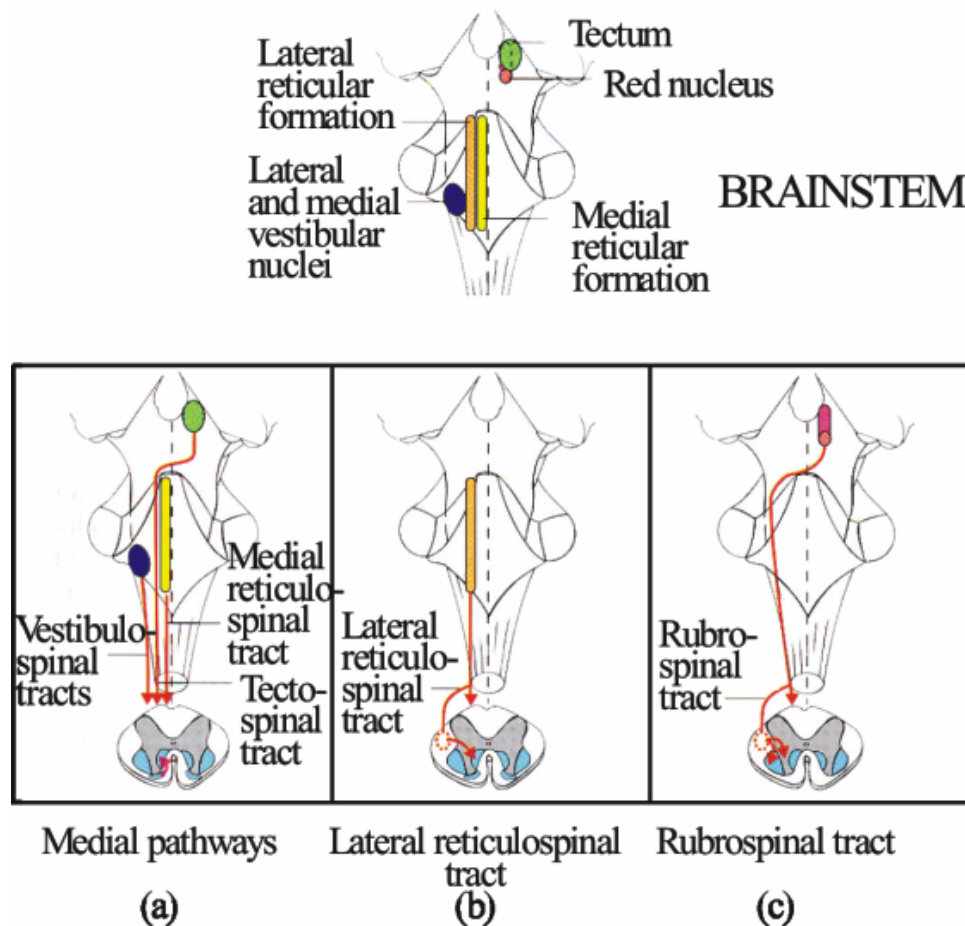


Fig. 1.17: Drawing representing the three motor pathways from the brainstem to the spinal cord (adapted from Human Physiol. Roades, 2002).

Efferents from the vestibular nuclei to the spinal cord

The vestibular nuclei project to the motoneurons of the spinal cord in two distinct tracts: the lateral vestibulo-spinal tract (LVST) and the medial vestibulo-spinal tract (MVST). The LVST is located ipsilaterally and projects directly to the extensor motoneurons of the forelimb and the hindlimb, and indirectly through interneurons to the flexor motoneurons of both limbs. This pathway also innervates monosynaptically the motoneurons responsible for neck movements. In contrast, the MVST projects contralaterally to the central cervical nuclei

responsible for neck movements. In addition, the vestibular nuclei project indirectly to the spinal cord through the formation reticularis.

1.3: Lesions of the corticospinal (CS) system

1.3.1: General aspects: lesions of the CS system at different levels

Different parameters strongly influence the effects of lesions of the CS system and functional recovery: the type of lesion, the extent and precise location of the lesion, the time post-lesion of behavioural evaluation, the type of the observed movements. Three levels of injury affecting the CS system have been studied in sub-human primates: 1) at the cortical level (Sloper et al 83; Passingham et al 83; Nudo and Milliken 96; Rouiller et al 98; Nudo 99; Liu and Rouiller 99), 2) along the corticospinal pathway through lesions of the pyramids (Tower 40; Bucy 57; Bucy 66; Lawrence and Kuypers 68a; Lawrence and Kuypers 68b; Beck and Chambers 70; Hepp-Reymond and Wiesendanger 72; Woolsey et al 72; Hepp-Reymond et al 74; Lawrence and Hopkins 76; Schwartzmann 78; Kucera and Wiesendanger 82; Chapman and Wiesendanger 82; Hepp-Reymond 82) and 3) closer to their termination in the spinal cord itself (Holmes and May 09; Bernhard et al 53; Denny-Brown 66; Aoki and Mori 79; Galea and Darian-Smith 97a; Galea and Darian-Smith 97b; Sasaki et al 04).

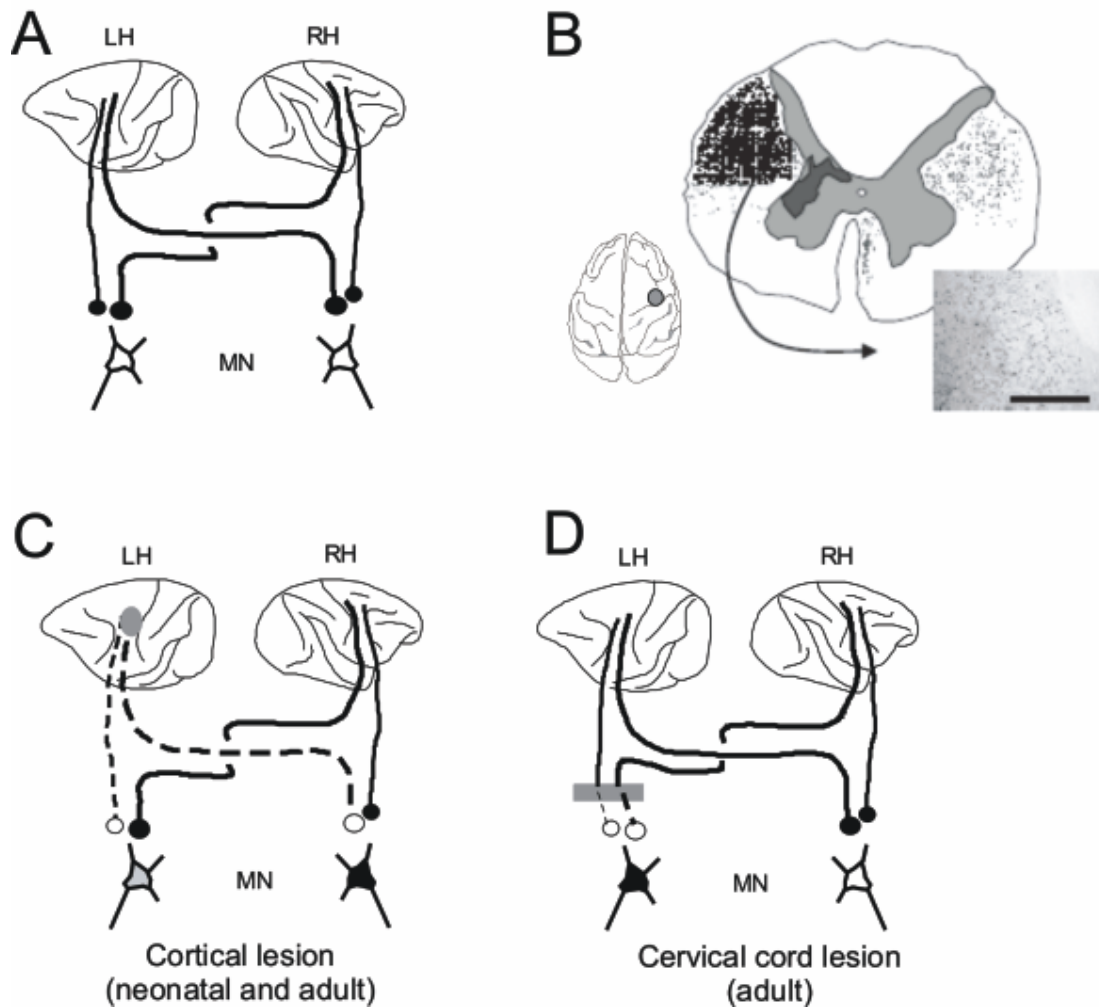


Fig. 1.18: Panel B shows the location of CS axons as seen at cervical level, after injection of BDA in the right M1 hand area forming a main contralateral component (the dorsolateral funiculus) comprising approximately 90% of the CS fibres and two ipsilateral components (10 % of the CS fibres), corresponding to the ipsilateral dorsolateral funiculus and ventral funiculus. Note the presence of some ventral contralateral fibres. As a consequence, MNs are influenced mainly by CS axons from the contralateral cortex and, to a lesser extent, by ipsilateral CS axons (panel A). The MNs in white are completely unaffected MNs, grey MNs are partially affected and black MNs are completely de-afferented CS inputs. Panel A: CS projections in an intact animal. Panel C: as a result of unilateral cortical lesion in M1 in the left hemisphere (LH), there is a dramatic loss of CS input on contralateral MNs (black), whereas the ipsilateral MNs (grey) are only deprived of the minor ipsilateral CS input. Panel D: unilateral cervical lesion aimed at the dorsolateral funiculus. As a consequence, only the ipsilateral MNs are deprived of CS input. In spinal lesion, the whole supraspinal afferences are interrupted.

Cortical lesions:

Rouiller and Liu (1999) studied the consequences of unilateral destruction of hand area M1 identified with ICMS in macaque monkeys (as depicted in panel C of Fig. 1.18). The behavioural consequences on the precision grip were assessed by comparison with pre-lesion manual dexterity. A permanent lesion of M1 hand area was induced by ibotenic acid infusion, and this was followed by a dramatic paresis of the opposite hand. The paresis lasted two months and was followed by an incomplete recovery of manual dexterity, reaching a plateau after six months post-lesion at a level corresponding to a performance of 30% of the pre-lesion score. Reversible inactivation experiments established that the ipsilateral PM played a major role in the recovery (Liu and Rouiller 99; Frost et al 03), in line with other studies in human (e.g. (Seitz et al 98; Sawaki et al 03; Werhahn et al 03). Nudo and Milliken (1996) studied the functional consequences of an ischemic infarct of the motor cortex in squirrel monkeys. They used the ICMS technique to map the primary motor cortex before and after the cortical lesion and precision grip tests to evaluate the fine motor performances of the animals. They arrived to two important conclusions: first, the motor cortex adjacent to the lesion is capable of functional re-organisation in adult squirrel monkeys and, second the extent of the functional re-organisation depends on the regular motor training occurring after the cortical infarct. A few days after the unilateral cortical lesion, they observed a dramatic loss of function of the contralateral hand with a good level of recovery of function around 60 days after the lesion (Nudo and Milliken 96; Nudo et al 96b). In human patients, a study showed that stroke in focal subcortical area just above M1 induced a reorganisation of the premotor cortex ipsilateral to the lesion. The patients showed a good motor recovery, which can be attributed to this reorganisation (Fridman 2004).

Pyramidal lesions

The recovery for postural and proximal limb movements is generally rapid and complete after a bilateral pyramidotomy. Manual dexterity as assessed by precision grip reappeared, but the time necessary to develop effective grip force increased (Hepp-Reymond 82). In another model of pyramidal tract lesions, when particular care was taken to limit the lesion to the pyramidal tract on both sides, the lesioned monkeys were able to sit, stand and climb, they had synchronous locomotion but they did not fully recover independent movements of the fingers. In this study, the animals subjected to bilateral lesion limited to the pyramidal tract, recovered weakly their manual performances several weeks post-lesion. At that time point, a certain closure of the fingers could be seen in attempts to catch food with the hand. Animals with unilateral pyramidal lesions showed no impairment of the hand contralateral to the lesion, while the ipsilateral hand showed a better recovery than the animals subjected to bilateral pyramidal lesions. (Lawrence and Kuypers 68b). In an other study investigating pyramidal lesions in sub-human primates, Schwartzman qualitatively evaluated the behavioural consequences of an unilateral pyramidal lesion in macaque monkeys. Two animals were subjected to complete transection of the left pyramid and showed an immediate paresis of the precision grip of the ipsilateral hand, with a remarkable recovery starting already 6 weeks post-lesion. After 3 years post-lesion, the animals showed no remarkable paresis of the ability in the hand ipsilateral to the lesion (Schwartzmann 78).

Cervical lesions:

Cervical hemisections of the spinal cord in primates were studied by Holmes in 1909. In rhesus macaques subjected to complete hemisection of the first cervical segment of the spinal cord, he observed a considerable reduction in the number of giant cells in the motor cortical layer

V, whereas between a third and a half of the number of the cells remained present; he concluded to certain shrinkage of the Betz' cells affected by the lesion.

Hemi-section of the spinal cord and pyramidotomy are considerably different: a unilateral lesion at pyramidal level interrupts CS fibres coming from the motor cortex of one hemisphere, whereas a spinal hemi-section has more complex consequences: it affects crossed CS projections from the opposite motor cortex and the uncrossed CS projections from the homolateral motor cortex, as well as other tracts like the rubrospinal and the reticulospinal tracts, the ascending sensory tracts and even the propriospinal system, but it does not affect the undecussated CS axons originating from the opposite motor cortex. As very few remaining axons may be sufficient to induce a noticeable recovery of function, some of these remaining uncrossed CS neurones (up to 10 %) may cross the midline below the lesion and recruit the deafferented motoneurons to improve the control exerted by the motor cortex contralateral to the spinal hemisection. A study in new born and juvenile macaque monkeys subjected to spinal hemisection at C3 level reported a dramatic loss of function in a manual dexterity task, though transient (Galea and Darian-Smith 97a; Galea and Darian-Smith 97b). The monkeys were trained to perform a prehension task using the precision grip between the thumb and the index finger to retrieve a small piece of food with a certain force. Immediately after the lesion, a severe flaccid hemi-paresis affecting the forelimb took place. Within 60 to 90 days after the spinal lesion, a remarkable recovery of function occurred in the hand directly affected by the cervical hemisection, although some behavioural deficits persisted, such as loss of the pre-shaping prior grasping and a weakening of the muscles implicated in the opposition between thumb and index finger. The hand contralateral to the lesion remained normal, with comparable scores compared to the period before the cervical lesion.

The modified trajectories of movement can be due to a change of strategy resulting from the paresis by using less affected muscles groups. In accordance with the observation of a

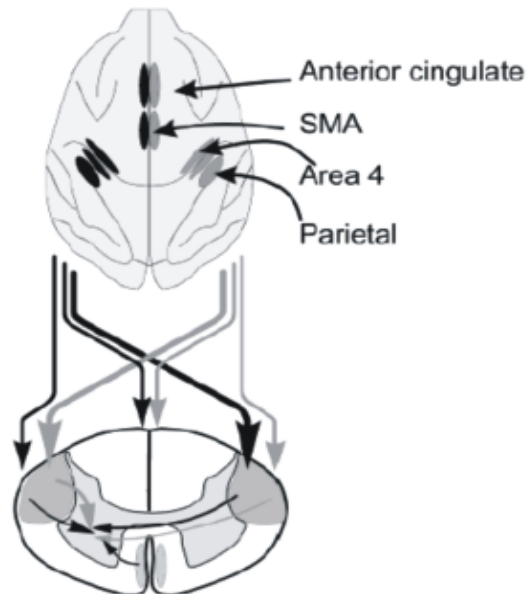
dramatic reduction of CS projections to the spinal cord caudally to the lesion, the functional recovery was believed to be due to the enhancement of the transmission of information through the remaining fibres rather to a regeneration or substantial reconstruction of the lesioned CS projections.

A change of strategy to perform the task can also explain the noticeable recovery of function. In the lesioned monkeys, an incomplete recovery of hand function started already 30 days after the lesion, and after another 30 days, the recovery of manual dexterity, although incomplete, was observed (Galea and Darian-Smith 97a; Galea and Darian-Smith 97b). The explanations for the partial recovery of precision grip ability after cervical hemisection are presented in Fig. 1.19. This drawing summarizes the intact remaining CS pathways expected to play a crucial role in recovery.

In a recent study, Alstermark and colleagues analysed in what extent the contribution of non-monosynaptic pathways could play a role in the recovery mechanisms in monkeys subjected to cervical cord hemisection at C4-C5 level. Electrophysiological recordings post-lesion showed disynaptic volleys interpreted to go through the C3-C4 propriospinal system and were interpreted as strongly participating to the functional recovery, occurring already a few days after surgery (Sasaki et al 04). The authors have not mentioned the fact that the delay measured in the motoneurons after stimulation of the motor cortex and attributed to the disynaptic propriospinal system left intact in the ventral part of the spinal cord could possibly be due to the lower velocity of conduction of action potentials along slow CS fibres.

In Galea's study on cervical lesion in macaque monkeys, the analysis of the data obtained with labelling of corticospinal neurones showed that a small amount of CS axons re-crossed the midline at cervical level and therefore could play a role in the recovery of manual dexterity after unilateral cervical lesions of the CST (Galea and Darian-Smith 97a).

A. Corticospinal projections with terminals in the left spinal cord



B. Spread of endings of corticospinal axons spared by left cervical 'hemisection'

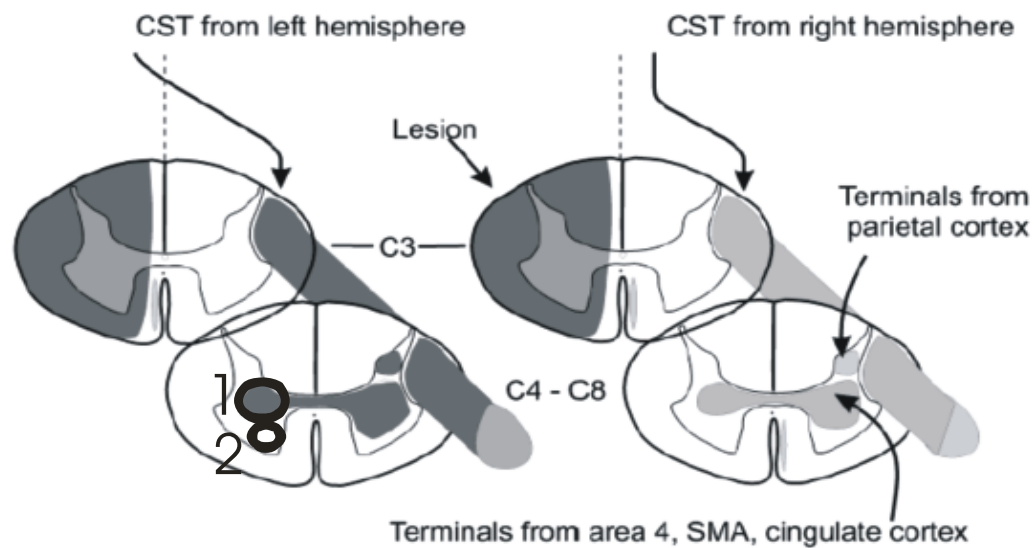


Fig. 1.19: A: Distribution of terminals of anterogradely stained CS fibres in the cervical spinal cord. The left motor cortex and its projections are represented in black and the right motor cortex and its projections are represented in grey. B: Summary of the distribution of CS fibres terminating in the grey matter of the cervical spinal cord after hemisection. Left: decussating axons from left hemisphere. Right: distribution of axons from the right hemisphere. Note the localisation of lamina VIII (1) and lamina IX (2) (adapted from Galea and Darian-Smith, 1997a).

1.3.2: Physiopathology of the spinal cord lesions

Lesions of the central nervous system result in permanent consequences in adult mammals. Histological analysis after traumatic injury shows that the normal neural tissue is replaced by a scar made of neo-formed fibrous network, and sometimes by a fluid-filled cyst.

The consequences of a spinal cord injury (SCI) depend on the extent, the location, the spinal level and the nature of the injury. In human patients, the vertebral canal is rigid and does not allow elastic compensatory volume absorption in case of an oedema following the inflammatory processes. In our study, the laminectomy absorbs a part of the increased pressure due to the oedema. A concussion of the spinal cord is a transient functional depression of the cord without anatomical damage. In contrast, a contusion of the cord results in a permanent deficit.

The primary injury is the mechanical impact, represented in the present study by the lateral transection of the spinal cord with a surgical blade. The secondary injuries that take place are vascular alterations that occur immediately, followed by biochemical alterations from minutes to hours. Then from hours to weeks after the injury, the cellular processes consisting in inflammation and apoptosis take over and finally there is a disturbance of the fibre tract through de-myelination, Wallerian degeneration and scar formation (Bareyre and Schwab 03).

The dynamics of spinal cord injury is triphasic: an acute phase occurs immediately after the injury followed by a sub-acute phase made of reactive gliosis with a local increased number of astrocytes and a late-phase, lasting from weeks to months after the injury.

Acute phase:

The acute phase starts with an alteration in the microvasculature of the central grey matter. The necrotic alterations quantitatively increase in the grey matter in the first hours after injury. The erythrocytes penetrate in the area adjacent to the central canal. The posterior part of the grey matter is often free of lesions, except in our case where the site of injury itself is the left

posterior part of the spinal cord. The ischemia that follows induces cell death. The disruption of the walls of the blood vessels results in vasogenic oedema reaching its maximum in the first days after injury and increases the local compression of the nerve fibres of the spinal cord. An unbalanced ionic equilibrium in the neural environment, calcium in particular, can also modify the excitability of surviving neurones.

An important inflammatory process increases the oedema formation by releasing inflammatory mediators in the extracellular liquid that increase the permeability of the blood vessels and the oedema. All these events are called the secondary injury. In human patients, a treatment applied immediately after the spinal cord injury consisting in the administration corticosteroids decreases these effects and limits to some extent the subsequent damages to the neural tissue.

The Wallerian degeneration is the degeneration following axotomy and results in the distal formation of retraction's bulb. The axon loses its myelin sheath and small axons are affected before larger ones. The fragments of myelin are phagocytosed by the macrophages. Most part of the histopathological findings derives from rodent models, but the main consequences such as necrosis have also been observed in primates.

Sub-acute phase:

The sub-acute phase consists of the inflammatory response to the first phase. One or two days after the injury, an increased number of astrocytes results from proliferation of the cell population (including Schwann cells, meningeal cells and fibroblasts) but these cells are neurophysiologically inactive. Their function seems to be the phagocytosis of cellular debris of damaged neurones (Schwab and Bartholdi 96).

Long-term phase: weeks to months after injury

Late lesions are accompanied with loss of myelin sheaths in the white matter, and often terminate with a fluid-filled cyst, surrounded by white matter tissue. Astrocytes accumulate at the margin of the lesion and form a scar separating the wound from the intact spinal cord. Three weeks after the lesion, Wallerian degeneration occurred, particularly in the larger diameter axons.

Remyelination of axons has been observed but had the following two properties: the distance between Ranviers node was particularly short, and the myelin sheaths were particularly thin. After 1 month, the majority of axons showed abnormal thin sheaths, a state that was present up to 3-6 months post injury.

The lesion scar

The major cells responsible for the scar are the astrocytes, in cooperation with secondary cell types like microglial cells, macrophages and other inflammatory cells. The scar in the spinal cord is characterised by the presence of hypertrophic astrocytes. They are located between the dense network of intermediate filaments and the necrotic and intact tissue. The scar is more prominent in adult tissue than in immature CNS. The scar has been described as a “physiological stop pathway” and not only as a physical impedimentum through its great density of intermediate filaments, suggesting an active inhibitory role of the scar.

Apoptosis

In a study focusing on apoptosis of neurones in monkeys following spinal cord hemisection at thoracic 1 level, a certain number of apoptotic cells were counted a week after the lesion on rostral and caudal sections from the lesion site. But these apoptotic cells were not

localised in the funiculus dorsolateralis containing the CST axons, the RST or the reticulospinal tract, but rather in the ascending pathways (Crowe et al 97).

1.4: Functional recovery

After lesion of the spinal cord in mammals, neuronal mechanisms involved in functional recovery include recuperation from spinal shock, re-myelination and spontaneous sprouting of axons. There are two levels of recovery : i) at the cortical level with colonisation of neighbouring areas unaffected by the lesion, ii) recovery at the lesion site including compensatory sprouting (Raineteau et al 02), and iii) sprouting remote from the lesion. These are so to say the anatomophysiological correlates of functional recovery. Other extrinsic factors can not be excluded even though they are difficult to evaluate. For example, the impact of every day training to perform a stereotyped task; the animal has then the opportunity to associate other possible movements with the rigidity of the affected muscles in a change of strategy that at term can be enhanced (see e.g. (Nudo et al 96b).

Plasticity

It is well known that the cortical functional organisation is highly plastic, even in adult mammal, in relation to use and/or injury. Several external events are at the origin of cortical plasticity (including functional reorganisation), such as learning, practice, cortical injury, spinal cord injury, peripheral injury (e.g. limb amputation (Schieber and Deuel 97).

In our model of unilateral cervical spinal cord lesion resulting from interruption of the dorsolateral funiculus, functional recovery can result from the recruitment of pathways not used normally (and spared by the lesion), or through newly established pathways. In the latter case, one can imagine a regeneration of the transected axons or a compensatory sprouting, taking place in the rubrospinal, reticulospinal or vestibulospinal projections, in case of their incomplete

interruption, or in recruitment of various components of the corticospinal tract spared by the lesion, as proposed by Galea and Darian-Smith (1997 a). In addition, a possible role played by the long propriospinal pathway has been demonstrated in the rat after spinal cord lesion (Bareyre, F. M. et al., 2004) and was also postulated in the monkey after C4-C5 hemi-section (Nudo et al 96a).

1.4.1: General considerations

In primates, a partial hemi-section of the spinal cord at cervical level made in juvenile monkeys (C3 level) resulted in an immediate severe hemi-paresis of the limb ipsilaterally to the lesion. A good general recovery of function was observed already 30 after the lesion, but a residual impairment persisted, described as slower precision grip movements and a defect in the pre-shaping (Galea and Darian-Smith 97b). Different mechanisms are involved in recovery of function in untreated animals subjected to SCI: cortical reorganisation, spinal reorganisation, compensatory sprouting. In addition, changes of behavioural strategy were observed in primate to compensate the neuronal deficit following a CNS lesion (Friel and Nudo 98). The recovery of function can also be mediated through plastic changes and sprouting in the lesioned spinal cord. Remaining fibres can produce, even caudally to the lesion, a compensatory process that mediates supraspinal information to the denervated motoneurons (Schwab and Bartholdi 96).

1.4.2: Cortical mechanisms involved in functional recovery: Plasticity

In their study of the somatotopical organisation of M1 in great apes, Leyton and Sherrington first described the “functional instability of cortical motor points” that can be defined now as cortical plasticity (Leyton and Sherrington 17). Nudo and colleagues performed a cortical lesion in the hand area identified through ICMS technique as responsible for hand movements in squirrel monkeys. The lesion was produced by a micro coagulation of blood vessels entering in the motor cortex. They observed an immediate deficit of the opposite hand

followed 4-5 months after the ischemic infarct by a noticeable functional recovery of hand movements. They attributed this recovery of function mainly to the reorganisation of primary motor cortex (Nudo and Milliken 96). A better recovery was obtained if rehabilitative therapy based on precision grip training took place (Nudo et al 96b). Liepert and colleagues investigated the cortical mechanisms responsible for a functional recovery in human patients suffering from stroke in the motor cortex. They observed that, in these patients, intracortical inhibition was reduced as compared to healthy subjects (Liepert et al 00).

1.4.3: Other pathways involved

1.4.3.1: Rubrospinal pathway

In their model of bilateral pyramidotomy in monkey, Lawrence and Kuypers attributed to some extent the functional recovery to the role played by the rubrospinal tract, involved in finger movements (Lawrence and Kuypers 68b). In their study, macaque monkeys were first subjected to complete bilateral pyramidal lesions, and in a second phase, a first group of animals was subjected to an unilateral lesion of the so-called medial system (vestibulospinal tract, reticulospinal tract mainly) and a second group of animals was subjected to a unilateral lesion of the lateral system (rubrospinal tract). The first group showed a much weaker effect of the second lesion on the manual dexterity, compared to the group of animal with an interruption of the rubrospinal tract.

1.4.3.2: Reticulospinal pathway

In a study performed by Saruhashi and collaborators (1996) on spinal injured rats, the possible role played by serotonergic (5HT) pathway in functional recovery was investigated. The authors noticed the presence, 3-4 weeks after lumbar hemisection of the spinal cord, of 5-HT

fibres crossing the scar which were believed to contribute, at least in part, to the locomotor recovery observed ipsilaterally (Saruhashi et al 96). In their study on primate hemisection of the cervical cord, Galea and Darian-Smith (1997 a) attributed a substantial part of the functional recovery of the precision grip in the lesioned monkeys to the remaining fibres of the reticulospinal tract spared by their model of lesion (Galea and Darian-Smith 97b).

1.4.4: Role of Propriospinal neurones in functional recovery after spinal cord injury (SCI)

A recent study (Bareyre et al 04) showed that long propriospinal neurones played a crucial role in functional recovery of function after spinal cord lesion. After thoracal hemisection of adult rats, the number of long propriospinal axons increased and penetrated in the white matter of the spinal cord to reach their target located caudally to the spinal lesion. Surprisingly, a peak of sprouting has been noted 3 weeks after the SCI, followed by a light decrease up to 12 weeks after SCI. Electrophysiological assessment of this pathway showed a longer latency of EMG recordings in SCI rats, in comparison to the sham group of animals.

1.5: Regeneration in the central nervous system (CNS)

1.5.1: Introduction

Classically, consequences of injury to the CNS of adult mammals were considered to be permanent because of the inability of CNS neurones to regenerate their functional axonal and dendritic connections, in contrast to the peripheral nervous system. This inability of injured neurones to regenerate in the CNS is not predominantly due to an intrinsic deficit of self regrowth possibilities but mainly due to growth inhibitory environmental factors. Several conditions are needed to allow regeneration of CNS neurones after traumatic injury: first, the

survival of the neurone itself and, second, the extension of the sectioned axon to the right target, and then the re-myelination and formation of functional synapses. All these steps are possible targets for experimental enhancement of regeneration (Horner and Gage 00).

Inhibitory environment:

Regeneration of axons is normally inhibited by the gliotic scar. Indeed, the application of chondroitinase in the medium enhanced the regeneration of axotomised neurones. The chondroitinase is an enzyme that digests certain components of the fibrous tissue of a scar and allows a better regeneration of injured axons by decreasing the mechanical barrier. In addition, the growth cone at the distal end of an axotomised neurone of the CNS collapses in contact with oligodendrocytes' myelin. The several methods needed to prove actual regeneration of functional nervous structures are shown in Fig. 1.20.

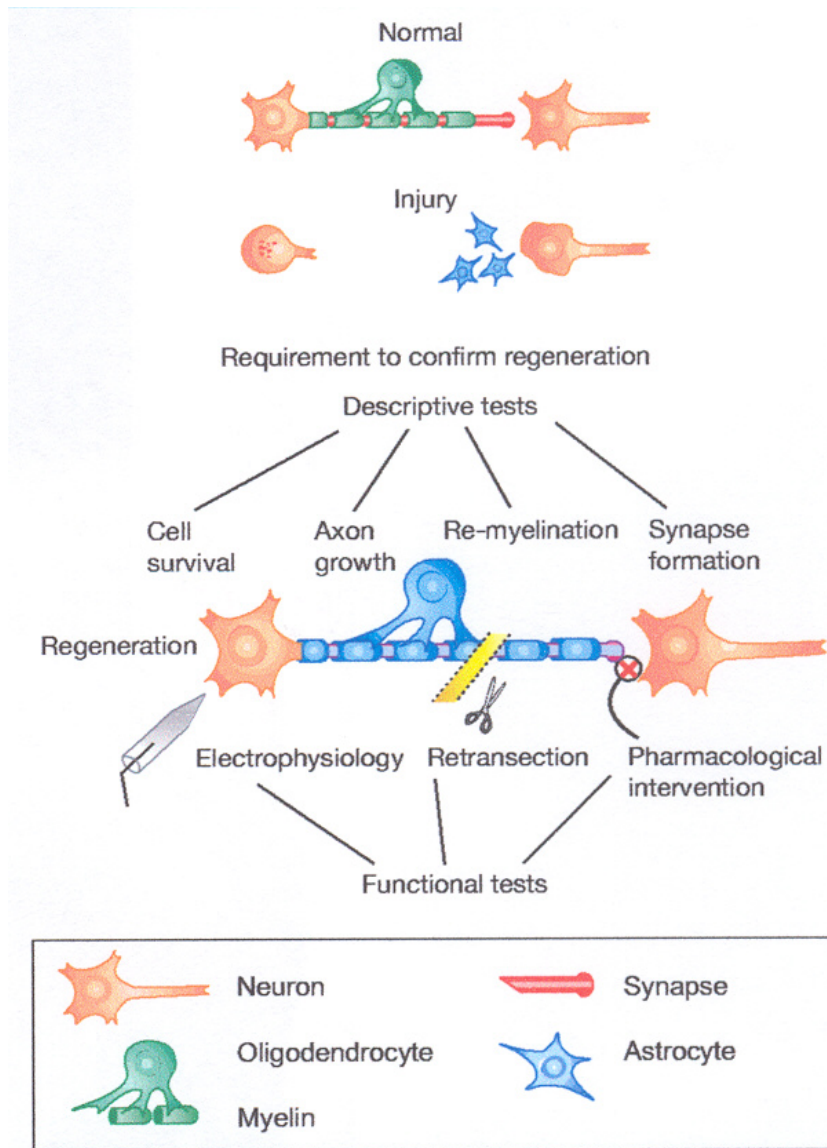


Fig. 1.20: Drawing summarising the required events to confirm regeneration after CNS axotomy. Different tests to confirm if there is regeneration or that the observed functional recovery is due to sprouting are presented (adapted from Horner, P. J. et al., 2000).

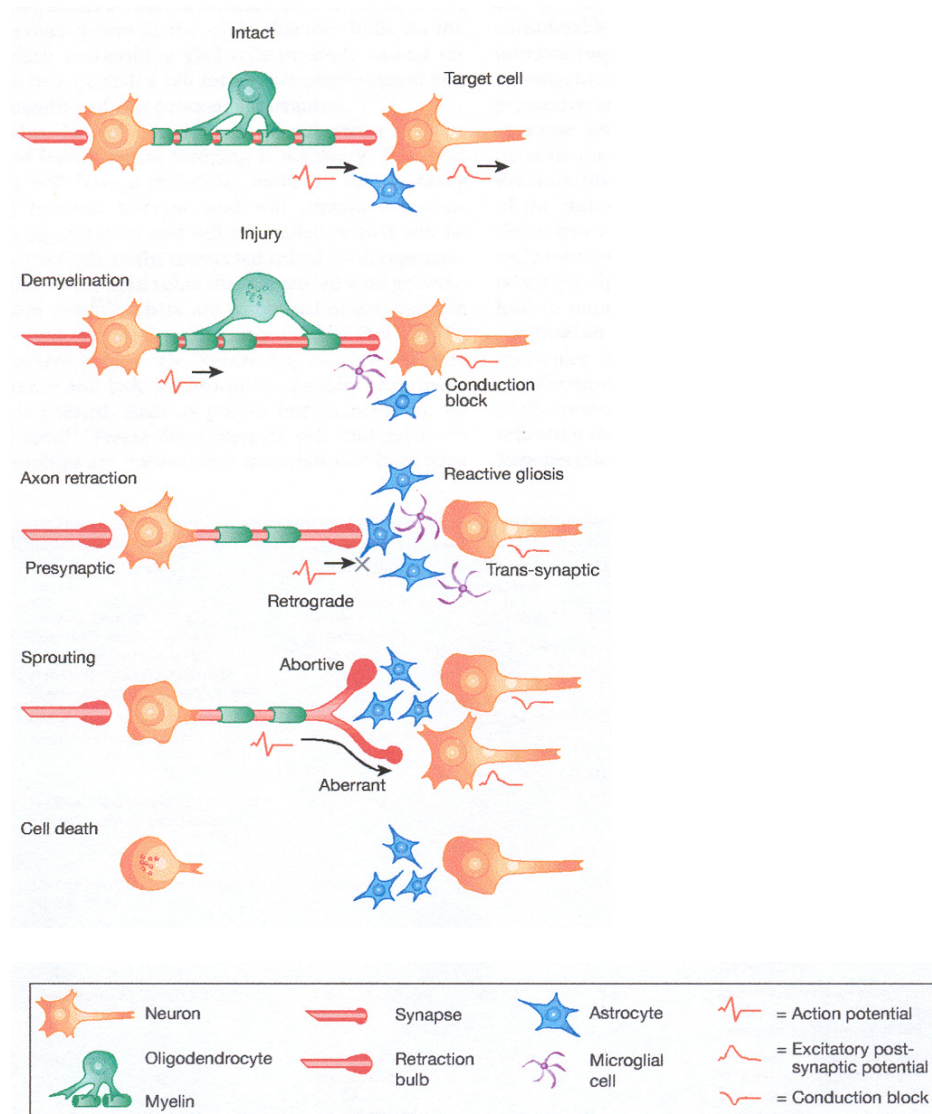


Fig. 1.21: Summary of the different events that can occur after axotomy of CNS neurones (adapted from Horner, P. J. et al., 2000).

In severe cases of lesion to CNS axons, no repair occurs. The result is a de-myelination of the axon, its retraction leads to a loss of trans-synaptic transmission of information. In surviving neurones, sprouting can occur, resulting in renewal of synaptic connections, when possible (absence of scar, short distance between axon and target), the very last event being of course cell death (Fig. 1.21).

1.5.2: The history of attempts to approach of CNS regeneration

The first related observation of CNS regeneration in adult mammals was made by Aguayo and David in the early eighties. They showed in SCI rats a regeneration of axons within a peripheral nerve implanted with auto-graft technique making a sciatic nerve “bridge” from the medulla oblongata and a more caudal part in the spinal cord (Fig. 1.22 A). They observed that HRP-stained axons originating from the CNS appeared up to 30 weeks after implantation in an environment consisting of PNS (Fig. 1.22 B). In other words, CNS axons can grow in an environment made of Schwann cells instead of oligodendrocytes, but they stopped their growth when arriving in contact with CNS environment, made of oligodendrocytes ; (David and Aguayo 81; McGee and Strittmatter 03).

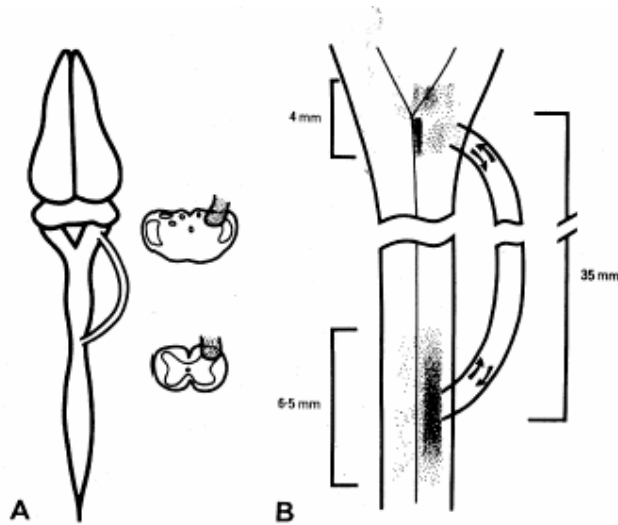


Fig. 1.22: This figure presents the results of the first proven growth of axons of central nervous system in adult mammals in a peripheral nervous system environment. Panel A shows the origin and insertion of the peripheral nerve bridge, providing a permissive environment in which CNS axons can grow. The resulting staining of fibres is shown in B (adapted from David, S. and Aguayo A. J., 1981).

1.5.3: Different approaches to CNS regeneration

Since the discovery of the possible enhancement of regeneration of neural tissue after CNS injury, two main directions of research have been followed: first to promote directly regeneration of axotomised neurones and, second, by decreasing the inhibitory effect of the CNS environment on axonal growth.

1.5.3.1: Direct approach: Promote the regeneration

These approaches consist in the replacement of the damaged or lost neural cells, with new potent cells coming from, for example, differentiated stem cells, or by replacement of damaged white matter by using bridges made of peripheral nerve grafts or an artificial matrix. In the case of the destruction of the soma of motoneurons in the cervical spinal cord, no regeneration is possible.

Several techniques have been developed with the aim of cellular replacement, such as implantation of cultured stem cells or of Olfactory Ensheathing Glial cells (OEG) cultivated and re-implanted to promote axonal regeneration and to obtain functional recovery in spinal injured rats subjected to complete spinal transection (Santos-Benito and Ramon-Cueto 03). The OEG cells have been chosen for their remaining cellular division capacities in the adult mammals CNS.

Another approach to promote axonal regeneration in the adult CNS is the application of neurotrophic factors such as Brain Derived Neurotrophic Factor (BDNF) or other neurotrophic factors (mainly neurotrophines NT-3 and NT-4) at the site of the lesion after axotomy. There are reports, including in man, that other molecules normally present could play a neuroprotective role, like the erythropoietin, or could promote neurological recovery like methylprednisolone (MP). In a study made by Nash and colleagues in the rat, they associated these two strategies in adult rat subjected to spinal cord injury: implantation of OEG cells and application in situ of MP

(Nash et al 02). They observed in treated animals an increase of the elongation of axotomised axons, compared to the sham group of rats.

An interesting approach of enhancement of cortical function after lesion is the development in vitro of cultured adult cortical progenitor cells coming from pre-frontal cortex of primate that are re-implanted in CNS at the site of a cortical lesion made by micro-injection of ibotenic acid. Previous unpublished data show the survival of these re-implanted cells in vivo, the following step being the functional impact of these neurones on the enhancement of recovery of motor function (Brunet et al 03).

1.5.3.2: Indirect approach: suppression of the inhibitory growth environment

To balance the respective role of direct enhancement of regeneration using neurotrophic factors or the indirect strategy through the decrease of the growth inhibitory role of glial environment, Schwab and Thoenen (1985) made a study comparing directly these two possible mechanisms. They compared the growth ability of CNS neurones in culture by placing them in the middle of two bridges, one containing sciatic nerve explant (PNS) and the other, placed on the opposite side, containing optic nerve explant (CNS). The neurones they used were newborn rats NGF responding neurones. They observed first that no neurone grew in the optic nerve explant bridge whereas the sciatic nerve explant contained a high number of growing axons. Thus, they added NGF in the medium in both situations and they observed that axons in contact with the CNS environment (inside the optic nerve) could not be overcome by the outgrowth effect of NGF. This observation shows the extremely strong inhibiting effect of the glia of the CNS versus PNS and versus the known promotion of growth by NGF.

1.5.4: Regeneration in spinal cord

The immediate reaction of axotomised neurones is not to die but to exhibit an initial regenerative response, enhanced by the over expression of the Growth Associated Protein gene

(GAP-43; Fig. 1.23). These neurones are able to sprout locally, but not to elongate the axotomised axon on a long distance. After this unfruitful attempt to regenerate, the neuron switches to an atrophic state (Schwab and Bartholdi 96).

Sparing of function after incomplete spinal cord sections

As the spinal cord of higher mammals possesses its own organised neuronal structure, it is able to perform rhythmic activity such as walking or swimming with a very small percentage of remaining descending fibres that initiate the pattern generation. In cat studies, the neural networks located in the spinal cord also called central pattern generator (CPG) allows recovery of gait 2-3 weeks after complete spinal cord section at thoracic level. Two main components are involved in the recovery of locomotion in spinal cats: the locomotor pattern generator that is self-sufficient to produce rhythmic activity of motoneurons, associated with the sensory inputs that give important information to regulate the final output to the muscles (Bouyer and Rossignol 03).

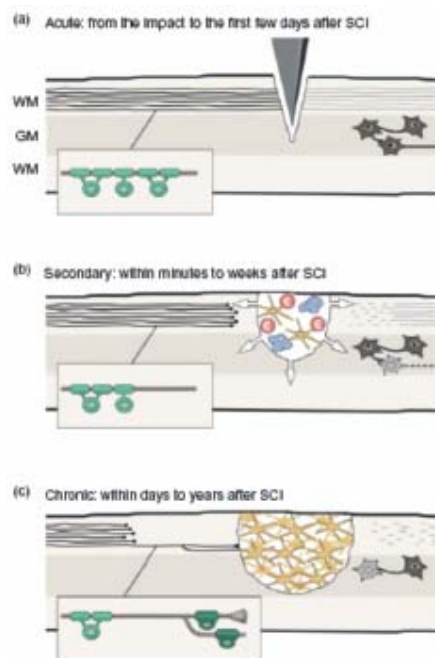


Fig. 1.23: Drawing summarising the different stages of histological deficits in the spinal cord after axotomy: A: acute events. B: The activation of the immune system takes place in the secondary phase as well as a down

regulation of myelin and loss of cytoskeletal proteins, symptom of cell death. In the chronic phase (C), the Wallerian degeneration of the distal axons took place. Simultaneously, GAP 43 is over expressed, showing an attempt of axonal regrowth. Dark green: Schwann cells, light green: oligodendrocytes, blue: macrophages, yellow: astrocytes, red: neutrophils, black: neurones.

1.6: Nogo: a myelin associated growth inhibiting protein

1.6.1: Identification of Nogo as a possible growth inhibitory agent

Two observations led to the concept that myelin was a possible inhibitor of neural tissue re-growth factor after injury in CNS adult mammals. The first observation was the regeneration of neural tissue in the PNS after injury, which was observed in the last century starting with Ramon y Cajal; the attempts to observe regeneration in adult mammals CNS remained unfruitful until Agayo and David's (1981) work in grafting peripheral nerve over injured spinal cord and the observation of a regeneration of CNS axons. The second observation was based on the observation that the regeneration of neural tissue present in newborn mammals, as their CNS fibres are still not myelinated.

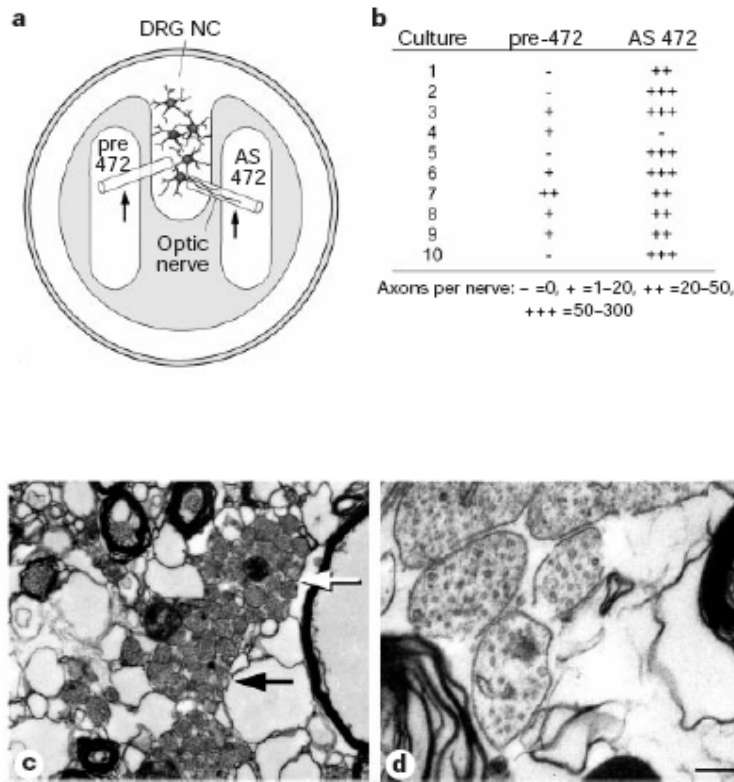


Fig. 1.24: This figure (a) represents the growth of neurites of dorsal root ganglion cells in presence of AS 472, that is an antiserum of rats directed against the Nogo-A peptide, in contrast to the absence of growth in a medium (pre-472) that does not contain this antiserum. The quantification of the number of axons per nerve from 10 similar experiments is shown in b and clearly demonstrates the enhancement of growth of neurite when the Nogo A peptide was neutralised. Microphotograph in c shows the presence of regenerated axon bundles (arrows) when AS 472 was injected and, in d, the regenerating axons in contact with myelin in the same conditions (adapted from Chen et al 00).

Three different directions have been investigated recently to assess quantitatively the growth inhibitory function of oligodendrocytes' myelin after CNS injuries: the first consisted in deleting the oligodendrocytes and the myelin in vitro from the medium, the second consisted in neutralising the growth inhibitory effect of myelin using a monoclonal antibody directed against Nogo, the myelinic protein that plays the major part of the inhibiting effect and, third, using mice or rats that have been auto-immunised with myelin and exhibited regenerative sprouting (Schwab 04).

Several myelin components have been identified to play an inhibitory role against regrowth of axons after injury in adult: the first identified component was Nogo but rapidly other molecules have been identified playing an additional role: Myelin Associated Glycoprotein (MAG), and the more recently identified Oligodendrocyte Myelin Glycoprotein (OMgp) (Filbin 03).

1.6.2: Molecular structure of the different forms of Nogo.

Three different molecular forms of Nogo have been identified: Nogo-A, Nogo-B and Nogo-C (Fig. 1.25). Nogo A is the longest isoform, with 1163 amino acids. It is mainly produced by oligodendrocytes in adult mammalian brain (Schwab 04). The functions of Nogo B, which is present in several types of tissue including adult neurons, and Nogo C, present in muscles, is not known. The protein Nogo A is largely present in the CNS and possesses two trans-membrane domains and an extra-cellular loop, indicative of a location in the membrane of oligodendrocytes. According to specific staining studies conducted by Brösamle and Schwab (2000) Nogo A acts on the neurones through membrane receptors called NgR, which is the plasma membrane receptor for the 66 aminoacid loop common to Nogo-A, -B and -C: Nogo-66 (Fournier et al 01). This NgR receptor mediates the inhibitory activity of Nogo-A and interacts with other myelin associated inhibitory proteins like the myelin associated glycoprotein (MAG) (Domeniconi et al 02), or oligodendrocytes and myelin associated glycoproteins (OMgp). A co-receptor to NgR called p75 interacts also with Nogo, MAG and OMgp (Wang et al 02); (Fig 1.26). The Nogo-66 membran domain has been identified as the major active part of Nogo (GrandPré et al 00). The transmission of the information to the nucleus of the neurone is made by the activation of the Rho A cascade (Fig. 1.26). The inhibitory effect of Nogo is shown in Fig. 1.26 in the two lower panels: on the left panel, a DRG neurone in presence of Nogo shows

extremely limited and short dendrites whereas on the right panel, another DRG neurone in presence of laminin shows greater amount and longer dendrites.

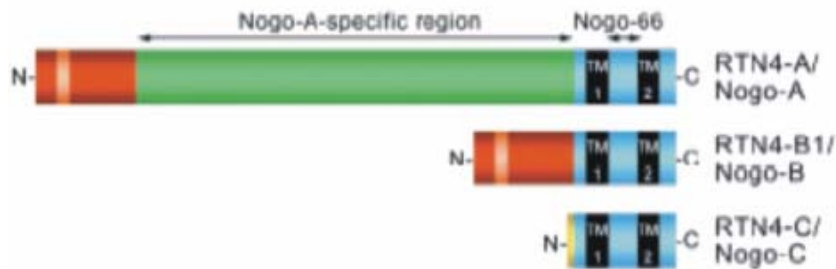


Fig. 1.25: Drawing representing the three isoforms Nogo A, B and C (adapted from Oertle and Schwab 03).

1.6.3: Function of Nogo A

Nogo-A is integrated in the myelinic membrane of the oligodendrocytes in the CNS and therefore has been identified after purification as one of the inhibitor of axon regeneration (Schwab and Caroni 88). The exact function of Nogo A in normal animals is still poorly understood whereas, after CNS injury, 2-3 particular domains of Nogo A are responsible for neurite growth inhibition, growth cone collapse and inhibition of fibroblast spreading (Schwab 04).

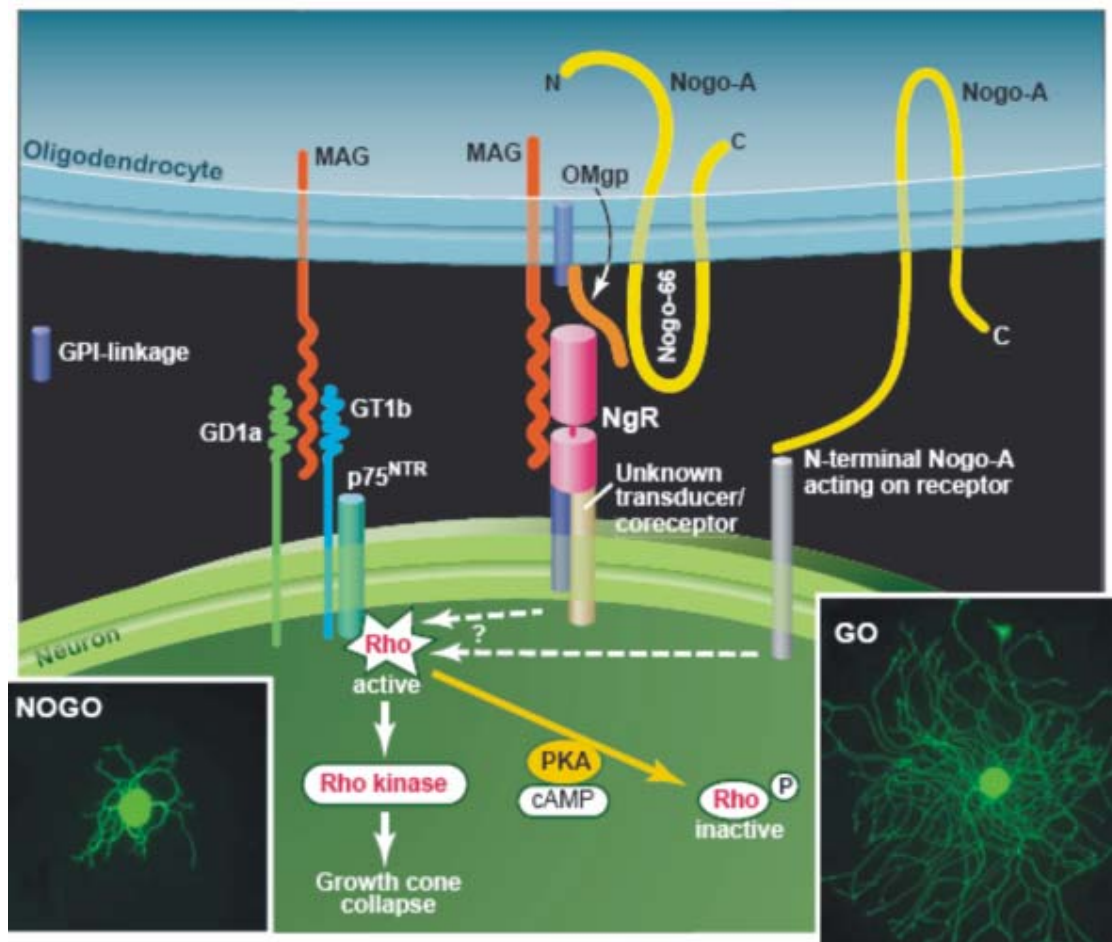


Fig. 1.26: Drawing representing the interaction between the three different transmembrane proteins of oligodendrocytes having an inhibitory role in neurite growth and the receptor NgR (in pink) of the neurones of central nervous system. Myelin Associated Glycoproteins (MAG) are in red, Oligodendrocyte Myelin Glycoprotein (OMgp) in orange and the 66 domain of Nogo A in yellow. Even if there are two pathways or more outside the cell in the Myelinic protein and the receptor, all seem to interact through the Rho kinase cascade inside the neurone, leading to an inhibition of neurite growth (adapted from Woolf and Bloechlinger 02).

1.6.4: Blocking the activity of Nogo with a monoclonal antibody

Two approaches to block the activity of Nogo have been investigated. First, using a monoclonal antibody (e.g. IN-1) that recognises and inactivates Nogo. Second, by applying a competitive inhibitory molecule that interferes at the receptor of Nogo on the oligodendrocyte membrane and thus prevents the effect of Nogo (GrandPré et al 02). A third method, based on the molecular biology technique, is to produce strains of mice that are Nogo- deficient, which

resulted in the observation of no regeneration of severed axons. This technique is controversial, as it does not take into account the compensatory mechanisms of the CNS to allow a “normal” neurologic development of the animal (Zheng et al 03).

The inactivation of Nogo results from the interaction between Nogo and its specific monoclonal antibody (IN-1 see below) that recognises and binds the extracellular part of Nogo-A. It ends in the internalisation of the complex of Nogo and the monoclonal antibody, captured in an intracellular vesicle. It is important to note that no compensatory mechanism expressing a greater amount of Nogo after its neutralisation by the monoclonal antibody in the oligodendrocytes has been observed (Dodd, unpublished data).

Two main effects of Nogo inactivation have been observed: the regeneration of axotomised neurones and a generally enhanced plasticity of the remaining intact neurones. Chen and colleagues (2000) replicated the experiment of Schwab and Thoenen (1985) consisting in comparing the growth of dorsal root ganglion neurones (DRG) in PNS environment versus CNS environment *in vitro*. With the same protocol (Fig. 1.24), they compared the growth of DRG axons in two optic nerves (CNS environment), one treated with a pre-immuserum or pre-472 (Fig.1.24a left) and one treated with the anti-Nogo antibody AS-472 (Fig. 1.24 right). Their results showed the positive effect of AS 472 on the growth of DRG axons also in the presence of CNS environment (optic nerve). The results obtained in ten similar experiments are presented in Fig. 1.24 B and shows that in nine out of ten experiments AS-472 enhanced the growth of DRG axons over several millimetres, whereas only one out of ten experiments with pre-472 shows a positive effect. Brösamle and colleagues compared the anatomical consequences of a lesion of the corticospinal tract in two groups of rats: a control group and a group treated with the monoclonal anti-Nogo antibody (Schnell and Schwab 90; Schwab and Schnell 91; Schnell and Schwab 93; Bregman et al 95; Thallmair et al 98; Raineteau et al 99; Wenk et al 99; Brösamle et al 00). The histological reconstruction of longitudinal sections of the spinal cord around the

lesion site shows an impressive elongation of CS fibres in the group of anti-Nogo treated animals (Fig. 1.27), on a distance of several mm in case of maximal regeneration (Fig. 1.28), whereas no elongation of severed axons was observed in the control group (Figs. 1.27 and 1.28).

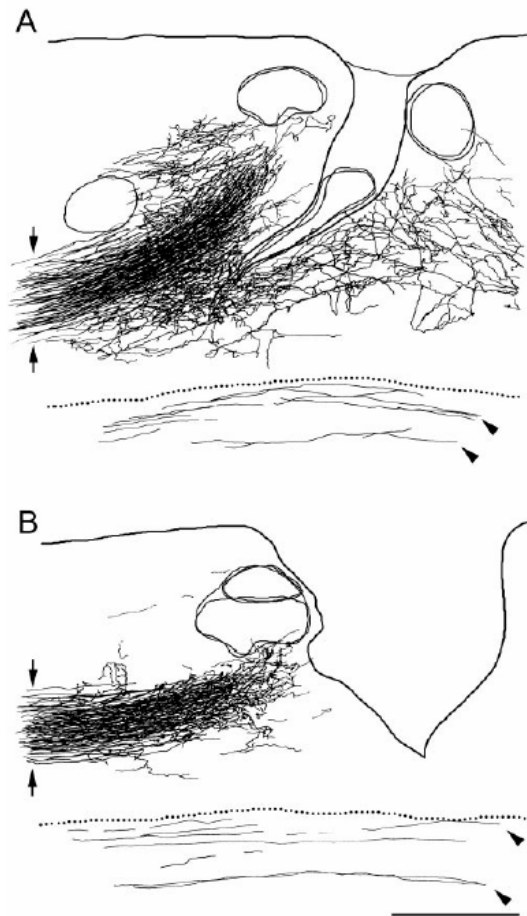


Fig. 1.27: Reconstruction of a few adjacent saggital sections of rat spinal cord in two rats subjected to a spinal lesion using camera lucida. In A, the animal has been treated with IN-1 directed against Nogo A, while in B the animal received the control inactive antibody. Note that in B, the stained CS axons do cross or turn around the lesion to migrate distally on several millimetres, in contrast to the untreated animal (B). Resulting cysts in the scar can be seen (adapted from Brösamle et al 00).

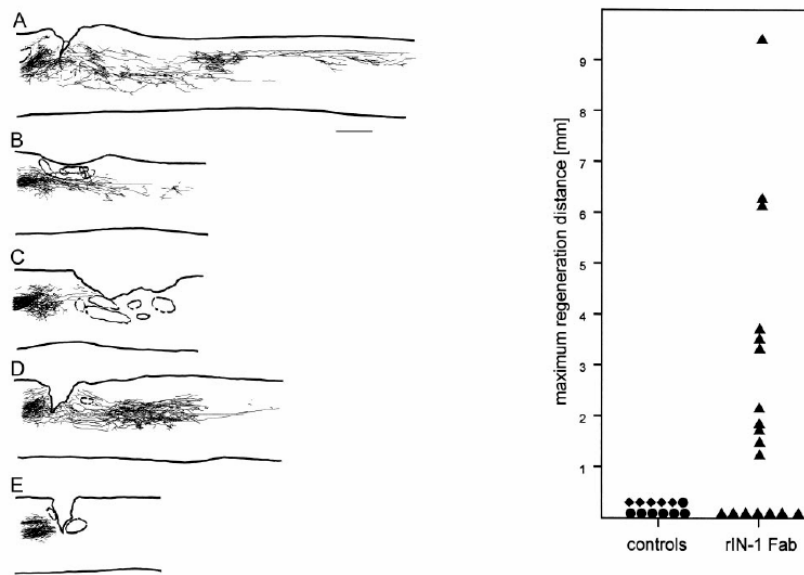


Fig 1.28: Left: Reconstruction from photomicrographs showing in 5 rats that regenerated CST fibres can growth over a long distance. Right: length of regenerated CST axons in different spinal cord injured rats, control versus treated (rIN-1 fab) rats. Scale bar in A: 1mm. (adapted from Brösamle C. et al., 2000).

The conclusions of these studies are that rats subjected to spinal cord injury resulting in large axotomy show consistent signs of regeneration of CNS neurones over a long distance when treated with the anti-Nogo antibody, in comparison to control animals with the same type of lesion without any treatment. A further step needed to conclude to regeneration would be to observe synaptic connections between the elongated axotomised axons and their neuronal target. Fig. 1.29 shows the consistent arborisation of the CST axons after anti-Nogo treatment (low magnification A and B) and the presence of varicosities at higher magnification (arrow heads in C-F) that strongly resemble to pre-synaptic *boutons* (G).

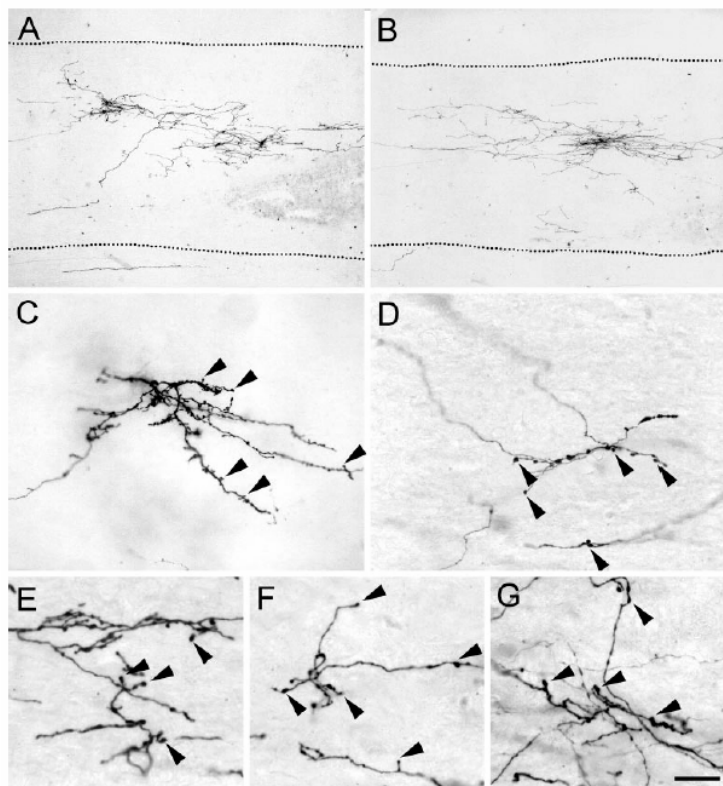


Fig. 1.29: Photomicrographs showing in A and B the arborisation of regenerated CST fibres caudally to the spinal cord lesion. Higher magnification in panels C-F of these arborisations showing a large number of varicosities (arrowheads) that could be synaptic *boutons*. At even higher magnification (G), the authors conclude that these varicosities are presynaptic *boutons*. Scale bar: In A-B: 250 μm , in C-F: 30 μm and in G: 15 μm . (adapted from Brösamle et al 00).

In a study made in rats subjected to bilateral transection of the CST and treated with the anti Nogo antibody IN-1, Raineteau and colleagues (2002) observed a reorganisation of the termination of RST fibres in the ventral horn of the cervical spinal cord. These terminations made close appositions to retrogradely stained motoneurons of Rexed lamina IX (Fig. 1.30). Microstimulation of the RST confirmed the functional reorganisation of the RST (Raineteau et al 02). In a previous study, Blöchlinger and colleagues investigated the reorganisation of motor fibres in rats subjected to unilateral transection of the CST and treated with the same anti-Nogo antibody IN-1. Using electron microscopy, they found an increased sprouting of corticobulbospinal fibres crossing the midline associated with the new formation of synapses in the treated group of animals, whereas no such synapses were found in a control group (Blöchlinger et al 01).

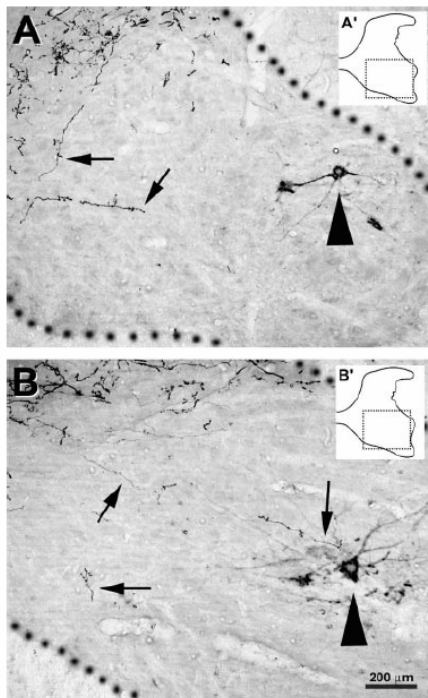


Fig. 1.30: Photomicrographs showing the penetration of the rubrospinal tract fibres in the ventral horn of the spinal cord in rats treated with the IN-1 antibody. Here are shown the invasion in the medial position to the proximal population of motoneurons, in A at C6 level and in B at C7 level (adapted from Raineteau et al 02).

1.6.5: Strategy developed to inactivate NOGO in situ and in vivo or how to deliver IN-1 with maximum efficacy

The first approach consisted of implanting at the lesion site, a capsule containing genetically modified hybridoma cells which produce in situ the IN-1 antibody (Z'Graggen et al 98). To have a better control over the delivery of the antibody in situ regarding the concentration, the total amount of antibody delivered and the duration of the treatment, the second approach consisted in temporarily implanting an osmotic pump containing the antibody and connected to the lesion site with a tube delivering the antibody at a constant rate.

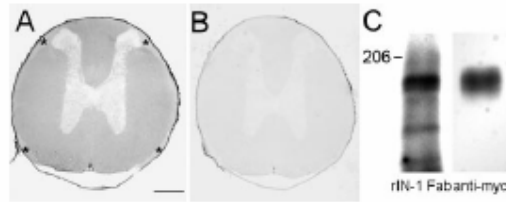
Close interaction between Nogo and IN-1:

Fig. 1.31: Photomicrographs showing in panel A the distribution of IN-1 antibody in the spinal cord and, in panel B, the distribution of a control secondary antibody that does not stain the section of the spinal cord. In panel C, a Western Blot experiment shows the great analogy between IN-1 protein and Nogo A when Nogo A is combined with a bacterial protein that shows the same band as IN-1. Scale bar: 300 μ m (adapted from Brösamle et al 00).

Figure 1.31 shows in panel A that, after specific staining, IN-I is homogenously and largely distributed in the spinal white matter of adult rats, whereas in panel B, the control secondary antibody is not significantly stained. In panel C, the correspondence between the two columns demonstrates the high specificity of recognition between the complex Nogo-A and IN-1 on the left and Nogo-A combined with a bacterial protein on the right side (Brösamle et al 00).

1.6.6: Improvement of motor performance in rats treated with Anti-Nogo A antibody

The anatomical observation of regenerated axons is not sufficient in itself to improve the functional recovery, since re-establishment of synapses to the right target is required. Several studies using different methods of inactivation of Nogo A in adult rats and analysing the functional recovery of locomotion observed a clear improvement of function, quantified by the BBB score (Merkler et al 01; GrandPré et al 02; Kim et al 03). An important electrophysiological study showed a clear improvement of function in rats subjected to complete thoracic spinal cord section and treated with the IN-1 antibody in comparison with animals treated with an inactive antibody. The EMG recordings (Fig. 1.32) show a clear recovered typical alternation of

excitation of the motoneurons responsible for locomotion in IN-1 treated animals (Fouad et al 01; Merkler et al 01).

Control mAb

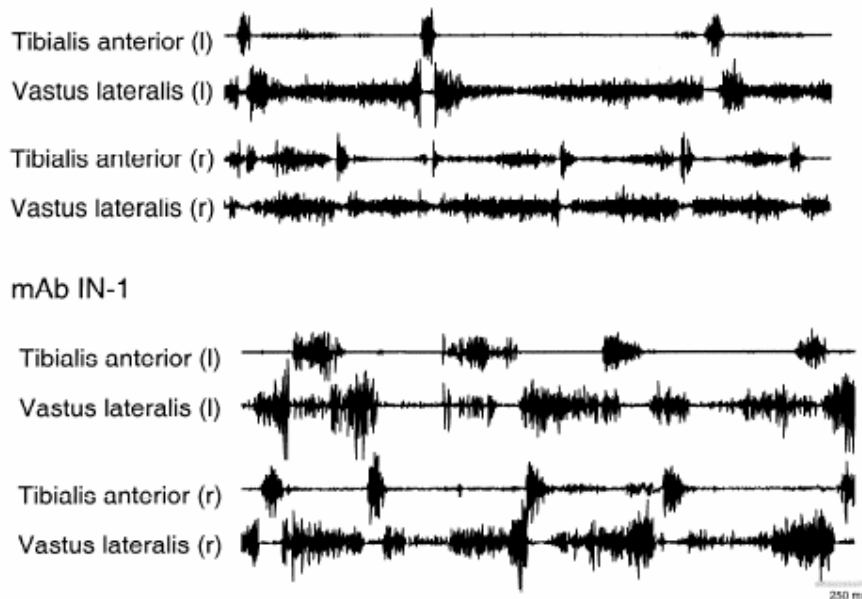


Fig. 1.32: Figure showing a comparison of EMG activity recorded in rats after a spinal cord section during locomotion in (A) animals treated with a control antibody compared to (B) animals treated with the IN-1 antibody. The pattern of EMG activity in (B) is much closer to the normal alternated pattern of electrical activity of locomotor muscles than in (A) (adapted from Fouad, K. et al., 2001).

1.7: Aim of the present thesis and methodological strategies

1.7.1: Goals

The general goal of the present thesis is to determine whether the neutralisation of Nogo, a strategy successfully applied in the rat (Schnell and Schwab 90; Schwab and Schnell 91; Schnell and Schwab 93; Bregman et al 95; Thallmair et al 98; Raineteau et al 99; Wenk et al 99; Brösamle et al 00) can be transposed to the primate, namely monkeys, as a preliminary step towards a future application of this strategy to spinal cord injured patients. More specifically, the present thesis aims at addressing the following questions:

- What are the behavioural consequences of a spinal cord hemisection at cervical level in monkeys, with emphasis on manual dexterity?
- How the motor maps in M1 are affected by the cervical hemisection?
- Do the axotomised CS neurones survive or die?
- What is the benefit of a treatment based on inactivating the growth inhibitory activity of Nogo infused immediately after a cervical hemi-section?

1.7.2: Brief survey of the methodological strategies

1.7.2.1 Behaviour

To assess the integrity of the supraspinal control of the manual dexterity, in particular through the corticomotoneuronal pathway, we focused our behavioural analysis on precision grip tasks already used in previous studies in our laboratory (Rouiller et al 98; Liu and Rouiller 99).

1.7.2.2: Role of the cerebral cortex in behavioural tasks: reversible pharmacological inactivation

The putative role of a given motor cortical area in functional recovery of manual dexterity after cervical lesion can be assessed using transient inactivation in that cortical area. Three methods of inactivation can be used: i) cooling of the cortex, with the disadvantage of the limitation of the control of the extent of the inactivated area, ii) infusion of a local anaesthetic (e.g. lidocaine), iii) infusion of muscimol. We used infusion of muscimol, which is a γ -amino butyric acid (GABA) agonist, which has been used with success in our laboratory (e.g. Liu and Rouiller, 1999; Kermadi et al., 1997). Similarly, previous work has shown that muscimol indeed plays an inhibiting role on the performance of hand movement in macaque monkeys, resulting in an excessive inhibition of cortical neurones silencing the efferent pyramidal tract neurones and weakening the total muscle activity (Matsumura et al 91); (Kubota 96).

1.7.3: Electrophysiology

To evaluate the functional organisation of the hand area in the primary motor cortex and its re-organisation after an interruption of the corticospinal tract, a suitable method is the ICMS, first designed and used by Asanuma and Sakata (1967) in the motor cortex of the cat.

In the present study, we investigated the functional organisation of M1 using ICMS, particularly in the hand area, which's state depends on the integrity of the corticospinal projections. M1 hand area mapping in both hemispheres was performed at two time points: before the spinal cord lesion and after lesion when the animal had reached the maximal level of recovery in the behavioural tasks. The functional reorganisation of both hemispheres can be compared in a single animal, because the electrophysiological mapping has been done in the same conditions before and after the spinal cord lesion. This strategy allowed a direct quantitative comparison of the number of sites that elicited movements when stimulated and a direct comparison of the current intensities needed to elicit a response.

1.7.4: Anatomy

Two aspects of the anatomical consequences of a spinal cord lesion were investigated. First, the structure of the different motor centres at cortical, subcortical and spinal levels using two staining methods: the most commonly used Nissl-staining and a staining based on an antibody recognising the non-phosphorylated neurofilaments of pyramidal neurones called SMI-32. Second, a further analysis was based on the transport of two distinct anterogradely transported molecules along CST axons: biotinylated dextran amine (BDA) was injected in the right hemisphere whereas dextran green (DG) was injected in the left hemisphere.

1.7.5: Treatment

In order to follow a comparable protocol of treatment application that has been done in the rat experiments conducted by Schwab and colleagues, the antibody application was done immediately after the lesion, directly into the cerebrospinal fluid space in the theca via a tube placed 2-3 mm above the cervical lesion. The antibody was applied during 4 weeks using an osmotic pump that delivered the antibody at a constant speed. The control monkeys received a common IgG while the treated animals receive the 11 C 7 antibody directed against Nogo.

List of references for chapter 1

- 1: Alstermark,B., Isa,T., Ohki,Y. & Saito,Y. (1999) Disynaptic pyramidal excitation in forelimb motoneurons mediated via C₃-C₄ propriospinal neurons in the *Macaca fuscata*. *Journal of Neurophysiology*, **82**, 3580-3585.
- 2: Alstermark,B., Ogawa,J. & Isa,T. (2004) Lack of monosynaptic corticomotoneuronal EPSPs in rats: disynaptic EPSPs mediated via reticulospinal neurons and polysynaptic EPSPs via segmental interneurons. *Journal of Neurophysiology*, **91**, 1832-1839.
- 3: Andersen,P., Hagan,P.J., Phillips,C.G. & Powell,T.P.S. (1975) Mapping by microstimulation of overlapping projections from area 4 to motor units of the baboon's hand. *Proc.R.Soc.London.SerB.*, **188**, 31-60.
- 4: Aoki,M. & Mori,S. (1979) Recovery of hindlimb movement elicited by motor cortical stimulation after spinal hemisection in monkeys. In Ito,M. (ed), *Integrative control functions of the brain*. Elsevier, Amsterdam, pp. 152-154.
- 5: Asanuma,H. & Sakata,H. (1967) Functional organization of a cortical efferent system examined with focal depth stimulation in cats. *Journal of Neurophysiology*, **30**, 35-54.
- 6: Baker,S.N., Olivier,E. & Lemon,R.N. (1998) An investigation of the intrinsic circuitry of the motor cortex of the monkey using intra-cortical microstimulation. *Experimental Brain Research*, **123**, 397-411.
- 7: Bareyre,F.M., Kerschensteiner,M., Raineteau,O., Mettenleiter,T.C., Weinmann,O. & Schwab,M.E. (2004) The injured spinal cord spontaneously forms a new intraspinal circuit in adult rats. *Nature Neuroscience*, **7**, 269-277.

- 8: Bareyre, F.M. & Schwab, M.E. (2003) Inflammation, degeneration and regeneration in the injured spinal cord: insights from DNA microarrays. *Trends in Neurosciences*, **26**, 555-563.
- 9: Beck, Ch.H. & Chambers, W.W. (1970) Speed, accuracy, and strength of forelimb movement after unilateral pyramidotomy in Rhesus monkeys. *Journal of comp. and Physiol. Psychol. (Monograph)*, **2, part 2**, 1-22.
- 10: Belhaj-Saïf, A. & Cheney, P.D. (2000) Plasticity in the distribution of the red nucleus output to forearm muscles after unilateral lesions of the pyramidal tract. *Journal of Neurophysiology*, **83**, 3147-3153.
- 11: Bennett, K.M.B. & Lemon, R.N. (1996) Corticomotoneuronal contribution to the fractionation of muscle activity during precision grip in the monkey. *Journal of Neurophysiology*, **75**, 1826-1842.
- 12: Bennett, K.M.B. & Lemon, R.N. (1994) The influence of single monkey corticomotoneuronal cells at different levels of activity in target muscles. *J. Physiol. (Lond.)*, **477**, 291-307.
- 13: Bernhard, C.G., Bohm, E. & Petersen, J. (1953) Investigations on the organization of the cortic-spinal system in monkeys (*Macaca mulatta*). *Acta physiologica scandinavica*, **29, Suppl. 106**, 79-103.
- 14: Blöchliger, S., Weinmann, O., Schwab, M.E. & Thallmair, M. (2001) Neuronal plasticity and formation of new synaptic contacts follow pyramidal lesions and neutralization of Nogo-A: A light and electron microscopic study in the pontine nuclei of adult rats. *Journal of Comparative Neurology*, **433**, 426-436.
- 15: Bortoff, G.A. & Strick, P.L. (1993) Corticospinal terminations in two new-world primates: Further evidence that corticomotoneuronal connections provide part of the neural substrate for manual dexterity. *Journal of Neuroscience*, **13**, 5105-5118.
- 16: Bouyer, L.J. & Rossignol, S. (2003) Contribution of cutaneous inputs from the hindpaw to the control of locomotion. II. Spinal cats. *Journal of Neurophysiology*, **90**, 3640-3653.
- 17: Bregman, B.S., Kunkel-Bagden, E., Schnell, L., Dai, H.N., Gao, D. & Schwab, M.E. (1995) Recovery from spinal cord injury mediated by antibodies to neurite growth inhibitors. *Nature*, **378**, 498-501.
- 18: Brösamle, C., Huber, A.B., Fiedler, M., Skerra, A. & Schwab, M.E. (2000) Regeneration of lesioned corticospinal tract fibers in the adult rat induced by a recombinant, humanized IN-1 antibody fragment. *Journal of Neuroscience*, **20**, 8061-8068.
- 19: Brunet, J.F., Pellerin, L., Magistretti, P. & Villemure, J.G. (2003) Cryopreservation of human brain tissue allowing timely production of viable adult human brain cells for autologous transplantation. *Cryobiology*, **47**, 179-183.
- 20: Bucy, P.C. (1957) Is there a pyramidal tract? *Brain*, **80**, 376-392.

- 21: Bucy,P.C. (1966) Destruction of the pyramidal tract in the monkey. *Journal of Neurosurgery*, **25**, 1-20.
- 22: Burman,K., Darian-Smith,C. & Darian-Smith,I. (2000) Macaque red nucleus: Origins of spinal and olivary projections and terminations of cortical inputs. *Journal of Comparative Neurology*, **423**, 179-196.
- 23: Caminiti,R., Ferraina,S. & Johnson,P.B. (1996) The sources of visual information to the primate frontal lobe: a novel. *Cereb.Cortex.*, **6**, 319-328.
- 24: Chapman,C.E. & Wiesendanger,M. (1982) Recovery of function following unilateral lesions of bulbar pyramid in the monkey. *Electroencephalog.Clin.Neurophysiol.*, **53**, 374-387.
- 25: Chen,M.S., Huber,A.B., Van der Haar,M.E., Franck,M., Schnell,L., Spillmann,A.A., Christ,F. & Schwab,M.E. (2000) Nogo-Ais a myelin-associated neurite outgrowth inhibitor and an antigen for monoclonal antibody IN-1. *Nature*, **403**, 434-438.
- 26: Clower,W.T. & Alexander,G.E. (1998) Movement sequence-related activity reflecting numerical order of components in supplementary and presupplementary motor areas. *Journal of Neurophysiology*, **80**, 1562-1566.
- 27: Crowe,M.J., Bresnahan,J.C., Shuman,S.L., Masters,J.N. & Beattie,M.S. (1997) Apoptosis and delayed degeneration after spinal cord injury in rats and monkeys. *Nat.Med.*, **3**, 73-76.
- 28: David,S. & Aguayo,A.J. (1981) Axonal elongation into peripheral nervous system "bridges" after central nervous system injury in adult rats. *Science*, **214**, 931-933.
- 29: Deiber,M.P., Honda,M., Ibañez,V., Sadato,N. & Hallett,M. (1999) Mesial motor areas in self-initiated versus externally triggered movements examined with fMRI: Effect of movement type and rate. *Journal of Neurophysiology*, **81**, 3065-3077.
- 30: Denny-Brown,D. (1966) *The Cerebral Control of Movements*. Liverpool University Press, Liverpool.
- 31: Domeniconi,M., Cao,Z., Spencer,T., Sivasankaran,R., Wang,K., Nikulina,E., Kimura,N., Cai,H., Deng,K., Gao,Y., He,Z. & Filbin,M. (2002) Myelin-associated glycoprotein interacts with the Nogo66 receptor to inhibit neurite outgrowth. *Neuron*, **35**, 283-290.
- 32: Dum,R.P. & Strick,P.L. (1996) Spinal cord terminations of the medial wall motor areas in macaque monkeys. *Journal of Neuroscience*, **16**, 6513-6525.
- 33: Dum,R.P. & Strick,P.L. (1991) The Origin of Corticospinal Projections from the Premotor Areas in the Frontal Lobe. *J.Neurosci.*, **11**, 667-689.
- 34: Feldman,M.L. (1984) Morphology of the neocortical pyramidal neuron. In Peters,A. & Jones,E.G. (eds), *Cerebral cortex*. Plenum Press, New York and London, pp. 123.

- 35: Fetz,E.E., Cheney,P.D. & German,D.C. (1976) Corticomotoneuronal connections of precentral cells detected by post-spike averages of EMG activity in behaving monkeys. *Brain Res.*, **114**, 505-510.
- 36: Filbin,M.T. (2003) Myelin-associated inhibitors of axonal regeneration in the adult mammalian CNS. *Nat.Rev.Neurosci.*, **4**, 703-713.
- 37: Fouad,K., Dietz,V. & Schwab,M.E. (2001) Improving axonal growth and functional recovery after experimental spinal cord injury by neutralizing myelin associated inhibitors. *Brain Res.Brain Res.Rev.*, **36**, 204-212.
- 38: Fournier,A.E., GrandPré,T. & Strittmatter,S.M. (2001) Identification of a receptor mediating Nogo-66 inhibition of axonal regeneration. *Nature.*, **409**, 341-346.
- 39: Friel,K.M. & Nudo,R.J. (1998) Recovery of motor function after focal cortical injury in primates: compensatory movement patterns used during rehabilitative training. *Somatosens.Mot.Res.*, **15**, 173-189.
- 40: Frost,S.B., Barbay,S., Friel,K.M., Plautz,E.J. & Nudo,R.J. (2003) Reorganization of remote cortical regions after ischemic brain injury: A potential substrate for stroke recovery. *Journal of Neurophysiology*, **89**, 3205-3214.
- 41: Gabernet,L., Meskenaite,V. & Hepp-Reymond,M.C. (1999) Parcellation of the lateral premotor cortex of the macaque monkey based on staining with the neurofilament antibody SMI-32. *Experimental Brain Research*, **128**, 188-193.
- 42: Galea,M.P. & Darian-Smith,I. (1994) Multiple corticospinal neuron populations in the macaque monkey are specified by their unique cortical origins, spinal terminations, and connections. *Cereb.Cortex*, **4**, 166-194.
- 43: Galea,M.P. & Darian-Smith,I. (1997a) Corticospinal Projection Patterns Following Unilateral Section of the Cervical Spinal Cord in the Newborn and Juvenile Macaque Monkey. *J.Comp.Neurol.*, **381**, 282-306.
- 44: Galea,M.P. & Darian-Smith,I. (1997b) Manual dexterity and corticospinal connectivity following unilateral section of the cervical spinal cord in the macaque monkey. *Journal of Comparative Neurology*, **381**, 307-319.
- 45: Geyer,S., Matelli,M., Luppino,G., Schleicher,A., Jansen,Y., Palomero-Gallagher,N. & Zilles,K. (1998) Receptor autoradiographic mapping of the mesial motor and premotor cortex of the macaque monkey. *Journal of Comparative Neurology*, **397**, 231-250.
- 46: Ghez,C. (1975) Input-output relations of the red nucleus in the cat. *Brain Res.*, **98**, 93-308.
- 47: GrandPré,T., Li,S. & Strittmatter,S.M. (2002) Nogo-66 receptor antagonist peptide promotes axonal regeneration. *Nature*, **417**, 547-551.
- 48: GrandPré,T., Nakamura,F., Vartanian,T. & Strittmatter,S.M. (2000) Identification of the NOGO inhibitor of axon regeneration as a reticulon protein. *Nature*, **403**, 439-444.

- 49: Graziano, M.S.A., Taylor, C.S.R. & Moore, T. (2002) Complex movements evoked by microstimulation of precentral cortex. *Neuron*, **34**, 841-851.
- 50: He, S.-Q., Dum, R.P. & Strick, P.L. (1995) Topographic organization of corticospinal projections from the frontal lobe: Motor areas on the medial surface of the hemisphere. *J. Neurosci.*, **15**, 3284-3306.
- 51: He, S.-Q., Dum, R.P. & Strick, P.L. (1993) Topographic organization of corticospinal projections from the frontal lobe: Motor areas on the lateral surface of the hemisphere. *Journal of Neuroscience*, **13**, 952-980.
- 52: Hepp-Reymond, M.C., Trouche, E. & Wiesendanger, M. (1974) Effects of unilateral and bilateral pyramidotomy on a conditioned rapid precision grip in monkeys (*Macaca fascicularis*). *Experimental Brain Research*, **21**, 519-527.
- 53: Hepp-Reymond, M.C. & Wiesendanger, M. (1972) Pyramidotomy in monkeys: effect on force and speed of a conditioned precision grip. *Brain Res.*, **36**, 117-131.
- 54: Hepp-Reymond, M.-C. (1982) Lésions expérimentales dans le système nerveux central. *Pädiat. Fortbildk. Praxis*, **53**, 160-177.
- 55: Holmes, G. & May, W.P. (1909) On the exact origin of the pyramidal tracts in man and other mammals. *Brain*, **32**, 1-43.
- 56: Holstege, G. (1991) Descending motor pathways and the spinal motor system: limbic and non-limbic components. *Prog. Brain Res.*, **87**, 307-421.
- 57: Holstege, G., Blok, B.F. & Ralston, D.D. (1988) Anatomical evidence for red nucleus projections to motoneuronal cell groups in the spinal cord of the monkey. *Neuroscience Letters*, **95**, 97-101.
- 58: Holstege, J.C. & Kuypers, H.G.J.M. (1987) Brainstem projections to spinal motoneurons: an update commentary. *Neuroscience*, **23**, 809-821.
- 59: Horner, P.J. & Gage, F.H. (2000) Regenerating the damaged central nervous system. *Nature*, **407**, 963-970.
- 60: Ikeda, A., Yazawa, S., Kunieda, T., Ohara, S., Terada, K., Mikuni, N., Nagamine, T., Taki, W., Kimura, J. & Shibasaki, H. (1999) Cognitive motor control in human pre-supplementary motor area studied by subdural recording of discrimination/selection-related potentials. *Brain*, **122**, 915-931.
- 61: Illert, M., Lundberg, A. & Tanaka, R. (1976a) Integration in descending motor pathways controlling the forelimb in the cat. 1. Pyramidal effects on motoneurons. *Experimental Brain Research*, **26**, 509-519.
- 62: Illert, M., Lundberg, A. & Tanaka, R. (1976b) Integration in descending motor pathways controlling the forelimb in the cat. 2. Convergence on neurones mediating disinaptic cortico-motoneuronal excitation. *Experimental Brain Research*, **26**, 521-540.

- 63: Illert, M. & Tanaka, R. (1976) Transmission of corticospinal I.P.S.P.'s to cat forelimb motoneurons via high cervical propriospinal neurons and Ia inhibitory interneurons. *Brain Res.*, **103**, 173-176.
- 64: Jenny, A.B. & Inukai, J. (1983) Principles of motor organization of the monkey cervical spinal cord. *Journal of Neuroscience*, **3**, 567-575.
- 65: Kermadi, I., Liu, Y., Tempini, A., Calciati, E. & Rouiller, E.M. (1998) Neuronal activity in the primate supplementary motor area and the primary motor cortex in relation to spatio-temporal bimanual coordination. *Somatosens.Mot.Res.*, **15**, 287-308.
- 66: Kermadi, I., Liu, Y., Tempini, A. & Rouiller, E.M. (1997) Effects of reversible inactivation of the supplementary motor area (SMA) on unimanual grasp and bimanual pull and grasp performance in monkeys. *Somatosens.Mot.Res.*, **14**, 268-280.
- 67: Kim, J.E., Li, S.X., GrandPré, T., Qiu, D. & Strittmatter, S.M. (2003) Axon regeneration in young adult mice lacking Nogo-A/B. *Neuron*, **38**, 187-199.
- 68: Kubota, K. (1996) Motor cortical muscimol injection disrupts forelimb movement in freely moving monkeys. *NR*, **7**, 2379-2384.
- 69: Kucera, P. & Wiesendanger, M. (1982) Does sprouting of uncrossed corticospinal fibers account for the functional recovery following unilateral pyramidal lesion in monkeys? *Neurosci.Letters.suppl.*, **10**, 274.
- 70: Kurata, K. (1991) Corticocortical inputs to the dorsal and ventral aspects of the premotor cortex of macaque monkeys. *Neurosci.Res.*, **12**, 263-280.
- 71: Kurata, K. (1994) Site of origin of projections from the thalamus to dorsal versus ventral aspects of the premotor cortex of monkeys. *Neurosci.Res.*, **21**, 71-76.
- 72: Kurata, K. & Hoffman, D.S. (1994) Differential effects of muscimol microinjection into dorsal and ventral aspects of the premotor cortex of monkeys. *J.Neuropsychiol.*, **71**, 1151-1164.
- 73: Kwan, H.C., MacKay, W.A., Murphy, J.T. & Wong, Y.C. (1978) An intracortical microstimulation study of output organization in precentral cortex of awake primates. *J.Physiol (Paris)*, **74**, 231-233.
- 74: Lawrence, D.G. & Hopkins, D.A. (1976) The development of motor control in the Rhesus monkey: evidence concerning the role of corticomotoneuronal connections. *Brain*, **99**, 235-254.
- 75: Lawrence, D.G. & Kuypers, H.G.J.M. (1968b) The functional organization of the motor system. I. The effects of bilateral pyramidal lesions. *Brain*, **91**, 1-14.
- 76: Lawrence, D.G. & Kuypers, H.G.J.M. (1968a) The functional organization of the motor system in the monkey. II. The effects of lesions in the descending brainstem pathways. *Brain*, **91**, 15-36.

-
- 77: Lawrence,D.G., Porter,R. & Redman,S.J. (1985) Corticomotoneuronal synapses in the monkey:light microscopic localization upon motoneurons of intrinsic muscles of the hand. *Journal of Comparative Neurology*, **232**, 499-510.
- 78: Lemon,R. (1988) The output map of the primate motor cortex. *Trends Neurosci.*, **11**, 501-506.
- 79: Lemon,R.N. (1993) Cortical control of the primate hand. *Experimental Physiology*, **78**, 263-301.
- 80: Lemon,R.N. (1999) Neural control of dexterity: what has been achieved? *Experimental Brain Research*, **128**, 6-12.
- 81: Lemon,R.N., Baker,S.N., Davis,J.A., Kirkwood,P.A., Maier,M.A. & Yang,H.S. (1998) The importance of the cortico-motoneuronal system for control of grasp. *Novartis.Found.Symp.*, **218**, 202-215.
- 82: Lemon,R.N., Maier,M.A., Armand,J., Kirkwood,P.A. & Yang,H.W. (2002) Functional differences in corticospinal projections from macaque primary motor cortex and supplementary motor area. *Adv.Exp.Med.Biol.*, **508**, 425-434.
- 83: Lemon,R.N., Muir,R.B. & Mantel,G.W. (1987) The effects upon the activity of hand and forearm muscles of intracortical stimulation in the vicinity of corticomotor neurones in the conscious monkey. *Experimental Brain Research*, **66**, 621-637.
- 84: Leyton,A.S.F. & Sherrington,C.S. (1917) Observations on the excitable cortex of the chimpanzee, orang-utan and gorilla. *Q.J.Exp.Physiol.*, **11**, 135-222.
- 85: Liang,F., Moret,V., Wiesendanger,M. & Rouiller,E.M. (1991) Corticomotoneuronal connections in the rat: Evidence from double-labeling of motoneurons and corticospinal axon arborizations. *Journal of Comparative Neurology*, **311**, 356-366.
- 86: Liepert,J., Storch,P., Fritsch,A. & Weiller,C. (2000) Motor cortex disinhibition in acute stroke. *Clinical Neurophysiology*, **111**, 671-676.
- 87: Liu,Y. & Rouiller,E.M. (1999) Mechanisms of recovery of dexterity following unilateral lesion of the sensorimotor cortex in adult monkeys. *Experimental Brain Research*, **128**, 149-159.
- 88: Luppino,G., Matelli,M., Camarda,R. & Rizzolatti,G. (1993) Corticocortical connections of area F3 (SMA-proper) and area F6 (pre-SMA) in the macaque monkey. *Journal of Comparative Neurology*, **338**, 114-140.
- 89: Luppino,G., Matelli,M. & Rizzolatti,G. (1990) Cortico-cortical connections of two electrophysiologically identified arm representations in the mesial agranular frontal cortex. *Exp Brain Res*, **82**, 214-218.
- 90: Maier,M.A., Armand,J., Kirkwood,P.A., Yang,H.W., Davis,J.N. & Lemon,R.N. (2002) Differences in the corticospinal projection from primary motor cortex and supplementary motor area to macaque upper limb motoneurons: An anatomical and electrophysiological study. *Cerebral Cortex*, **12**, 281-296.

- 91: Maier, M.A., Bennett, K.M.B., Hepp-Reymond, M.-C. & Lemon, R.N. (1993) Contribution of the monkey corticomotoneuronal system to the control of force in precision grip. *Journal of Neurophysiology*, **69**, 772-785.
- 92: Maier, M.A., Illert, M., Kirkwood, P.A., Nielsen, J. & Lemon, R.N. (1998) Does a C3-C4 propriospinal system transmit corticospinal excitation in the primate? An investigation in the macaque monkey. *J.Physiol.(Lond.)*, **511**, 191-212.
- 93: Matelli, M. & Luppino, G. (1996) Thalamic input to mesial and superior area 6 in the macaque monkey. *Journal of Comparative Neurology*, **372**, 59-87.
- 94: Matelli, M., Luppino, G. & Rizzolatti, G. (1985) Patterns of cytochrome oxidase activity in the frontal agranular cortex of the macaque monkey. *Behavioural Brain Research*, **18**, 125-136.
- 95: Matelli, M., Luppino, G. & Rizzolatti, G. (1991) Architecture of superior and mesial area 6 and the adjacent cingulate cortex in the macaque monkey. *Journal of Comparative Neurology*, **311**, 445-462.
- 96: Matsumura, M., Sawaguchi, T., Oishi, T., Ueki, K. & Kubota, K. (1991) Behavioral deficits induced by local injection of Bicuculline and Muscimol into the primate motor and premotor cortex. *Journal of Neurophysiology*, **65**, 1542-1553.
- 97: Matsuyama, K., Kobayashi, Y., Takakusaki, K., Mori, S. & Kimura, H. (1993) Termination mode and branching patterns of reticuloreticular and reticulospinal fibers of the nucleus reticularis pontis oralis in the cat: An anterograde PHA-L tracing study. *Neurosci.Res.*, **17**, 9-21.
- 98: Matsuzaka, Y., Aizawa, H. & Tanji, J. (1992) A motor area rostral to the supplementary motor area (presupplementary motor area) in the monkey: Neuronal activity during a learned motor task. *Journal of Neurophysiology*, **68**, 653-662.
- 99: Matsuzaka, Y. & Tanji, J. (1996) Changing directions of forthcoming arm movements: Neuronal activity in the presupplementary and supplementary motor area of monkey cerebral cortex. *Journal of Neurophysiology*, **76**, 2327-2342.
- 100: McGee, A.W. & Strittmatter, S.M. (2003) The Nogo-66 receptor: focusing myelin inhibition of axon regeneration. *Trends in Neurosciences*, **26**, 193-198.
- 101: McKiernan, B.J., Marcario, J.K., Karrer, J.H. & Cheney, P.D. (1998) Corticomotoneuronal postspike effects in shoulder, elbow, wrist, digit, and intrinsic hand muscles during a reach and prehension task. *Journal of Neurophysiology*, **80**, 1961-1980.
- 102: Merkler, D., Metz, G.A.S., Raineteau, O., Dietz, V., Schwab, M.E. & Fouad, K. (2001) Locomotor recovery in spinal cord-injured rats treated with an antibody neutralizing the myelin-associated neurite growth inhibitor Nogo-a. *Journal of Neuroscience*, **21**, 3665-3673.
- 103: Miller, L.E., Van Kan, P.L.E., Sinkjær, T., Andersen, T., Harris, G.D. & Houk, J.C. (1993) Correlation of primate red nucleus discharge with muscle activity during free-form arm movements. *J.Physiol.(Lond.)*, **469**, 213-243.

- 104: Mori,S., Matsuyama,K., Miyashita,E., Nakajima,K. & Asanome,M. (1996) Basic neurophysiology of primate locomotion. *Folia Primatologica*, **66**, 192-203.
- 105: Murphy,J.T., Wong,Y.C. & Kwan,H.C. (1985) Sequential activation of neurons in primate motor cortex during unrestrained forelimb movement. *Journal of Neurophysiology*, **53**, 435-445.
- 106: Nakamura,K., Sakai,K. & Hikosaka,O. (1998) Neuronal activity in medial frontal cortex during learning of sequential procedures. *Journal of Neurophysiology*, **80**, 2671-2687.
- 107: Nakamura,K., Sakai,K. & Hikosaka,O. (1999) Effects of local inactivation of monkey medial frontal cortex in learning of sequential procedures. *Journal of Neurophysiology*, **82**, 1063-1068.
- 108: Nash,H.H., Borke,R.C. & Anders,J.J. (2002) Ensheathing cells and methylprednisolone promote axonal regeneration and functional recovery in the lesioned adult rat spinal cord. *Journal of Neuroscience*, **22**, 7111-7120.
- 109: Nathan,P.W., Smith,M. & Deacon,P. (1996) Vestibulospinal, reticulospinal and descending propriospinal nerve fibres in man. *Brain*, **119**, 1809-1833.
- 110: Nieuwenhuys,R., Voogd,J. & Huijzen,C. (1988) *The human central nervous system a synopsis and atlas* Springer-Verlag, Berlin.
- 111: Nudo,R.J. (1999) Recovery after damage to motor cortical areas. *Current Opinion in Neurobiology*, **9**, 740-747.
- 112: Nudo,R.J. & Milliken,G.W. (1996) Reorganization of movement representations in primary motor cortex following focal ischemic infarcts in adult squirrel monkeys. *Journal of Neurophysiology*, **75**, 2144-2149.
- 113: Nudo,R.J., Milliken,G.W., Jenkins,W.M. & Merzenich,M.M. (1996a) Use-dependent alterations of movement representations in primary motor. *J Neurosci.*, **16**, 785-807.
- 114: Nudo,R.J., Wise,B.M., SiFuentes,F. & Milliken,G.W. (1996b) Neural substrates for the effects of rehabilitative training on motor recovery after ischemic infarct. *Science*, **272**, 1791-1794.
- 115: Oertle,T. & Schwab,M.E. (2003) Nogo and its paRTNers. *Trends Cell Biol.*, **13**, 187-194.
- 116: Olivier,E., Baker,S.N., Nakajima,K., Brochier,T. & Lemon,R.N. (2001) Investigation into non-mono synaptic corticospinal excitation of macaque upper limb single motor units. *Journal of Neurophysiology*, **86**, 1573-1586.
- 117: Palmer,S.S. & Fetz,E.E. (1985) Effects of single intracortical microstimuli in motor cortex on activity of identified forearm motor units in behaving monkeys. *J.Neurophysiol.*, **54**, 1194-1212.
- 118: Passingham,R.E. (1996) Functional specialization of the supplementary motor area in monkeys and humans. *Adv.Neurol.*, **70**, 105-116.

- 119: Passingham,R.E., Perry,V.H. & Wilkinson,F. (1983) The long-term effects of removal of sensorimotor cortex in infant and adult rhesus monkeys. *Brain*, **106**, 675-705.
- 120: Petit,L., Courtney,S.M., Ungerleider,L.G. & Haxby,J.V. (1998) Sustained activity in the medial wall during working memory delays. *Journal of Neuroscience*, **18**, 9429-9437.
- 121: Phillips,C.G. & Porter,R. (1977) Corticospinal neurones, their role in movement. *Monographs of the Physiol. Soc. - No. 34*. Academic Press, London, New York, San Francisco, pp. 450pp.
- 122: Picard,N. & Strick,P.L. (1996) Motor areas of the medial wall: A review of their location and functional activation. *Cereb.Cortex*, **6**, 342-353.
- 123: Poliakov,A.V. & Schieber,M.H. (1999) Limited functional grouping of neurons in the motor cortex hand area during individuated finger movements: A cluster analysis. *Journal of Neurophysiology*, **82**, 3488-3505.
- 124: Porter,R. (1987) Corticomotoneuronal projections: synaptic events related to skilled movement. *Proc.R.Soc.Lond.B.*, **231**, 147-168.
- 125: Preuss,T.M., Stepniewska,I., Jain,N. & Kaas,J.H. (1997) Multiple divisions of macaque precentral motor cortex identified with neurofilament antibody SMI-32. *Brain Res.*, **767**, 148-153.
- 126: Preuss,T.M., Stepniewska,I. & Kaas,J.H. (1996) Movement representation in the dorsal and ventral premotor areas of owl monkeys: A microstimulation study. *J.Comp.Neurol.*, **371**, 649-675.
- 127: Raineteau,O., Fouad,K., Bareyre,F.M. & Schwab,M.E. (2002) Reorganization of descending motor tracts in the rat spinal cord. *European Journal of Neuroscience*, **16**, 1761-1771.
- 128: Raineteau,O., Z'Graggen,W.J., Thallmair,M. & Schwab,M.E. (1999) Sprouting and regeneration after pyramidotomy and blockade of the myelin-associated neurite growth inhibitors NI 35/250 in adult rats. *European Journal of Neuroscience*, **11**, 1486-1490.
- 129: Rexed,B. (1954) A cytoarchitectonic atlas of the spinal cord in the cat. *J.Comp Neurol.*, **100**, 297-379.
- 130: Rizzolatti,G., Luppino,G. & Matelli,M. (1996) The classic supplementary motor area is formed by two independent areas. *Adv.Neurol.*, **70**, 45-56.
- 131: Rouiller,E.M., Moret,V., Tanné,J. & Boussaoud,D. (1996) Evidence for direct connections between the hand region of the supplementary motor area and cervical motoneurons in the macaque monkey. *European Journal of Neuroscience*, **8**, 1055-1059.
- 132: Rouiller,E.M., Yu,X.H., Moret,V., Tempini,A., Wiesendanger,M. & Liang,F. (1998) Dexterity in adult monkeys following early lesion of the motor cortical hand area: the role of cortex adjacent to the lesion. *European Journal of Neuroscience*, **10**, 729-740.

- 133: Santos-Benito,F.F. & Ramon-Cueto,A. (2003) Olfactory ensheathing glia transplantation: a therapy to promote repair in the mammalian central nervous system. *Anat.Rec.*, **271B**, 77-85.
- 134: Saruhashi,Y., Young,W. & Perkins,R. (1996) The recovery of 5-HT immunoreactivity in lumbosacral spinal cord and locomotor function after thoracic hemisection. *Exp.Neurol.*, **139**, 203-213.
- 135: Sasaki,S., Isa,T., Pettersson,L.G., Alstermark,B., Naito,K., Yoshimura,K., Seki,K. & Ohki,Y. (2004) Dexterous Finger Movements in Primate without Monosynaptic Corticomotoneuronal Excitation. *Journal of Neurophysiology*.
- 136: Sawaki,L., Werhahn,K.J., Barco,R., Kopylev,L. & Cohen,L.G. (2003) Effect of an α_1 -adrenergic blocker on plasticity elicited by motor training. *Experimental Brain Research*, **148**, 504-508.
- 137: Schieber,M.H. (2001) Constraints on somatotopic organization in the primary motor cortex. *Journal of Neurophysiology*, **86**, 2125-2143.
- 138: Schieber,M.H. & Deuel,R.K. (1997) Primary motor cortex reorganization in a long-term monkey amputee. *Somatosens.Mot.Res.*, **14**, 157-167.
- 139: Schieber,M.H. & Hibbard,L.S. (1993) How somatotopic is the motor cortex hand area? *Science*, **261**, 489-492.
- 140: Schnell,L. & Schwab,M.E. (1990) Axonal regeneration in the rat spinal cord produced by an antibody against myelin-associated neurite growth inhibitors. *Nature.*, **343 no 6255**, 269-272.
- 141: Schnell,L. & Schwab,M.E. (1993) Sprouting and regeneration of lesioned corticospinal tract fibres in the adult rat spinal cord. *European Journal of Neuroscience*, **5**, 1156-1171.
- 142: Schwab,M.E. (2004) Nogo and axon regeneration. *Current Opinion in Neurobiology*, **14**, 118-124.
- 143: Schwab,M.E. & Bartholdi,D. (1996) Degeneration and regeneration of axons in the lesioned spinal cord. *Physiological Reviews*, **76**, 319-370.
- 144: Schwab,M.E. & Caroni,P. (1988) Oligodendrocytes and CNS myelin are nonpermissive substrates for neurite growth and fibroblast spreading in vitro. *Journal of Neuroscience*, **8**, 2381-2393.
- 145: Schwab,M.E. & Schnell,L. (1991) Channeling of developing rat corticospinal tract axons by myelin-associated neurite growth inhibitors. *Journal of Neuroscience*, **11**, 709-721.
- 146: Schwartzmann,R.J. (1978) A behavioral analysis of complete unilateral section of the pyramidal tract as the medullary level in *Macaca mulatta*. *Annals of Neurology*, **4**, 234-244.

- 147: Seitz,R.J., Hoflich,P., Binkofski,F., Tellmann,L., Herzog,H. & Freund,H.J. (1998) Role of the premotor cortex in recovery from middle cerebral artery infarction. *Arch.Neurol.*, **55**, 1081-1088.
- 148: Shima,K., Mushiake,H., Saito,N. & Tanji,J. (1996) Role for cells in the presupplementary motor area in updating motor plans. *Proc.Natl.Acad.Sci.USA*, **93**, 8694-8698.
- 149: Shima,K. & Tanji,J. (1998) Both supplementary and presupplementary motor areas are crucial for the temporal organization of multiple movements. *Journal of Neurophysiology*, **80**, 3247-3260.
- 150: Shinoda,Y., Yokota,J.I. & Futami,T. (1981) Divergent projection of individual corticospinal axons to motoneurons of multiple muscles in the monkey. *Neurosci.Letters*, **23**, 7-12.
- 151: Sloper,J.J., Brodal,P. & Powell,T.P.S. (1983) An anatomical study of the effects of unilateral removal of sensorimotor cortex in infant monkeys on the subcortical projections of the contralateral sensorimotor cortex. *Brain*, **106**, 707-716.
- 152: Tanji,J. (1994) The supplementary motor area in the cerebral cortex. *Neurosci.Res.*, **19**, 251-268.
- 153: Tanné,J., Boussaoud,D., Boyer-Zeller,N. & Rouiller,E.M. (1995) Direct visual pathways for reaching movements in the macaque monkey. *NR*, **7**, 267-272.
- 154: Thallmair,M., Metz,G.A.S., Z'Graggen,W.J., Raineteau,O., Kartje,G.L. & Schwab,M.E. (1998) Neurite growth inhibitors restrict plasticity and functional recovery following corticospinal tract lesions. *Nature Neurosci.*, **1**, 124-131.
- 155: Tower,S.S. (1940) Pyramidal lesion in the monkey. *Brain*, **63**, 36-90.
- 156: Vorobiev,V., Govoni,P., Rizzolatti,G., Matelli,M. & Luppino,G. (1998) Parcellation of human mesial area 6: cytoarchitectonic evidence for three separate areas. *Eur.J.Neurosci.*, **10**, 2199-2203.
- 157: Wang,K.C., Kim,J.A., Sivasankaran,R., Segal,R. & He,Z. (2002) P75 interacts with the Nogo receptor as a co-receptor for Nogo, MAG and OMgp. *Nature*, **420**, 74-78.
- 158: Wassermann,E.M., Pascual-Leone,A. & Hallett,M. (1994) Cortical motor representation of the ipsilateral hand and arm. *Experimental Brain Research*, **100**, 121-132.
- 159: Wenk,C.A., Thallmair,M., Kartje,G.L. & Schwab,M.E. (1999) Increased corticofugal plasticity after unilateral cortical lesions combined with neutralization of the IN-1 antigen in adult rats. *Journal of Comparative Neurology*, **410**, 143-157.
- 160: Werhahn,K.J., Conforto,A.B., Kadom,N., Hallett,M. & Cohen,L.G. (2003) Contribution of the ipsilateral motor cortex to recovery after chronic stroke. *Annals of Neurology*, **54**, 464-472.
- 161: Wiesendanger,M. (1981) The pyramidal tract. Its structure and function. *Handbook of behavioral neurobiology*, **5**, 401-491.

- 162: Wiesendanger,M. (1986) Recent developments in studies of the supplementary motor area of primates. *Rev.Physiol.Biochem.Pharmacol.*, **103**, 1-59.
- 163: Wiesendanger,R. & Wiesendanger,M. (1985) The thalamic connections with medial area 6 (supplementary motor cortex) in the monkey (*Macaca fascicularis*). *Experimental Brain Research*, **59**, 91-104.
- 164: Woolf,C.J. & Bloechlinger,S. (2002) It takes more than two to NOGO. *Science*, **297**, 1132-1134.
- 165: Woolsey,C.N., Gorska,T., Wetzel,A., Erickson,T.C., Earls,F.J. & Allman,J.M. (1972) Complete unilateral section of the pyramidal tract at the medullary level in *Macaca Mulatta*. *Brain Res.*, **40**, 119-123.
- 166: Yang,H.W. & Lemon,R.N. (2003) An electron microscopic examination of the corticospinal projection to the cervical spinal cord in the rat: lack of evidence for cortico-motoneuronal synapses. *Experimental Brain Research*, **149**, 458-469.
- 167: Yazawa,S., Ikeda,A., Kunieda,T., Ohara,S., Mima,T., Nagamine,T., Taki,W., Kimura,J., Hori,T. & Shibasaki,H. (2000) Human presupplementary motor area is active before voluntary movement: subdural recording of Bereitschaftspotential from medial frontal cortex. *Experimental Brain Research*, **131**, 165-177.
- 168: Z'Graggen,W.J., Metz,G.A.S., Kartje,G.L., Thallmair,M. & Schwab,M.E. (1998) Functional recovery and enhanced corticofugal plasticity after unilateral pyramidal tract lesion and blockade of myelin-associated neurite growth inhibitors in adult rats. *Journal of Neuroscience*, **18**, 4744-4757.
- 169: Zheng,B.H., Ho,C., Li,S.X., Keirstead,H., Steward,O. & Tessier-Lavigne,M. (2003) Lack of enhanced spinal regeneration in Nogo-deficient mice. *Neuron*, **38**, 213-224.

Chapter 2: Methods: general aspects	91
2.1: Overview of the experimental protocol:	91
2.1.1: Animal model and retention conditions:	91
2.1.2: Habituation to the primate chair	93
2.2: Training and behavioural tests	95
2.2.1: Quantative behavioural tests	96
2.2.1.1: “Modified Brinkman board” test	96
2.2.1.2: “Drawer task” test	97
2.2.2: Qualitative behavioural tests	99
2.2.2.1: “Displacement” test	99
2.2.2.2: “Foot prehension” test	100
2.2.2.3: “Ballistic arm movement” test	101
2.2.2.4: “Brachiation” and “up side down hanging” tests	101
2.3: Surgical procedures	103
2.3.1: Common aspects	103
2.3.1.1: Pre-medication	103
2.3.1.2: Anaesthesia	103
2.3.1.3: Post operative care	104
2.3.1.5: General care	105
2.3.2: Chronic stimulation chambers implantation	106
2.3.3: Spinal cord hemi-section and implantation of osmotic pump	107
2.4: Post-lesion investigations	110
2.4.1: Intracortical microstimulation	110
2.4.2: Cortical inactivation experiment	113
2.4.3: Injections of neuroanatomical tracers in the motor cortex	113
2.5: Anatomical procedures	114
2.5.1: Sacrifice and CNS dissection	114
2.5.2: Gastrocnemius muscle dissection	114
2.5.3: Histological sections preparation and staining	115
2.5.3.1: Nissl staining	115
2.5.3.2: SMI-32	115
2.5.3.3: Biotinylated Dextran amine (BDA)	116
2.5.3.4: Anti-fluorescein reaction	116
2.5.4: Reconstruction of the spinal cord lesion	117
2.5.5: Morphometrical analysis	117

Chapter 2: Methods: general aspects

2.1: Overview of the experimental protocol:

2.1.1: Animal model and retention conditions:

Two species of young adult macaque were used in this study: *Macaca mulatta* (rhesus monkeys) and *Macaca fascicularis* (cynomolgus monkeys or crab eating monkeys). The animals are kept in groups of four animals in the same 13 cubic meters room (245cm x 220cm x240cm) containing two cages in which they can be individually separated (Fig. 2.1). The retention conditions are in accordance with the federal rules for animal protection and applied by the local veterinary authorities. Animal care was given by two animal room keepers, 7 days a week. The monkeys had always free access to water. The animals were free to move in the retention room, except at 7 a.m. when the animal keepers placed them in the cages to allow capture of the monkeys for the behavioural training and tests. The rewards obtained during the behavioural tests were thus the first access to food during the day. After the behavioural tests, the monkeys received additional food during the rest of the day in the form of cereal pellets and fruits (apple, banana) or vegetable (carrot). When coming back from the behavioural session, the monkeys were again free to move in the retention room and could thus interact with their room-mates. The monkeys did not receive food anymore from 5 p.m. during the night. The weight of the animals was checked daily, except on week-end. As a rule imposed by veterinary authorities, the behavioural and electrophysiological experiments were interrupted in case of loss of weight of 10 % or more, until the monkey regained its initial weight.



Fig. 2.1: Retention room containing two cages. These cages are used also in stereotyped displacements like climbing from the floor to the ceiling of a cage, descending back to the floor and jumping from one cage to the other (A=60cm and B=130cm).

Six monkeys were involved in this study. The first two monkeys (Intact 1 and 2) have not been subjected to spinal cord injury and served as control in the anatomical part of the project. Two monkeys (Ctrl 1 and 2) subjected to spinal cord injury, were involved in the behavioural, electrophysiological and anatomical protocols and were treated with an inactive control antibody. The last two monkeys (Treat 1 and 2) followed the same protocols than the control animals but were treated with the anti-Nogo antibody (Table 2.1).

Animal	Given name	Species	Age	Weight	Sex	Lesion	Anti-Nogo Treatment	ICMS
Intact 1	Ginko	Rhesus	8	11 kg	M	No	No	No
Intact 2	Ruth	Fascicularis	5	5 kg	F	No	No	No
Ctrl 1	Caramel	Rhesus	4	4 kg	M	Yes	No	Yes
Ctrl 2	Stein	Rhesus	4	4 kg	M	Yes	No	Yes
Treat 1	Frank	Rhesus	4	4 kg	M	Yes	Yes	Yes
Treat 2	Antoine	Fascicularis	6	5.5 kg	M	Yes	Yes	Yes

Table 2.1: This table summarises the characteristics of the three groups of animals involved in this study. The values of age and weight of each monkey have been taken into account before the sacrifice.

2.1.2: Habituation to the primate chair

The normal unfolding of experimental events from the time the animals learned to enter in the primate chair (Fig. 2.2) to the time of sacrifice ranged from 10 months up to 20 months. This variability is mainly due to two main factors: first the normal inter-individual variability concerning the learning abilities and the tolerance to the experimental protocol, particularly during the electrophysiological mapping of the cortex, and the time needed by the neuroanatomical tracers to migrate from the cortex to the spinal cord (see below). Other factors played a secondary role, such as the synchronisation between collaborators: for example the availability of neurosurgeon to perform the spinal cord lesion, the availability of the anti-Nogo antibody.

The first step that can last several weeks consisted in the habituation of the animal to come in the primate chair on his own, without direct manipulation by the experimenter (Fig. 2.2). The second step was to train the animal for the different behavioural tests every open day of the week, and the total amount of food was balanced following the evolution of the body weight and the motivation to perform the task. However, there was no food deprivation, except that rewards during the behavioural tests were the first access to the food of the day. The normal amount of food daily provided for an animal weighting under 5 kg, in addition to the rewards delivered in

the behavioural tests, consisted in half a banana and half an apple, completed with cereal “croquettes” specially designed for primates’ needs. Bigger animals received an increased portion, up to the double, for 10 kg monkeys.

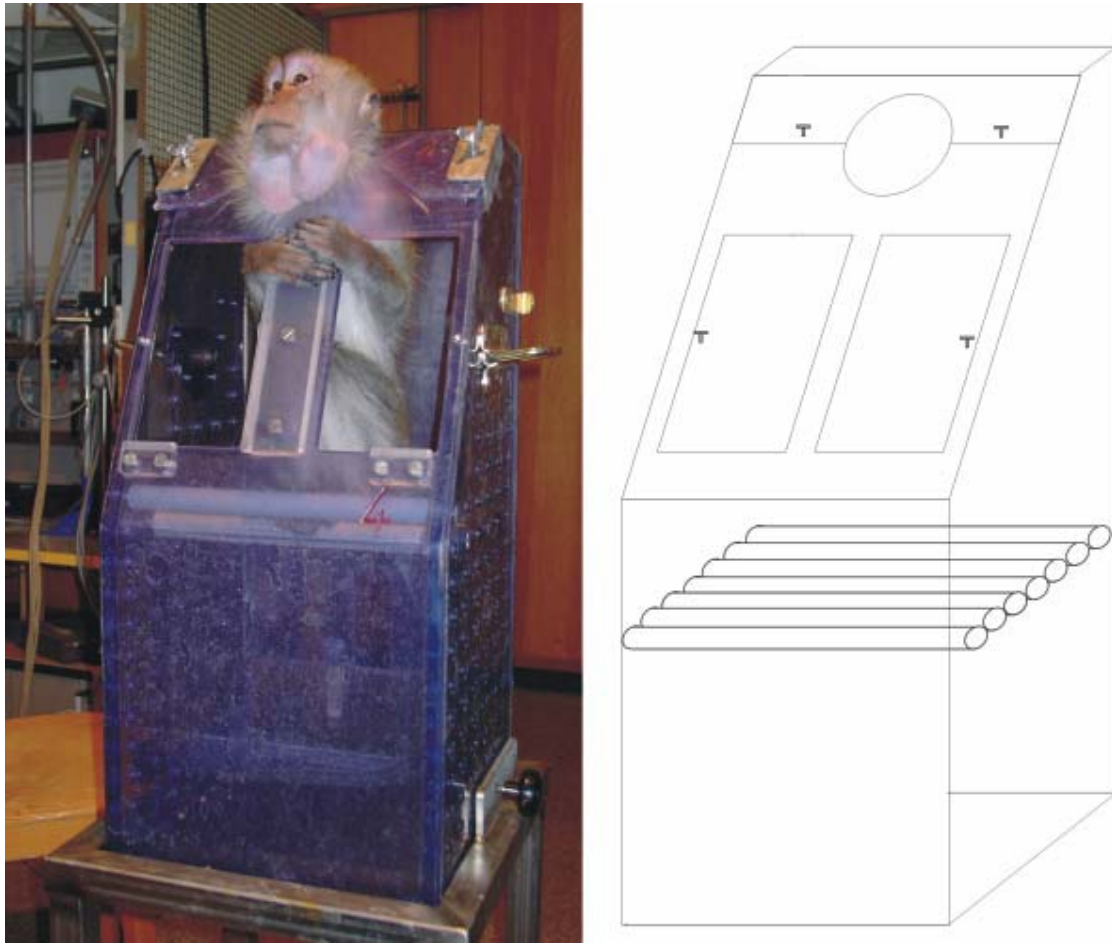


Fig. 2.2: primate chair used for the behavioural and electrophysiological experiments.

For the behavioural and electrophysiological sessions, the animal sat in a primate chair, in which it was restrained at the neck’s level (Fig. 2.2). The hands are relatively free of movements and can be tested one after the other, through right and left windows that can be opened separately. The level of the seat can be adjusted to get the most comfortable position, the back of the animal being lightly flexed.

2.2: Training and behavioural tests

The experimental unfolding is divided in four main periods: the first lasted about 3 to 5 weeks. It consisted of the habituation of the animal to come on his own in the primate chair that was connected to the cage by a tunnel of 80 cm long. The procedure to obtain a good collaboration of the animal was to provide food only in the primate chair, and in extreme cases partial food restriction was episodically used. The monkey learned to perform the various behavioural tasks (i.e. the Brinkman board test) until it reached a stable level of performance. The second period consisted in the acquisition of data. Its duration depended on the stability of the animal's performance and ranged between three to seven months. The third period was the post-lesion period, which started immediately after the spinal cord lesion (day 0). Following the surgery, during a first phase of 1 to 2 weeks, the animal's general state improved rapidly. The duration of this first phase depended on the extent of the spinal cord lesion. In a second phase, the animal was regularly trained in order to assess the functional recovery until it reached again a stable level of performance in the behavioural tests. At the end of this period of recovery, neuronal tracers (BDA, Dextran green) were injected in M1 on both hemispheres. This event corresponded to the beginning of the fourth period, whose aim was to allow enough time to the neuroanatomical tracers to migrate along the corticospinal tract.

Food pellets used in the behavioural tests consisted of small pieces made of dried banana powder or glucose powder (see Fig. 2.3), compressed in a round shape of about 4 mm in diameter. Dried raisins were occasionally given to increase the motivation of the animal, for example to perform a particularly difficult step of learning. Again, no aversive re-enforcement was used.

2.2.1: Quantative behavioural tests

These tests were normally performed at the same time of the day, one task after the other during each session. The position of the experimental setup was kept fixed with respect to the primate chair in order to keep the same prehension movements patterns. All behavioural task sessions were video recorded for off-line analysis.

2.2.1.1: “Modified Brinkman board” test

Manual dexterity was assessed using the so-called “modified Brinkman Board” task, as described previously (Rouiller et al 98;Liu and Rouiller 99). Briefly, the monkey sat in a primate chair in front of a Perspex modified "Brinkman board" (10 cm x 20 cm) containing 50 holes randomly distributed, 25 holes being oriented horizontally and 25 vertically (Fig. 2.3). The board was inclined with an angle of 40° from the horizontal plane. The dimensions of the holes (15 mm X 8 mm and 6 mm deep) allowed the penetration of the index finger and the thumb to retrieve a food pellet by performing the so-called "precision grip", consisting of the opposition of thumb and index finger. The monkeys performed this manual dexterity task alternatively with one or the other hand, 4 to 5 times a week. One to 2 weekly sessions were quantitatively analysed from video recordings. An attempt was considered as successful when the monkey grasped a pellet with the fingers and transported it to the mouth. Two behavioural scores were quantified: the number of slots successfully retrieved within 30 or 45 seconds and the time spent in individual slots to pick up the pellets. For the horizontally oriented slots analysis, the rotation of the wrist was also taken in consideration: pronation of the wrist results in internal grip (I) while supination of the wrist resulted in external grip (E). As the laboratories in which the behavioural tests were conducted were not soundproofed, the animal could be distracted by external noises and therefore, a musical background was given in order to mask the external noises.

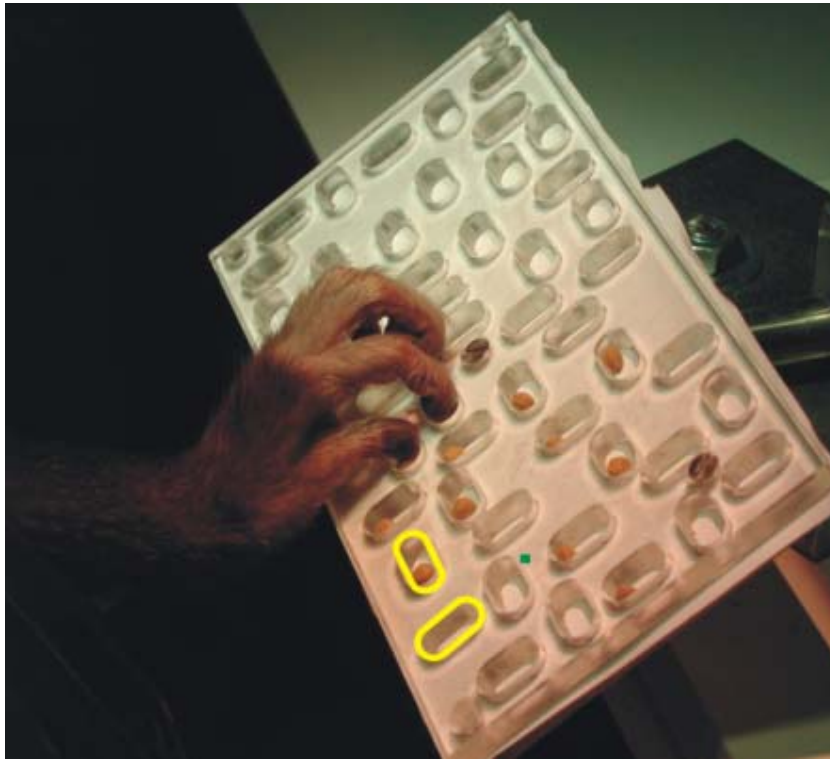


Fig. 2.3: Brinkman board. Perspex board made of 50 slots randomly distributed and containing pellets, 25 slots are vertically oriented and 25 are horizontally oriented.

2.2.1.2: “Drawer task” test

To test the ability and the velocity of complex movements, the animals were trained to perform the standard so-called “reach and grasp” drawer task (Fig. 2.4) (Kazennikov et al 94;Kermadi et al 97;Kermadi et al 98;Kermadi et al 00). In front of the setup, the animal placed its hands on two touch-sensitive “starting” pads, thus initiating a trial. The monkey saw the drawer behind the gates through a window. The start signal was the opening of one of the two gates that let it reach the knob of the drawer either with the left or the right hand. With one hand (unimanual task), the animal grasped the knob and pulled it to open the drawer against the force of a spring placed back to the drawer that slowed the pulling movement. The animal had to open the drawer until the drawer remained mechanically fixed in the fully open position. Then the animal picked the food reward (pellet or raisin) placed in the well of the drawer and brought it

back through the gate to its mouth. During the entire trial, the other (unused) hand remained on its pad. A series of trials (n=20) was executed with one hand followed by the same number of trials with the other hand.

Contact sensors and photoelectric cells were used for assessing discrete time points (“triggers”) of the different steps of the movements sequence to perform the “reach and grasp drawer” opening task. The opening of the right or left gate corresponded to the “go-signal” indicating to the animal that it can initiate the movement sequence. The time triggers allowed to define three periods: i) from the starting pad through the gate to the knob, ii) the time period spent to grasp the knob and to fully open the drawer, iii) the time to pick the reward and to retrieve the hand outside the gate. These signals were used for computational analysis: reaching time (RT) was the time difference between onset hands from the pad and reaching to the knob; pulling time (PT) was the time necessary to fully open the drawer and the withdrawal time (WT) the time used to return to the mouth through the gate that recorded the passing signal. A touch sensitive signal at the bottom of the well in the drawer detected the presence of the finger giving the time spent by the index finger in the well to pick up the pellet (picking time = PIT). Successful trials were selected according to the following criteria: adequate level of motivation and absence of disturbing factors such as unattended noises, direct movement from the starting pad to the knob, success to retrieve the food piece from the well and transport back to the mouth. The successful trials were labelled in the computer file with a trigger. In summary, the “drawer” task not only tested manual dexterity but also the ability to develop a minimal level of force to open the drawer.

2.2.2: Qualitative behavioural tests

2.2.2.1: “Displacement” test

Unrestrained displacements of the animal inside the retention room were video recorded before the spinal cord lesion, during the recovery period and when the recovery level reached its maximum (plateau) as assessed by the quantitative behavioural tests. By placing food morsels at specific locations inside the room, the animals could be repeatedly brought to perform different displacements: to climb from the floor to the ceiling of the room, to climb down to the floor again and to jump horizontally from one cage to the other (Fig. 2.5). These tests enabled to evaluate the capacity of an animal to use and coordinate its forelimbs and hindlimbs.

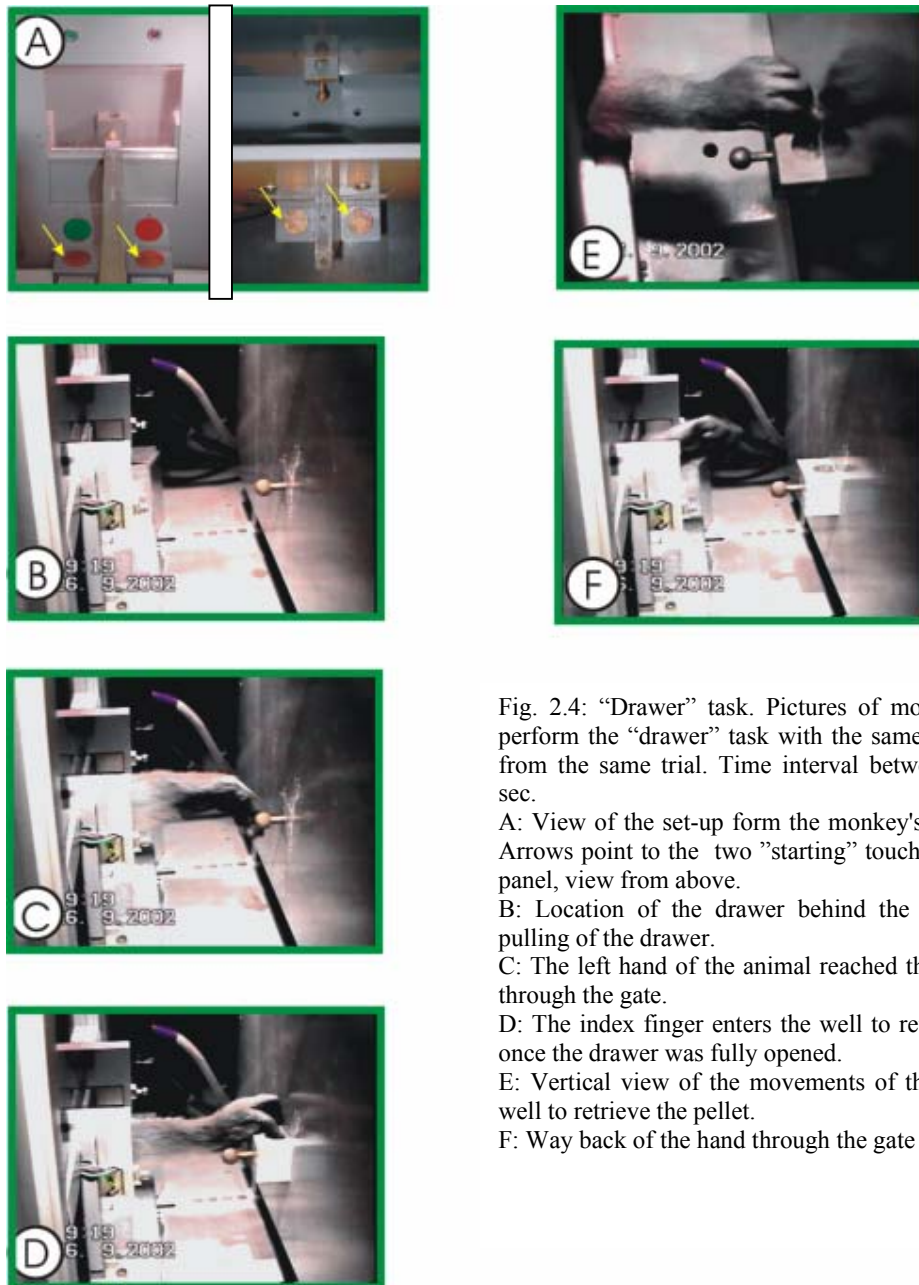


Fig. 2.4: “Drawer” task. Pictures of movement sequences to perform the “drawer” task with the same hand. Pictures come from the same trial. Time interval between each picture is 1 sec.

A: View of the set-up from the monkey's position (left panel). Arrows point to the two “starting” touch sensitive pads. Right panel, view from above.

B: Location of the drawer behind the gates to execute the pulling of the drawer.

C: The left hand of the animal reached the knob of the drawer through the gate.

D: The index finger enters the well to retrieve the food pellet, once the drawer was fully opened.

E: Vertical view of the movements of the index finger in the well to retrieve the pellet.

F: Way back of the hand through the gate to the mouth

2.2.2.2: “Foot prehension” test

At the end of a behavioural training session (“Brinkman board” test), two or three times a week, the animal was trained to pick up food morsels with its toes in the so-called “foot prehension” task. The animal sat in another type of primate chair, in which the animal was only restrained by its neck fixed in a rigid necklace, leaving it a great number of degrees of movement

for the forelimbs and hindlimbs. The reward, held by the experimentalist, was placed at low level to avoid hand prehension. The animal made an extension of the hindlimb to place the foot close to the reward and made a flexion of all toes and a flexion of the ankle to grip the reward and bring it first to the hand and finally to its mouth. The aim of this test was to observe if the animal was still able to perform the task with both feet, immediately after the spinal cord injury, and how it eventually improved during the recovery period.

2.2.2.3: “Ballistic arm movement” test

To assess the level of motor reaction ability, seated in the standard primate chair with one or two windows opened, the animal had to catch flying “croquettes” thrown by the experimentalist in its direction, using one or both hands. This task, referred to as the “ballistic arm movement” test was video-recorded. The coordination of movements of both limbs (in the bimanual catching situation), the initial position and the pre-shaping movement of the fingers of both hands were carefully observed and analysed.

2.2.2.4: “Brachiation” and “up side down hanging” tests

During brachiation, which consists in locomotion using hands along the ceiling of the retention room (Fig. 2.5), the animals had to move to reach a location where food morsels were placed. “Up side down hanging” consists in hanging from the ceiling using the feet. The animal moves in that position to grasp dried raisins stuck to the wall of the retention room by the experimentalist. The location of the dried raisins was far enough from the cage and the floor not to be directly taken by the animal.



Fig. 2.5: retention room. In a retention room, two cages allowed the separation of the animals to come in the primate chair and to isolate them after a surgical operation. The ceiling made from a metallic grid allowed to test “brachiation” and “up side down hanging” (see text).

2.3: Surgical procedures

2.3.1: Common aspects

The general protocol for anaesthesia, surgery, monitoring of the state of the animal was derived from procedures routinely used in this laboratory (Kermadi et al 97;Kermadi et al 98;Rouiller et al 98;Liu and Rouiller 99;Liu et al 02) . All surgeries were conducted under aseptic conditions.

2.3.1.1: Pre-medication

Anaesthesia was induced with an intra-muscular (i.m.) injection of Ketamine (Ketalar, Parke-Davis, 5 mg/kg). Atropine was injected i.m. (0.05 mg/kg) to reduce bronchial secretions. The area of the body to be operated and the femoral posterior region were shaved with an electric razor and with shaving cream. To prevent oedema formation, the animal received also an i.m. injection of dexamethason (Dexacortin 0.1mg/kg). To decrease post-operative pain and infection risks, the analgesic carprofen (Rimadyl 4 mg/kg) and an antibiotic (Albipen 0.22mg/kg) were injected subcutaneously.

2.3.1.2: Anaesthesia

In the operating room, the femoral vein was cannulated and a mixture of 1/3 volume propofol 1% (Fresenius®) and 2/3 volume glucose 4% solution was injected continuously. A stenosis of the vein was prevented by the use of a peristaltic pump with a constant perfusion rate. The level of anaesthesia was adjusted in regard to the following parameters which were monitored during the entire surgery: heart rate, oxygen saturation of arterial blood, respiration rate, expired CO₂, and central body temperature measured in the anal canal. The average amount

of injected propofol/glucose mixture to obtain a stable anaesthesia was 0.1 ml/min/kg. We used a warming blanket whose temperature was continuously adapted to the body temperature to avoid hypothermia. If necessary, during painful phases of the surgery (e.g. trepanation), a bolus of ketamine (50 mg/h) was added to the perfusion with propofol. After surgery, the animal normally recovered from anaesthesia around 15 to 30 minutes after offset of the propofol delivery.

In case of short operation time, or in case of impossibility to perform the intravenous injection of propofol solution, an i.m. injection of a mixture of 1 volume of Rompun for 3 volumes of Ketalar was performed to obtain a deep anaesthesia. This second method of anaesthesia was rarely used because it caused a decrease of heart rate in the minutes following the injection and it was more difficult to rapidly regulate the level of anaesthesia. Moreover, the time required to recover from anaesthesia was longer in such a case.

2.3.1.3: Post operative care

Standard post-operative care consisted in providing an antibiotic (per os with Synulox® 12.5 mg/kg or s.c. with Albipen® 0.22 mg/kg) and an analgesic (carprofen Rimadyl® 4 mg/kg) treatment to prevent post-operative infection and pain. This treatment was administrated during one week or more if required. The operated animals received during 3 to 4 days (even longer if needed) a daily injection or per os administration of Rimadyl and an every two days injection of Albipen or per os daily administration of Synulox (12.5 mg/kg). The operation scar was carefully disinfected with Betadine and dried with an antiseptic powder (Batramycine). A survey of the various pharmacological treatments is given in Table 2.2.

Table 2.2: Summary of the various treatments used for animal care

Name	Active molecule	Indication	Application	dosage
Albipen®	Ampiciline	Antibiotic ad inj	s.c.	0.22mg/kg
Atropine®	Atropinum sulfate 0.5 mg	Anticholinergic	i.m.	0.025mg/kg
Batramycine®	Bacitracine	Antibiotic powder	Surface application	
Dexacortin®	Dexamethasone	Anti-inflammatory ad inj.	i.m.	0.1mg/kg
Ketalar®	Ketamine	Sedatif ad inj	i.m.	6 mg/kg
Rompun®	Xylasine 2%	Sedatif ad inj	i.m.	0.15mg/kg
Nebacetine®	Neomycine + bacitracine	Antibiotic sol	Surface application	
Rimadyl ®	Carprofen 50mg / 1ml	Analgesic ad inj	s.c.	4 mg/kg
Rimadyl ®	Carprofen 20 mg	Analgesic comp	p.o.	4 mg/kg
Synulox®	Amoxicilinum	Antibiotic comp	p.o.	12.5 mg/kg
Morrhulan	Morrhuae oleum	Scar	Surface application	

Abbreviations: s.c.: sub cutaneous injection; i.m.: intramuscular injection; p.o.: Per os administration; ad inj.: to be injected; sol: liquid solution. Dosage: per kilogram of body weight.

2.3.1.5: General care

To evaluate the general state of each animal, attention was paid on every deviation from usual behaviour for this particular monkey such as loss of appetite, prostration, pain symptoms (although sometimes difficult to detect), weight loss, quality and abundance of fur. Pain can be detected through these symptoms: prostration, apathy, unusual posture, change of behaviour with room-mates or experimentalist, loss of appetite, etc. If this state persisted even treated with drugs or isolation of the animal, a meeting between the collaborators involved in animal cares (animal

keepers, experimentalists and veterinarian) was organised and the decision to sacrifice the animal was taken in case no health improvement could be obtained.

In some rare cases, after repetitive surgeries, the suture of the skin did not close adequately. In such a case, the procedure was to dissociate the maximum of skin from sub cutaneous structures to obtain more elasticity by decreasing the tension between the two pieces of skin. The scar was cleaned almost every day, with particular care to infection symptoms, using Betadine® and Batramycine® added with subcutaneous injections of Albipen®. In case of repetitive re-opening of scar, the animal was isolated in a cage to avoid scratching by the other animals sharing the retention room.

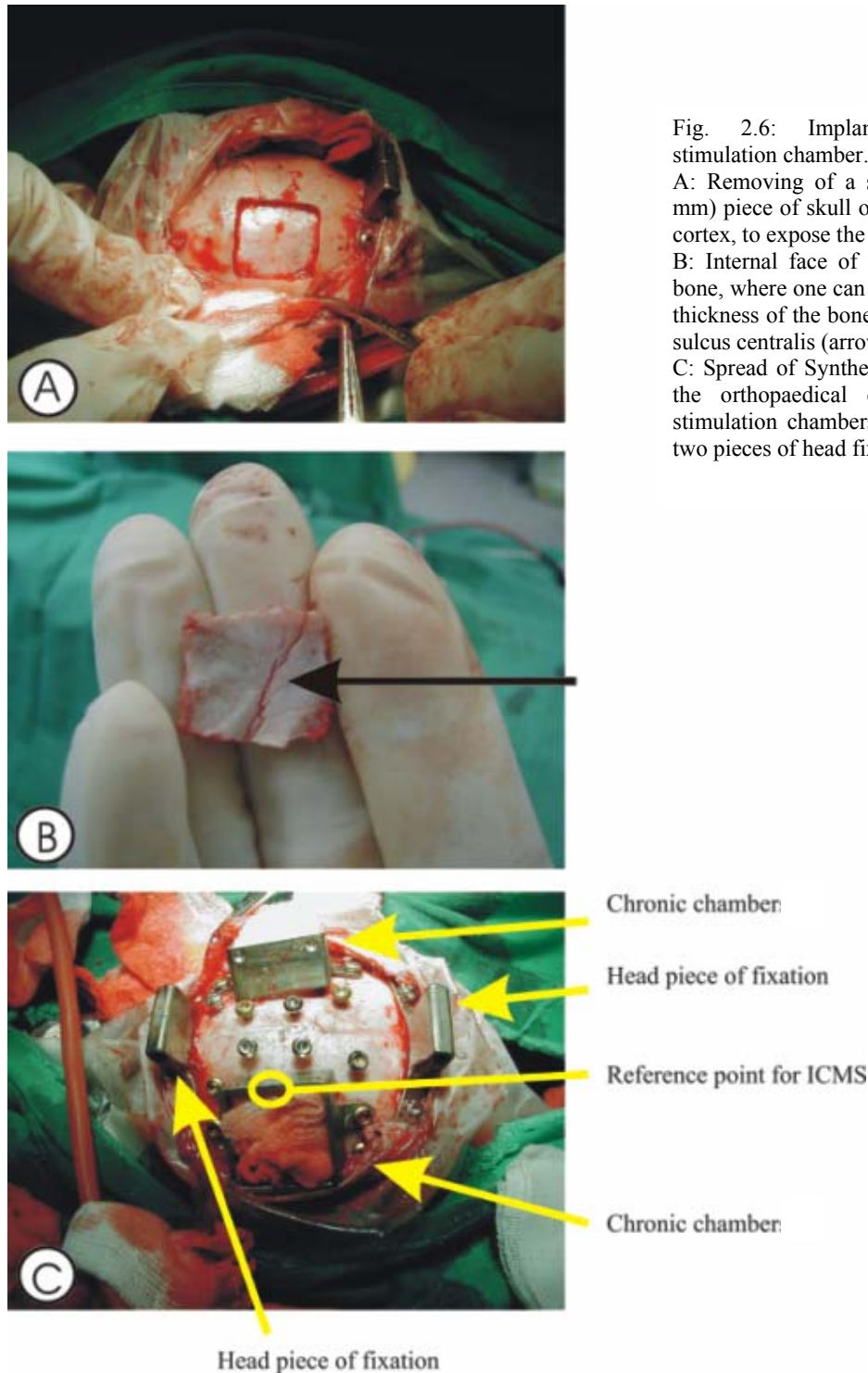
2.3.2: Chronic stimulation chambers implantation

For mapping of the motor cortex with intracortical microstimulation (ICMS), the monkey was subjected to a surgical procedure to implant chronic stimulation chambers. (Fig. 2.6). Lying in a decubitus ventral position, the animal's head was fixed in the stereotaxic framework using ear bars and infraorbital and palatine fixation. The surface of the skull was cleaned and the midline identified. Two stainless steel fixation bars were fixed over the skull, one placed rostrally and the other placed caudally. A reference point was marked with a sterile pencil 15 mm rostrally to the ear bars and 13 mm laterally from midline. This point served as reference to place the centre of the chronic stainless steel stimulation chambers over M1 hand area on each hemisphere. A square was drawn to delineate the future position of the chambers, along which the bone was drilled. The corresponding piece of bone was removed thus exposing the dura-mater on a surface corresponding to the chamber. The position of the sulcus centralis was identified on the internal face of the removed piece of bone and used as landmark for initiating later on the mapping in the appropriate zone (Fig. 2.6 B). Both chambers were fixed to the skull

with titan bone surgery Synthes® screws (Stratec Medical) and closed with an ad-hoc cover. Different methods have been used to fix and stabilise the fixation headpieces that supported two kinds of forces; the voluntary movements of the animal when it was restrained and externalisation forces originating in the reconstruction of fibrous tissue over the skull that slowly pushed the head pieces screws out of the bone. The fixation headpieces and the two chronic chambers were secured by application of orthopaedic cement (Palacos Gentamycinum®, Essex Chemie), anchored to the skull with additional titan bone surgery screws implanted around the chronic chambers (Fig. 2.6 C). The muscles and the skin were sutured and the animal recovered from anaesthesia usually 15-30 minutes after interruption of the venous perfusion with propofol. After implantation of the chronic chambers, ICMS sessions took place in order to map M1 on both hemispheres, as described below (paragraph 2.4.1). Behavioural tests were continued in parallel to the ICMS sessions.

2.3.3: Spinal cord hemi-section and implantation of osmotic pump

The optimal position to expose the posterior cervical region was obtained by placing a pillow under the monkey's chest that was lying in a ventral decubitus position and by dorsally flexing its head. Under sterile conditions, a vertical midline skin incision was performed from C2 to T1. The fascia was cut and the spinal processes from C2 to T1 were dissected. A hemi-laminectomy of C6 was then performed. The dura-mater was exposed and incised paramedially on the left side (Fig. 2.7). Under microscope observation, the dorsal root entry



zones were easily identified. To complete the left unilateral section of the cord at C7/C8 border, the dorsal root entry zone was the most medial landmark. From this target, a surgical blade (no 11, Paragon®) was inserted 4 mm perpendicularly to the spinal cord, and the section was

prolonged laterally to completely cut the dorsolateral funiculus. The surgical procedure to obtain this type of lesion was previously tested immediately before sacrifice on three monkeys involved in previous anatomical studies. The anatomical material available has been used to determine the rostro-caudal level where the dorsal rootlets entering respectively the 7th and the 8th cervical segments meet, corresponding to the rostral zone of the spinal portion covered by the 6th cervical lamina. The aimed lesion is located caudal with respect to the pool of the biceps motoneurons but rostral to the pool of triceps, forearm and hand muscles motoneurons (Jenny and Inukai 83). An osmotic pump was then placed (see below) before the muscles and the skin were sutured. After the cervical cord lesion, the post operative care consisted in the isolation of the animal in a small individual cage to avoid excessive moves and to deliver the standard post-op medication.

To deliver in situ the antibody treatment immediately after the spinal cord lesion, an osmotic pump was used with a size allowing the delivery of a volume of 2 ml of solution in two weeks (Alzet®, 2ML2). The pump was implanted subcutaneously or inside the neck musculature, caudally to the lesion site. It was connected to the lesion site by a polyethylene tube of 1 mm of diameter at the pump side and reduced to ca 100 μ m at the intrathecal side located a few mm rostrally to the cervical lesion level. The concentration of antibody in sterile PBS solution was 3.7 mg/ml, and the speed flow was 5 μ l/h. The mechanism of drug delivery of an osmotic pump is the following: one elastic tank containing the solution to inject is surrounded by a tank containing a solution at high osmotic concentration. Extracellular fluid attracted by this osmotic gradient comes in through the pump wall into this external tank and thus compresses the inside tank containing the drug to deliver. The inside pressure increases and the drug is delivered through the unique way out of the pump: a metallic tube in which the polyethylene tube is attached.

After two weeks of treatment, a surgery under anaesthesia with propofol was performed to replace the empty osmotic pump with a second one in order to deliver the antibody for another

two weeks. When the pump was localised by simple palpation, the scar was reopened and the pump was pulled out, taking great care of letting the polyethylene tube in place. Then the empty pump was removed and replaced by the full one, plugged directly on the outside aperture of the polyethylene tube. The skin was sutured, and the animal was put back in its cage and isolated a few hours. After removal of the pump, the inside bag was emptied with a syringe to check how much solution was delivered in the two preceding weeks, considering for instance the possibility of an occlusion of the catheter.

2.4: Post-lesion investigations

After recovery from the surgery aimed at damaging unilaterally the cervical cord lasting 2-3 days, the animals were subjected to daily behavioural tests in order to establish the deficits in motor control as a result of the cervical hemi-section. This post-lesion behavioural evaluation lasted several months, in order to quantify the time course and extent of motor control restitution. When behavioural scores reached a plateau, indicative of a saturation of the functional recovery, the animal was considered for the post-lesional ICMS mapping.

2.4.1: Intracortical microstimulation

To map the M1 hand area on both hemispheres (both pre- and post-lesion), tungsten microelectrodes were inserted via the chronic chambers into the motor cortex, 30 degrees from vertical which is about perpendicular to the surface of the dura mater (Fig. 2.7). Before each ICMS session the impedance of the electrode was checked, ranging from 0.1 to 0.3 MOhms, as well as its shape to avoid a bare tip exceeding 100 micrometers in length, and an eventual hook. At the beginning of the daily ICMS session, the chronic stimulation chamber was opened and the inside was cleaned with sterile compresses and Betadine. The depth "zero" along an electrode

penetration was defined as the position where the stimulating microelectrode touched the surface of the dura. The position of the electrode on the same plane than the cortical surface was selected following the rostrocaudal axis for the x-axis and the mediolateral axis for the y-axis. The parameters of stimulation were standard (Sessle and Wiesendanger 82; Rouiller et al 94a; Rouiller et al 94b; Kermadi et al 97; Liu and Rouiller 99): 35 ms duration trains of 12 electric pulses of 0.2 ms duration each were presented once every 2 seconds. ICMS was applied from starting 2 mm under the depth “zero” and then repeated at 1 mm steps in depth. At the first ICMS point, a medium current intensity level was tested (40-60 microAmps) and then the current intensity was progressively decreased to establish the threshold at which a movement could still be identified. In absence of response, a maximal of current of up to 80 microAmps was briefly applied to confirm the absence of ICMS effect. The limit in depth of the explored cortical region was considered to be reached when no responses were recorded with the intensity of 80 microAmps at two successive points in depth. The hand area in M1 was outlined by performing electrode penetrations at 2 mm steps along the medio-lateral and rostro-caudal axes. The animals were trained to let their arm being held by the experimentalist, in a relatively relaxed position. Depending on the compliance of the animal to be manipulated, up to 5 or 6 tracks were investigated in one daily session. At the end of the daily ICMS session, the inside of the chamber was cleaned with Betadine. To decrease the formation of fibrous tissue over the exposed dura-mater, a square of Silastic® was placed in contact with the dura-mater, a few drops of liquid antibiotic Nebacetine and cotton compresses were added.

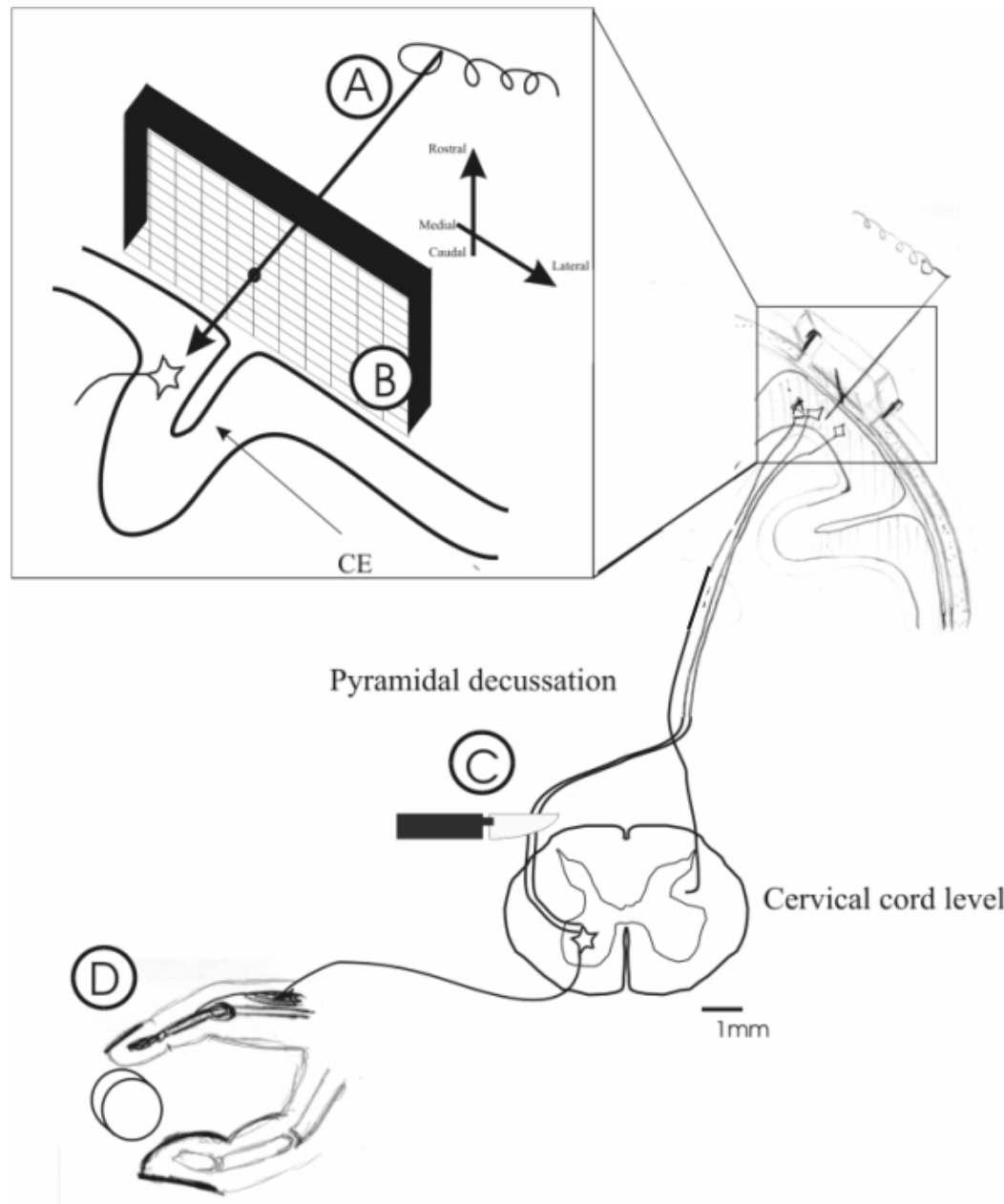


Fig. 2.7: ICMS drawing representing the intracortical microstimulation (ICMS) procedure.

A: Penetration of a microelectrode (arrow) in the motor cortex according to a x-y grid system (B) positioned with respect to the wall of the chronic chamber.

B: 2 dimensional map on the surface of the motor cortex in the rostrocaudal and mediolateral axis.

C: Spinal cord hemi-section interrupting the crossed corticospinal tract on the left side at cervical level, originating from the right hemisphere.

D: Target muscles of the interrupted corticospinal fibres.

2.4.2: Cortical inactivation experiment

To evaluate the role played by a given motor cortical area in the recovered manual dexterity after the spinal cord lesion, a restricted zone of motor cortex previously identified by intracortical microstimulation (ICMS) was transiently inactivated through in situ microinjections of a gabaergic agonist, muscimol (Kermadi et al 97). This agent was injected using a 10 μ l Hamilton micro-syringe positioned at different sites, delivering an amount of 1.5 μ l muscimol solution per site, for 2 sites along 2-5 tracks distributed in the target zone. The injection sites were usually defined in order to inactivate most of the hand area of M1, based on the expected diffusion of muscimol (2 mm around the injection site) in the cerebral cortex (Martin 1991). The animal performed the behavioural manual dexterity test with each hand before and 30 minutes after the muscimol infusion. These sessions were also video tape recorded, for off-line processing.

2.4.3: Injections of neuroanatomical tracers in the motor cortex

At the end of the post-lesional ICMS mapping sessions, tracers were injected in the cortical area of M1 responsible for hand movements, an area that has been defined by ICMS. The coordinates of the sites of injections were chosen on surface ICMS maps and depth according to the ICMS effects observed, aiming to label the entire hand area of M1. We considered that the tracers covered a distance of around 1.5 – 2 mm from an injection site for an injection of 2 μ l per site. After opening of the chamber and cleaning of the dura-mater surface, the reference point was defined in the same way described previously for ICMS procedure. The anterograde tracer injected in the right (contralesional) hemisphere was Biotinylated Dextran Amine (BDA, Molecular Probe®, 10% in saline). In the left hemisphere, the fluorescent anterograde tracer Fluorescein Dextran (Molecular Probe®, 10% in saline, 30 μ l) was injected. Sites of injection were determined based on ICMS data, both pre- and post-lesion.

2.5: Anatomical procedures

2.5.1 Sacrifice and CNS dissection

For sacrifice, sedation was first induced with ketamine, as mentioned above, followed by a deep anaesthesia obtained by i.p. injection of a lethal dose of pentobarbital (90 mg/kg). The chest of the animal was opened to access the heart. To avoid micro thrombi in vasculature during perfusion, an injection of heparin (1 ml) in the left ventricle was added before the perfusion. The animals were perfused transcardially with 0.4 litre of 0.9% saline, followed by 4 litres of fixative (4% solution of paraformaldehyde in 0.1 M phosphate buffer, pH=7.6). Perfusion was continued with 3 solutions of sucrose of increasing concentration (10% in fixative, 20 and 30 % in phosphate buffer). Care was taken to place the body of the animal in an optimal position for dissection; the head was lightly flexed on the chest to reproduce the normal angle of flexion of the cranio cervical articulation. The brain and the spinal cord were dissected and stored in a 30% sucrose solution for cryoprotection during several days.

2.5.2: Gastrocnemius muscle dissection

To analyse the loss of inputs to the distal muscles of the hind limb, the volume of both Gastrocnemius muscles was measured after perfusion. The Gastrocnemius muscle was chosen for its easiness to be retrieved. Its origin is located in the inferior part of the lateral and medial epicondyles femorales and its insertion is of the Achilles' tendon. These structures are easy to find and little inter-individual differences are due to the dissection itself. We separated the body of the muscle from the neighbouring structures (the musculus tibialis anterior and the tibial bone) and we resected it at both origin and insertion. We measured the volume of the body of the muscle by water immersion.

2.5.3: Histological sections preparation and staining

Frozen sections of the brain were cut in the frontal plane at a thickness of 50 µm. The spinal cord was cut sagittally at the site of the lesion and transversally at the level of the first cervical segments as well as of thoracic segments caudally to the lesion. The histological sections were distributed into eight series for the brain and 3 series for the spinal cervical cord.

2.5.3.1: Nissl staining

One series of section of the brain was Nissl-stained. Nissl staining consists in cresyl violet reliable and permanent stain used for light microscopy. The principle is to remove fat from tissue sections by passing through graded concentrations of ethanol solutions and rehydrated by passing the sections mounted on slides through decreasing concentration of ethanol solutions. The ethanol solutions differentiate the stain causing myelin and other fatty components to lose colour whereas pericarya retained the colour. “Like a fine wine, cresyl violet solution improves with age”.

2.5.3.2: SMI-32

One series of brain and spinal cord sections was processed to reveal SMI-32 staining. SMI-32 is an antibody that recognises specifically neurofilaments in pyramidal neurones. The sections were rinsed 2-3 times in a PBS solution and then incubated 10 min. in H₂O₂ 1.5% before being rinsed again 2 times in PBS solution. The sections were incubated for the first time overnight at room temperature in the following solution: 58.8 ml PBS-T, 1.2 ml horse serum and 20µl SMI-32 antibody. After being rinsed 3 times 10 min. in PBS solution, the sections were incubated 30 min in a solution made of 40 ml PBS, 800 µl horse serum and 200 µl biotinylated

anti-mouse solution (Vector BA 2000®). The last step was to rinse 3 times the sections in PBS solution.

2.5.3.3: Biotinylated Dextran amine (BDA)

One series of brain and spinal cord sections was processed to visualise BDA, as previously described (Rouiller et al 94a; Rouiller et al 94b). Sections were rinsed 4 times in PBS-T (phosphate buffer 0.01M pH 7.4 NaCl 0.9% and Triton 0.3%) for 30 min. The ABC reaction itself consisted in an overnight incubation at room temperature in a solution made of 10 ml PBS-T added with 2 drops of A and 2 drops of B. The DAB reaction revealed the staining and consisted in letting the sections 20 min in a solution made of 20 ml phosphate buffer 0.1 M at pH 7.4, 10 mg DAB and 660µl H₂O₂ 0.3%. Finally, the sections were rinsed 3 times in phosphate buffer 0.1 M at pH 7.4.

2.5.3.4: Anti-fluorescein reaction

One series of brain and spinal cord sections were processed to visualise Fluorescein dextran. The sections were rinsed 3 times in TBS-T solution: Tris HCl, 0.05 M NaCl 0.9% and Triton 0.3%, pH 8.0. Then the sections were incubated overnight at room temperature in the first antibody: anti-fluorescein (rabbit IgG 40 µl) 1:250 in TBS-T (10 ml). They were then rinsed 2 times 10 min in TBS-T and 1 time 10 min in phosphate buffer.

The ABC reaction is the same as described in 2.5.3.3. The sections were washed 2 times in 0.1 M phosphate buffer at pH 7.4, 1 time in distilled water and 2 times in 0.05 M cacodylate buffer at pH 7.2. The DAB reaction started with pre-incubation in DAB solution made of 40 ml 0.05 M cacodylate buffer pH7.2 added with 20 mg DAB. The sections were then incubated 5 to 15 min in 10 ml DAB solution added with 200 µl H₂O₂. They are washed then 3 times in 0.05 M cacodylate buffer, 1 time in distilled water and 1 time in phosphate buffer 0.1 M at pH 7.4. TBS

is preferable over phosphate buffer to avoid formation of ionic complexes such as calcium or magnesium.

2.5.4: Reconstruction of the spinal cord lesion

The lesion site was reconstructed from camera lucida drawings of individual consecutive sagittal Nissl-stained sections of the spinal cervical cord. An alignment of the drawings allowed reconstruction of the location and extent of the lesion on a frontal view of the spinal cervical cord.

2.5.5: Morphometrical analysis

To evaluate the effect of the cervical hemi-section on CS neurones in the motor cortex in both hemispheres, we selected a few coronal sections through motor cortical areas where no electrode penetration had been made for ICMS. These areas were located in the medial wall of the gyri praecentralis in M1 and more rostrally, in the supplementary motor area (SMA). On SMI-32 stained material, well stained lamina V pyramidal cells were easily identifiable even using low magnification (x100). They were counted on sections covering a large part of the rostrocaudal extension of the medial M1 and SMA, and their number was plotted. Since, particularly in the contralateral M1, some cells were faintly stained and would have escaped observation at low magnification; this analysis was repeated on some sections using a higher magnification (x400) which led to a better identification. The number of SMI-32 stained lamina V cells and the projected surface of their cell body were obtained from digitised photomicrographs using appropriate software (Olympus DP 10® and Neurolucida®). The neurones included in this analysis were SMI-32 positive, had a visible nucleus and were located in layer V. Because of the presence of large apical dendrites, the limits of the soma along their

axis was sometimes difficult to define, we therefore considered that along large apical dendrites, the soma ended at a distance of 20 μm from the nucleus.

List of references for chapter 2

- 1: Jenny,A.B. & Inukai,J. (1983) Principles of motor organization of the monkey cervical spinal cord. *Journal of Neuroscience*, **3**, 567-575.
- 2: Kazennikov,O., Wicki,U., Corboz,M., Hyland,B., Palmeri,A., Rouiller,E.M. & Wiesendanger,M. (1994) Temporal structure of a bimanual goal-directed movement sequence in monkeys. *Eur.J.Neurosci.*, **6**, 203-210.
- 3: Kermadi,I., Liu,Y. & Rouiller,E.M. (2000) Do bimanual motor actions involve the dorsal premotor (PMd), cingulate (CMA) and posterior parietal (PPC) cortices? Comparison with primary and supplementary motor cortical areas. *Somatosensory and Motor Research*, **17**, 255-271.
- 4: Kermadi,I., Liu,Y., Tempini,A., Calciati,E. & Rouiller,E.M. (1998) Neuronal activity in the primate supplementary motor area and the primary motor cortex in relation to spatio-temporal bimanual coordination. *Somatosens.Mot.Res.*, **15**, 287-308.
- 5: Kermadi,I., Liu,Y., Tempini,A. & Rouiller,E.M. (1997) Effects of reversible inactivation of the supplementary motor area (SMA) on unimanual grasp and bimanual pull and grasp performance in monkeys. *Somatosens.Mot.Res.*, **14**, 268-280.
- 6: Liu,J., Morel,A., Wannier,T. & Rouiller,E.M. (2002) Origins of callosal projections to the supplementary motor area (SMA): A direct comparison between pre-SMA and SMA-proper in macaque monkeys. *Journal of Comparative Neurology*, **443**, 71-85.
- 7: Liu,Y. & Rouiller,E.M. (1999) Mechanisms of recovery of dexterity following unilateral lesion of the sensorimotor cortex in adult monkeys. *Experimental Brain Research*, **128**, 149-159.
- 8: Rouiller,E.M., Babalian,A., Kazennikov,O., Moret,V., Yu,X.-H. & Wiesendanger,M. (1994a) Transcallosal connections of the distal forelimb representations of the primary and supplementary motor cortical areas in macaque monkeys. *Experimental Brain Research*, **102**, 227-243.
- 9: Rouiller,E.M., Liang,F., Babalian,A., Moret,V. & Wiesendanger,M. (1994b) Cerebellothalamocortical and pallidothalamocortical projections to the primary and supplementary motor cortical areas: A multiple tracing study in macaque monkeys. *Journal of Comparative Neurology*, **345**, 185-213.

- 10: Rouiller,E.M., Yu,X.H., Moret,V., Tempini,A., Wiesendanger,M. & Liang,F. (1998) Dexterity in adult monkeys following early lesion of the motor cortical hand area: the role of cortex adjacent to the lesion. *Eur.J.Neurosci.*, **10**, 729-740.
- 11: Sessle,B.J. & Wiesendanger,M. (1982) Structural and functional definition of the motor cortex in the monkey (macaca fascicularis). *J.Physiol.(London)*, **323**, 245-265.

Chapter 3: Consequences of a unilateral section of the spinal cord at cervical level in primate: untreated (“control”) monkeys _____ 121

3.1: Introduction	121
3.2: Results	121
3.2.1: Anatomical data	121
3.2.1.1: Do CS neurones whose axon has been severed in the cervical cord degenerate?	125
3.2.1.2: Effect of the lesion on the rubrospinal tract	133
3.2.2: Behavioural data	135
3.2.2.1: General aspects immediately after the spinal cord lesion	135
3.2.2.2: Manual dexterity	135
3.2.2.3: Qualitative behavioural test:	146
3.2.3: ICMS data	152
3.2.3.1: Mapping of M1 hand area before and after cervical cord lesion in the contralateral hemisphere	152
3.2.3.2: Mapping of M1 hand area in the ipsilesional hemisphere	158
3.2.3.3: Comparison of thresholds in the contralesional hemisphere	162
3.2.3.4: Progressive changes of ICMS effects during the recovery period	164
3.2.3.5: Time course of ICMS changes and time course of behavioral recovery	167
3.2.3.6: Does the progressively re-established hand area contribute to the recovery	169
3.3: Discussion:	170
3.3.1: Discussion related to the anatomical data (fate of CS neurones after cervical cord lesion)	170
3.3.1.1: Extent of the cervical lesion	170
3.3.1.2: Soma area measurement	171
3.3.1.3: Technical considerations	172
3.3.1.4: CS cells survival after transection of the CS tract: comparison with previous studies	172
3.3.1.5: Considerations related to the recovery from CS tract lesion	176
3.3.2: Discussion related to the ICMS data (plasticity of motor cortical maps induced by the cervical lesion)	178
3.3.2.1: Technical considerations	178
3.3.2.2: Pathways affected by the lesion:	179
3.3.2.3: Extent and time course of functional recovery	181
3.3.2.4: Mechanisms of functional recovery:	182

Chapter 3: Consequences of a unilateral section of the spinal cord at cervical level in primate: untreated (“control”) monkeys

3.1: Introduction

This chapter presents the results obtained in two control animal experiments: Ctrl1 and Ctrl2. A first anatomical sub-chapter will describe the extent and the location of the cervical cord hemisection with the consequences in the cerebral cortex of the unilateral interruption of the corticospinal tract. The second sub-chapter presents the behavioural results subdivided in two categories: quantitative and qualitative tests of motor control. Finally, the last sub-chapter will present the electrophysiological data. The results are discussed at the end of this chapter.

3.2: Results

3.2.1: Anatomical data

Anatomical data derived from previous experiments and from the two control monkeys included in the present study provided a basis to address basic issues related to spinal cord lesions. First of all, the precise location of the CS axons in the cervical enlargement of normal monkeys was derived from material obtained in a previous study (Rouiller et al 96). In this study, two intact macaque cynomolgus monkeys were subjected to a unilateral injection of the anterograde tracer BDA in the hand representation of M1 or SMA. In the animal where BDA was injected in the M1 hand representation, BDA-labelled CS axons formed three groups of fibres in the cervical cord (Fig. 3.1A). The majority of CS fibres occupied the contralateral dorso-lateral funiculus, representing in this animal 86% of all CS fibres labelled. Also in the dorsolateral funiculus, but ipsilaterally with respect to the injection in M1, CS axons were observed, representing a proportion of 11.6%. Finally, a relatively small tract of BDA-labelled

CS fibres was found in the ipsilateral ventral funiculus (2.4%). This distribution of CS axons at cervical level is largely consistent with that observed at lumbar level as a result of massive BDA injection in the M1 hindlimb area in macaque monkeys (Lacroix et al 04).

For ethical reasons and in order to maintain proper post-lesion health conditions, the lesion of the cervical cord was limited to one side and focussed on the main CS tract running in the dorsolateral funiculus. For both lesioned animals, the extent of the lesion was assessed by reconstructing the incision site from histological sections (Fig. 3.1B). In the first animal (Ctrl1; top panel in Fig. 3.1B), the knife penetrated near the insertion site of the dorsal rootlets and travelled ventrally down to the ventral side of the spinal cord. It cut most of the left dorsolateral funiculus, the lateral part of the ventral horn and the white matter lying immediately ventrally to the latter. The dorsal, the ventromedial and lateral parts of the ventrolateral funiculi were preserved. This knife cut thus sectioned most if not all of the CS fibres descending through the left dorsolateral funiculus (whose position in a normal animal is shown in Fig. 3.1A), but preserved the fibres on the opposite side. In the second animal (Ctrl2; bottom panel of Fig. 3.1B), the section was larger and only the dorsal and the ventromedial funiculi were preserved on the lesioned side.

BDA has been injected in the M1 hand region in order to confirm that the CS tract has been interrupted by the lesion. However, despite transport times of 21 (Ctrl1) and 36 days (Ctrl2), BDA did not reach the level of the lesion, and its transport could only be demonstrated from the site of injection down to the first cervical segments.

SMI-32 also stained axons of lamina V pyramidal cells in the white matter under the cerebral cortex. Therefore, we treated spinal cord sections with SMI-32 to determine if this marker also stained the distal part of the axon and, if yes, whether this labelling can be used to assess the extent of the lesion. In both lesioned monkeys, on a transverse spinal cord section at thoracic level, the dorso-lateral funiculus on the side contralateral to the lesion contained

numerous stained axons (Fig. 3.1E). In contrast, no or rare stained axons were seen in the dorsal and dorsolateral funiculi on the side of the lesion (Fig. 3.1D). On transverse sections taken from the first cervical segments, stained CS axons were observed bilaterally in the dorsolateral funiculus. On sagittal sections at the level of the lesion, numerous stained fibres were seen in the dorsolateral funiculus rostrally to the lesion, whereas very few remained visible in the dorsolateral funiculus caudally to the lesion (Fig. 3.2). This observation suggests that the section interrupted most of the portion of the CS tract running in the dorsolateral funiculus unilaterally. All stained CS axons ended at the level of the knife-cut and the tip of some of them was swollen corresponding to retraction bulbs, indicative of a retraction process. To clarify if some spontaneous regeneration of the severed axons had occurred, we looked for the presence of processes crossing the site of the knife-cut as well as for axons bending away from their normal course to turn around the lesion. Neither SMI-32 labelled fibres crossing the knife-cut nor bent axons in the dorsolateral funiculus were observed. However, some few darkly stained processes were sometimes seen locally at the level of the lesion. As the intensity of their staining was different from that observed in CS axons in the dorsolateral funiculus, but was similar to that of dendrites in the adjacent grey matter, these structures were assumed to be dendrites of local neurones extending into the damaged tissue.

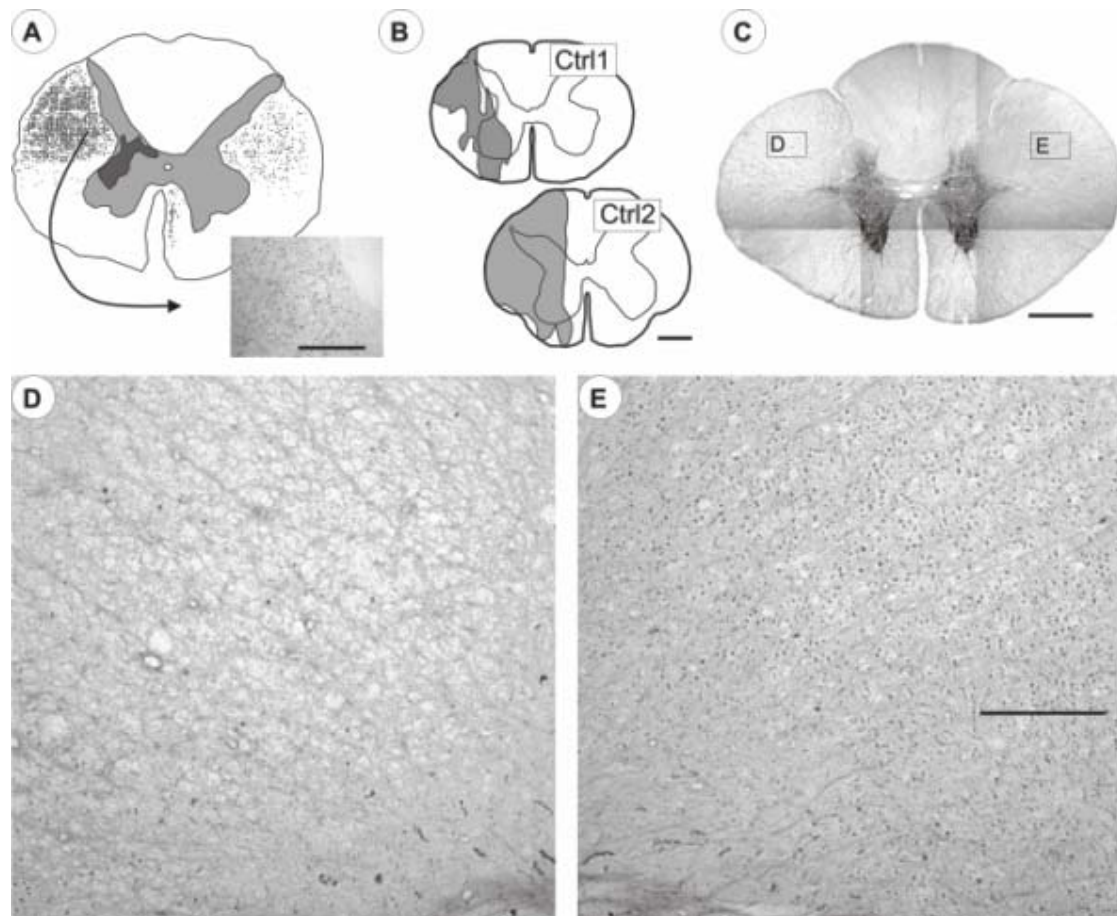


Fig. 3.1: Anatomy of spinal cord

A: Cross-section of the cervical spinal cord at the upper part of the cervical enlargement showing the distribution of BDA labelled CS axons as a result of BDA injection in the right M1 of an intact monkey. These data were derived from a previous set of experiments (Rouiller et al 96). In the white matter, each labelled CS axon is represented by a dot corresponding to the position of its cut diameter when focussing on top of the section. The light grey area corresponds to the grey matter. The dark grey spot indicates the position of ramifying CS axons in the grey matter, thus forming a dense terminal field where boutons are visible. As indicated by the arrow, a small region of the section is illustrated by a photomicrograph, on which one sees a part of the dorsolateral funiculus and a portion of the grey matter in the dorsal horn (upper right part of the photomicrograph). In the white matter, the cut CS axons labelled with BDA appear as black dots. See text for detailed and quantitative descriptions. Scale bar: 500 μ m.

B: Location and extent of the lesion (grey area), performed at C7 in Ctrl1 (top section) and Ctrl2 (bottom section). Scale bar = 2 mm.

C: Frontal section of the spinal cord processed for SMI-32, on which rectangles display the position of the photomicrographs shown in panels D and E. Scale bar: 1 mm.

D and E: Density of SMI-32 stained CS axons in the left and right dorsal funiculi caudal to the left hemi-section. Labelled CS axons appear as black dots. Note the paucity of CS axons below the lesion on the left side (D) in contrast to the right unlesioned side (E). Scale bar: 200 μ m.



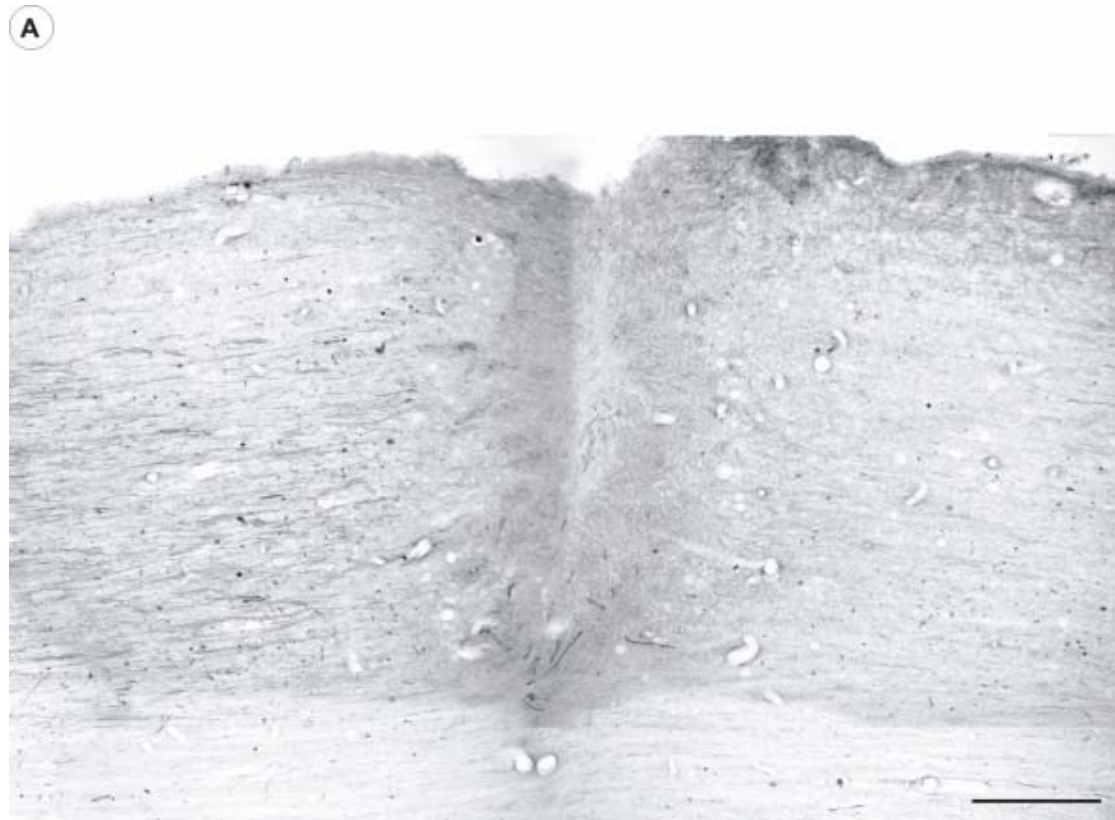
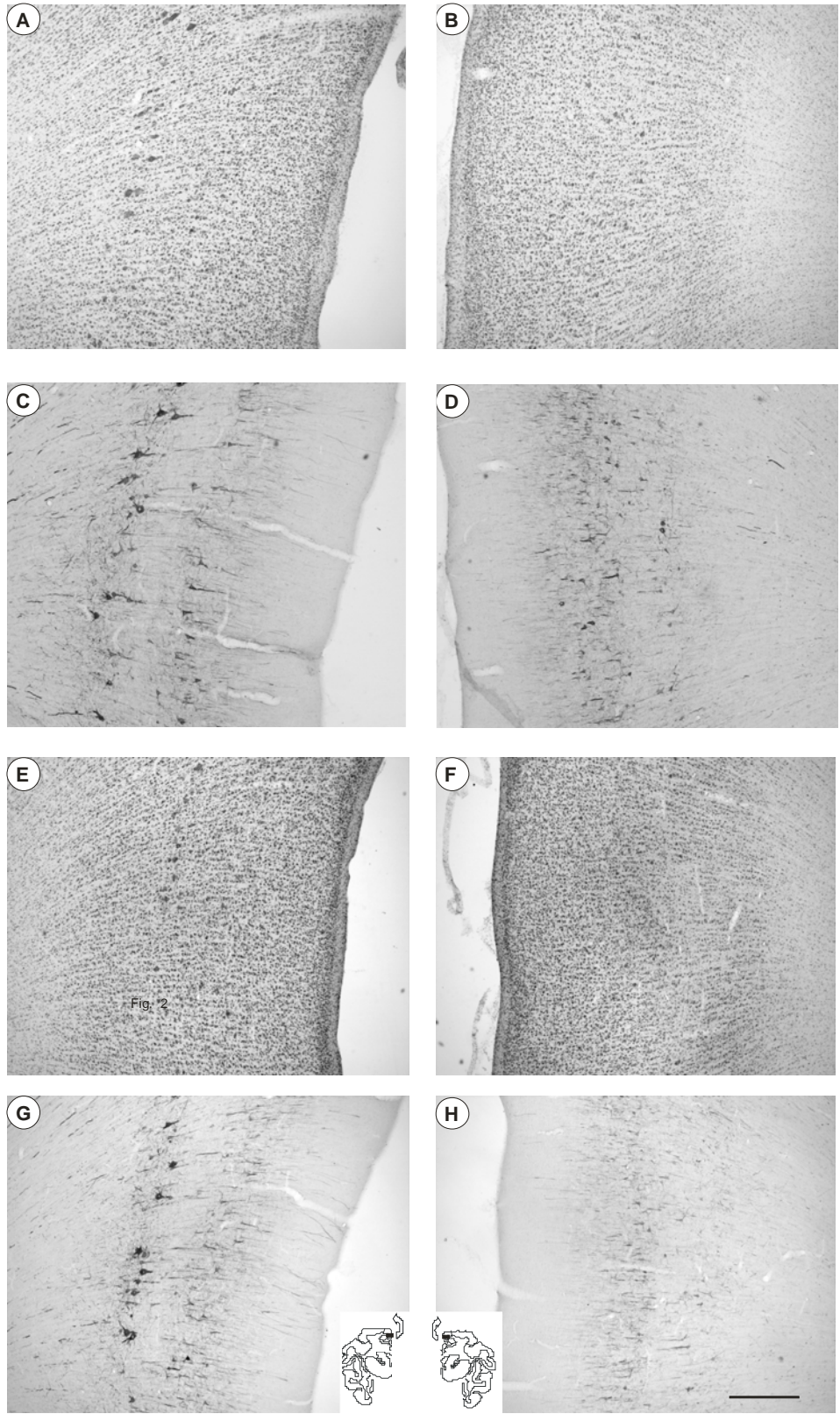


Fig. 3.2 : Saggital section of the spinal cord taken at the level of the lesion (arrow) in Ctrl2. Note on the left (rostral to the lesion) the presence of numerous SMI-32 stained CS axons, whereas on the right (caudal to the lesion) no CS axon is visible, except a few labelled processes ventrally most likely corresponding to dendrites (see text). Scale bar: 500 μ m.

3.2.1.1: Do CS neurones whose axon has been severed in the cervical cord degenerate?

To address this question, coronal sections of the brain of the two lesioned monkeys were processed for Nissl or for SMI-32 staining. The hand region of motor cortex which has been affected by the repeated penetrations of tungsten electrodes during the electrophysiological mapping and subjected to an injection of BDA was not suitable for such an analysis. However, CS neurones in M1 represent about 35% of the whole population, the remaining CS neurones being dispersed mainly among non-primary motor areas, such as the caudal portion of the supplementary motor cortex (SMA-proper), the premotor cortex (PM), the cingulate motor areas (CMA), and somatosensory areas. The analysis focussed on the most medial part of M1, whose

vertical position above the cingulate sulcus allowed an easy comparison between the two hemispheres on the same coronal section. This M1 region contains CS neurones which normally project down to the lumbar segments but whose axons have been sectioned by the cervical lesion. The analysis was extended rostrally to include SMA-proper and pre-SMA. To avoid counting bias related to the presence of cortex curvatures, the quantitative analysis was restricted to regions where the cell columns are perpendicular to the cortex surface. On Nissl-stained sections, M1 (Fig. 3.3 A) and SMA-proper (Fig. 3.3 E) ipsilateral to the cervical lesion were characterised by the presence of numerous and large perikaria in layer V (typical pyramidal cells), the layer of origin of the CS tract. In the contralateral M1 (Fig. 3.3 B) and SMA proper (Fig. 3.3F), in contrast, the layer V appeared strongly impoverished of large pyramidal cell bodies. The same observations were made on SMI-32 stained material (Fig. 3.3 C and D for M1 and 3.3 G and H for SMA-proper). To clarify if CS neurones were more affected than other lamina V neurones, the number of SMI-32 stained neurones in lamina V of SMA-proper and pre-SMA was compared between both hemispheres because it is known that pre-SMA does not contain CS neurones (Luppino et al 94). In pre-SMA, the number of SMI-32 positive neurones was relatively low, but comparable for the two hemispheres (Fig. 3.3 I). In contrast, in SMA-proper, the number of positive neurones was lower in the contralateral SMA-proper than in its counterpart (Fig. 3.3 I). A similar tendency in term of hemispheric difference was found for the number of SMI-32 positive neurones in CMA (not shown).



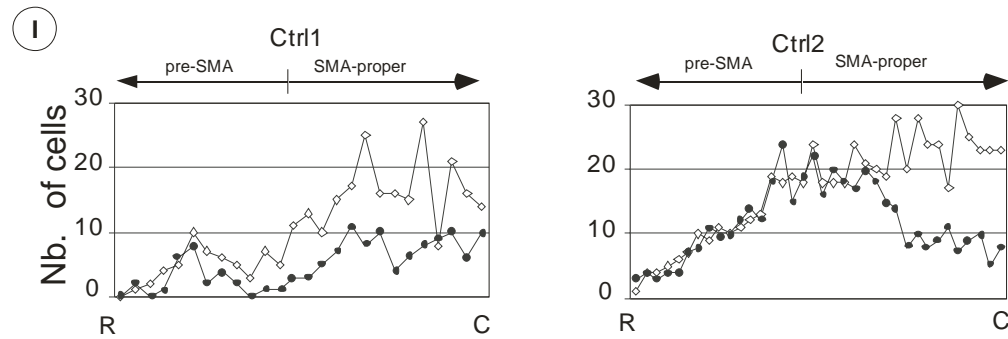


Fig. 3.3: A, B, C and D: Photomicrographs showing a part of M1 on both hemispheres in Ctrl 1 on Nissl-stained (A and B) or on SMI-32 treated (C and D) histological sections. Note that the number of large Nissl-stained as well as large and darkly positive SMI-32 neurones in layer V was clearly higher in the left hemisphere (A and C) as compared to the right hemisphere (B and D), as a result of a left hemi-section of the cervical cord at C7. Section C/D is adjacent to section A/B. D,E,F and G: Photomicrographs showing a part of SMA-proper in Ctrl 1 on Nissl-stained (D and E) or on SMI-32 treated (F and G) histological sections.

I: Number of SMI-32 positive neurones observed with a magnification of 40x in layer V in pre-SMA and SMA-proper in Ctrl1 and Ctrl2 on individual sections arranged from rostral (R) to caudal (C) along the abscissa. Open diamonds are for the (left) hemisphere, homolateral to the cervical lesion, whereas filled dots are for the hemisphere contralateral to the lesion.

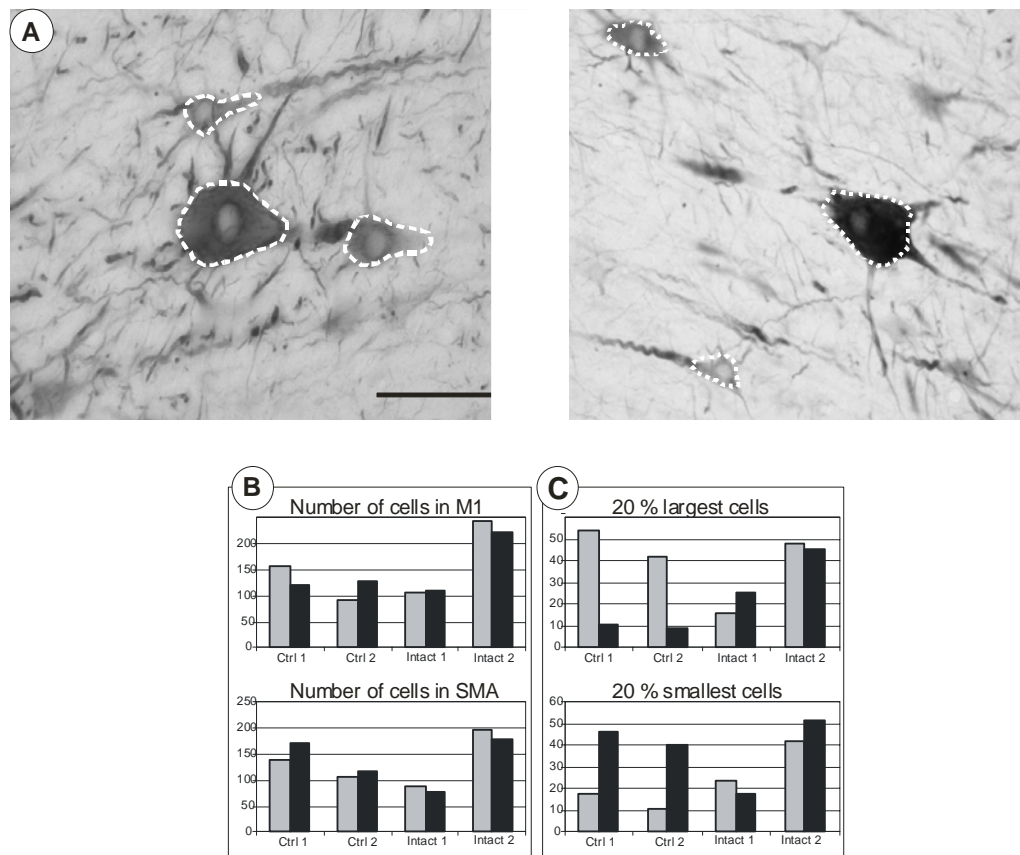


Fig. 3.4:

A: Photomicrograph of SMI-32 stained pyramidal cells in layer V of M1 on the left hemisphere (left panel) and on the right hemisphere (right panel), illustrating the typical staining restricted to pyramidal cells with their axons and dendrites. The three neurones are representative of the cell body sizes frequently met during the analysis. The nucleus and the apical dendrite directed to the right are easily identifiable. The dashed outline illustrates the criteria applied in order to define the soma area (see methods). Scale bar: 50 μ m.

B: Total number of SMI-32 stained cells in layer V of M1 and SMA-proper in the two lesioned monkeys (Ctrl1, Ctrl2) and, for comparison, in two intact monkeys, in the left (grey) and right (black) hemispheres. For the two lesioned monkeys, the right hemisphere is contralateral to the cervical lesion. Due to the relative large difference of the size of the analysed cortical region from one animal to another the total number varied from one animal to the next. However, there was no substantial difference between the two hemisphere within each animal.

C: Same data as in B, but only the numbers of SMI-32 stained neurones belonging to the 20% lowest or upper percentiles with respect to their somatic size are indicated for each hemisphere. Clearly, the two lesioned monkeys showed a predominance of smallest neurones in the right hemisphere (black) whereas the largest neurones were found more frequently on the left hemisphere (grey).

These observations suggest that the large pyramidal cells of layer V in the contralateral hemisphere have degenerated as a result of the cervical lesion. However, as an alternative

explanation, the neurones could also have shrunken and/or reduced their expression of non-phosphorylated neurofilaments, thereby losing their strong SMI-32 staining. In fact, in the two lesioned monkeys, faintly stained neurones were rather frequent in the contralateral M1 and SMA (Fig. 3.4A) and they could have escaped from the counting procedure which was done observing the sections with a low magnification factor (40x). The lamina V neurones were therefore re-counted and their surface measured on several sections using a higher magnification factor (400x).

The analysis was conducted in the two lesioned monkeys (Ctrl 1 and Ctrl 2) and, for comparison, on material taken from two unlesioned animals (Intact1, Intact2). For each monkey, the total number of SMI-32 positive neurones in layer V was comparable between the two hemispheres (Fig. 3.4B). To investigate whether CS cells' shrinkage took place as a result of the cervical lesion, measurements of soma areas were performed in each hemisphere, separately for M1 and SMA-proper (Fig. 3.5). In M1, the box plot distribution shows that the somatic cross-sectional areas in the two intact monkeys do not differ significantly between the left and the right hemispheres. In contrast, in the two lesioned (untreated) animals (Ctrl 1 and Ctrl 2), the somatic cross-sectional areas of the SMI-32 positive neurones in layer V were significantly smaller in the (right) hemisphere affected by the cervical hemisection than in the (left) ipsilesional hemisphere (Fig. 4, top panel). In SMA-proper, no statistically significant difference of somatic cross-sectional area was observed between the two hemispheres in both intact and lesioned monkeys (Fig. 3.5, bottom panel). For each monkey, the soma area values were stored in an Excel file, and ranked from the smallest to the largest. For each soma area value, it was kept track whether the corresponding SMI-32 positive layer V neurone was located in the ipsilateral versus contralateral hemisphere with respect to the lesion. Two sub-populations of layer V neurones, each amounting to 20% of the cells of the whole population, were then investigated separately. The first one pooled the neurones with the lowest soma areas, the second one, those with the largest soma

areas. The numbers of neurones from each hemisphere in each of these 2 sub-populations were calculated and plotted. For the lesioned animals (Ctrl 1 and Ctrl 2), the results indicate that the majority of the largest cells were located in the ipsilateral hemisphere and that the majority of the smallest neurones were located in the contralateral hemisphere, with respect to the cervical lesion (Fig. 3.4 C). These differences were statistically significant (Chi-square test, $p < 0.05$). For the unlesioned animals such differences were not observed (Chi-square test, $p > 0.05$), and some areas were comparable in both hemispheres. These data therefore indicate that following a section of their axon in the cervical cord, the CS neurones underwent histological changes, such as shrinkage of their soma and/or a reduction of expression of non-phosphorylated neurofilaments. In contrast, no massive neuronal cell death could be demonstrated, since there was no significant decrease of the cell number in the hemisphere contralateral to the lesion.

To clarify if the changes were restricted to lamina V or if they also affected lamina III neurones, the staining density of four microphotographs of the left and right M1 have been calculated and compared. The results indicate that the mean density was comparable in both hemispheres for layers I to IV, but decreased for layer V in the contralateral hemisphere as compared to the ipsilateral one (Fig. 3.5). This observation thus supports the idea that the shrinkage of soma and reduction of SMI-32 expression occurs essentially in layer V, most likely in CS axotomised neurones.

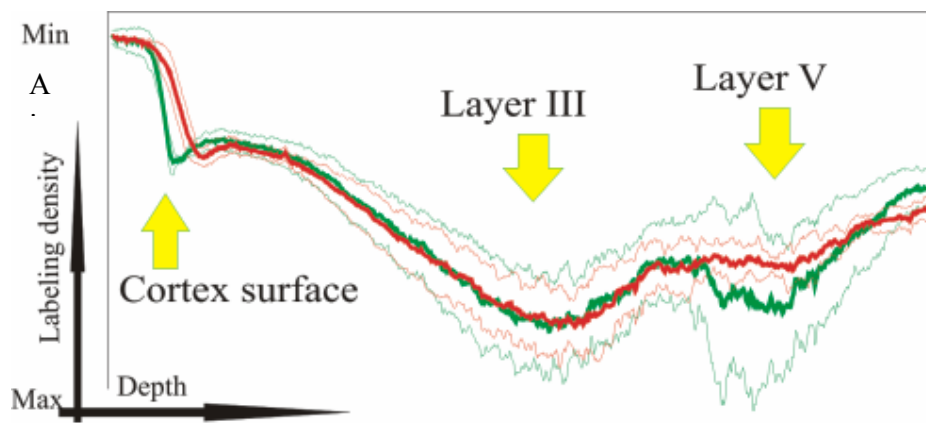


Fig. 3.5 A: Pixel density analysis along an axis perpendicular to the cortical surface on frontal sections of M1 stained with an antibody directed against neurofilaments of pyramidal cells (SMI-32). Data for the left hemisphere (homolateral to the lesion) are represented by the red lines, whereas the green lines are for the right hemisphere (contralateral to the lesion). The average density values (thick lines, with standard deviations represented by the thin lines) exhibit a comparable peak of high density of SMI-32 staining in layer III of both hemispheres. In contrast, the peak of high density of SMI-32 staining in layer V is present only in the left hemisphere but not in the right hemisphere. This result supports the notion that the decrease of SMI-32 staining is limited to layer V of the contralesional side.

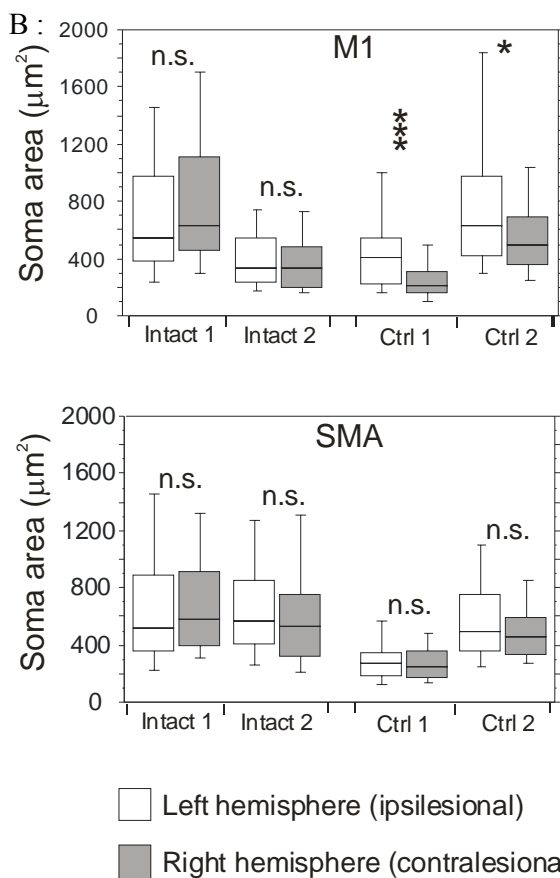


Fig. 3.5 B: Box plots showing the distribution of somatic cross-sectional areas of SMI-32 positive neurons in layer V in M1 (top panel) and SMA-proper (bottom panel) for two intact animals (Intact 1 and Intact 2) and for the two lesioned (untreated) monkeys (Ctrl 1 and Ctrl 2). The soma areas did not follow a normal distribution and therefore were graphically represented in the form of box plots (putting emphasis on the median value rather than the mean value). Accordingly, the statistical analysis was conducted using a non-parametric unpaired test (see below). In the box plots, the horizontal line in the box corresponds to the median value, whereas the top and bottom of the box are for the 75 and 25 percentile values

respectively. The top and bottom extremities of the vertical lines on each side of the box are for the 90 and 10 percentile values, respectively. The white boxes are for the left hemisphere, ipsilateral to the cervical hemisection in the 2 lesioned monkeys. The gray boxes are for the right hemisphere, opposite to the lesion in the 2 lesioned monkeys. A statistical comparison between the two hemisphere was conducted for each animal using the non-parametric Mann and Whitney test. In M1, the two lesioned monkeys exhibited a significant difference of soma area across hemispheres ($*=p<0.01$; $***=p<0.0001$), whereas the other comparisons did not show any statistically significant difference ($n.s.=p>0.05$).

3.2.1.2: *Effect of the lesion on the rubrospinal tract*

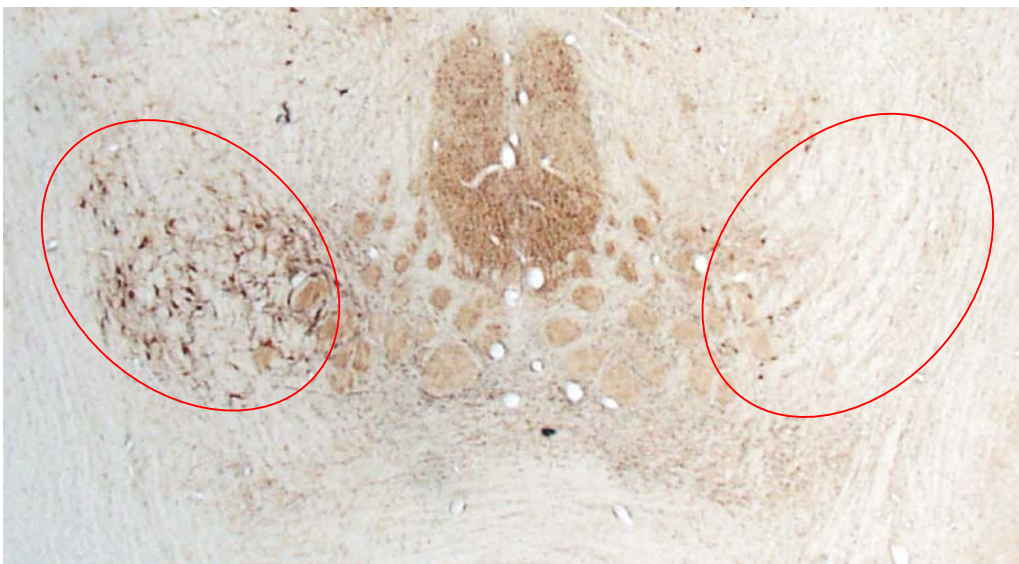


Fig. 3.6: A representative SMI-32 stained section through the middle part of the red nucleus pars magnocellularis in Ctrl2 (Red circle). Note the difference in the number of SMI-32 stained cells between the left and right red nucleus.

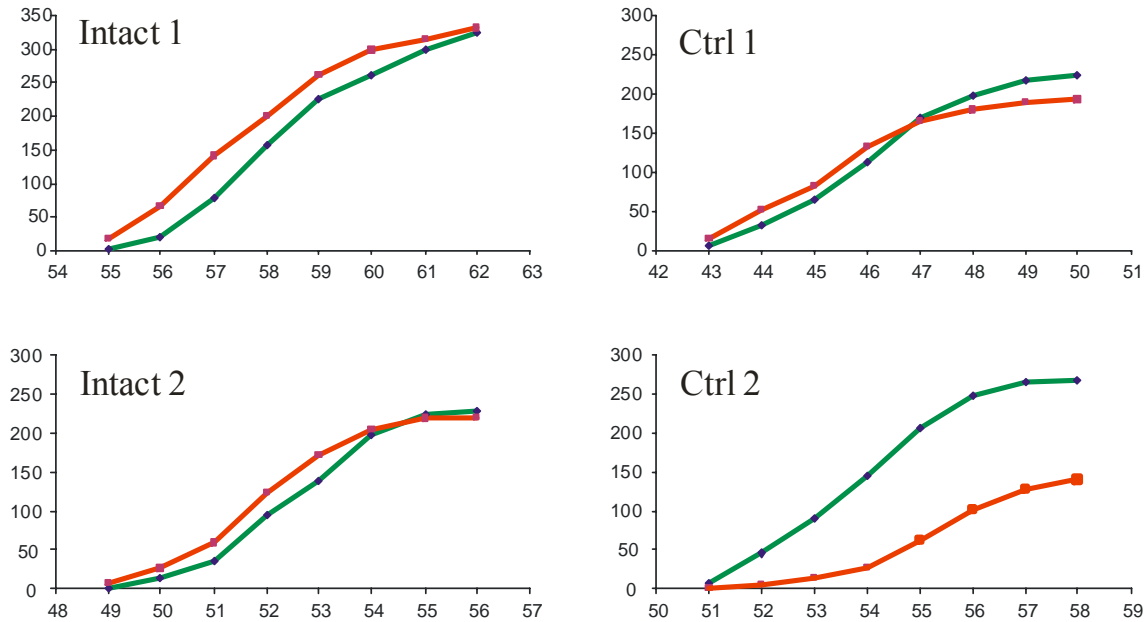


Fig 3.7: Cumulative number of SMI-32 stained neurones in the red nucleus along the rostro-caudal axis.

In Ctrl 1, the lesion spared the ventrolateral part of the cervical white matter leaving most rubrospinal axons intact. In contrast, the larger lesion in Ctrl 2 interrupted many rubrospinal axons leading to a marked decrease of SMI-32 labelling in the contralateral RN. The abscissa axis represents the sections number and the ordinate axis represents the number of SMI-32 neurones. The green diamonds represent the number of SMI-32 neurones in left RN (ipsilesional) and the red squares represent the number of neurones in the right RN (contralesional).

In Ctrl 2, the Red Nucleus contralateral to the cervical hemisection showed, in SMI-32 stained sections, a decrease of SMI-32 stained cells in the Magnocellular part (Fig. 3.6) in comparison to the ipsilateral red nucleus. The quantitative data in Figure 3.7 show that the contralateral Red Nucleus has been affected by the hemisection in a greater extent in Ctrl 2 than in Ctrl 1, the latter animal exhibiting a number of SMI-32 neurones in the red nucleus on both sides close to the unlesioned animals (Intact 1 and 2). The difference between Ctrl 1 and Ctrl 2 is thus consistent with the larger size of the cervical lesion in the latter animal, thus affecting a larger portion of the rubrospinal tract in Ctrl 2 than in Ctrl 1.

3.2.2: Behavioural data

3.2.2.1: General aspects immediately after the spinal cord lesion

The two lesioned monkeys (Ctrl 1 and 2) woke up normally about one hour after the end of the propofol anaesthesia when they returned to their cage. When awake, the animals sat in the cage, in an abnormal and asymmetric position, resulting from a prominent and remaining stretching of the hindlimb ipsilateral to the cervical lesion. In addition, an immediate paresis of the elbow, wrist and hand was observed. Consequently, the animals were strongly handicapped for maintaining the standing posture and for walking. The ipsilesional forelimb was maintained in a flexed position at the level of the elbow and the fingers were all flexed and unused when food was presented to the animal. Movements of the ipsilesional shoulder were preserved. In contrast, no deficit was observed for the forelimb and hindlimb contralateral to the lesion. A few hours after, if forced to use the affected hand, the animal was able to catch a large piece of fruit by pushing further and altogether the flexed fingers in direction of the palm of the hand. No precision grip movement of the fingers was possible during a few days. In addition, the function of the urinary bladder remained under voluntary control and no incontinence was observed.

3.2.2.2: Manual dexterity

To assess the functional impairment following a lesion of the dorsolateral funiculus tract at cervical level on the left side, the manual dexterity of the animals was quantitatively tested with the modified Brinkman board task and the “drawer” task. In the first task, the animals had to retrieve food pellets from 50 slots randomly distributed, 25 vertically oriented and 25 horizontally oriented. In the second one, the animals had to unimanually open a drawer and retrieve a food reward (see methods).

3.2.2.2.1: "Modified Brinkman board»

To quantify the manual dexterity of the monkeys performing the precision grip task, we analysed off-line the video recordings of the performances of the monkeys in the modified Brinkman board task. We quantified two indexes of performances: the number of successfully retrieved pellets within a certain time (45 seconds) and the time in milliseconds spent by the fingers (mainly the index finger) in each well to perform the precision grip. A score of 0 in the first analysis can be due either to a devastating motor deficit or to lack of motivation to perform the task. These two interpretations can be distinguished in the second analysis, as the monkey will spend time in the wells if motivated to try to grasp pellets even if impaired whereas in case of lack of motivation the time spent in the wells remains equal to zero.

First quantitative evaluation of the Brinkman board: nb of pellets retrieved

The main axis of the behavioural evaluation after unilateral cervical lesion is the comparison of performance for the ipsilesional hand before versus after lesion. Even though, a comparison between both hands in each animal is useful to show the unilateralism of the lesion and to confirm that the decrease of the daily performance is not due to a lack of motivation but to motor impairment.

The results shown in Figure 3.8 represent the performance in precision grip task of each hand for monkey Ctrl 1 from 60 days before the cervical lesion until reaching a new plateau of performance after recovery, about 100 days post-lesion. The reference day (day 0) is the day when the cervical cord lesion took place. Each dot corresponds to the number of successfully retrieved pellets by each hand (right hand in green and left hand in red) within 45 seconds in each daily session. During the pre-lesion period, the performance of each hand slightly increased

to reach a plateau, indicative of a relatively modest training effect. In Ctrl 1, immediately after the spinal cord lesion, the left hand (ipsilateral to the lesion) showed a complete deficit of motor performance (behavioural score = 0) while the right hand (contralateral to the lesion) showed a modest deficit of 10%. During the two weeks post-lesion, the affected hand recovered most of its ability to perform the precision grip, reaching up to 80 % of its pre-lesion score, while the contralateral hand rapidly returned to a performance nearly similar to the pre-lesion score.

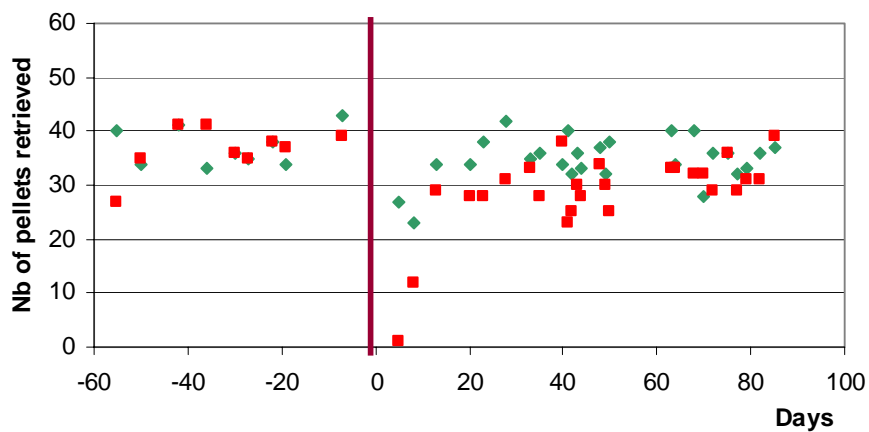


Fig. 3.8: Precision grip scores of monkey Ctrl 1 using the right hand (green squares) or the left hand (red diamonds; affected by the lesion), 60 days before the spinal cord lesion up to 90 days after. Vertical and horizontal wells were pooled together.

No significant differences in the precision grip score between the right and the left hand were observed in the period of stable performance immediately before the spinal cord lesion.

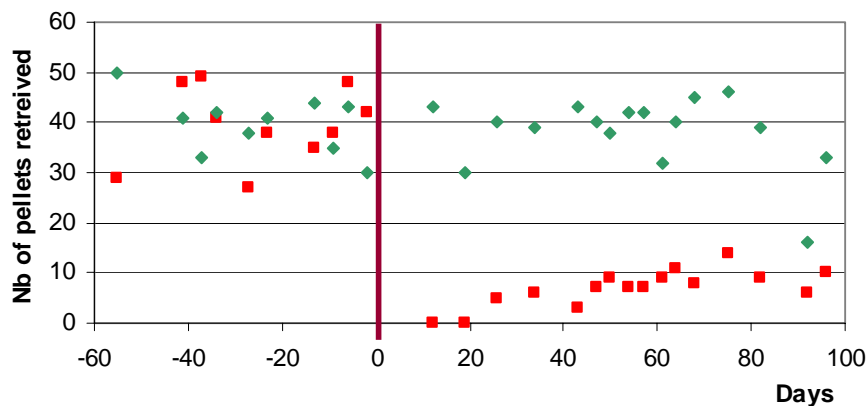


Fig. 3.9: Precision grip performances of monkey Ctrl 2. Same conventions as in Fig. 3.8. Vertical and horizontal wells were pooled together.

Considering the plateau level reached after the spinal cord lesion, monkey Ctrl 1 recovered almost completely. Furthermore, the recovery was very rapid, since already three weeks after the spinal lesion the animal reached with the affected hand a score of about 80 %, as compared to the pre-lesion score. Nevertheless, the video recordings of monkey Ctrl 1 eighty-five days after the lesion revealed a dexterous use of the index finger with fine extension and flexion, associated however with a slightly diminished thumb use.

In monkey Ctrl 2 the contralesional hand was not affected by the lesion, whereas the ipsilesional hand was clearly affected (Fig. 3.9). The time course of functional recovery for the affected hand was shorter for Ctrl 1, namely less than three weeks after the spinal cord lesion for Ctrl 1, as compared to the two months needed to Ctrl 2 to reach a plateau at about 25 % of the pre-lesion score.

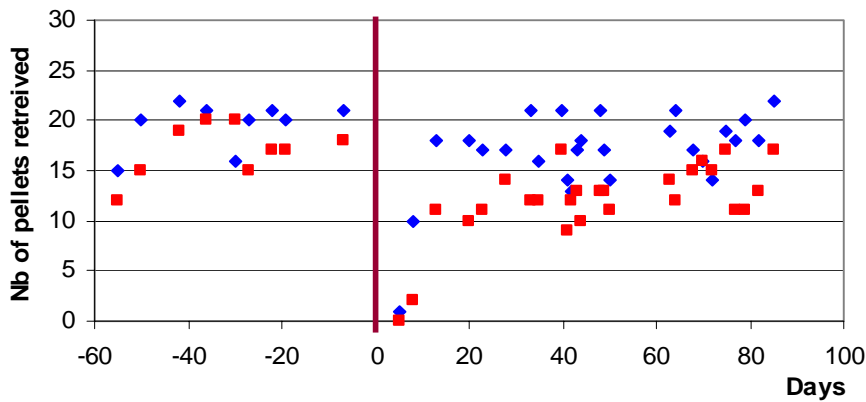


Fig. 3.10: This graph represents the number of successfully retrieved pellets within 45 sec performed by monkey Ctrl 1 in the “Brinkman board” task separately for vertical (blue diamonds) and horizontal (red squares) slots.

Let’s focus our attention on the ipsilesional hand performance in monkeys Ctrl 1 and Ctrl 2. First, Ctrl 1 showed during the training period a different ability of precision grip between the vertically oriented and the horizontally oriented slots, exhibiting a better score for the vertically oriented ones (Fig. 3.10). After the cervical cord lesion, this tendency was even augmented. Using non-parametric statistical analysis, the number of successfully retrieved pellets in the vertically oriented slots within 45 sec. was significantly larger ($P < 0.002$) than the number of retrieved pellets in the horizontally oriented slots (Fig. 3.10).

In Ctrl 2, there was no difference of score between vertically and horizontally oriented slots at the end of the pre-lesion period. In sharp contrast, after the cervical cord lesion, no recovery of function was observed for the horizontal slots whereas the recovery was about 30 % for the vertically oriented slots when reaching a post-lesion plateau (Fig. 3.11).

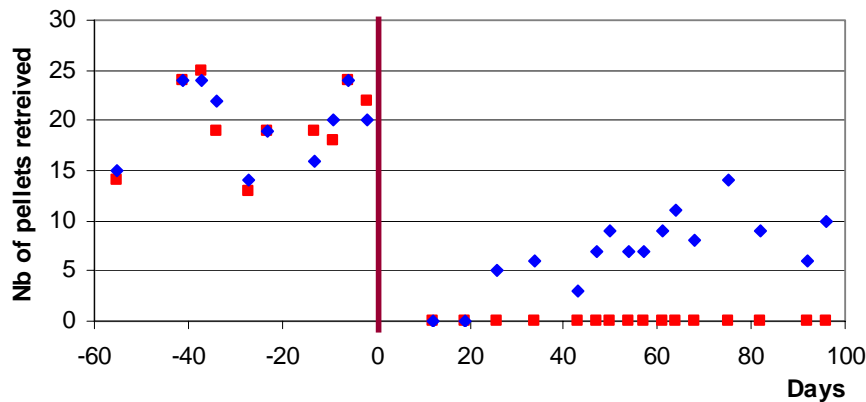


Fig. 3.11: Precision grip performances of the left (affected) hand in monkey Ctrl 2 for the vertically oriented slots (blue) and the horizontally oriented slots (red).

In the same animal, after the period of recovery, the shape of the precision grip using the left hand was analysed in video sequences. A slight flexion of the index finger helped by the flexion of the wrist allowed the animal to empty the vertically oriented slots by pushing the food reward against the external face of the thumb. This pattern of grip does not correspond to the “standard” precision grip, thus representing a strategy of substitution. In contrast, the animal was unable to perform the horizontally oriented task (Fig. 3.11).

The “Brinkman Board” task can be influenced by the distraction of the animal during the test or his level of motivation. To better separate the real motor ability of fingers, we analysed the time spent by the thumb and the index finger to retrieve the pellets from the wells. The time spent in a slot is the interval separating the precise time of penetration of the index finger in the well from the time when the pellet was completely retrieved of the well.

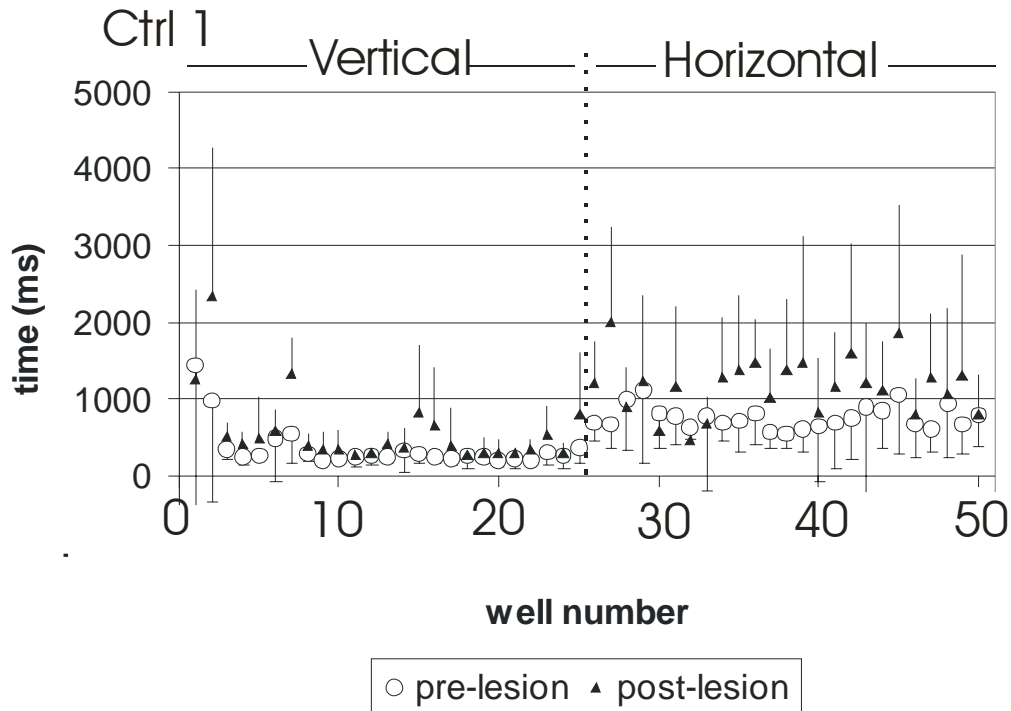


Fig. 3.12: Diagram showing for each slot of the Brinkman board task the average time (ms) spent in the slot to retrieve the pellet. The ID numbers 1-25 correspond to the vertically oriented wells, and the ID numbers 26-50 correspond to the horizontally oriented slots.

In the monkey Ctrl 1 (Fig. 3.12), we can observe that the fingers remained a significantly longer time in the wells oriented horizontally in the post-lesion period, as compared to the pre-lesion period. In monkey Ctrl 2 (Fig. 3.13), the performances showed a significant increase of the time spent in the vertically oriented slots post-lesion, whereas the comparison between the period pre- and post-lesion was not possible for the horizontally oriented slots due to the complete loss ability to grasp the horizontal pellets post-lesion.

In several specific slots, for example the vertically oriented slot number 17 in Ctrl 2, the time spent was clearly larger than the mean. This is due to the position of the slots in the board that obliged the animal to perform a special inclination of the wrist to empty this particular slot.

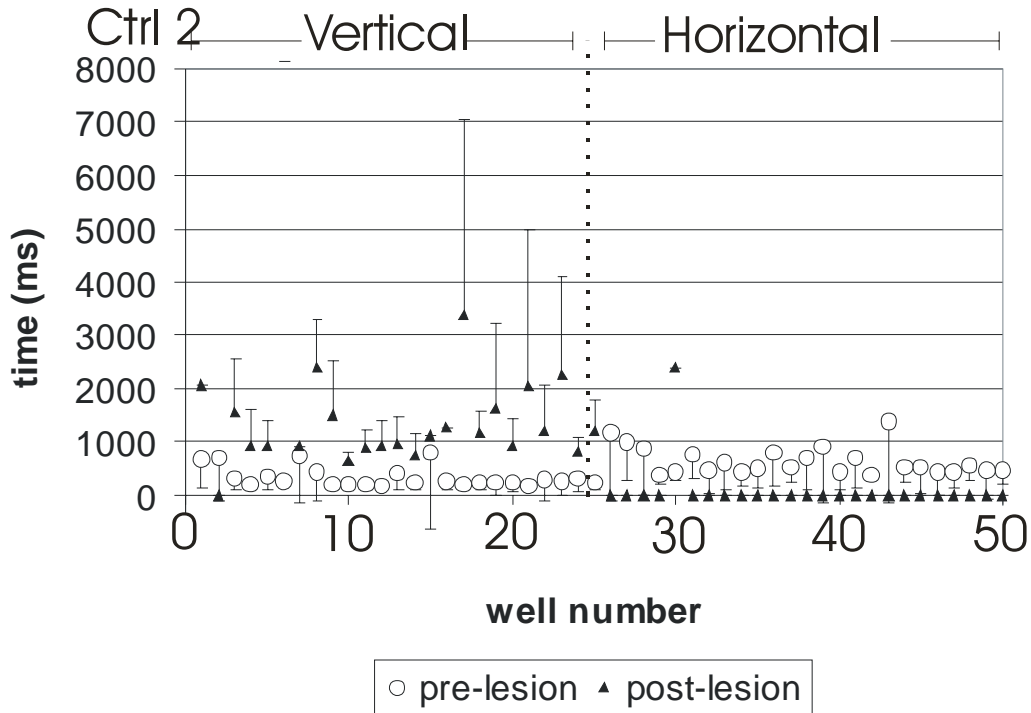


Fig. 3.13: Diagram showing the time (in ms) spent in the wells in monkey Ctrl 2. Same conventions as in Fig. 3.12.

This second quantitative analysis of the Brinkman board task based on time spent in the slots generally confirmed the observations based on the direct evaluation of the number of pellets retrieved within 45 seconds (Figs. 3.8 to 3.11), thus indicating in addition an adequate level of motivation of the two monkeys.

3.2.2.2.2: Role played by the Primary Motor cortex in recovery of precision grip

To assess the putative role played by the hand area of M1 of either hemisphere in the recovery of manual dexterity post-lesion, we transiently inactivated this area previously identified with ICMS technique (see below) through microinjections of muscimol at several sites in one or the other hemisphere (see Figs. 3.18 A and 3.19). The animal performed with each hand the precision grip task a few minutes before the infusion of muscimol. The animal repeated the same test with each hand 30 to 40 minutes after the infusion during the effective period of

action of the muscimol. Twenty four hours after infusion, the effect of muscimol disappeared and the performance of the animal returned to normal.

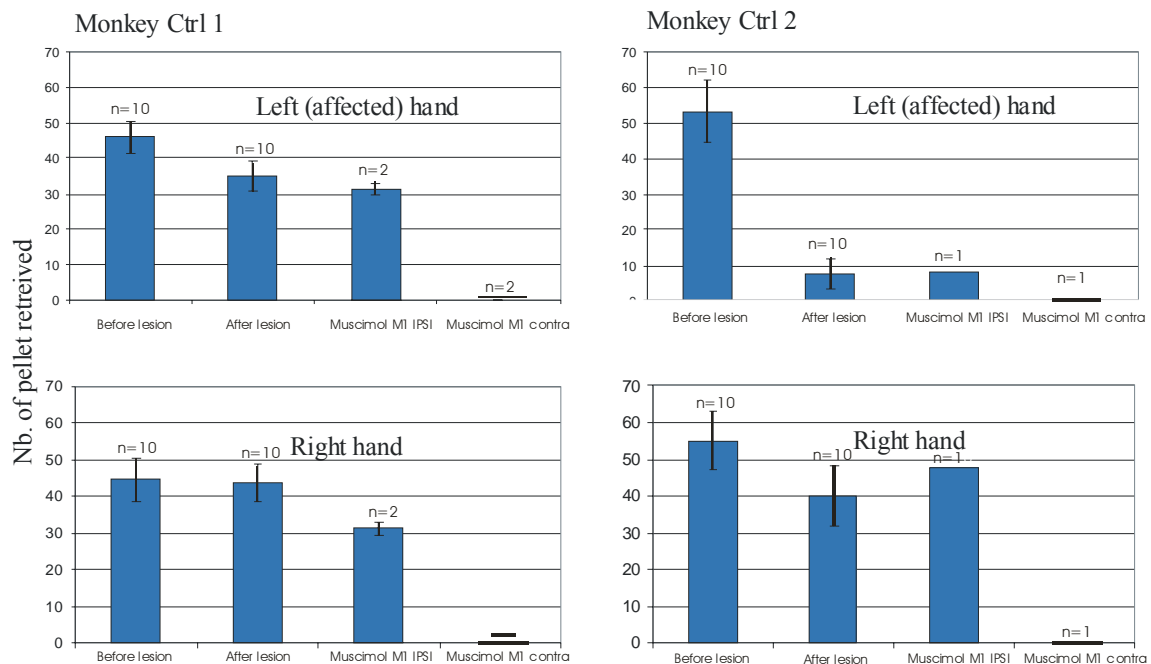


Fig. 3.14: Diagrams presenting the average of the scores of the ipsilesional hand in the precision grip task (in 45 sec) before the spinal cord lesion, after the spinal cord lesion at the plateau level of recovery (first and second bins from the left). The third and fourth bins (from the left) are the score after the muscimol infusion, in the ipsilateral hemisphere (Muscimol M1 ipsi) and in the contralateral hemisphere (Muscimol M1 contra), respectively. Scores for vertical and horizontal slots were pooled.

After the muscimol infusions in the hand area of M1, in both animals Ctrl1 and 2, there was a dramatic impairment of the precision grip ability with the hand opposite to the site of infusion of muscimol (Fig. 3.14 “Muscimol M1 contra”), whereas the infusion in the ipsilateral M1 (with respect to the tested hand) did not affect the precision grip scores. For the right hand, these data confirm the efficacy of the muscimol reversible inactivation strategy. For the left hand, these data demonstrate that the contralesional (right) M1 hand area plays an important role in the recovery following the left hemi-section of the cervical cord.

3.2.2.2.3: Drawer task:

Three main temporal aspects of the motor control of the forelimb were quantified in the drawer task: the time interval for the forelimb and the wrist to move from the start pad to the knob of the drawer (reaching time = RT), time for the fingers to fully open the drawer (pulling time = PT) and the time interval to pick up the food reward inside the drawer (picking time = PIT). In Fig. 3.15 A, each dot corresponds to the mean time interval values of the 20 trials performed during a daily session. The means of the time interval values obtained in the last 20 sessions before the cervical cord lesion are shown in Fig. 3.15 B, and compared to intervals obtained in four post-lesion sessions. The mean of RT was lightly increased after the cervical cord lesion, showing that monkey Ctrl 2 reached the knob and tried to open the drawer. In contrast, as the animal could not open the drawer (PT) nor pick up the food reward (PIT), the post-lesion values decreased to zero (Fig 3.15 B). A few sessions have been excluded from the analysis as their results could not match with the unfolding of the task (negative or exaggerated time intervals). The data in Fig. 3.15 demonstrate that the monkey Ctrl 2 did not exhibit any long term impairment for reaching. In contrast, post-lesion PT and PIT values dropping to zero are indicative of a long-term inability to exert any force to pull the drawer and to perform the precision grip to grasp the reward. Of course, the inability to open the drawer prevented the picking of the reward inside the drawer (PIT post-lesion = 0).

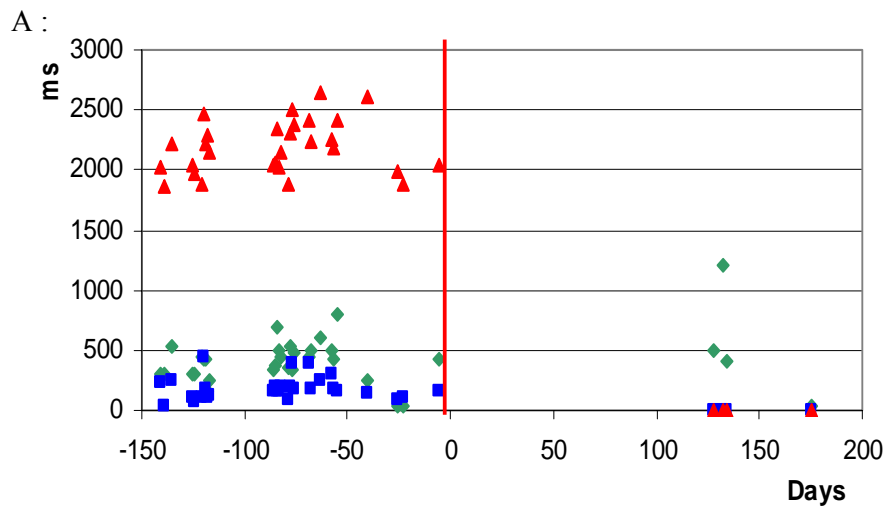


Fig. 3.15 A: Drawer task time intervals for the left hand performed by monkey Ctrl 2, 150 days before the left cervical lesion (day =0) up to 200 days after the lesion. Three time intervals have been taken into consideration: the reaching time (RT, green diamonds), the pulling time (PT, blue squares) and the picking time (PIT, red triangles). Time in milliseconds.

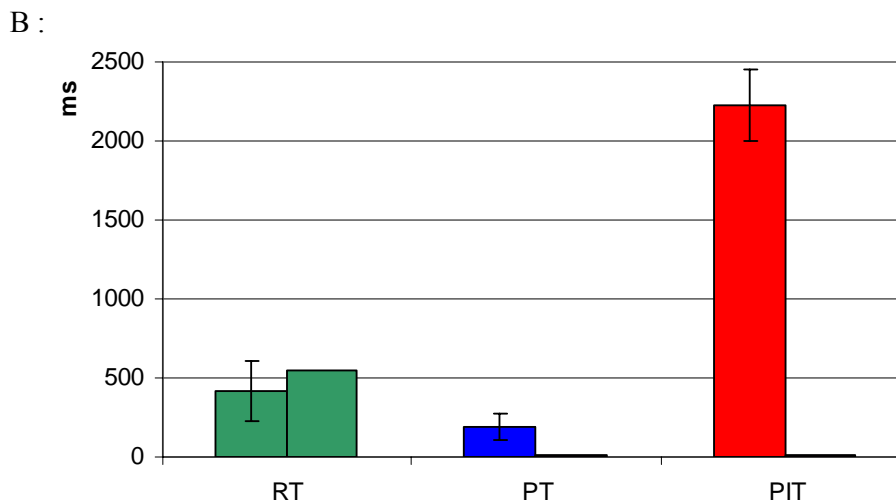


Fig. 3.15 B: Histograms showing the means and the standard deviation of the three time intervals as defined in the text: Reaching time (RT), pulling time (PT) and picking time (PIT). The intervals are compared before (left columns) and after the cervical lesion (right columns). The number of values obtained after the cervical lesion is too low ($n = 4$) to allow statistical analysis. The population of values taken before the cervical cord lesion is limited to the 20 last sessions before the lesion. Data are for monkey Ctrl 2.

3.2.2.3: *Qualitative behavioural test:*

3.2.2.3.1: "Displacement" tests:

Using food rewards, the experimentalist motivated the animals to move inside the animal room in unrestrained conditions. The following events were taken into consideration: jump from the floor of the room to the top of the cage, the different uses of the limbs to take off and to land during the jump from the top of one cage to another cage and a description of the movements made in the up side down hanging (from the ceiling) and the brachiation. Particular attention was paid on the observation of the use and the movement of the affected limbs in such displacements. Immediately after the spinal cord lesion, Ctrl 2 used mainly the unaffected (right) limbs to move in the room, showing a close to complete paresis of the left limbs. In the following days, some movements of the left hindlimb reappeared during the walk, although an important asymmetry of mobilisation of the limbs remained. Before the spinal cord lesion, Ctrl2 used during these tasks both hindlimbs to jump from one cage to the other cage in the room.



Fig. 3.16 A: Monkey Ctrl 2 showing the standard sitting position on the cage following the spinal cord lesion. The ipsilesional hind limb is in extension, and the ipsilesional forelimb is relaxed, the fingers remaining flexed.

Qualitative analysis of jump abilities:



Fig. 3.16 B: Picture showing the jump of monkey Ctrl 2 from one cage to the other cage before the spinal cord lesion. Note the normal use of both hindlimbs through symmetric extension.



Fig. 3.16 C: A few days after the spinal cord lesion, the animal (Ctrl 2) was unable to fully control its affected (left) hindlimb when landing on a cage.



Fig. 3.16 D: Nine months after the cervical cord lesion, the animal avoided to use its ipsilesional hind limb to land and used the contralesional one only.

Post-lesion, monkeys Ctrl 1 and 2 showed an extension of the affected hindlimb when they were sitting (Ctrl 1 in Fig. 3.16 A). Three to four days after the spinal cord lesion, they showed enough force in the affected hand to climb along the lateral grid of a cage to reach the top of the room. A couple of hours after the lesion, both animals could help the affected hand with the unaffected hand in order to grasp relatively big morsels of food (5–6 cm in size) and, a few days after, even with the affected hand.



Fig. 3.17 A: Picture taken before the spinal cord lesion, showing Ctrl 2 during brachiation using the ipsilesional forelimb to support the whole body weight.



Fig. 3.17 B: Ctrl 2 a few days after the spinal cord lesion.



Fig. 3.17 C: 6 months after the spinal cord lesion, Ctrl 2 was not able to put all its body weight on the affected hindlimb.

By sticking raisins at specific locations on the wall of the retention room, the animals were obliged to use the ceiling grid performing brachiation movements or “up-side-down” position to reach the food reward (Fig. 3.17 A: before the cervical cord lesion, B: a few days after, and C: 6 months after the lesion in monkey Ctrl 2). In Fig. 3.17 A, the animal showed no differences in the alternative use of its left and right hand during brachiation. The movement was balanced and no asymmetry between the use or position of the left or right part of the body was observed. In Fig. 3.17 B, the animal moved slowly. The movement was asymmetric, the time spent hanged by the left affected forelimb was shorter than the time spent hanged by the right hand. The left hand remained flexed and the wrist was more involved in the grip when the left forelimb was supporting the whole body weight than the right forelimb. As shown in Fig. 3.17 C, taken 6 months after the cervical lesion, a deficit remained permanent consisting in the “up-side-down hanging”: the animal supported the whole body weight mainly on the right hindlimb, perhaps using its left hindlimb to balance the position.

3.2.2.3.2: “Jump” test

To perform the “jump” test, the monkeys Ctrl 1 and Ctrl 2 were asked to jump from one cage to the other cage inside the retention room (Ctrl 2, Fig 3.16 B-D). Before the cervical cord lesion, monkey Ctrl 2 used its left or right hindlimb (Fig 3.16 B) to initiate the jump without any difficulties. The landing on the second cage was normal, with flexion of both hindlimbs. Several days after the cervical cord lesion, the position of the body during the jump was asymmetric, resulting from the weakness of the left hindlimb (Fig 3.16 C). The animal landed on the second cage with the only help of the right hindlimb as the left hindlimb showed a clear paresis, particularly in the flexion movements. Around nine months after the cervical cord lesion, a certain asymmetry of movement during the jump test was observed (Fig 3.16 D), even if a limited recovery of the left hindlimb flexion took place. The animal landed always on the right hindlimb.

3.2.2.3.3: “Foot prehension” test

Before the spinal cord lesion, the monkeys were trained to grasp the “croquettes” (large food pellets) presented by the experimentalist with the only help of the foot. Each foot was trained alternatively. The decomposition of the movement of the foot showed first a movement of the hindlimb from the floor of the chair to the reward and an extension of the toes to catch the reward. Then the flexed toes grabbed the reward to bring it to the hand that finally brought it to the mouth. After the spinal cord lesion, the animals were unable to grasp the “croquettes” with the only help of the foot, and this deficit was persistent several months after the lesion.

3.2.2.3.4: “Ballistic arm movement” (BAM) test

The « Ballistic arm movement » test was designed to evaluate the ability of the monkey to perform a rapid and coordinated visually guided motor reaction of prehension of moving object using both hands. The movement is comparable to the action of catching a ball with two hands. Before the spinal cord lesion, the animal showed that he was able to grasp with the right or left hand alone, as well as with both hands simultaneously. In cases of bimanual prehension, several aspects of movements were qualitatively taken into consideration. We observed the speed of reaction, the appropriate coordination of both hands regarding the synchronous opening of the hands and the preshaping, consisting in the anticipated extension of the fingers to catch the reward.

After a short training period, the animal was able to catch with one or both hands at the same time the thrown food morsels. The analysis of video recordings in slow motion showed, in the bimanual catching, a symmetric speed of both hands to reach the flying reward. After the cervical lesion (7 months), the analysis showed an impairment of the ipsilesional hand to contribute to the task, the left fingers remaining flexed and the general movement (extension of the elbow and anterior rotation of the shoulder) was asymmetric. Overall, it was slower on the ipsilesional side.

3.2.2.3.5: Summary of the qualitative behavioural tests

To summarise the behavioural status of the animals Ctrl 1 and Ctrl 2 before and after the cervical cord lesion, the severity of the cervical cord lesion can be roughly estimated immediately at the end of the surgery, when the animal recovers from the anaesthesia. The symptoms are the paresis of the affected left hand, resulting in the impossibility to perform a extension followed by an active flexion of the fingers to grasp relatively large food morsels.

The ability to perform movements can be estimated through a scale made of points. The minimum was 1 point, given when the animal was absolutely unable to perform the corresponding movement; two points were given when the animal was unable to perform the task appropriately but if tentative movements were observed; three points was the score reflecting the ability of the animal to perform the task with difficulties and more slowly; four points were given when the animal was able to perform the task likewise before the cervical cord lesion. The table 3.1 summarises the results obtained in the different behavioural tasks following this behavioural scale.

	Ctrl1		Ctrl2	
	Few days after SCI	Several months after SCI	Few days after SCI	Several months after SCI
Jump	1	4	1	3
Hanging	2	Not tested	2	3
Brachiation	1	Not tested	1	3
BAM (left hand)	1	Not tested	1	2
Foot prehension	1	2	1	2
Shape of grip: vertical slots	1	4	1	3
Horizontal slots	1	3	1	2

Table 3.1: Scores obtained in the qualitative behavioural tests 5 days after the spinal cord injury and at the end of the period of recovery for Ctrl 1 and Ctrl 2. Scores: see text. BAM: “ballistic arm movement”.

3.2.3. ICMS data

3.2.3.1: Mapping of M1 hand area before and after cervical cord lesion in the contralateral hemisphere

Although we will focus here on subtle and progressive changes of the motor map in M1 taking place during the few weeks following the lesion, it is imperative to first describe the detailed properties of the motor map as it appears before the lesion. The hand area of M1 was

thus extensively mapped in daily ICMS sessions taking place during the two months preceding the lesion. In the present paragraph, the pre-lesion motor map will be compared to the motor map re-established extensively 2 and 4.5 months after the lesion in Monkeys Ctrl 1 and Ctrl 2, respectively. The issue of the progressive changes taking place shortly after the lesion during the recovery period will be addressed below in paragraph 3.2.3.4.

3.2.3.1.1: Before lesion

On a surface map of M1 (Fig. 3.18 A, left column), each electrode penetration is represented at its corresponding position by a symbol indicating the body territory activated at the lowest ICMS current still eliciting a movement. Diamonds indicate the locations where the most excitable stimulation point along the electrode track induced a movement of digits of the contralateral hand. In the left column, the solid line surrounding the diamonds thus delineates the hand representation in the contralateral M1. In monkey Ctrl 2, the position of the chronic chamber allowed to investigate more rostral territories than in monkey Ctrl 1. As a result, a second, smaller hand area located more rostrally was observed in Ctrl 2, which corresponds most likely to a territory in the premotor cortex (PM) where ICMS elicited digit movements, but at higher thresholds than in the M1 hand area. In both monkeys (Fig. 3.18 A, left column), the M1 hand area was surrounded by territories where ICMS at the lowest current elicited more proximal movements of the forelimb (wrist, elbow, shoulder) or movements of face muscles.

3.2.3.1.2 After lesion

The post-lesion ICMS maps, established after the functional recovery had reached a plateau, are shown in the right column of Figure 3.18 A. Most ICMS sites effective before the lesion remained micro-excitable after the lesion. However, there were dramatic changes with respect to the precise body territory activated at a given ICMS site. These changes affected

mainly the hand areas in both M1 and PM, which occupied post-lesion a significantly diminished cortical surface. In monkey Ctrl 1, with a section presumably interrupting most of the CS tract but preserving considerable amount of the lateral and ventral spinal white matter (Fig. 3.1), the M1 hand area surface decreased from about 72 mm² (pre-lesion) to 24 mm² (post-lesion), thus representing a drop of 67%. In monkey Ctrl 2, the lateral and ventral funiculi were nearly completely sectioned, resulting in an even more dramatic decrease of the surface of M1 hand area, dropping from 36 mm² to 4 mm² (89% decrease). In this animal, the rostral hand area in PM was even more affected since no movements at all could be elicited after the lesion. The M1 hand areas remaining after the lesion are delineated by a dashed contour in the right column of Fig. 3.18 A. Territories separating the dashed contour from the solid contour are sites where ICMS elicited digits movements before the lesion, replaced by movements of other muscles (grey symbols) or non micro-excitabile sites (X) post-lesion. Most of the sites addressing other muscles post-lesion elicited movements of face or wrist muscles. In other words, some of the pre-lesion hand points have been filled by adjacent body territories. There were also changes of territories outside the pre-lesion hand areas, but clearly less dramatic.

In the above computation leading to 67% and 89% decrease of hand area in the ICMS surface map observed as a result of the lesion in monkeys Ctrl 1 and Ctrl 2, respectively, one cannot exclude the influence of a possible bias. Indeed, there was an underestimation of the hand territory lying in the rostral bank of the central sulcus, where a penetration all the way down the bank was represented by a single point on the surface map of Figure 3.18 A. For this reason, as done and explained in the next paragraph, one may consider not only one ICMS site for each penetration (corresponding to the lowest threshold), but all ICMS sites tested. As reported in Figure 3.19 for Ctrl 1, 67 ICMS sites generated distal (hand) movements pre-lesion, a number dropping to 21 sites post-lesion, thus representing a drop of 69%. For monkey Ctrl 2, the number of ICMS sites eliciting distal movements dropped from 74 to 2 after the lesion, corresponding to

a decrease of 97% (Fig. 3.20). These values reflecting the decrease of hand ICMS sites, particularly for monkey Ctrl 2, thus support the notion of underestimation of the territory buried in the rostral bank of the central sulcus on the surface map such as in Figure 3.18 A.

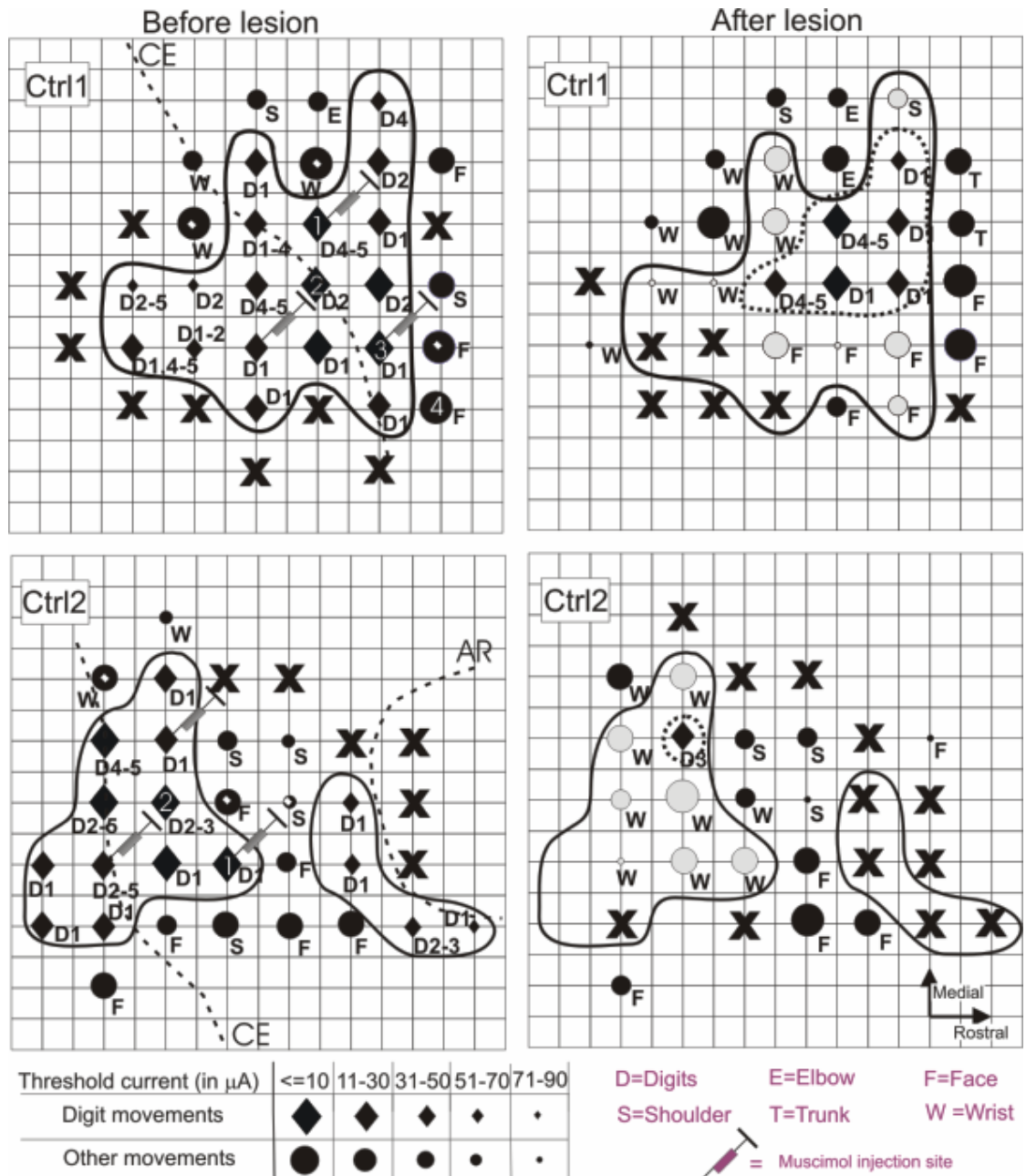


Fig. 3.18 A: Somatotopic map in the motor cortex on the right (contralateral) hemisphere in the region of the hand area, before (left column) and after (right column) the cervical lesion. The pre-lesion maps were established by daily ICMS sessions conducted during the 2 months preceding the lesion. The post-lesion maps were derived from daily

ICMS sessions starting 2 and 4.5 months after the lesion in monkeys Ctrl 1 and Ctrl 2, respectively and lasted about 2 months each. The data are presented on a surface view of the brain. Each symbol represents the location of penetration with an electrode for ICMS. The ICMS data given for each symbol is representative for the site of stimulation where the effect was observed at the lowest current intensity along the considered electrode track. The letter next to each symbol indicates the body territory activated at threshold for each track (see letter codes in the bottom right). The current intensity at threshold (in μA) is indicated by the size of the symbols (see bottom left). Hand area(s), outlined by a solid line, was defined as a cortical region where ICMS at lowest threshold elicits movements of the fingers (electrode tracks represented by diamonds). The map is given for monkey Ctrl 1 (top two panels) and monkey Ctrl 2 (bottom two panels), as established by ICMS before (left two panels) and after lesion (right two panels). Symbol X means that ICMS did not elicit any visible movement of muscles. Symbols in grey are for sites belonging to the hand area before lesion, which became part of other territories post-lesion. The grid in the background indicates steps of 1 mm. In the pre-lesion maps (left column), symbols outside the hand area with a small white rectangle indicate electrode penetrations along which hand movements were obtained, but not at the lowest current producing ICMS effect (see Fig. 3.18 B for a representation of all electrode penetrations along which hand muscles effects were observed). The position of the tracks in which ICMS was repeated on a weekly basis during the period of recovery are pointed by numbers (1-4 for monkey Ctrl 1, see Fig. 3.25; 1-2 for monkey Ctrl 2, see Fig. 3.26). Syringes point to ICMS sites where muscimol was infused in order to inactivate M1 (see text). In order to make sure that the entire "post-lesion" hand representation was reversibly inactivated, the sites of infusion of muscimol were rather selected based on the "pre-lesion" map, exhibiting a larger hand representation than post-lesion. On the pre-lesion maps (left column), the approximate positions of the central (CE) and arcuate (AR) sulci are indicated by dashed lines.

threshold intensities, whereas the diamonds outside these areas are the points where a movement of another muscular group than the fingers was elicited with a lower threshold of current. Same convention as in Fig. 3.18 A.

In the ICMS data shown in Fig. 3.18 A, only the effect obtained at the lowest threshold was represented for each electrode penetration. As a consequence, cortical territories influencing hand muscles were underestimated since one observed activations of hand muscles along electrode penetrations in which the lowest threshold stimulation affected other muscles. For this reason, Fig. 3.18 B shows all electrode penetrations along which hand muscles effects were observed, even if the effect was not the lowest stimulation current along the track. As expected (Fig. 3.18 B), there were ICMS hand points outside the hand area as defined in Fig 3.18 A. Considering also these extra hand sites, there was again a reduction of the overall hand area when comparing pre- and post-lesion, in line with the data discussed in Fig. 3.18 A for the “classical” defined hand area. The same conclusion of a reduction of ICMS sites eliciting activation of hand muscles can be drawn from histograms showing the relative (%) distribution of all ICMS sites by body territories (Figs. 3.19 and 3.20).

3.2.3.2: Mapping of M1 hand area in the ipsilesional hemisphere

If changes in the motor map were expected in the hemisphere contralateral to the cervical hemi-section (Fig. 3.18 A and B), one may wonder whether the ipsilateral hemisphere was affected. In the light of the small proportion of uncrossed CS projection (5-10%; see (Rouiller et al 96), one would predict that the motor map changes ipsilaterally are likely to be modest, if any. The consequences of a unilateral cervical lesion on the motor map of the ipsilesional primary motor cortex are illustrated in Figure 3.21. On the contrary to the above prediction, a substantial reduction of the hand representation was also observed on the ipsilesional hemisphere, representing a drop in surface of about 52% and 77% in monkeys Ctrl 1 and Ctrl 2, respectively.

Taking into account all sites eliciting digit movements, the drop was as follows. In monkey Ctrl 1, the number of digit ICMS sites pre-lesion was 79%, diminished to 39% post-lesion (51% reduction). Reciprocally, the ICMS sites eliciting movements of other territories (wrist, elbow, shoulder, trunk, face) in Ctrl 1 was 77 pre-lesion and 78 post-lesion, whereas the number of non-effective sites was 57 and 82 pre- and post-lesion respectively. In monkey Ctrl 2, the pre- and post-lesion ICMS digit sites were 81 and 29 (64% reduction). For the other territories, the numbers of ICMS sites in Ctrl 2 were 72 and 70, pre- and post-lesion whereas the number of non-excitabile sites was 139 and 158 respectively. In conclusion, the motor map was significantly affected in the ipsilesional hemisphere, but to a lesser extent than in the contralateral hemisphere.

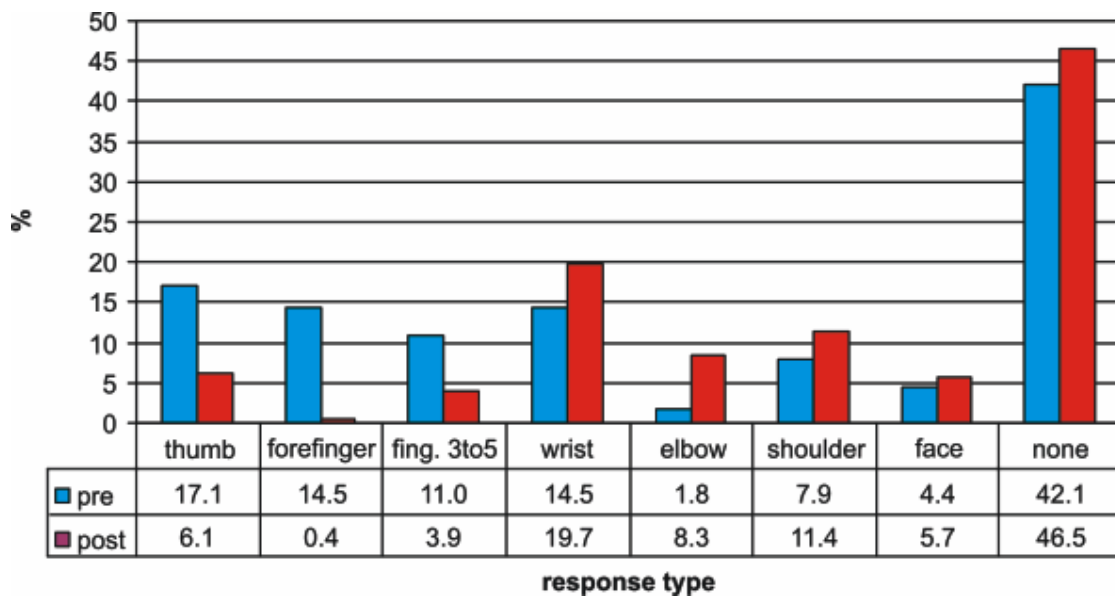


Fig. 3.19: Comparison of the relative distribution (%) of body territories where ICMS elicited movements in monkey Ctrl 1 before (pre) and after (post) the cervical hemi-section. The sum of all bins is 100% for each (pre/post) condition. Data for contralesional hemisphere. "None" is for sites which were not micro-excitabile.

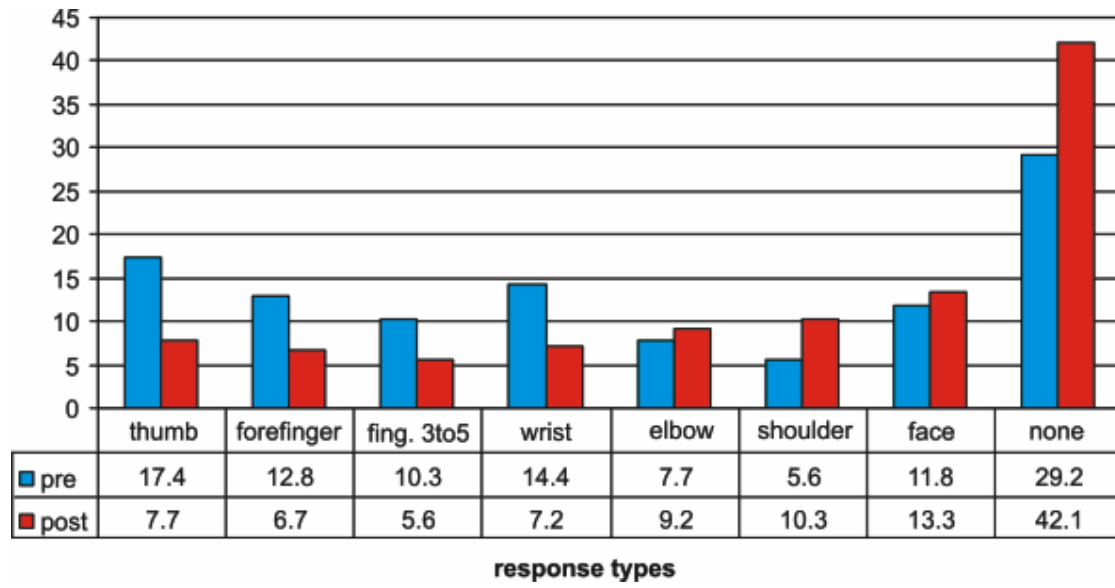


Fig. 3.20: Comparison of elicited movements in monkey Ctrl 2 during ICMS sessions conducted before (pre) and after (post) the cervical cord lesion. (Same conventions as in Fig. 3.19)

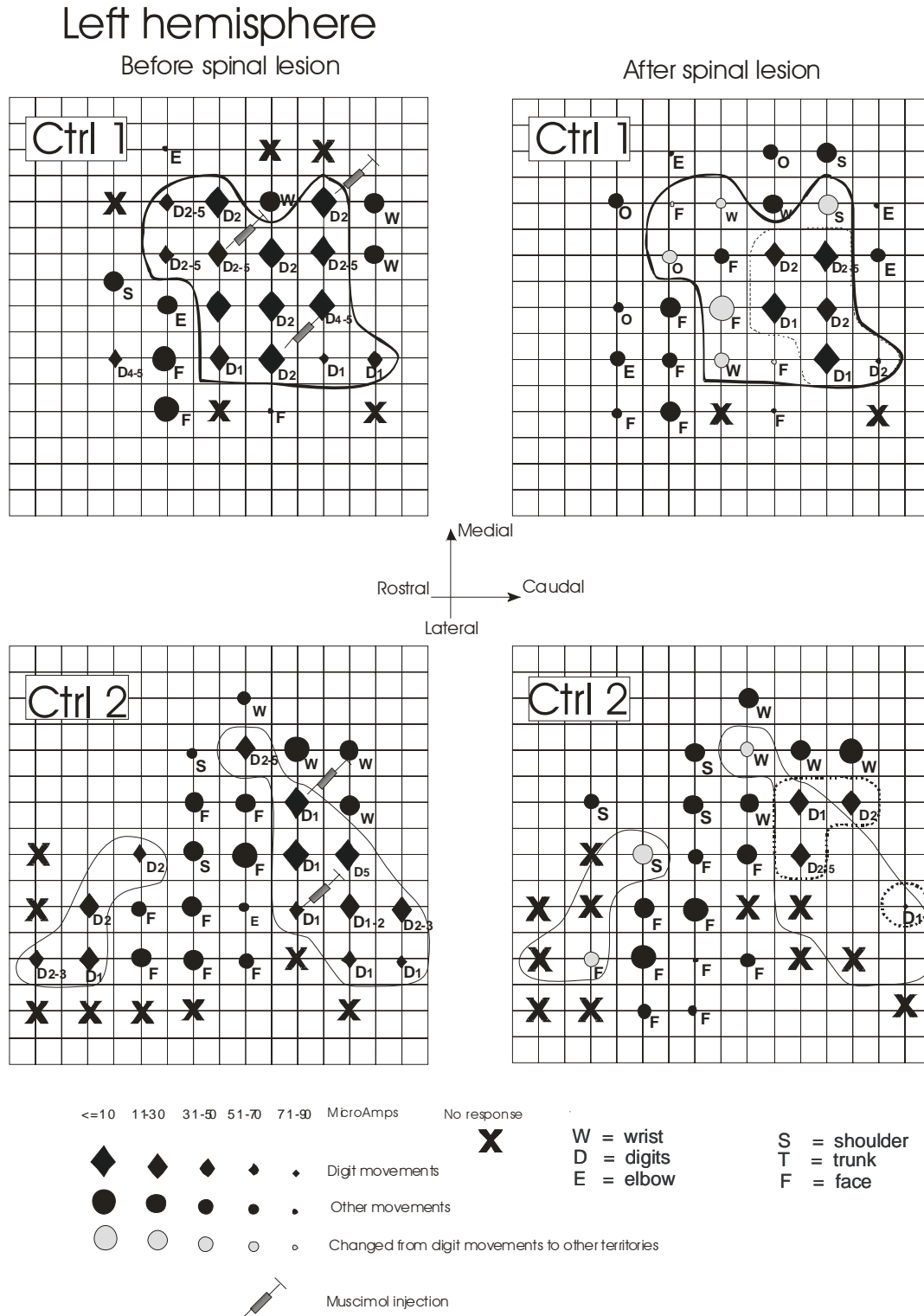


Fig. 3.21: Somatotopic map in motor cortex of the left hemisphere (ipsilesional) in monkey Ctrl 1 (upper panels) and Ctrl 2 (lower panels) before (left column) and after (right column) the cervical cord injury.

3.2.3.3: Comparison of thresholds in the contralesional hemisphere

The surface of the contralesional M1 hand area post-lesion dramatically decreased after the lesion (Figs. 3.18 A and B) and the number of sites eliciting digit movements post-lesion was also reduced (Figs. 3.19 and 3.20). They were replaced by sites eliciting forelimb proximal or face movements or, in some cases, the sites became non micro-excitabile. These observations were expected because the lesion reduced greatly or completely the number of CS neurons accessing directly to the motoneurons placed caudally to the lesion (i.e. motoneurons innervating the finger muscles), but preserved access to the motoneurons placed more rostrally via collaterals. As a consequence of the diminished access to finger motoneurons, one would predict that a higher stimulation current would be necessary to elicit finger movements than before the lesion. To test this prediction, we compared the ICMS thresholds required to elicit movements from stimulation at the same stereotaxic points before and after the lesion, in the later case when the behavioral score reached the plateau. In contrast to Fig. 3.18 A where only the best ICMS site along each electrode penetration was represented, several sites of stimulation were considered along each track for the ICMS threshold comparison (Figs. 3.22 and 3.23). The mean threshold values had a large variability as indicated by large SD bars and no systematic and significant difference of threshold appears between pre- and post-lesion values. Based on the body territories affected, ICMS sites were grouped in three sets (Fig. 3.24): distal (movements of the digits), proximal (movements of the wrist, elbow or shoulder) and face. A mean value of thresholds (with the standard deviation) has been obtained for these three groups, pre- and post-lesion (Fig. 3.24). Surprisingly, for both animals, the threshold stimulation current to elicit either finger, proximal forelimb or face movements remained comparable pre- and post-lesion (no statistically significant difference; Mann Whitney U-test, $p > 0.05$).

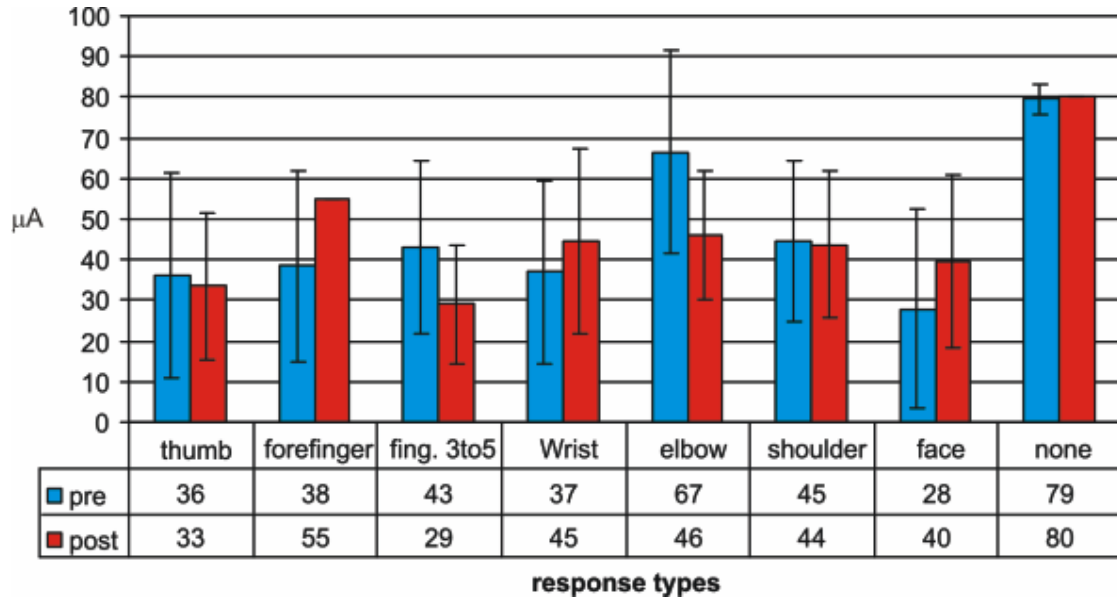


Fig. 3.22: For Monkey Ctrl 1, comparison of ICMS threshold before (blue) and after (red) cervical cord lesion in the different body territories where movements were elicited by ICMS. The numbers below correspond, in μA , to the average of lowest intensity of current needed to elicit the movement of the corresponding body territory. The value of $80 \mu\text{A}$ in the rightmost bins is the maximal intensity tested at sites where no ICMS effect was observed.

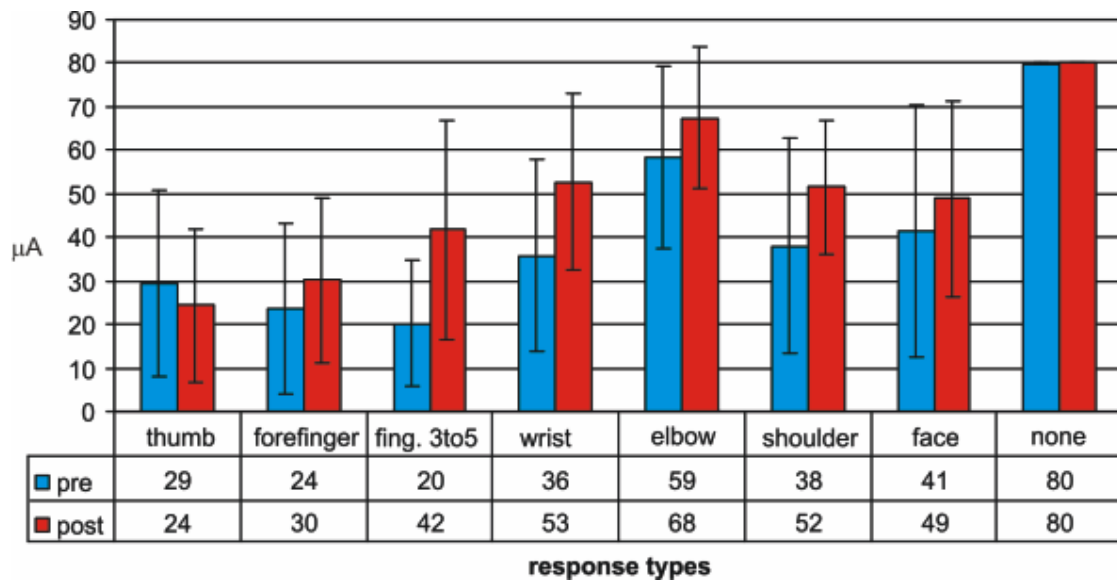


Fig. 3.23: Monkey Ctrl 2, comparison of ICMS threshold before (blue) and after (red) the cervical cord lesion (same conventions as in Fig. 3.22).

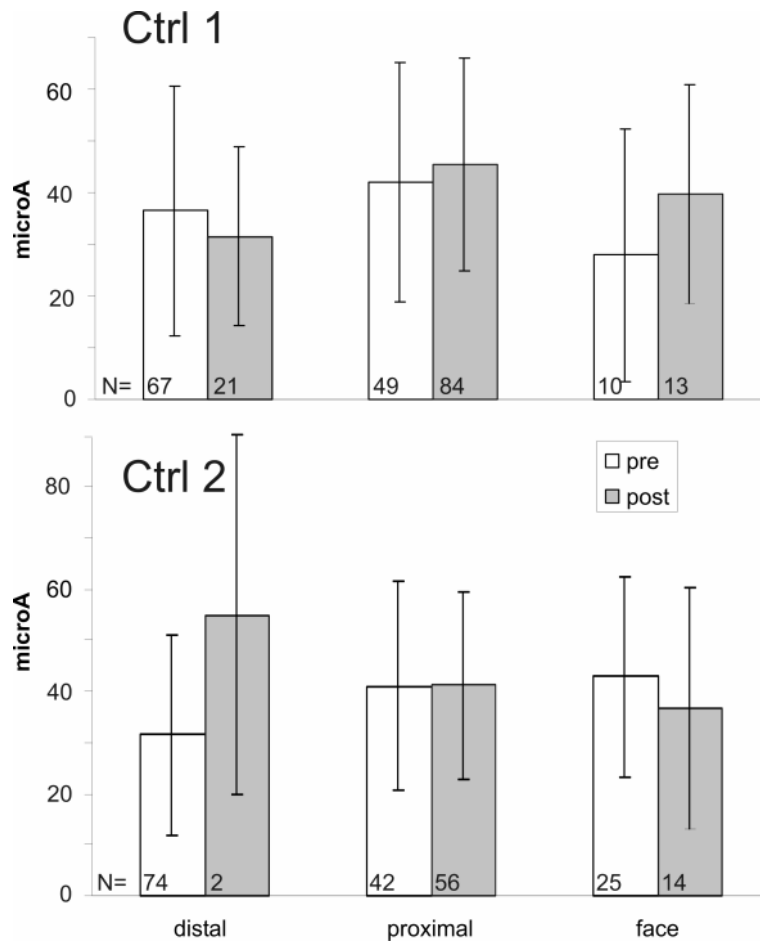


Fig. 3.24: For M1 contralateral to the lesion, the bars indicate the average ICMS current at threshold with standard deviations to elicit movements of forelimb "distal" muscles (fingers), forelimb "proximal" muscles (wrist, elbow, shoulder) or "face" muscles. The average values are derived from all responsive ICMS sites cumulated before ("pre-") and after ("post-") lesion, separately for the two monkeys. The pre-lesion ICMS threshold data were collected during the 2 months preceding the lesion, whereas the post-lesion ICMS threshold data were collected during a period of 2 months, starting 2 and 4.5 months after the lesion in Ctrl1 and Ctrl2, respectively. The number of ICMS sites considered to establish these data (given in the bottom of each bin) was lower post-lesion than pre-lesion because some ICMS sites became non-microexcitable post-lesion. Note that the ICMS thresholds were not significantly different pre- and post-lesion.

3.2.3.4: *Progressive changes of ICMS effects during the recovery period*

The ICMS data shown in Fig. 3.18, limited to two time points, do not address the question of the time course of the plastic changes post-lesion and to what extent the temporal evolution of plastic changes parallels the time course of behavioral recovery. To address this question, we conducted ICMS experiments repetitively at short time intervals during the few weeks following

the lesion in the contralesional hemisphere. Daily ICMS sessions on alert monkeys were, however, limited to 30-60 minutes, allowing a number of electrode penetrations ranging from 3 to 6, in general. Thus, a complete mapping of the hand area in M1 (like in Fig. 3.18 A) requires 10 to 20 daily sessions on each hemisphere. Therefore, a complete mapping of the hand area at weekly intervals post-lesion during the recovery was not undertaken, also to avoid an additional deficit to that initially induced by the cervical cord lesion. For these reasons, a limited number of electrode track locations were selected (see Fig. 3.18 A), where ICMS experiments were systematically repeated approximately every 7 days during the period of functional recovery (days 2-6 to days 40-48 post-lesion; Figs. 3.25 and 3.26). Four electrode track positions were selected for the repetitive ICMS protocol, as illustrated in Fig. 3.25 for monkey Ctrl 1. Three of the tracks (#1, 2, 3) belonged to the pre-lesion hand territory while ICMS along the fourth track elicited twitches of face muscles ("F").

A repetition of ICMS at the same locations two days post-lesion yielded quite different results in the hand area. In the electrode tracks #1 and #3, ICMS did not elicit movements of the fingers any more, but produced movements of more proximal muscles or failed to induce any observable movement (Fig. 3.25, second column from the left). Along the electrode track #2 (Fig. 3.25), the number of sites where ICMS elicited finger movements decreased dramatically (seven before the lesion and only one post-lesion). In addition, the finger movements produced at the latter site were obtained at a higher current intensity than that necessary to elicit movements of other territories (wrist). Note that ICMS conducted along the electrode track initially performed in the face area of M1 did not show any significant change of representation during the entire recovery period (Fig. 3.25, bottom line).

Eight days post-lesion, a limited re-appearance of finger movements in the hand area occurred. In electrode track # 2, four points along the track elicited finger movements, as compared to one point 7 days before. Again, these ICMS sites were less sensitive than other sites

triggering movements of other body territories (wrist). One site where ICMS elicited finger movements re-appeared at that time point along electrode track #3 (black star), but once more this was not the site of maximal excitability. Finger movements were observed to re-appear in electrode track #1 as well, after 22 days. ICMS sessions performed at day 22 or more post-lesion confirmed this tendency of a re-appearance of ICMS sites addressing hand muscles. The immediate post-lesion dramatic loss of virtually all sites producing finger movements pre-lesion was replaced by a progressive, incomplete, re-establishment of sites where finger movements occurred as a result of ICMS (black ticks pointed by stars in the three top lines, days 22 to 40 of Figure 3.25). Along electrode track #2, stimulation of the site of lowest threshold elicited finger movements, thus re-establishing a hand representation post-lesion.

Consistent progressive ICMS data were observed in monkey Ctrl 2, as shown by repetitive ICMS sessions performed during recovery along two electrode penetrations (Fig. 3.26). All sites where ICMS elicited finger movements were replaced, at six and thirteen days post-lesion, by wrist movements. Later on in track #1, in parallel to the progressive functional recovery, a few sites where finger movements could be elicited by ICMS re-appeared (27, 41 and 48 days post-lesion). However, these few re-established hand points did not correspond to the lowest threshold along the electrode penetration on the long term and therefore the location of the electrode penetration on the surface map does not correspond to a hand representation (Fig. 3.18 A). In this animal (Ctrl2), we also observed electrode penetrations in the pre-lesion hand area along which there was no re-appearance of sites eliciting hand movements (track #2 in Fig. 3.26), after the elimination of such ICMS sites immediately after lesion. These observations indicate that the phenomenon of map plasticity in parallel to the recovery is limited and its occurrence appears to be related to the size of the lesion. Indeed, substantially more ICMS digit sites reappeared post-lesion in monkey Ctrl 1 subjected to a smaller lesion than in monkey Ctrl 2 with a larger cervical cord lesion.

3.2.3.5. Time course of ICMS changes and time course of behavioral recovery

The progressive ICMS changes observed in monkey Ctrl 1 during the few weeks post-lesion (Fig. 3.25) indicate that sites eliciting finger movements, which nearly completely disappeared as a result of the lesion, re-appeared in a stable manner in the 3 tested penetrations after 15-22 days. This time point was correlated with the behavioral recovery curve of the same monkey (Ctrl 1), showing that a substantial degree of recovery of 50% was reached after about 2 weeks. In monkey Ctrl 2, the recovery of manual dexterity was clearly less prominent and slower, with a small, but consistent, ability to again perform the grasping movement from 25 days post-lesion. As seen in the progressive ICMS assessment during the few weeks post-lesion (Fig. 3.26), the first time point at which sites eliciting finger movements re-appeared was 27 days. Although these data are limited to two monkeys and to a limited set of ICMS penetrations, there is some evidence for a correlation between the behavioral recovery and the progressive plastic changes of the hand representation in the motor cortex contralateral to the lesion.

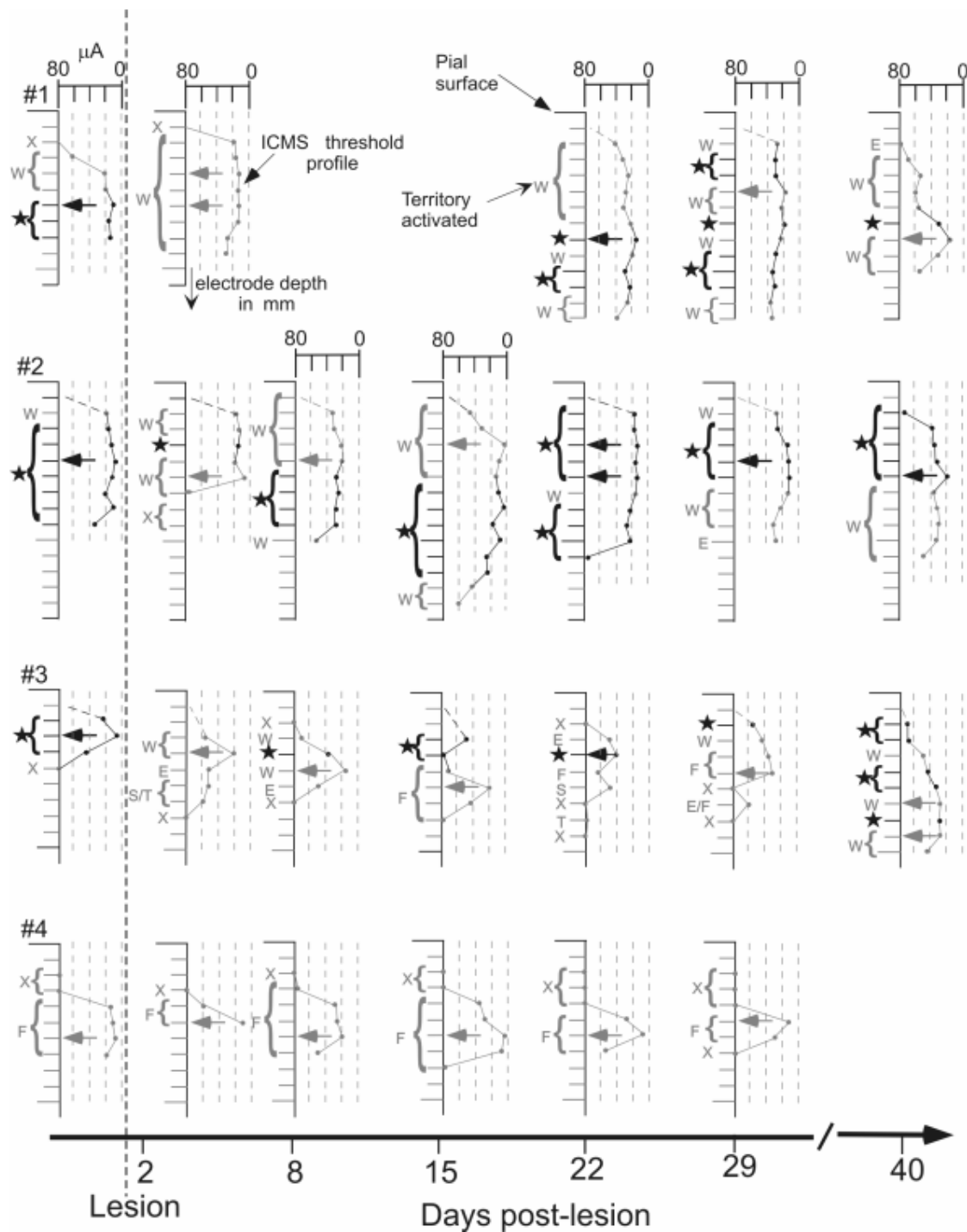


Fig. 3.25: In order to establish the time course and extent of progressive plastic changes taking place during the recovery period, four cortical sites were penetrated repetitively in M1 contralateral to the cervical lesion, and ICMS was applied at the same sites on a period of 40 days post-lesion (abscissa). The data obtained for four electrode penetrations are presented here for monkey Ctrl 1 (the vertical bars with horizontal ticks numbered 1 to 4). The top of the four vertical bars corresponds to the surface of the dura. Then, ticks correspond to progressively deeper ICMS sites, separated from each other by 1 mm. The four bars on the left of the vertical dashed line are ICMS data before

lesion. The ICMS effects observed at each site are indicated with a grey letter (W=wrists; F=face; E=Elbow; S=Shoulder; T=Trunk) or with a black star in case of movements of the fingers. At each site, on a scale at the right of each electrode penetration, the threshold at which the ICMS effect was observed is indicated (between 0 and 80 μ A). The depth at which the current was the lowest along the corresponding electrode penetration is indicated by an arrow. Non-microexcitable sites are indicated by X symbol.

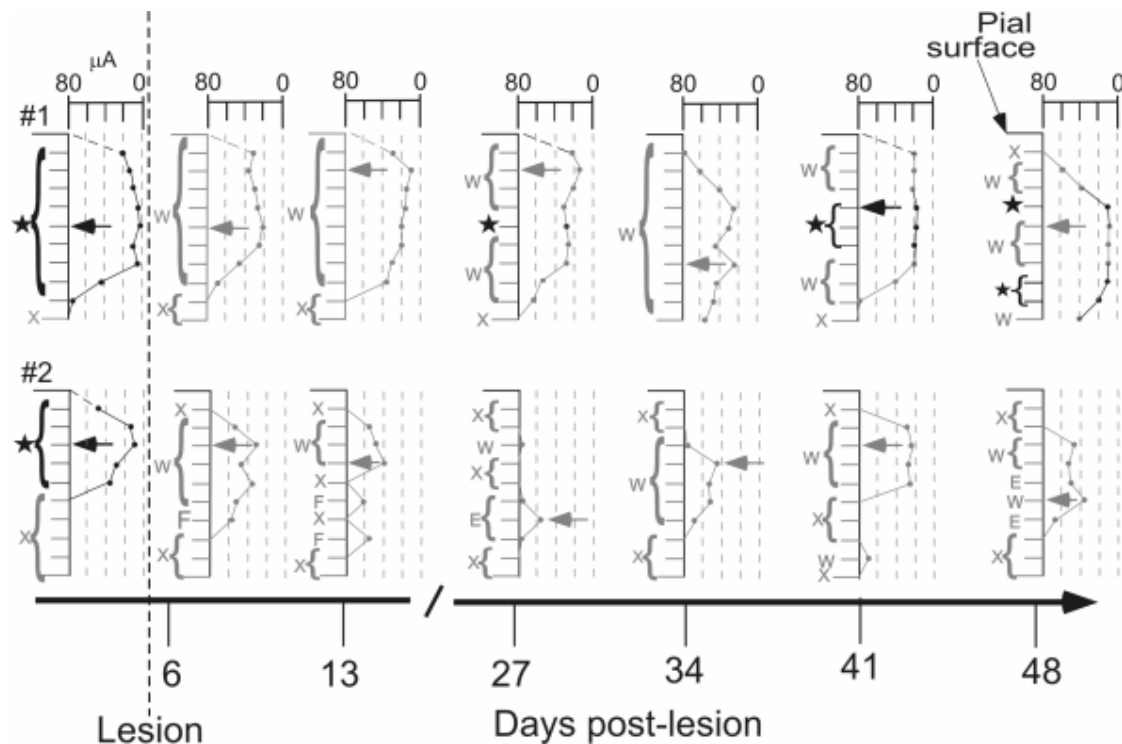


Fig. 3.26: Progressive plastic changes taking place along two electrode penetrations in monkey Ctrl 2 during the period of recovery of manual dexterity. Same conventions as in Fig. 3.25.

3.2.3.6: Does the progressively re-established hand area contribute to the recovery

To address this question, reversible inactivation sessions of M1 in the ipsilateral or contralateral hemispheres were performed 3 and 5 months post-lesion in monkeys Ctrl 1 and Ctrl 2, respectively. In a typical inactivation session obtained by infusion of muscimol, the manual dexterity task was initially performed just before the muscimol infusion and repeated 30 minutes after completion of the muscimol injections - a time point at which its effect is well established. A pre- and post-inactivation manual dexterity score was thus determined for each hand. Before

infusion of muscimol, the behavioral score of the affected hand was that corresponding to the plateau of incomplete recovery (Fig. 3.14). In both monkeys, a reversible inactivation of the ipsilesional M1 did not affect noticeably the recovered manual dexterity score of the hand homolateral to the cervical lesion, which thus remained at the recovery plateau level. In sharp contrast, a reversible inactivation of the contralesional M1, including the re-established hand area, led to a total inability to make coordinated finger movements as reflected by a manual dexterity score dropping to zero (the same level as immediately after the lesion). This second observation demonstrates that the contralateral M1 contributes substantially to the incomplete recovery, in contrast to the ipsilesional M1. Recovery from inactivation using muscimol is slow (several hours) and therefore could not be tested within the same inactivation session. However, the day after, the animal had fully recovered its manual dexterity from before the inactivation session.

3.3: Discussion:

3.3.1: Discussion related to the anatomical data (fate of CS neurones after cervical cord lesion)

3.3.1.1: Extent of the cervical lesion

Following a hemisection of the cervical cord at level C7/C8, most pyramidal neurones in layer V of the contralateral motor cortex survived. However, in M1, the axotomised neurones exhibited a significant shrinkage of their soma and a parallel decrease of SMI-32 immunoreactivity. A critical evaluation of the lesion position and extent indicates that most of the left dorsolateral funiculus was sectioned in both animals, although a small proportion may have been spared in monkey Ctrl 1. In spite of the absence of direct quantitative measures, it seems safe to estimate that 80-90% of the drive normally provided directly by the CS system to

spinal segments caudal to the lesion (and including that of the spared uncrossed projections) has been eliminated. This important loss of descending influence was corroborated by the flaccid paresis of the hand and leg observed immediately after the lesion and by the inefficacy of intracortical microstimulation (ICMS) to elicit hand and finger movements during the period immediately following the lesion.

3.3.1.2: Soma area measurement

The quantification of SMI-32 positive neurones in layer V, together with the determination of their soma area, led to the main conclusion of the present study that most axotomised CS neurones in M1 survived but shrank (Figs. 3.4). The median values of soma areas of SMI-32 positive neurones in layer V obtained in M1 in the two intact animals ranged from 329 to 631 μm^2 . In the lesioned monkeys Ctrl 1 and Ctrl 2, the range of median values of soma areas in the left hemisphere (ipsilateral to the cervical hemisection) was 401 to 627 μm^2 . In SMA-proper, the median values of soma areas ranged from 253 to 594 μm^2 across hemispheres and animals. These data indicate that there was a substantial variability of soma areas across monkeys. However, the soma areas values are generally consistent with the average diameter of 34.5 μm reported for CS neurones in *Macaca mulatta* (Nudo et al 95), as well as with the range of diameters (10 to 58 μm) obtained from CS neurones retrogradely labelled as a result of tracer injection in the spinal cord (Murray and Coulter 81). More directly, the soma area values of Figure 3.5 B are consistent with the areas derived from the dimensions of six intracellularly labelled CS neurones (Gosh and Porter 88), ranging from 650 to 1000 μm^2 . In addition to inter-individual differences, different shrinkage factors of the tissue during fixation and histological processing may explain the wide variability from one animal to the next (Fig. 3.5 B). The shrinkage of the CS axotomised neurones appeared clearly in M1 but, in SMA-proper, although

the soma areas tended to be smaller in the hemisphere contralateral to the lesion than in the ipsilateral one, this difference was not statistically significant (Fig. 3.5 B). The less dramatic impact of the lesion on SMA-proper as compared to M1 in term of shrinkage of the axotomised neurones, as seen in Fig. 3.5 B, can be explained by the lower number of CS neurones in SMA-proper than in M1. Therefore, measurements conducted on a general population of pyramidal neurones in layer V involve proportionally less axotomised CS neurones in SMA-proper than in M1, explaining why the difference was smaller in the former than the latter area.

3.3.1.3: Technical considerations

It is worth to mention here that the reduction of the anterograde transport velocity of BDA after injection in the contralateral M1 in the monkeys Ctrl 1 and Ctrl 2 was unexpected. In intact animals, the transport time that we used here would have been fully sufficient to stain CS fibres down to the thoracic segments (Rouiller et al 96), whereas in the two lesioned animals, it only enabled to stain CS axons down to the rostral most cervical segments. In young and juvenile macaques subjected to a spinal hemisection similar transport times were used successfully (Galea and Darian-Smith 97a). The reasons for the slow transport velocity in the present study are unknown, but the age of the animals at the time of the lesion as well as the duration of the survival time following the lesion could contribute to explain for this difference. In rodents, it has been observed that axotomy reduces the retrograde transport velocity in a way that varies in function of the time from the moment of the lesion to that of the injection of the tracer (Tseng et al 95).

3.3.1.4: CS cells survival after transection of the CS tract: comparison with previous studies

Cell death has long been used as tracing method (retrograde degeneration) enabling to identify the cells of origin and the course of projecting systems, although its feasibility has been

questioned (Kuypers 81). Following a section of the CS tract, such changes have been reported in the layer V of motor cortex of primates (Levin and Bradford 38; Walker and Richter 66; Pernet and Hepp-Reymond 75), including human subjects (Holmes and May 09; Bronson et al 78). In the macaque monkey, a quantitative analysis of Nissl stained material indicated that up to 63% of the pyramidal cells disappeared from layer V following a complete unilateral pyramidal transection (pyramidotomy) and, in addition, the large pyramidal neurones were more affected than the small ones (Pernet and Hepp-Reymond 75). The present observations at **low magnification** on Nissl and SMI-32 stained material (Fig. 3.3) would lead to conclusions consistent with these previous studies, suggesting that many large pyramidal neurones may have disappeared from layer V in M1 and SMA-proper. However, our quantitative analysis of the SMI-32 stained material at **high magnification** led to another conclusion. SMI-32 positive cells are mostly projecting neurones and, in the intact animal, the large layer V neurones in M1, presumably CS neurones, belong to the well stained elements (Campbell and Morrison 89). In our experiments, the comparison of both hemispheres for the number of SMI-32 stained neurones in M1 and in SMA did not show any significant cell loss in the hemisphere contralateral to the lesion. However, comparing the projected soma surface of the stained cells in both hemispheres showed that the layer V neurones in M1 are significantly smaller in the contralateral hemisphere, thus indicating shrinkage of these neurones. In addition, the intensity of the SMI-32 cell staining was fainter in the hemisphere opposite to the lesion. These observations indicate that the layer V neurones survived but shrank. The shrinkage of the large pyramidal cells and the decrease of SMI-32 immunoreactivity could account for the discrepancy of the observations made at different magnifications in Nissl and SMI-32 stained material. The large cells shrank to the dimensions of other layer V neurones and thus lost their typical appearance in Nissl stained sections. The survival of at least a large portion of the CS neurones is confirmed by several other observations, which also demonstrated that the damaged CS fibres

still reach the spinal segments rostral to the lesion. First, retrogradely stained neurones in the hand and foot region of the contralateral M1 were found after injecting a retrograde tracer just rostrally to a cervical spinal hemisection (Galea and Darian-Smith 97a). Second, although the transport time was inadequate to stain CS axons down to the lesion site, BDA injections in the M1 hand region of monkeys Ctrl 1 and Ctrl 2 stained numerous fibres down to the pyramids and entered the first cervical segments. Third, our SMI-32 stained material showed positive axons in the dorsolateral funiculi at locations rostral to the lesion, presenting a comparable pattern of labelling of CS axons on both sides. Caudally to the lesion, SMI-32 stained axons nearly fully disappeared from the dorsolateral funiculus on the lesioned side. Since the axons of numerous large layer V pyramidal cells of M1 are SMI-32 positive, many of the stained axons in the dorsolateral funiculus are presumably CS axons. Altogether these data show that the sectioned CS axons survived and did not retract significantly from the lesion level (not more than 0.5 – 1 mm; Fig. 3.2). This is in accordance with the distribution of apoptotic elements in the spinal cord of lesioned monkeys which are mainly found in the white matter caudal to a lesion affecting descending tracts (Crowe et al 97). In conclusion, these considerations and the present SMI-32 data contradict the notion of a substantial loss of CS neurones after lesion of the spinal cord in primates, put forward by some authors on the basis of Nissl-stained material (Holmes and May 09; Levin and Bradford 38; Pernet and Hepp-Reymond 75; Hains et al 03b). How to reconcile then the present observation of a survival of axotomized CS neurones with these retrograde degeneration data reported earlier? First of all, shrunken but rescued CS neurones may have been interpreted as a disappearance of large layer V neurones, as this can be seen on Nissl material, especially at low magnification (Fig. 3.3). The use of the specific SMI-32 marker represents a clear advantage over Nissl material, to better identify the relevant population of neurones on which to perform counts and measurements. Second, most retrograde degeneration studies are cases in which the CS tract lesion was a pyramidotomy, a lesion thus located closer from the

soma than our cervical hemisection, leading to a higher probability of cell loss than after lesion located more caudal. The latter explanation is however unlikely because in one of these earlier studies the lesion was at cervical level and the authors concluded to a significant cell loss (Holmes and May 09), in contradiction to the present results.

Highly relevant is the presence in the literature of observations in the primate and on Nissl material fully in line with the present results. Indeed, Tower (1940), Lassek (1948), Bronson et al. (1978) all reported a large survival of CS axotomised neurones, irrespective of whether the lesion was a pyramidotomy or affected the spinal cord itself (Tower 40; Bronson et al 78). In particular, Lassek (1948) met this conclusion based on a highly careful examination of cell size and cell appearance in layer V, as we did here using another marker, SMI-32. These detailed observations in both Nissl and SMI-32 materials demonstrate that the axotomised CS neurones lost some of their typical appearance and shrank, changes that were apparently not detected by the authors concluding to cell loss, possibly because they focussed their observations on the large layer V neurones without paying enough attention to smaller (shrunken) pyramidal cells.

The same controversy appears to be present in rodents. In the rat, it has recently been demonstrated that, after transection of the main CS tract (95% of CS axons, running in the dorsal funiculus) at T9 level, a significant proportion (40%) of the CS neurones projecting to this thoracic level underwent apoptosis one week after injury (Hains et al 03a). At four weeks after injury, the same authors estimated the cell loss to be around 35-40% of the CS neurones. As discussed by Hains et al. (2003), considering that about 40% of CS axons reach the T9 level, the cell loss thus represents about 14% of all CS neurones. In the present study, considering that the lesion was at cervical level, a comparable rate of cell loss would have resulted in a substantially larger loss of cell. The data presented in Figure 3.4 argue that, in contrast to the rat, there was no cell loss after cervical cord hemisection in the monkey. To explain such a species difference, one should consider that, in the monkey, the CS axons have been axotomised at a distance from the

soma longer than in the rat, assuming that the further the lesion is from the soma the higher is the probability of survival. One may also speculate that, on their way, CS axons in the monkey may give rise to more collateral projections, establishing contacts which may favour survival. The evidence of a cell loss in the rat is however challenged by a study conducted in hamsters (Tower 40; Kalil and Schneider 75), showing clear evidence for a survival of most CS axotomised neurones after unilateral pyramidotomy. The latter observation argues against the notion that a section of the axon relatively close to the soma leads to a retrograde degeneration up to the cell body. Indeed, Kalil and Schneider (1975) observed that the retrograde degeneration of the axon was limited to a distance of 6-7 mm. The main difference between the two studies is that the observation of Hains (2003) was conducted after a survival time of 4 weeks, whereas Kalil and Schneider (1975) followed the changes up to 14 months.

What is then the difference between the studies concluding to a cell loss from those arguing for a cell survival, making the latter more plausible? Cell loss was a conclusion drawn from observations limited to the soma of the CS neurones in the cerebral cortex and without quantification of soma areas. In contrast, the studies supporting the scenario of cell survival not only examined in detail and quantitatively the situation in the cerebral cortex (counts of cells and measurements of soma areas), but also looked at in detail about the status of the CS axons rostral to the lesion. These reports (Tower 40; Kalil and Schneider 75) and the present study all provide evidence that the CS transected axons underwent a retrograde degeneration, but limited to a short distance above the lesion (a few mm), consistent with a survival of the soma of origin.

3.3.1.5: Considerations related to the recovery from CS tract lesion

As described in a paragraph, the two monkeys Ctrl 1 and Ctrl 2 subjected to the cervical cord lesion exhibited a spontaneous, incomplete recovery of the hand manual dexterity reaching,

after about 50 days, a level of 70 and 20% of the pre-lesion behavioural score in Ctrl 1 and Ctrl 2, respectively. One may think that the absence of death among the axotomized CS neurones is a factor favourable for such a remarkable spontaneous recovery. The large survival of axotomized CS neurones in primates thus represents good news in the context of developing treatments aimed at enhancing such recovery. Indeed, in primates, a rapid treatment post-lesion aimed at preventing cell loss does not seem necessary. In other words, in primates, treatments can be directly focussed on promoting regeneration of transected CS axons and/or triggering the recruitment of minor CS tracts preserved by the lesion. It has been shown that such preserved minor CS tracts can give rise to axonal sprouting, as observed in the rat even in absence of treatment (Weidner et al 01e). The large survival of axotomized CS neurones in primates is thus favourable for promoting *compensatory sprouting* from the transected axons along their trajectory, in order to recruit other descending pathways (e.g. rubrospinal projection), allowing a re-routing of motor commands to the motoneurones. Such a mechanism of *compensatory sprouting* was demonstrated to be enhanced in rats subjected to unilateral or bilateral pyramidotomy or to motor cortex lesion and treated with an antibody neutralising the neurite growth inhibition protein “Nogo” (Z'Graggen et al 98;Wenk et al 99;Raineteau et al 99;Raineteau et al 01;Raineteau et al 02a). The two monkeys subjected to cervical hemisection in the present study are animals representing a model to assess the degree of recovery after such a lesion, that will be compared in the near future to monkeys subjected to the same lesion but treated with the antibody neutralising “Nogo”.

The present study aimed at assessing the effect of partial spinal cord lesions, as well as the amount and time course of spontaneous recovery that can take place post-lesion. The understanding of such mechanisms is of strategic significance in the context of ongoing work leading to attempts to repair human spinal cord injury. In particular, such knowledge derived

from the present non-human primate model is crucial, because of the potential difficulties in translating work in the rat model of spinal cord injury to the human condition. In macaque monkeys, we used a skilled hand task to confirm that some spontaneous recovery can and do occur following a sub-total cervical hemi-section. Quantitative behavioral measures also demonstrate that the recovery is limited and may to some extent depend on compensatory strategies. Whatever the precise strategies are, reversible inactivation experiments clearly demonstrated the contribution of the contralesional primary motor cortex to the recovered function. These results are of significance in attempting to assess the impact of any interventions that might further improve recovery of function after spinal cord injury.

3.3.2: Discussion related to the ICMS data (plasticity of motor cortical maps induced by the cervical lesion)

3.3.2.1: Technical considerations

Data in Figure 3.18 show clear changes of cortical representations in M1 when comparing ICMS maps established before and after cervical hemi-section. In addition, the representation of body territories affected by the lesion (digits) exhibited post-lesion progressive changes, in parallel to the time course of recovery. These observations are based on the comparison of ICMS data derived from penetrations performed at the same cortical location at various time points, for instance before and after the lesion. However, one may question the intrinsic variability of the ICMS method. In other words, are ICMS changes attributed to a lesion clearly more prominent than variations observed along repetitive penetrations performed at the same location in an intact animal? To address this crucial question, a few ICMS penetrations at the same site were repeated during the pre-lesion period, while the monkeys were intact. Overall, in the two monkeys, six and two ICMS electrode penetrations were repeated either twice or even three times, respectively. The time interval between two repetitions ranged from 2 to 71 days (median value:

12 days). While one electrode penetration exhibited activation of different body territories at two time points (digits replaced by face), the 7 other repetitions of electrode penetrations were found to be very reproducible. More precisely, we observed similar body territories activated at lowest threshold, comparable sequences of movements observed along the track at various depths and consistent relative amplitudes of current needed to elicit the observed movements. These data argue for a good reproducibility of the ICMS method and, therefore, one can conclude that the ICMS plastic changes as described in Figures 3.18 A and B and following are substantial and reflect a true plasticity induced by the cervical lesion. Furthermore, such stability of ICMS data observed for electrode penetrations repeated up to three times is consistent with the notion that our protocol of stimulation did not generate damage of the cortical tissue due to over-penetration. This conclusion is in line with our previous work (Rouiller et al 98;Liu and Rouiller 99), where no deficit of manual dexterity was observed when the hand area was mapped using the same ICMS protocol while the animal was intact.

3.3.2.2: Pathways affected by the lesion:

The position and extent of the lesion at the transition between the seventh and eighth cervical segments (Fig. 3.1 B) indicates that most of the drive exerted by the motor cortex on finger muscle motoneurons was eliminated. In the macaque monkey, the location of the CS axons at cervical level, forming three different fascicles, is well established (Kuypers 81;Rouiller et al 96;Armand et al 97;Galea and Darian-Smith 97b). More quantitatively, as shown in a paragraph, unilateral injection of the anterograde tracer BDA in the hand area of M1 resulted in the following distribution of CS axons at cervical level. Nearly 90% of the CS axons originating from the injected hemisphere decussate, while the rest (about 10%) does not decussate, running along the ipsilateral dorso-lateral fasciculus, although a few CS axons (1-2%) travel along the ipsilateral ventro-medial fasciculus. Most of the left dorsolateral fasciculus was thus sectioned in

both animals (Fig. 3.1 B), although a small proportion may have been spared in monkey Ctrl 1. One may also not totally exclude the possibility that a few intraspinal collaterals of stem CS axons can travel for some distance within the spinal grey matter (Lawrence et al 85), and thus could still influence motoneurons in 1 or even 2 segments below the funicular lesion. Despite of the absence of direct quantitative measures, it seems safe to estimate that 80-90% of the drive normally provided directly by the CS system to spinal segments caudal to the lesion (and including that of the spared uncrossed projections) has been eliminated. In addition, the drive provided by other descending systems (particularly that of the rubrospinal projection) has been partially diminished as well.

The above mentioned distribution of CS axons at cervical level in the three components of the CS tract is consistent with the classical view of a vast majority (about 90%) of decussated CS axons travelling in the dorsolateral funiculus. However, the higher proportion of undecussated CS axons found in the ipsilateral dorsolateral funiculus than in the ipsilateral ventral funiculus contrasts with the classical view of more numerous undecussated CS axons in the ventral funiculus, as seen in macaca mulata or chimpanzee (Kuypers 81). This discrepancy can be explained by different zones of origin of the CS projection in M1, precisely restricted to the hand area in our study. In addition, the classical view is based on observations derived from tracing methods (anterograde degeneration, autoradiography), which do not allow identification and precise counts of individual CS axons, in contrast to BDA, suggesting that the latter method led to more accurate counts.

The clear loss of ICMS responsive sites in M1 during 1-2 weeks after the lesion (see Figs. 3.25 and 3.26) was interpreted primarily as the consequence of the transection of the CS axons mediating the control of M1 onto the corresponding distal muscle motoneurons, before some re-organization took place. However, one may question to what extent such observation relates to what has been referred to as “spinal shock”, although the physio-pathology of this phenomenon

remains largely unknown. We believe that both the small size of the spinal lesion and its greater impact on the white than gray matter is likely to generate a less prominent “spinal shock” than a larger spinal lesion as often observed in human subjects. In addition, the muscles supporting the finger movements of the affected hand were not flaccid. These considerations thus argue against a “spinal” phenomenon and rather support the notion that the loss of ICMS response is indeed due to lack of CS input.

3.3.2.3: Extent and time course of functional recovery

After subtotal hemi-section of the cervical cord at C7/C8 level, the time course of recovery of manual dexterity observed in the present work (about 50 days) is generally consistent with the 60-90 days reported following complete unilateral section of the cervical cord at C3 level in juvenile monkeys (Galea and Darian-Smith 97a). However, the latter authors reported persisting deficit, in line with our data demonstrating that the recovery is incomplete. The recovered grip movement can differ from the original pre-lesion pattern of movement, indicating that rehabilitation is, at least partly, based on the development of compensatory movements, as previously reported after cortical lesion (Friel and Nudo 98) or cervical cord lesion (Galea and Darian-Smith 97b). In the present case, the prehension of pellets was executed more slowly and the monkeys did not use the typical opposition of thumb and index finger, indicating that coordination of the fingers was affected. In one animal (Ctrl2), the thumb was even largely unused, being kept in a flexed position. As a result, the pellet was grasped essentially using the index finger by pushing the pellet towards the dorsal part of the flexed thumb or towards the palm of the hand.

Previous data derived from cortical lesions have shown that an intense rehabilitative training (frequent use of the impaired hand) improves the recovery and leads to a re-expansion of the digit representation (Nudo et al 96). Such intense rehabilitative training was not considered

here because our goal was to establish a baseline of “spontaneous” recovery for the cervical cord hemi-section model. Nevertheless, we cannot exclude that the daily manual dexterity testing (“modified Brinkman board” task) represented a mild rehabilitative training, which presumably led to a slightly better recovery than that obtained if the monkey would have been tested only after several months. The work of Nudo and collaborators (Nudo et al 96;Nudo 99) thus suggests that the decrease of the hand representation in the contralesional cortex would have been less dramatic if a more intense use of the affected hand had occurred.

3.3.2.4: Mechanisms of functional recovery:

The ICMS experiments confirm that a spinal cord lesion modifies cortical maps, as previously reported in monkeys (Jain et al 97;Jain et al 98) and human subjects (Puri et al 98;Green et al 98;Nelles et al 99;Green et al 99;Lotze et al 99;Marshall et al 00). However, in human subjects, the pre-lesion cortical map was not available and the post-lesion data were compared with a group of normal subjects, thus introducing a large variability in the data. In contrast, the monkey model as used here allows a comparison of the cortical map pre- and post-lesion. The present study thus provides evidence, for the first time, that the time course of recovery after hemi-section of the cervical cord parallels the progressive changes taking place in the somatotopic map in the motor cortex contralateral to the lesion. Although the parallel time courses of recovery and cortical plastic changes do not prove a causal relationship between the two phenomena, reversible inactivation of the reorganized motor cortex several months after the lesion abolished the manual dexterity regained during the recovery. In contrast, reversible inactivation of the motor cortex homolateral to the cervical lesion did not affect the recovered behavioral score. Consequently, a possible mechanism of recovery involving decussated CS axons originating from the ipsilesional cortex, sprouting in the intact spinal side before regaining control of deprived motoneurons by re-crossing the midline below the lesion is unlikely. These

observations support the notion that, although substantially diminished in size, the post-lesion hand territory in the contralesional M1 plays a crucial role in the partial rehabilitation.

The pathways through which the reorganized hand area in the contralesional M1 regains partial control of the muscles of the affected hand remains unclear. Previous data (Weidner et al 01) and preliminary observations from our laboratory indicate that there is no regeneration of the transected CS axons. Furthermore, we have evidence that most axotomized CS neurons in the contralateral M1 do not degenerate, but rather exhibit shrinkage of their soma. A mechanism of compensatory sprouting can come into play in the form of a re-innervation of the denervated motoneurons by undecussated CS axons originating from the contralesional M1 and crossing the midline at segmental level below the lesion. The time course of reorganization in M1 may thus reflect the time taken for such compensatory sprouting. One may also argue that the post-lesion control exerted by the contralesional M1 may be undertaken by decussated CS axons spared by the lesion. Such interpretation is unlikely, particularly for Ctrl2, considering the location and extent of the lesion (Fig. 3.1 B) and, in addition, such control would be effective immediately after the lesion. Indeed, the delayed recovery and progressive re-arrangement of the hand representation in M1 over several weeks are rather supportive of slow mechanisms of compensation via reorganized pathways, such as the undecussated CS axons running in the contralesional dorso-lateral and/or ventral lateral funiculi. Such a scenario of recovery involving minor CS tracts not affected by the lesion has been verified in the rat. Spontaneous sprouting of the CS ventral funiculus after lesion at cervical level of the main CS tract in the dorsal funiculus was found to parallel recovery (Weidner et al 01c). Elegantly, these authors observed that a combined lesion of both the CS dorsal and ventral funiculi eliminated sprouting and recovery in the rat. Based on these rat data, one may speculate that a larger cervical lesion at C7/C8 in the monkey (affecting the uncrossed CS tracts) would result in a slower and less prominent recovery, as compared to the monkeys of the present study. One should also not disregard the possibility of

compensatory sprouting taking place immediately above the lesion by forming new intraspinal circuits (e.g. (Weidner et al 01; Hill et al 01c; Bareyre et al 04) or at higher levels. For instance, both CS neurons not affected by the lesion and/or axotomized CS neurons may well sprout in the brainstem in order to recruit other descending pathways such as the rubrospinal or reticulospinal projection systems (Kuypers 81). However, in adult rats subjected to pyramidotomy, such post-lesional sprouting in the brainstem was substantial only after blockade of myelin-associated neurite growth inhibitors (Kuypers 81). This scenario of recovery via the brainstem is consistent with the observation of significant sprouting of the rubrospinal projection in the spinal cord, after pyramidotomy and blockade of myelin-associated neurite growth inhibitors (Raineteau et al 02b). Also consistent with such a scenario, in the contusive spinal cord injury model in the rat, a collateralization and penetration of reticulospinal fibers in the lesion matrix was observed (Hill et al 01) . In the present monkey study, the rubrospinal projection was partially (Ctrl 1) or substantially (Ctrl 2) affected by the lesion, in contrast to the ventromedially located reticulospinal tract largely unaffected by the cervical hemi-section. Therefore, the cortico-reticular and reticulospinal projections may have contributed to the observed behavioral recovery, more than the cortico-rubral and rubrospinal projections. Irrespective of the precise scenario of remodeling, it seems that the preservation of a small contingent of intact CS axons (the undecussated ones) is a necessary condition for the plastic changes in motor maps as observed here in Figs. 3.18, 3.25 and 3.26. Indeed, it was reported that ICMS did not elicit motor responses following a complete pyramidotomy (Hill et al 01a).

The re-routing of the control of hand muscles via remodeled connections appears very efficient functionally, as evidenced by the comparable ICMS thresholds before and after the lesion (Fig. 3.24). It should be noted that the comparison for distal movements is problematic in Ctrl 2, since only two sites eliciting digit movements were left at the time point at which the ICMS map was established post-lesion. Nevertheless, based on the data in Ctrl1, it appears that

the ICMS sites eliciting movements of the digits post-lesion did not exhibit elevated threshold. An absence of elevation of ICMS thresholds post-lesion was also observed for other movements, namely of face and proximal forelimb muscles (Fig. 3.24). The observation that ICMS thresholds were not significantly higher post-lesion (Fig. 3.24) may be explained, at least in part, by considering that threshold measurements were performed at a time period after the recovery had reached a plateau. One cannot thus exclude that ICMS thresholds were elevated during the recovery period.

The present data and previous studies in the rat (Weidner et al 01a) argue for a significant role played in the recovery by undecussated axons originating from the contralesional motor cortex and not affected by the lesion. However, further anatomical data are needed, derived from injection of an anterograde tracer in the contralesional motor cortex, in order to identify at which level undecussated CS axons sprout in order to compensate for the deficits induced by the cervical lesion. Such evidence of compensatory sprouting may be difficult to establish because it may well be present in a relatively limited number of CS axons and therefore difficult to detect while comparing with a normal animal.

List of references for chapter 3

- 1: Armand,J., Olivier,E., Edgley,S.A. & Lemon,R.N. (1997) Postnatal development of corticospinal projections from motor cortex to the cervical enlargement in the macaque monkey. *Journal of Neuroscience*, **17**, 251-266.
- 2: Bareyre,F.M., Kerschensteiner,M., Raineteau,O., Mettenleiter,T.C., Weinmann,O. & Schwab,M.E. (2004) The injured spinal cord spontaneously forms a new intraspinal circuit in adult rats. *Nature Neuroscience*, **7**, 269-277.
- 3: Bronson,R., Gilles,F.H., Hall,J. & Hedley-Whyte,E.T. (1978) Long term post-traumatic retrograde corticospinal degeneration in man. *Hum.Pathol.*, **9**, 602-607.
- 4: Campbell,M.J. & Morrison,J.H. (1989) Monoclonal antibody to neurofilament protein (SMI-32) labels a subpopulation of pyramidal neurons in the human and monkey neocortex. *J Comp Neurol.*, **282**, 191-205.

- 5: Crowe,M.J., Bresnahan,J.C., Shuman,S.L., Masters,J.N. & Beattie,M.S. (1997) Apoptosis and delayed degeneration after spinal cord injury in rats and monkeys. *Nat.Med.*, **3**, 73-76.
- 6: Friel,K.M. & Nudo,R.J. (1998) Recovery of motor function after focal cortical injury in primates: compensatory movement patterns used during rehabilitative training. *Somatosens.Mot.Res.*, **15**, 173-189.
- 7: Galea,M.P. & Darian-Smith,I. (1997a) Corticospinal projection patterns following unilateral section of the cervical spinal cord in the newborn and juvenile macaque monkey. *Journal of Comparative Neurology*, **381**, 282-306.
- 8: Galea,M.P. & Darian-Smith,I. (1997b) Manual dexterity and corticospinal connectivity following unilateral section of the cervical spinal cord in the macaque monkey. *Journal of Comparative Neurology*, **381**, 307-319.
- 9: Gosh,S. & Porter,R. (1988) Morphology of pyramidal neurones in monkey motor cortex and the synaptic actions of their intracortical axon collaterals. *J.Physiol.(London)*, **400**, 593-615.
- 10: Green,J.B., Sora,E., Bialy,Y., Ricamato,A. & Thatcher,R.W. (1998) Cortical sensorimotor reorganization after spinal cord injury - An electroencephalographic study. *Neurology*, **50**, 1115-1121.
- 11: Green,J.B., Sora,E., Bialy,Y., Ricamato,A. & Thatcher,R.W. (1999) Cortical motor reorganization after paraplegia - An EEG study. *Neurology*, **53**, 736-743.
- 12: Hains,B.C., Black,J.A. & Waxman,S.G. (2003) Primary cortical motor neurons undergo apoptosis after axotomizing spinal cord injury. *Journal of Comparative Neurology*, **462**, 328-341.
- 13: Hill,C.E., Beattie,M.S. & Bresnahan,J.C. (2001) Degeneration and sprouting of identified descending supraspinal axons after contusive spinal cord injury in the rat. *Experimental Neurology*, **171**, 153-169.
- 14: Holmes,G.L. & May,W.P. (1909) On the exact origin of the pyramidal tracts in man and other mammals. *Brain*, **32**, 1-42.
- 15: Jain,N., Catania,K.C. & Kaas,J.H. (1997) Deactivation and reactivation of somatosensory cortex after dorsal spinal cord injury. *Nature*, **386**, 495-498.
- 16: Jain,N., Florence,S.L. & Kaas,J.H. (1998) Reorganization of somatosensory cortex after nerve and spinal cord injury. *News Physiol.Sci.*, **13**, 143-149.
- 17: Kalil,K. & Schneider,G.E. (1975) Motor performance following unilateral pyramidal tract lesions in the hamster. *Brain Res.*, **100**, 170-174.
- 18: Kuypers,H.G.J.M. (1981) Anatomy of descending pathways. In Brooks,V.B. (ed), *Handbook of Physiology (The Nervous System)*, vol. II, part I. Am. Physiol. Soc., Bethesda, MD, pp. 597-666.

- 19: Lacroix,S., Havton,L.A., McKay,H., Yang,H., Brant,A., Roberts,J. & Tuszynski,M.H. (2004) Bilateral corticospinal projections arise from each motor cortex in the macaque monkey: a quantitative study. *J.Comp Neurol.*, **473**, 147-161.
- 20: Lawrence,D.G., Porter,R. & Redman,S.J. (1985) Corticomotoneuronal synapses in the monkey:light microscopic localization upon motoneurons of intrinsic muscles of the hand. *Journal of Comparative Neurology*, **232**, 499-510.
- 21: Levin,P.M. & Bradford,F.K. (1938) The exact origin of the cortico-spinal tract in the monkey. *J.Comp.Neurol.*, **68**, 411-422.
- 22: Liu,Y. & Rouiller,E.M. (1999) Mechanisms of recovery of dexterity following unilateral lesion of the sensorimotor cortex in adult monkeys. *Experimental Brain Research*, **128**, 149-159.
- 23: Lotze,M., Laubis-Herrmann,U., Topka,H., Erb,M. & Grodd,W. (1999) Reorganization in the primary motor cortex after spinal cord injury - A functional Magnetic Resonance (fMRI) Study. *Restor.Neurol.Neurosci.*, **14**, 183-187.
- 24: Luppino,G., Matelli,M., Camarda,R. & Rizzolatti,G. (1994) Corticospinal projections from mesial frontal and cingulate areas in the monkey. *NeuroReport*, **5**, 2545-2548.
- 25: Marshall,R.S., Perera,G.M., Lazar,R.M., Krakauer,J.W., Constantine,R.C. & DeLaPaz,R.L. (2000) Evolution of cortical activation during recovery from corticospinal tract infarction. *Stroke*, **31**, 656-661.
- 26: Murray,E.A. & Coulter,J.D. (1981) Organization of corticospinal neurons in the monkey. *J Comp Neurol*, **195**, 339-365.
- 27: Nelles,G., Spiekermann,G., Jueptner,M., Leonhardt,G., Müller,S., Gerhard,H. & Diener,H.C. (1999) Reorganization of sensory and motor systems in hemiplegic stroke patients - A positron emission tomography study. *Stroke*, **30**, 1510-1516.
- 28: Nudo,R.J. (1999) Recovery after damage to motor cortical areas. *Curr.Opin.Neurobiol.*, **9**, 740-747.
- 29: Nudo,R.J., Sutherland,D.P. & Masterton,R.B. (1995) Variation and evolution of mammalian corticospinal somata with special reference to primates. *Journal of Comparative Neurology*, **358**, 181-205.
- 30: Nudo,R.J., Wise,B.M., SiFuentes,F. & Milliken,G.W. (1996) Neural substrates for the effects of rehabilitative training on motor recovery after ischemic infarct. *Science*, **272**, 1791-1794.
- 31: Pernet,U. & Hepp-Reymond,M.-C. (1975) Retrograde Degeneration der Pyramidenbahnzellen im motorischen Kortex beim Affen (*Macaca fascicularis*). *Acta Anat.(Basel)*, 552-561.
- 32: Puri,B.K., Smith,H.C., Cox,I.J., Sargentoni,J., Savic,G., Maskill,D.W., Frankel,H.L., Ellaway,P.H. & Davey,N.J. (1998) The human motor cortex after incomplete spinal cord

- injury: an investigation using proton magnetic resonance spectroscopy. *J.Neurol.Neurosurg.Psychiatry*, **65**, 748-754.
- 33: Raineteau,O., Fouad,K., Bareyre,F.M. & Schwab,M.E. (2002) Reorganization of descending motor tracts in the rat spinal cord. *European Journal of Neuroscience*, **16**, 1761-1771.
- 34: Raineteau,O., Fouad,K., Noth,P., Thallmair,M. & Schwab,M.E. (2001) Functional switch between motor tracts in the presence of the mAb IN-1 in the adult rat. *Proceedings of the National Academy of Sciences of the United States of America*, **98**, 6929-6934.
- 35: Raineteau,O., Z'Graggen,W.J., Thallmair,M. & Schwab,M.E. (1999) Sprouting and regeneration after pyramidotomy and blockade of the myelin-associated neurite growth inhibitors NI 35/250 in adult rats. *European Journal of Neuroscience*, **11**, 1486-1490.
- 36: Rouiller,E.M., Moret,V., Tanné,J. & Boussaoud,D. (1996) Evidence for direct connections between the hand region of the supplementary motor area and cervical motoneurons in the macaque monkey. *European Journal of Neuroscience*, **8**, 1055-1059.
- 37: Rouiller,E.M., Yu,X.H., Moret,V., Tempini,A., Wiesendanger,M. & Liang,F. (1998) Dexterity in adult monkeys following early lesion of the motor cortical hand area: the role of cortex adjacent to the lesion. *Eur.J.Neurosci.*, **10**, 729-740.
- 38: Tower,S.S. (1940) Pyramidal lesion in the monkey. *Brain*, **63**, 36-90.
- 39: Tseng,G.F., Shu,J., Huang,S.J. & Wang,Y.J. (1995) A time-dependent loss of retrograde transport ability in distally axotomized rubrospinal neurons. *Anatomy and Embryology*, **191**, 243-249.
- 40: Walker,A.E. & Richter,H. (1966) Section of the cerebral peduncle in the monkey. *Arch Neurol*, **14**, 231-240.
- 41: Weidner,N., Ner,A., Salimi,N. & Tuszynski,M.H. (2001) Spontaneous corticospinal axonal plasticity and functional recovery after adult central nervous system injury. *Proceedings of the National Academy of Sciences of the United States of America*, **98**, 3513-3518.
- 42: Wenk,C.A., Thallmair,M., Kartje,G.L. & Schwab,M.E. (1999) Increased corticofugal plasticity after unilateral cortical lesions combined with neutralization of the IN-1 antigen in adult rats. *Journal of Comparative Neurology*, **410**, 143-157.
- 43: Z'Graggen,W.J., Metz,G.A.S., Kartje,G.L., Thallmair,M. & Schwab,M.E. (1998) Functional recovery and enhanced corticofugal plasticity after unilateral pyramidal tract lesion and blockade of myelin-associated neurite growth inhibitors in adult rats. *J.Neurosci.*, **18**, 4744-4757.

Chapter 4: Consequences of an unilateral section of the spinal cord at cervical level in primate treated with an antibody neutralizing the neurite growth inhibiting protein Nogo _____ 190

4.1: Introduction	190
4.2: Results	191
4.2.1: Anatomical data	191
4.2.1.1: Reconstruction of the spinal cord hemisection	191
4.2.1.2: BDA stained fibres around the lesion site	193
4.2.2: Behavioural data	198
4.2.3: ICMS data	210
4.2.3.1: Mapping of M1 hand area before and after cervical cord lesion	210
4.2.3.2: Distribution of ICMS sites in relation to the activated body territories	215
4.3: Discussion:	217

Chapter 4: Consequences of an unilateral section of the spinal cord at cervical level in primate treated with an antibody neutralizing the neurite growth inhibiting protein Nogo

4.1: Introduction

This second part of the results presents the data obtained in the two monkeys subjected to cervical hemi-section of the cervical cord treated with the anti-Nogo antibody: Treat 1 and Treat 2. The anatomical data are presented in the first sub-chapter, focusing on the extent of the cervical cord hemisection and the consequences in the cortical layers of M1. The behavioural data are presented in a second sub-chapter consisting of the quantitative evaluation of the deficits resulting from the cervical cord lesion, the extent and time course of recovery, as well as a qualitative approach of the general behaviour of the treated animals. The third sub-chapter summarises the electrophysiological data obtained with ICMS in these two animals focusing on the functional organisation of M1 in both hemispheres, particularly on the hand area. The general discussion follows in the fourth and last sub-chapter.

Monkeys Treat 1 and 2 were subjected to the same type of unilateral spinal cord section at C7-C8 level on the left side. The treatment was administered following the same protocol as for the two monkeys Ctrl 1 and 2. An osmotic pump was locally implanted that delivered continuously the antibody intrathecally a few mm above the level of the blade incision immediately after the lesion.

How can we know that the antibody has been appropriately administered to the treated animals? The blood sampling analysis of other macaque monkeys treated in the same conditions has been made by Novartis[®] that provided us with the anti-Nogo antibody. This analysis showed

the presence of the antibody in the blood of the treated animals during the four weeks of the treatment. Further analysis of macaque brain tissue treated with the anti-Nogo antibody in the same conditions has been made by Schwab and collaborators in Zurich. They showed (unpublished data) that the distribution of the anti-Nogo antibody is ubiquitous in the CNS (brain and spinal cord).

4.2: Results

4.2.1: Anatomical data

Two anatomical aspects have been particularly investigated in this section: the reconstruction of the spinal cord lesion to assess the extent of the lesion and the morphological changes at the cervical level using first, anterograde tracers injected in the motor cortex in both hemispheres to label the CST and, second, a cytological staining (SMI-32) applied post fixation to assess the cortical consequences of the cervical cord lesion.

4.2.1.1: Reconstruction of the spinal cord hemisection

The histological reconstruction of the spinal cord lesion in Treat 1 and Treat 2 is shown in Fig. 4.1 (left panel and right panels respectively). The spinal cord lesions in Treat 1 and Treat 2 were performed in the same way as in the control monkeys Ctrl 1 and Ctrl 2. The lesion was made at cervical level C7-C8 on the left side (see methods). Considering the differences of possible behavioural recovery of function with a small amount of preserved fibres, each animal will be discussed separately.

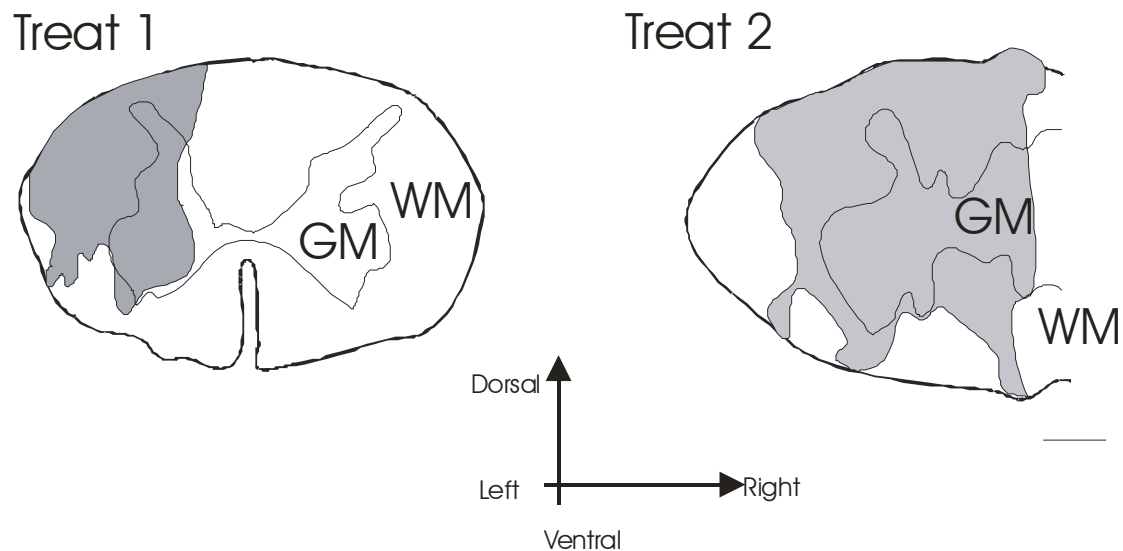


Fig. 4.1: Histological reconstruction of the spinal cord lesion at cervical level (C7-C8) on the left side in the transversal plane in monkeys Treat 1 (left panel) and Treat 2 (right panel). The extent of the lesion is represented in grey. In monkey Treat 1, the corticospinal and the rubrospinal tracts have been entirely transected whereas the ventromedial part of the white matter has been preserved. In monkey Treat 2, the lesion did not completely interrupt the corticospinal tract on the left side in its most lateral part, and the rubrospinal tract remained mostly unaffected by the lesion. GM: grey matter, WM: white matter. Scale bar: 1mm.

A crucial point in our study is the extent of the spinal cord lesion, and how it affected the different afferent and efferent tracts of fibres involved in motor control. In Treat 1, the corticospinal tract on the left side has been completely interrupted and the rubrospinal tract was also most likely completely interrupted (Fig. 4.1). In Treat 2, the cervical lesion affected most of the CST in the dorsolateral funiculus, sparing partly its most lateral part, whereas the rubrospinal tract remained mostly unaffected (Fig. 4.1 right panel). The other tracts such as the reticulospinal and the vestibulospinal tracts, located in the ventral part of the spinal cord, were preserved in both monkeys Treat 1 and Treat 2.

4.2.1.2: BDA stained fibres around the lesion site

To test for the presence of any regenerated fibres induced by the Anti-Nogo treatment caudally to the spinal cord lesion (as seen in the rat; see chapter 1), two anterograde tracers have been injected in the hand area of the M1: BDA in the right hemisphere and Dextran Green in the left hemisphere. In monkey Treat 1, BDA was injected 71 days and Dextran Green 57 days before the sacrifice of the animal. In monkey Treat 2, two injections of each tracer were performed. BDA was injected a first time 74 days before sacrifice in the hand area of the right hemisphere identified with ICMS and a second time, in a region located 8 mm more medially and 4 mm more caudally 69 days before sacrifice. Dextran Green injections were performed the same days as above, but in the left hemisphere; the first injection was aimed in the ICMS identified hand area of M1 and the second one in a cortical region located 7 mm more medially and 4 mm more caudally than the first injection. All injections were performed when the monkeys had reached a plateau of performance in the Brinkman board task, indicative of the end of the period of recovery. There long survival periods were applied (around 70 days) to allow the migration of the tracers all the way to the cervical level, in light of the fact that the axonal transport of the tracers seemed to be slowed by the axotomy of the CS fibres (see results of Ctrl animals in chapter 3). The observations made caudally to the spinal lesion, as shown in Figure 4.2 C did not match the results obtained in the anti-Nogo treated rats (Brösamle et al 00), where labelled corticospinal fibres have been detected caudally to the thoracal lesion, indicative of regeneration. In Treat 1 and Treat 2, no BDA labelled CS fibres have been observed caudally to the lesion, whereas CS labelled fibres were seen rostrally to the lesion, indicating an absence of clear axonal regeneration in our two treated monkeys. Nevertheless, in Treat 1, the presence of BDA stained axons were observed that do not follow the normal rostro-caudal axis of CST fibres or the medio-lateral axis of their collaterals; we observed a few CS axons oriented obliquely,

possibly corresponding to axons aiming around the lesion, (Fig. 4.2 A, B and D) a pattern not observed in normal untreated monkeys.

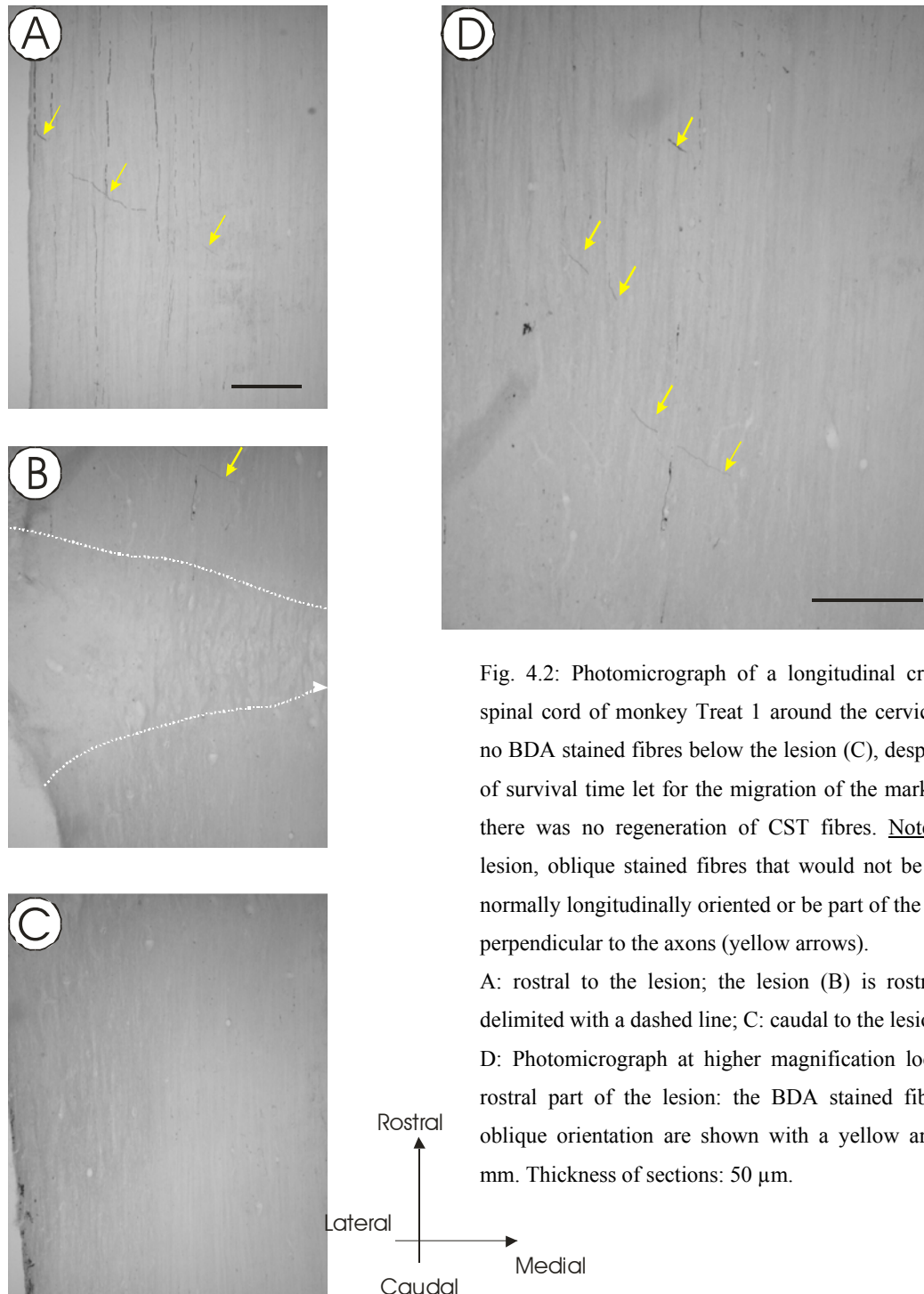


Fig. 4.2: Photomicrograph of a longitudinal cross-section of the spinal cord of monkey Treat 1 around the cervical lesion showing no BDA stained fibres below the lesion (C), despite the long period of survival time let for the migration of the marker, indicating that there was no regeneration of CST fibres. Note: rostrally to the lesion, oblique stained fibres that would not be part of the axons normally longitudinally oriented or be part of the collaterals that are perpendicular to the axons (yellow arrows).

A: rostral to the lesion; the lesion (B) is rostrally and caudally delimited with a dashed line; C: caudal to the lesion.

D: Photomicrograph at higher magnification located close to the rostral part of the lesion: the BDA stained fibres presenting an oblique orientation are shown with a yellow arrow. Scale bar: 1 mm. Thickness of sections: 50 μ m.

4.2.1.3 Morphological changes induced by the spinal cord lesion in the motor cortex of the treated monkeys

The observation of frontal sections of the primary motor cortex in monkeys Treat 1 and Treat 2 showed a clear decrease of the number of the giant Betz cells in the layer V in the right hemisphere, as a result of the left cervical cord lesion, as seen at low magnification (Fig. 4.3). However, as reported in chapter 3 for the monkeys Ctrl 1 and Ctrl2, we cannot rely on such superficial analysis at low magnification (100X). For that reason, we have undertaken a more detailed analysis at high magnification in SMI-32 sections in order to assess more precisely the number of SMI-32 positive neurones in layer V of both hemispheres, as well as their cross-sectional area.

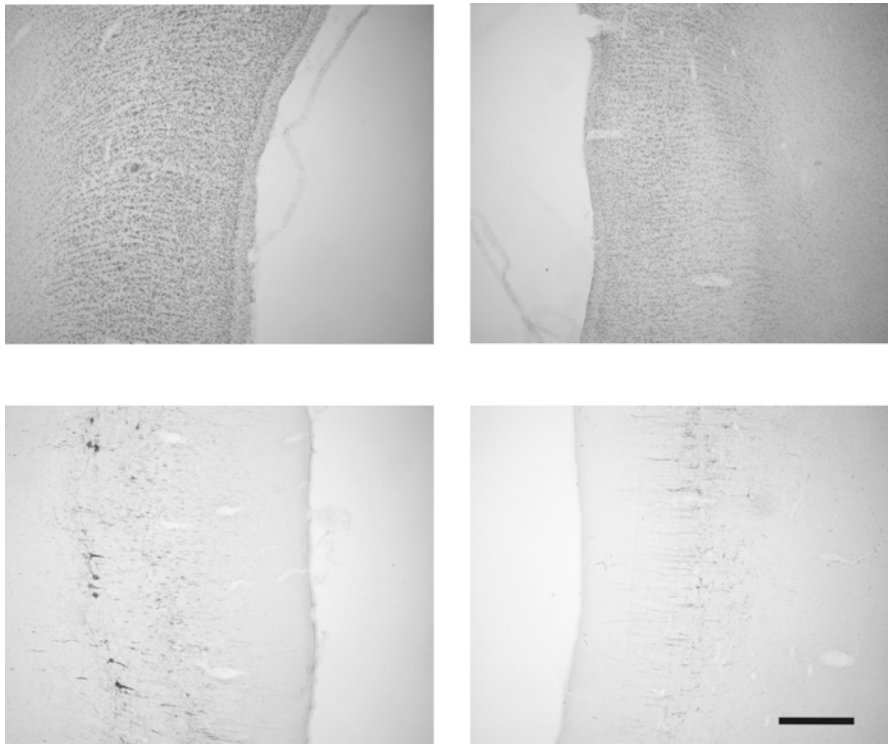


Fig. 4.3: Photomicrographs of frontal sections of the primary motor cortex of monkey Treat 1 in the medial wall (hindlimb area in M1). The two upper photomicrographs show the two hemispheres on a Nissl stained section. The two lower photomicrographs show the two hemispheres on an adjacent SMI-32 stained section. Scale bar: 500 μ m. The right panels represent the (right) contralesional hemisphere, whereas the two left panels represent the (left) ipsilesional hemisphere.

The histological consequences of the unilateral cervical lesion in the motor cortex have been analysed at high magnification (400X) in monkey Treat 1. The same method has been used

in this analysis based on four sections as in Ctrl 1 and Ctrl 2, but restricted to the primary motor cortex and to monkey Treat 1. In fact, the brain sections obtained in monkey Treat 2 were poorly stained with SMI-32 due to freezing artefacts. In monkey Treat 1, SMI-32 positive pyramidal neurones in layer V were not equally distributed with 157 neurones identified in M1 of the left hemisphere, in four sections (50 μm thick each), whereas 110 neurones have been found in the right hemisphere (Fig.4.4 leftmost left bins). At this point, this difference cannot be interpreted very clearly since one cannot exclude that this preliminary analysis was conducted on different volumes of tissues in the right and the left hemisphere. Nevertheless, to assess in more detail the consequences of the axotomy on the pyramidal neurones of M1, the same procedure of somatic area measurement has been followed (see chapter 3, Fig. 3.4) for monkey Treat 1 as for two control monkeys. The data in Treat 1 show that the majority of the neurones belonging to the upper 20th percentile with respect to their cross-sectional somatic area are in the left hemisphere (Fig. 4.4 middle bins). Reciprocally, the smallest neurones (lower 20th percentile) were more frequent in the right (contralesional) than the left (ipsilesional) hemisphere (2 out of 53) and (16 out of 37, Fig. 4.4 rightmost bins). The cervical hemisection thus results in shrinkage of pyramidal neurones in the layer V of the contralesional M1 in the monkey Treat 1, and this was also the case in the two control monkeys.

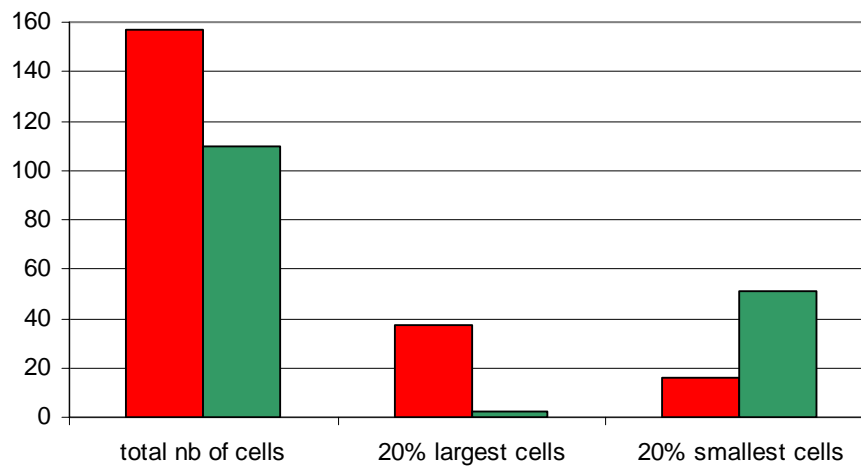


Fig. 4.4: Histograms of the distribution of the SMI-32 positive pyramidal neurones in layer V in the left hemisphere, ipsilateral to the lesion (red), and the right hemisphere, contralateral to the lesion (green), in monkey Treat 1. The left columns represent the total number of SMI-32 pyramidal neurones in the four analysed sections. The bins in the middle represent the distribution of the 20 % largest cells and the bins on the right represent the distribution of the 20 % smallest cells.

4.2.1.4: Muscular atrophy

The loss of central motor control results in muscular atrophy, as reported in chapter 3 for the control monkeys (Ctrl 1 and Ctrl 2). Table 4.1 lists the volume of the Gastrocnemius muscles dissected from the right and left hindlimbs in the treated monkeys Treat 1 and Treat 2. In comparison to the results obtained in intact animals, the muscle on the affected side presents an atrophy, as shown by a decrease of its volume of 28% for Treat 1 and about 15% for Treat 2. These results are not sufficient to make a relationship between the extent of the spinal lesion (greater in Treat1) and the amplitude of the muscular atrophy, but they indicate a trend in that direction, and need to be confirmed in a larger pool of animals. The left and right gastrocnemius muscles of a monkey subjected to a cervical hemi-section are shown in Fig. 4.5.

Monkey name	Volume left Gastrocnemius	Volume right Gastrocnemius	% atrophy
Treat 1 Frank (4 kg)	13ml	18ml	28%
Treat 2 Antoine (5.5 kg)	25 ml	29 ml	15%

Table 4.1: Comparison of volume of the Gastrocnemius muscle from left and right hindlimb.

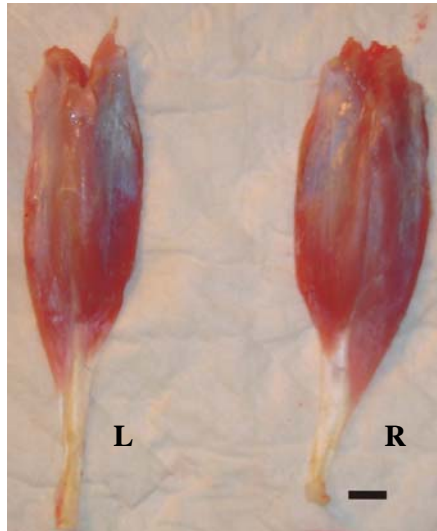


Fig. 4.5: Photograph of the left (L) and the right (R) dissected gastrocnemius muscles showing the technique adopted to allow a direct comparison of volume. Scale bar: 1 cm.

4.2.2: Behavioural data

4.2.2.1: Introduction: Immediate consequences of the cervical cord lesion

When monkeys Treat 1 and Treat 2 fully recovered from the general anaesthesia after the cervical cord lesion, they showed a dramatic impairment on the left side of the body, with a strong paresis of the left hand, while the prehension of the right hand could be stimulated with small pieces of food. The left hand remained closed a few days. The animals sat in an asymmetric position in their cages, this position resulting from a defect in the posture muscles of the back, as well as the muscles of the hip. The left hindlimb remained paretic in extension position most of the time in the first hours after surgery. The animals were very rapidly, if not

immediately, able to control their urination and defecation. No symptoms of pain were observed, but the animals received an analgesic treatment during this period of time.

4.2.2.2: Quantitative analysis

4.2.2.2.1: Brinkman board

The animals were trained to perform the Brinkman board task several months before the spinal cord lesion, until reaching a plateau of performance in the same conditions as in the experiments with the two Ctrl monkeys. Immediately after the spinal cord lesion, the manual dexterity performance, based on the number of successfully retrieved pellets within 45 sec., dramatically decreased for the left hand, ipsilateral to the lesion in monkeys Treat 1 and Treat 2 (Figs. 4.6 A and 4.6 B, respectively). In both animals, the performance of the right hand remained in general unaffected, although immediately after the cervical cord lesion a light decrease of performance (around 5-10%) was observed (Fig. 4.6). This may have been due to a change of posture in the primate chair after paresis of the left side or to a transient decrease of motivation, subsequent to surgery.

In monkey Treat 1, the dramatic loss of function in the precision grip of the left hand prevented the monkey being tested on the manual dexterity task for three weeks post lesion (Fig. 4.6 A, red squares). After about 35 days, a recovery took place, reaching a level of approximately 50 % of the pre-lesion score (Fig. 4.6 A).

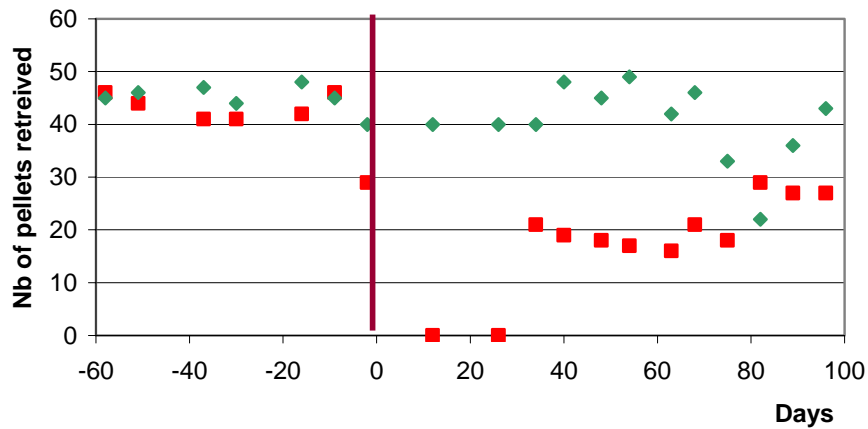


Fig. 4.6 A: Brinkman board scores for both hands (right hand: green diamonds and left hand: red squares) before and after the spinal cord lesion (day =0) in Treat 1. Horizontal and Vertical wells were pooled together.

The functional recovery of the left hand in monkey Treat 2 already occurred within the first three weeks post-lesion, reaching nearly 80 % of the pre-lesion score after 30 days (Fig. 4.6 B).

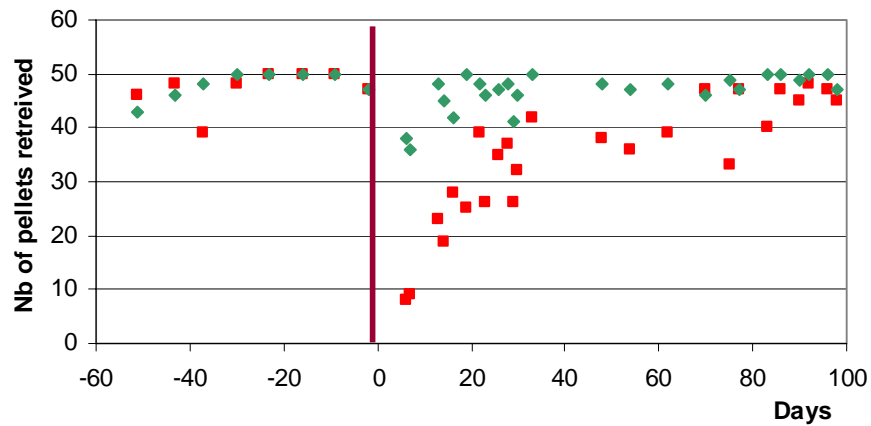


Fig. 4.6 B: Brinkman board scores for both hands of Treat 2 (right hand: green diamonds, left hand: red squares) before and after the spinal cord lesion (day=0). Horizontal and Vertical slots were pooled together.

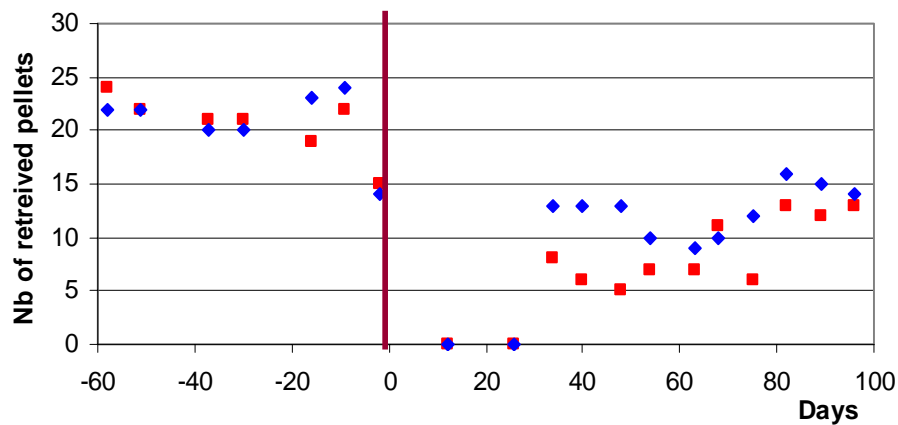


Fig. 4.7 A: Scores of the left hand (ipsilesional) of Treat 1, before and after the SCI, for the vertically oriented slots (blue diamonds) and horizontally oriented slots (red squares) of the Brinkman board task. The lesion occurred at day 0.

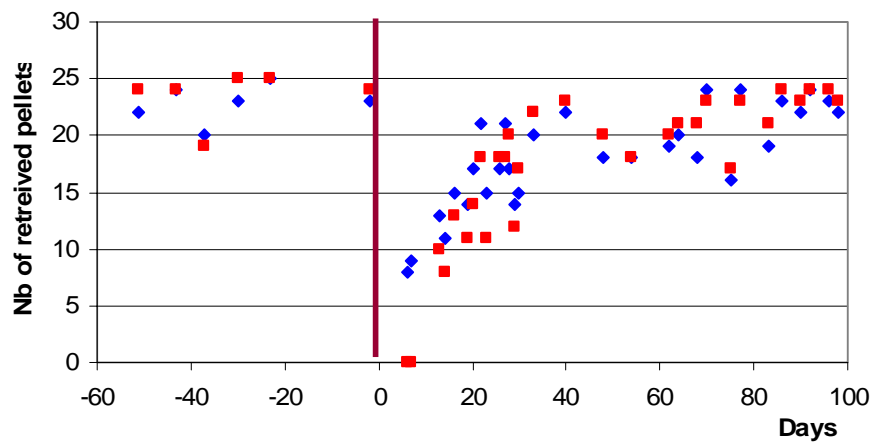


Fig. 4.7 B: Scores for the Brinkman board task of Treat 2. The score is represented with red squares for the horizontally oriented wells, and with blue diamonds for the vertically oriented wells. The lesion occurred at day 0.

Focusing our attention on the left hand directly affected by the spinal lesion in monkey Treat 1 (Fig. 4.7 A) no recovery of manual dexterity was observed for the vertically or horizontally oriented wells within the first three weeks post-lesion. After about 4 weeks, Treat 1 exhibited an incomplete recovery of manual dexterity, corresponding to scores for both vertically and horizontally oriented slots of about 50 % of the pre-lesion performance. In the monkey Treat 2

(Fig. 4.7 B), the recovery was more rapid, progressive and more efficient, reaching a level after 3 weeks of 80% of the pre-lesion performance. After 10 weeks, the recovery was nearly complete. As far as the type of movements recovered is concerned, in Treat 1, the recovered performance of the left hand to retrieve the pellets in the horizontally oriented slots was due to the recovered capacity to move the thumb individually, in a coordinated movement with the index finger. These movements are illustrated in Fig. 4.8. In monkey Treat 2, the recovered function of the manual dexterity seen in the Brinkman board post-lesion (Fig. 4.7 B) is due to the recovered capacity to perform the precision grip with the left thumb and index finger, allowing retrieval of the pellets in both vertically and horizontally oriented slots. The recovery processes was shorter in Treat 2 than in Treat 1.



Fig. 4.8: Photographs showing four consecutive sequences of movements of the left hand of Treat 1, 58 days after SCI, illustrating the use of the thumb while performing the precision grip. Delay between A-B-C-D: 1/24 of sec. One can see the mobilisation in a flexion and adduction movement of the thumb in a coordinated motor performance successfully leading to a precision grip.

4.2.2.2.2: Transient cortical inactivation of the hand area

In order to define the role played by the motor cortex on one or the other hemisphere, Treat 1 and Treat 2 were subjected to the same protocol of behavioural evaluation of manual dexterity before and after reversible inactivation of the left or the right cortical M1 hand area using infusions of muscimol. At the end of the period of functional recovery, when the animals

reached a plateau of performance, the ICMS mapping allowed to exactly locate the putative area of M1 responsible for the recovered hand movements (see below). This area was unilaterally and transiently inactivated with micro-injections of Muscimol (see methods) immediately after the performance of the Brinkman board task with either hand. During the first evaluation of manual dexterity, the performance was normal with both hands.

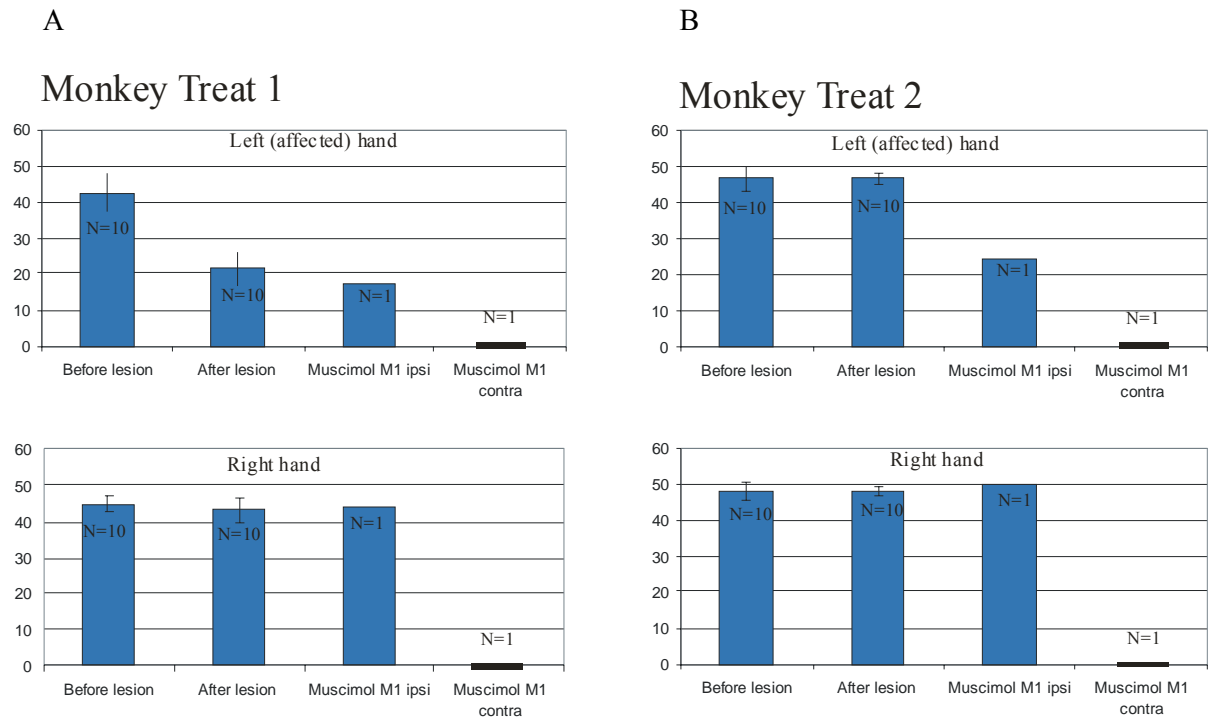


Fig. 4.9: Histograms showing the score of the Brinkman board test performed by monkey Treat 1 (A) and Treat 2 (B) before and after muscimol micro-injections in M1. Only one session of transient inactivation was performed in each animal.

In Fig. 4.9, the two leftmost bins show the average Brinkman board score in both orientation vertical and horizontal before and after lesion, as derived from 10 behavioural daily sessions. For the right hand, as expected, infusion of muscimol in the right hemisphere (M1 ipsi) did not affect the manual dexterity, which was, in contrast, dramatically reduced if muscimol was injected in the left hemisphere (M1 contra), indicative of the efficacy of the inactivation method (Fig. 4.9, two rightmost bins in the bottom panels). For the left hand (Fig. 4.9 top

panels), infusion of muscimol in the right hemisphere (M1 contra) dramatically suppressed the recovered performance (rightmost bin), confirming the crucial role played in the recovery by the contralateral hemisphere, as seen in the control monkeys (see chapter 3). An interesting result here, more in Treat 2 than in Treat 1, was a reduction of the recovered performance of the left hand by infusion of muscimol in the ipsilesional hemisphere (50% in Treat 2), in sharp contrast to what has been observed in the control monkeys (chapter 3, Fig. 3.14).

4.2.2.2.3: Drawer task

These data are presented in the same way as those obtained for monkey Ctrl 2. The monkeys were trained to perform the drawer task before the spinal lesion. Immediately after the lesion, the ability to open the drawer was lost, but both Treat 1 and Treat 2 were again able to perform the task with the left hand a few weeks after the spinal lesion, although the manual dexterity was not completely recovered. In other words, in contrast to the control monkeys (Ctrl 1 and Ctrl 2), the two treated monkeys were able to develop enough force to pull the drawer. The shape of the movement performed by the hand to open the drawer after the lesion was very similar to that before the spinal lesion. The correct performance of the task requires the recovery of enough force to grasp the knob against the resistance of the spring load exerted on the drawer. The time intervals between the different events are represented in Figs. 4.10 A and 4.10 B for monkeys Treat 1 and Treat 2, respectively. The reaching time (RT) is the time interval separating onset of the hand from the starting pad and contact with the drawer knob and is represented with green diamonds. The pulling time (PT), represented with blue squares, is the time interval between the start of the opening of the drawer and full opening. Finally, the picking time (PIT) is the time spent by the index finger and thumb inside the drawer to retrieve the food reward and is represented by red triangles. In Treat 1 and Treat 2, the three measured time intervals tended to

increase immediately after the cervical lesion, but then decreased during the recovery period to go back to values closer to the pre-lesion time intervals.

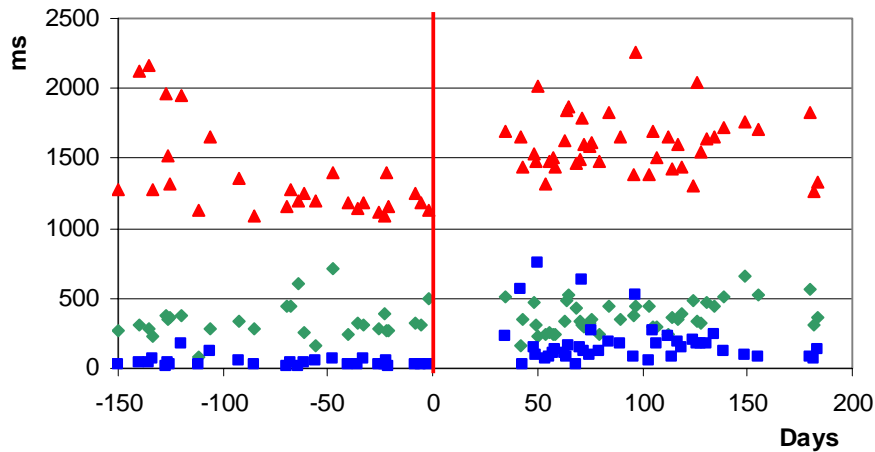


Fig. 4.10 A: Drawer task time intervals for the left hand performed by monkey Treat 1, from 150 days before the cervical lesion (day = 0) up to 200 days post-lesion. Three time intervals are presented here: the reaching time (RT, green diamonds), the pulling time (PT, blue squares) and the picking time (PIT, red triangles). Time in milliseconds.

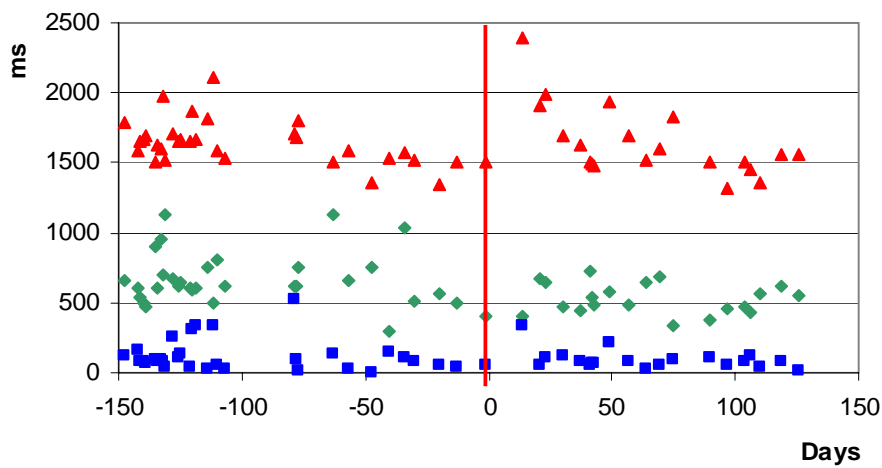


Fig. 4.10 B: Time intervals for the drawer task for monkey Treat 2. Same conventions as in Fig. 4.10 A.

The statistical analysis is presented in Figs. 4.10 C and D for monkey Treat 1 and Treat 2, respectively. In monkey Treat 1, the reaching time remained stable post-lesion, whereas both

time intervals, PT and PIT clearly increased. In Treat 2, all the data showed no difference between the pre-lesion period and the post-lesion period.

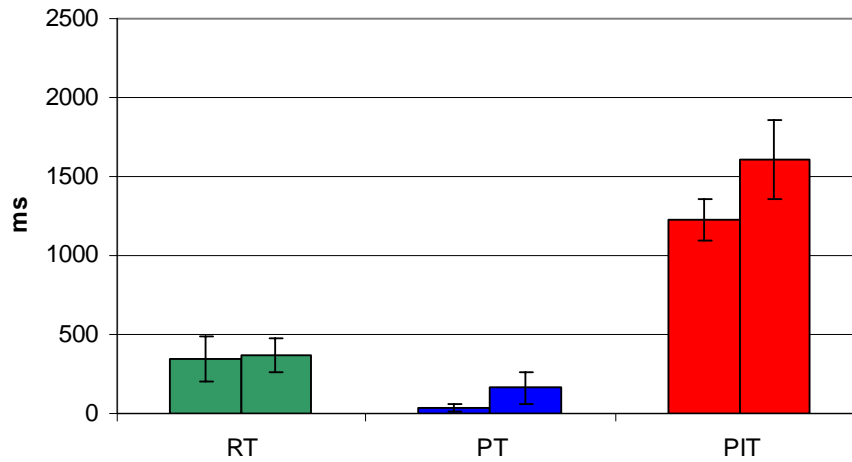


Fig. 4.10 C: Histograms presenting the mean and the standard deviation of the three time intervals for the drawer task, as defined in the text for monkey Treat 1: RT: reaching time (green), pulling time (PT) and picking time (PIT). The intervals are compared before (left column) and after the cervical lesion (right column). Twenty sessions were considered pre- and post-lesion.

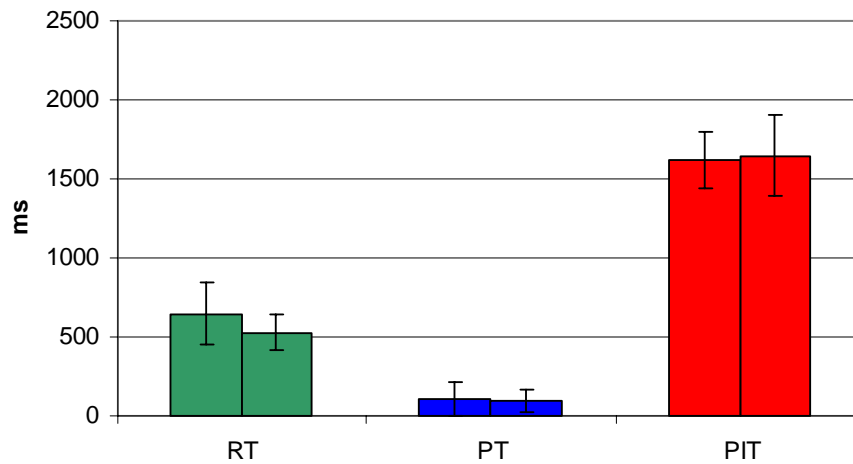


Fig. 4.10 D: Pre- and post-lesion comparison of time intervals in the drawer task for monkey Treat 2. Same conventions as in Fig. 4.10 C.

4.2.2.3: Qualitative data

Ballistic arm movement and brachiation test

Before the spinal cord lesion, both animals were trained to perform the so-called ballistic arm movement (see methods) during which they had to rapidly react in order to grasp with both hands a food reward thrown. The experimentalist threw the food reward in such a way that the animal had to perform a visually guided quick movement to grasp it. The movement was dissected in three phases: the first one (pre-shaping) consists in opening both hands with extension of the fingers, while advancing the hand in the direction of the approaching reward. The second phase consists in the catching itself: unification of both hands around the reward with flexion of the fingers. The third phase is the transfer of the reward back to the mouth, with flexion of both biceps with continuous flexion of fingers around the reward. After the period of recovery, no particular training was needed to improve the results of this task. Both animals Treat 1 and Treat 2 succeeded in the task. They exhibited a nearly normal sequence of movement, consisting of the opening of the hands and extension of the fingers of both hands, coupled with an external rotation of the shoulder, a contraction of the triceps allowing the hands to reach together the thrown food reward. There was no difference in the ability of the animals to catch the thrown reward with either hand. Similarly, both animals recovered noticeably during the weeks following the unilateral cervical cord lesion the ability to perform the brachiation test with either arm.

Foot prehension task, jumping test and “up-side-down hanging” test

The two monkeys Treat 1 and Treat 2 were not able to catch large food rewards with their ipsilesional toes several weeks after the cervical lesion. They never used again their left foot to perform this task: their toe remained parietic in a flexed position. In contrast, both animals showed a significant improvement for the hanging and jump tests, although they did not fully recovered the pre-lesion performance.

The qualitative behavioural data in monkeys Treat 1 and Treat 2 are summarised in Table 4.2.

	<i>Treat 1</i>		<i>Treat 2</i>	
	<i>Few days after SCI</i>	<i>Several months after SCI</i>	<i>Few days after SCI</i>	<i>Several months after SCI</i>
<i>Jump</i>	<i>1</i>	<i>3</i>	<i>2</i>	<i>3</i>
<i>Hanging (foot)</i>	<i>1</i>	<i>3</i>	<i>2</i>	<i>3</i>
<i>Brachiation</i>	<i>1</i>	<i>3</i>	<i>2</i>	<i>3</i>
<i>BAM (left hand)</i>	<i>Not tested</i>	<i>4</i>	<i>4</i>	<i>4</i>
<i>Foot prehension</i>	<i>1</i>	<i>2</i>	<i>1</i>	<i>2</i>
<i>Shape of grip: vertical</i>	<i>1</i>	<i>4</i>	<i>2</i>	<i>4</i>
<i>horizontal</i>	<i>1</i>	<i>3</i>	<i>1</i>	<i>4</i>

Table 4.2: Scores obtained in the qualitative behavioural tests 5 days after the spinal cord injury and at the end of the period of recovery for Treat 1 and Treat 2. Scores: 1: complete paresis of the limb, no possible voluntary movement; 2: marked paresis of the limb, unsuccessful trial with visible movements; 3: possible movements, successful trial with great difficulties; 4: successful trial with nearly complete movement. BAM = ballistic arm movement.

4.2.3: ICMS data

4.2.3.1: Mapping of M1 hand area before and after cervical cord lesion

The analysis of the changes occurring in the cortical motor maps investigated with the ICMS technique was two fold: in a first approach, the ICMS responses were represented at the cortical surface (Figs. 4.11, 4.12 and 4.13). The second approach consisted in comparing the total number of sites, before and after the spinal cord lesion, efficient to activate a body territory. The ICMS mapping was not done before the cervical cord lesion in monkey Treat 2 for schedule reasons, this is why only the ICMS map performed after the lesion is presented for this animal (Figs. 4.11, 4.12 and 4.13, lower right panel).

4.2.3.1.1: ICMS data for the contralesional hemisphere in Treat 1 and Treat 2

The animal Treat 1 exhibited, pre-lesion, typical hand area in M1 as well as a smaller hand area more rostral in PM (Fig. 4.11, left panel on top). The cervical lesion had a dramatic effect in the sense that the hand area in Treat 1 completely disappeared post-lesion: all ICMS sites previously eliciting finger movements of the left hand were replaced by wrist or face movements or became non-micro excitable in both M1 and PM (Fig. 4.11, upper right panel). One should however remember that the ICMS data in Fig. 4.11 display only one ICMS site per electrode penetration, namely at the lowest observed threshold only the corresponding penetration. If all ICMS sites eliciting finger movements of the left hand are considered (even at higher threshold), as shown in Fig. 4.12, the hand area is larger pre-lesion and, post-lesion, a few hand points were preserved but the entire hand area was dramatically reduced (Fig. 4.12, top panels). For the animal Treat 2, the ICMS data cannot be interpreted in detail in absence of pre-lesion map. However, a hand area was present post-lesion (Fig. 4.11 and 4.12), even when only lowest threshold were considered (Fig. 4.11).

lowest threshold elicited movements of the fingers (electrode tracks represented by diamonds). The map is given for monkey Treat 1 (top two panels) and monkey Treat 2 (bottom right panel), as established by ICMS before (left panel) and after lesion (right two panels). Symbol X means that ICMS did not elicit any visible movement of muscles. Symbols in grey are for ICMS sites belonging to the hand area before lesion, which became part of other territories post-lesion. The grid in the background indicates steps of 1 mm. Syringes point to ICMS sites where muscimol was infused in order to inactivate M1 (see text). In order to make sure that the entire “post-lesion” hand representation was reversibly inactivated, the sites of infusion of muscimol were rather selected based on the “pre-lesion” map, exhibiting a larger hand representation than post-lesion.

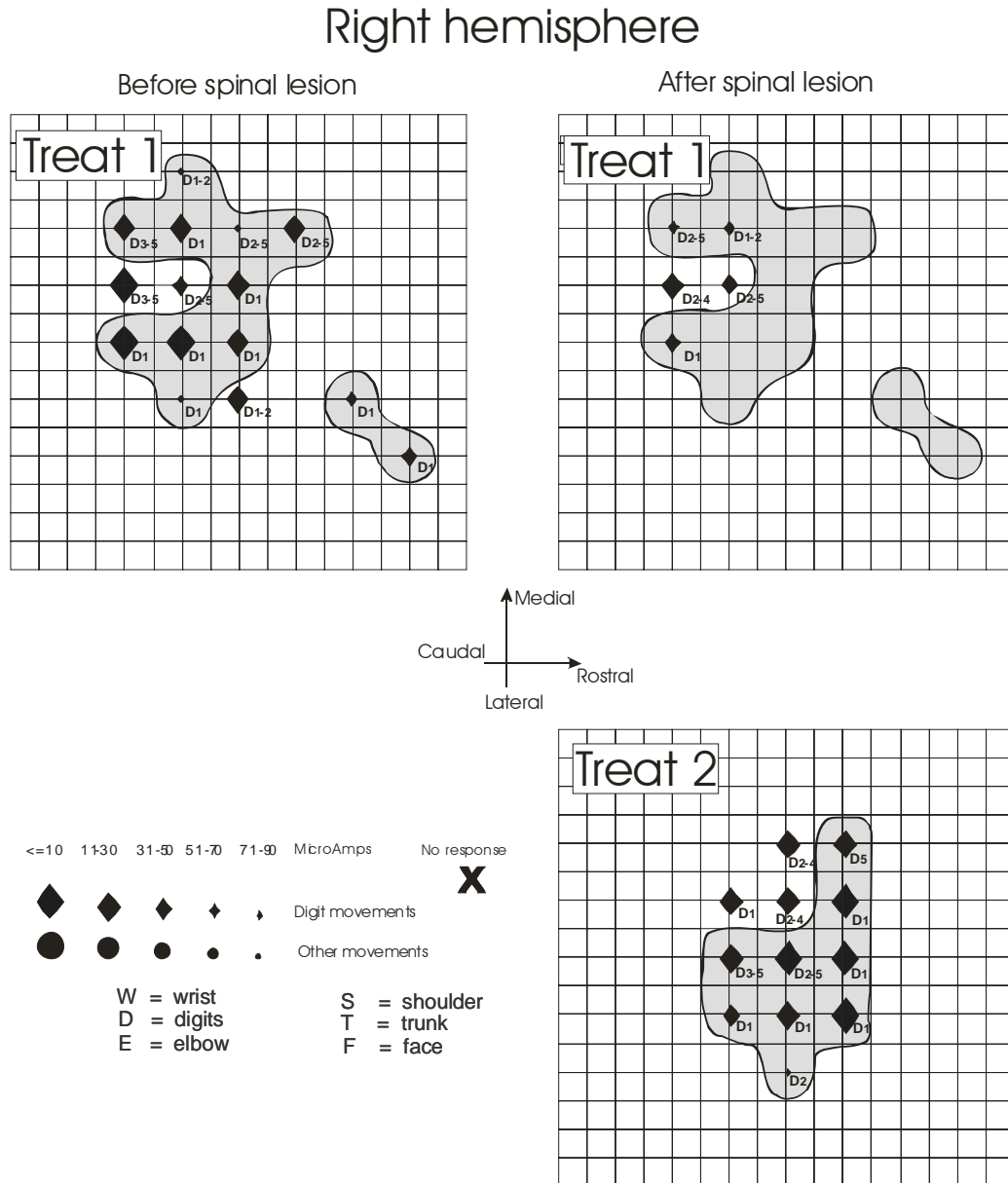


Fig. 4.12: Somatotopic map of M1 in the right hemisphere of Treat 1 and Treat 2, considering only the hand movements elicited by ICMS. Same conventions as in Fig. 4.11.

4.2.3.1.2: ICMS data for the ipsilesional hemisphere in Teat 1 and Treat 2.

Similarly to the control monkeys (Ctrl 1 and Ctrl 2), the animal Treat 1 also shows a decrease of the area of the (right) hand representation in the ipsilesional M1 and a disappearance of that in PM (compare left and right panels in the top of Fig. 4.13). The absence of pre-lesion map in Treat 2 did not allow to assess the impact of the lesion on the ipsilesional hemisphere in this animal. Considering only ICMS data for the hand, the same conclusion as above applies for Treat 1, in the sense of a reduction of the area of the hand representation (Fig. 4.14).

Left hemisphere

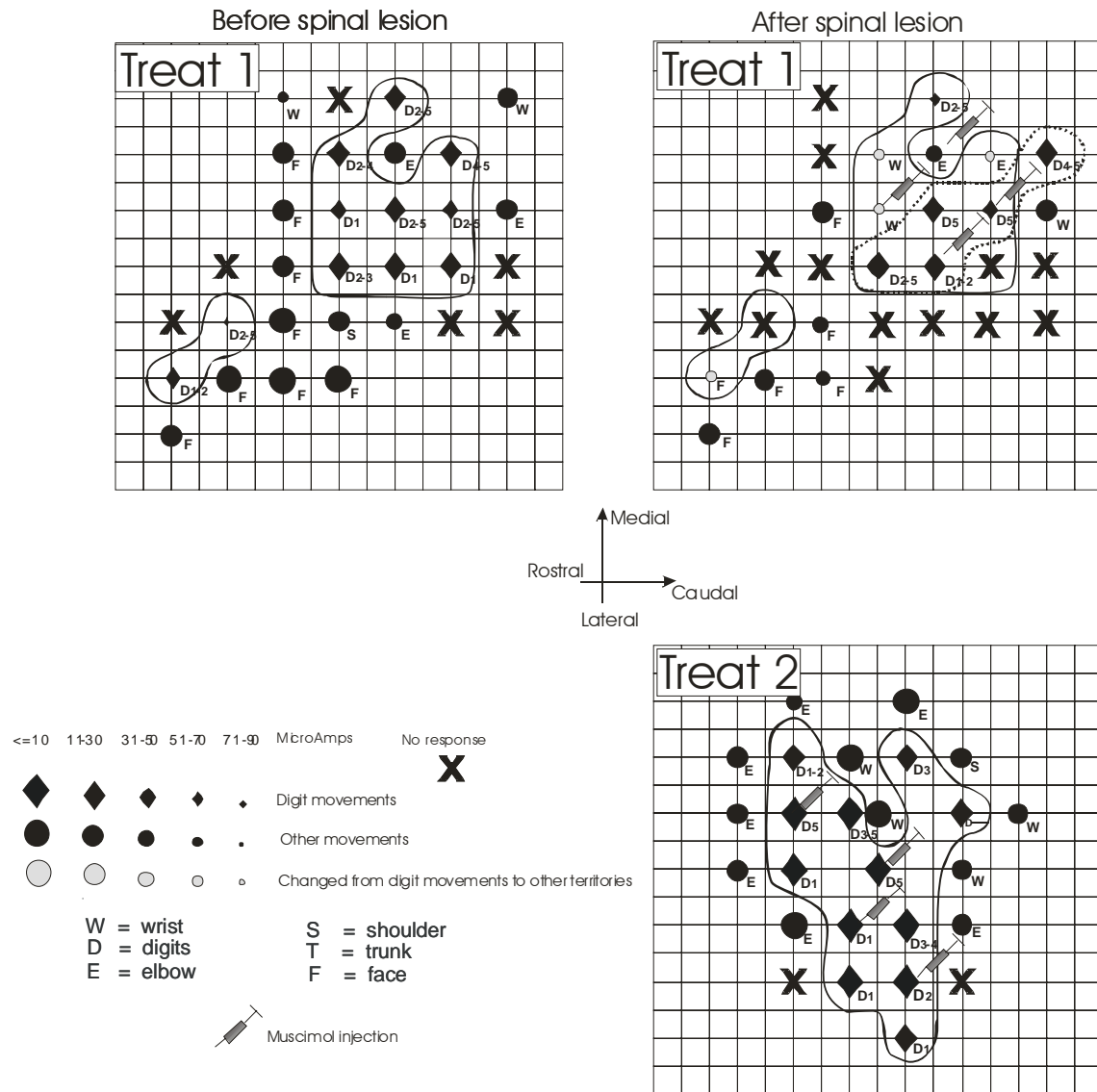


Fig. 4.13: somatotopic map of the left hemisphere (contralesional) in monkey Treat 1 before (upper left panel) and after (upper right panel) the cervical cord lesion in monkey Treat 1 and in monkey Treat 2 after the lesion (lower right panel). Same conventions as in Fig. 4.11.

1 (Figs. 4.15 and 4.16): the number of ICMS sites eliciting finger movement decreased post-lesion in both hemispheres. In the right hemisphere, these hand area ICMS sites were replaced by sites activating the wrist or became non micro-excitable (Fig. 4.15). This does not appear to be the case in the left hemisphere, except for the increase of the non-microexcitable sites.

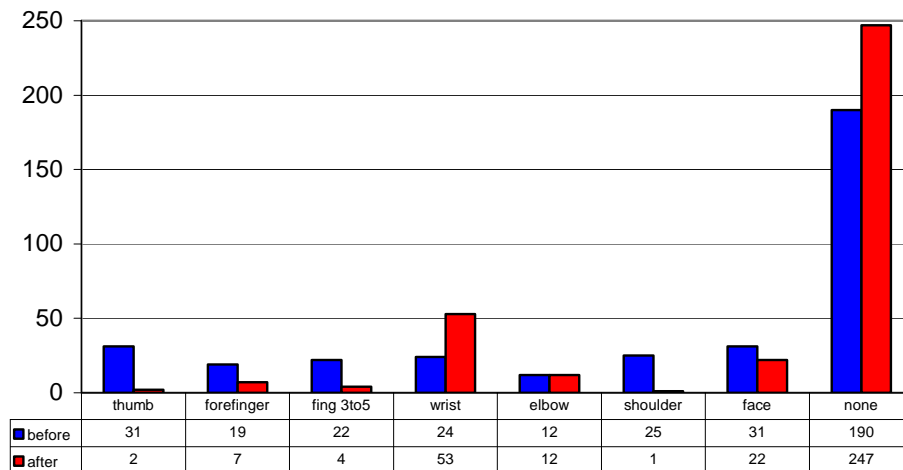


Fig. 4.15: Distribution of ICMS sites pre-lesion versus post-lesion for different body territories in the right hemisphere of monkey Treat 1. Each column represents the total number of ICMS elicited sites classified following their topography. The results obtained before the spinal cord lesion are presented in blue whereas the results obtained after the lesion are represented in red.

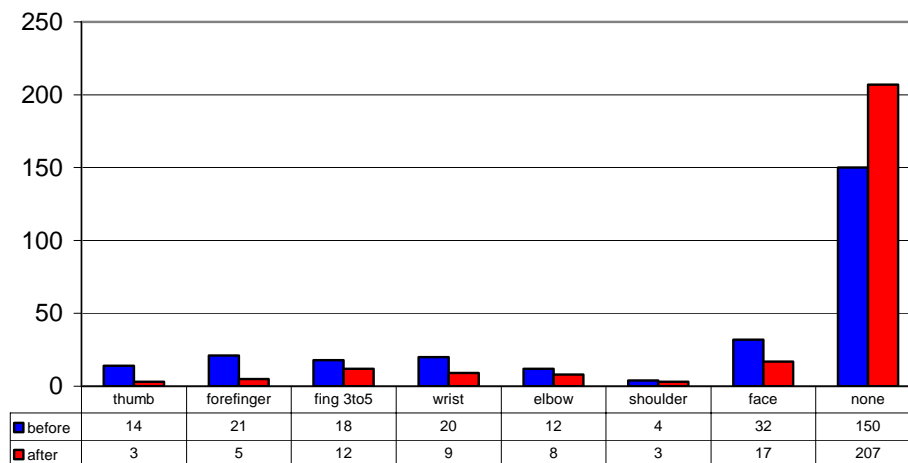


Fig. 4.16: ICMS data in the left hemisphere of Treat 1 (same conventions as in Fig. 4.15).

4.3: Discussion:

The detailed comparison of data obtained in the monkeys Treat 1 and Treat 2 with those in the control monkeys Ctrl 1 and Ctrl 2, thus addressing the issue of the efficacy of the anti-Nogo treatment, will be presented in chapter 5. As far as the treated monkeys are concerned (Treat 1 and Treat 2), it is important to emphasize here that the anti-Nogo treatment did not generate any substantial regeneration of the transected CS axons, in contrast to the rat data (Z'Graggen et al 98; Raineteau et al 99). Indeed, the BDA labelled CS axons affected by the lesion were clearly interrupted rostral to the lesion and no evidence for labelled axons caudal to the lesion was found, except a few axons exhibiting an unusual oblique orientation, possibly corresponding to CS axons going around the lesion..

Still on the anatomical point of view, the treated animals were characterized by shrinkage of the CS neurons in the contralesional hemisphere as compared to the ipsilesional one, in line with the data in the control animals (Chapter 3). Clearly, the anti-Nogo treatment did not reduce the shrinkage effect on the soma of the CS neurons after axotomy. One can also conclude that most CS neurones in the contralesional hemisphere survived to the cervical hemisection in the treated animals.

A very crucial observation in the two treated monkeys was an absence of deleterious secondary effect of the treatment. Indeed, the infusion of anti-Nogo did not modify the general behaviour of the monkeys and, in particular, no signs of pain were observed.

The last chapter will directly compare the other data obtained in this group of treated animals with the comparable data obtained in the control animals. In that sense, this last chapter will provide the conclusions of the question asked at the beginning concerning the observed improvement provided or not by the treatment of unilateral cervical cord lesion in macaque monkeys.

List of references for chapter 4:

- 1: Brösamle,C., Huber,A.B., Fiedler,M., Skerra,A. & Schwab,M.E. (2000) Regeneration of lesioned corticospinal tract fibers in the adult rat induced by a recombinant, humanized IN-1 antibody fragment. *Journal of Neuroscience*, **20**, 8061-8068.
- 2: Raineteau,O., Z'Graggen,W.J., Thallmair,M. & Schwab,M.E. (1999) Sprouting and regeneration after pyramidotomy and blockade of the myelin-associated neurite growth inhibitors NI 35/250 in adult rats. *European Journal of Neuroscience*, **11**, 1486-1490.
- 3: Z'Graggen,W.J., Metz,G.A.S., Kartje,G.L., Thallmair,M. & Schwab,M.E. (1998) Functional recovery and enhanced corticofugal plasticity after unilateral pyramidal tract lesion and blockade of myelin-associated neurite growth inhibitors in adult rats. *J.Neurosci.* **18**, 4744-4757.

Chapter 5: Direct comparison of recovery from cervical cord lesion between control (untreated) monkeys Ctrl 1 and Ctrl 2 and anti-Nogo treated monkeys Treat 1 and Treat 2.

5.1: Introduction	220
5.2: Comparisons	220
5.2.1: Extent of the cervical cord hemisection in control and treated monkeys	220
5.2.2: Behaviour	222
5.2.2.3: “Drawer” task	228
5.2.2.5: Role of the ipsilesional M1 in the recovery of function in Treat monkeys	232
5.3: Discussion	233
5.3.1: Mechanisms involved in the improvement of functional recovery	233
5.3.2: Conclusions	241

Chapter 5: Direct comparison of recovery from cervical cord lesion between control (untreated) monkeys Ctrl 1 and anti-Nogo treated monkeys Treat 1 and Treat 2.

5.1: Introduction

This last chapter presents the general discussion, focusing on the comparison of the data of the two control monkeys Ctrl 1 and Ctrl 2 with the two treated monkeys Treat 1 and Treat 2. This chapter is subdivided in two sub-chapters: the first one presents the anatomical and behavioural data that can be directly compared between the control animals and the treated animals and the second one consists in the discussion on the underlying mechanisms possibly involved in the recovery of function in the control and treated monkeys. We will focus our attention on the data pertinent to address our starting hypothesis: does the anti-Nogo treatment, enhancing the functional recovery in adult rats subjected to lesion of the central nervous system through regeneration of fibres, also improve recovery in our model of cervical cord hemisection in primate? In that direction we will select and compare the most relevant results presented in chapters 3 and 4.

5.2: Comparisons

5.2.1: Extent of the cervical cord hemisection in control and treated monkeys

The precise location and extent of the cervical cord hemisection are crucial parameters in order to assess the behavioural deficits. We will consider separately each animal, with emphasis on the destroyed neural structures affected by the surgical lesion. Three aspects will be taken here into consideration: first, the reconstruction of the cervical spinal cord showing anatomically the location and extent of the surgical section on the left side in the white and grey matter.

Second, assess whether the extent of the lesion is correlated behaviourally with the severity of the observed symptoms immediately after the lesion, for instance the ability of the monkey to use its left hand to grasp small pieces of food. The dynamic of the functional recovery has also been taken into consideration. Third, the electrophysiological data obtained with the ICMS will be compared across monkeys to determine if they reflect, to some extent, the severity of the cervical cord lesion.

As shown in Fig. 5.1, the location and extent of the lesion are substantially variable from one monkey to the next. As a consequence, it appears inadequate to make a general comparison of the “control” group (n = 2) versus the “treated” group (n = 2). We rather decided to make a more pertinent comparison of pairs of monkeys “matched” by exhibiting roughly comparable lesions. In the present case the monkey Ctrl 1 will be specifically compared to monkey Treat 2, because their lesion affected a fairly similar part of the dorsolateral funiculus and preserved a substantial, comparable part of the rubrospinal tract and, to a lesser extent, of the corticospinal tract (Fig. 5.1). A separate comparison will be made between the monkey Ctrl 2 and the monkey Treat 1, because both animals exhibit a lesion interrupting both the corticospinal tract and the rubrospinal tract (Fig. 5.1). In the following discussion, we will refer as “Pair 1” the comparison between the monkeys Ctrl 1 and Treat 2 and “Pair 2” the comparison between the monkeys Ctrl 2 and Treat 1.

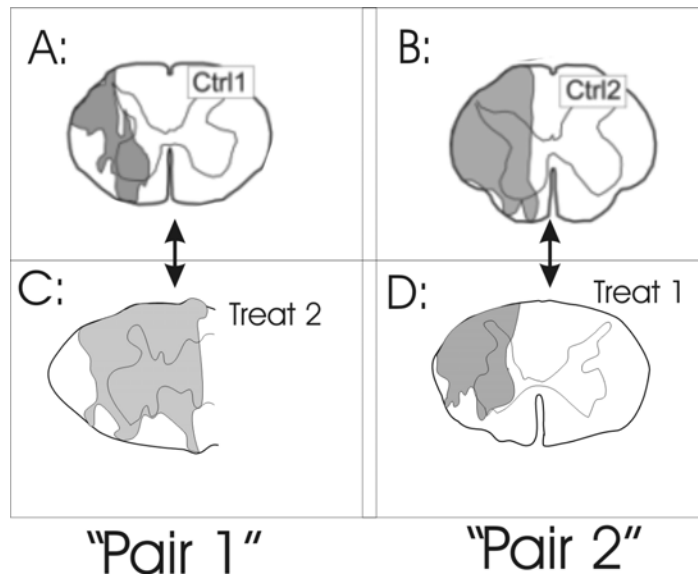


Fig. 5.1: Summary of the reconstruction of the cervical cord lesion in the control monkeys Ctrl 1 (A), Ctrl 2 (B) and the Treated monkeys Treat 1 (C) and Treat 2 (D). Scale bar: 1mm. The two arrows indicate the comparison within “matched” pairs of monkey with respect to their lesion properties.

5.2.2: Behaviour

All four monkeys exhibited a dramatic loss of manual dexterity of the ipsilesional hand immediately after the spinal cord hemisection but, on a general point of view, the treated monkeys recovered more rapidly and extensively than the control animals.

5.2.2.1: Qualitative behavioural data

Some “qualitative” behavioural tests such as the jump test, the up-side-down hanging test and the brachiation test did not show a difference between the control monkeys and the treated monkeys, taken within the two pairs of comparison. This result can be interpreted in the sense that those tests are not sensitive (or challenging) enough to detect a possible effect of the treatment. A similar conclusion can be drawn for the foot prehension test, since all four remained unable post-lesion to grasp with the toes of the left foot relatively big food morsels, in contrast to such ability present before the cervical cord lesion.

In sharp contrast, the “qualitative” test of Ballistic Arm Movement (BAM) turned out to be a very pertinent test.

177 days post-lesion

58 days posst-lesion



Fig. 5.2: Direct comparison between Ctrl 2 (left) and Treat 1 (right) in the ballistic arm movement task.

In the comparison “Pair 2”, the Ballistic Arm Movement (BAM) was executed in very different ways in monkeys Ctrl 2 and Treat 1. Monkey Ctrl 2, 177 days post-lesion, did not exhibit a pre-shaping of the left hand (extension of the fingers) to prepare the catch of the thrown food reward (Fig. 5.2, left column). In addition, an asymmetry between the velocity of movement of the right hand and the left forelimb was observed in Ctrl 2. In contrast, after a shorter period of recovery (58 days post-lesion, Fig. 5.2, right column), the monkey Treat 1 fully recovered the normal pattern of movement (pre-shaping of the two hands) and the velocity of movement was symmetric for both forelimbs. The monkey Ctrl 1 was not subjected to the BAM test and the monkey Treat 2 performed the Bam test post-lesion in an equivalent manner as Treat 1.

5.2.2.2: Quantitative behavioural test: Brinkman board test

The direct comparison within “Pair 2” (monkeys Ctrl 2 and Treat 1) for the Brinkman board test is presented in Fig. 5.3 for the horizontally oriented wells and in Fig. 5.4 for the vertically oriented wells. In both cases, one can see that the two animals exhibited a comparable and stable level of performance in the pre-lesion period and that the performance dramatically dropped to a score of 0 immediately after the cervical lesion. However, the extent and time course of recovery differed between the two monkeys, particularly for the horizontally oriented wells (Fig. 5.3). There was no recovery in monkey Ctrl 2 for the ability to grasp the horizontally oriented pellets (Fig. 5.3 blue diamonds), whereas monkey Treat 1 showed a substantial recovery, close to 60 % of the pre-lesion score (Fig. 5.3 orange squares). For the vertically oriented wells, the recovery observed in Ctrl 2 (Fig. 5.4, blue diamonds), partly due to a change of strategy in presence of the complete paresis of the left thumb (Fig. 5.6), was slower and less extensive than in Treat 1. The recovered performances for the Brinkman board test are given in

Table 5.1, expressed in percentage of the pre-lesion score. The average scores pre-and post-lesion can be compared in Fig. 5.5.

Horizontally oriented slots:

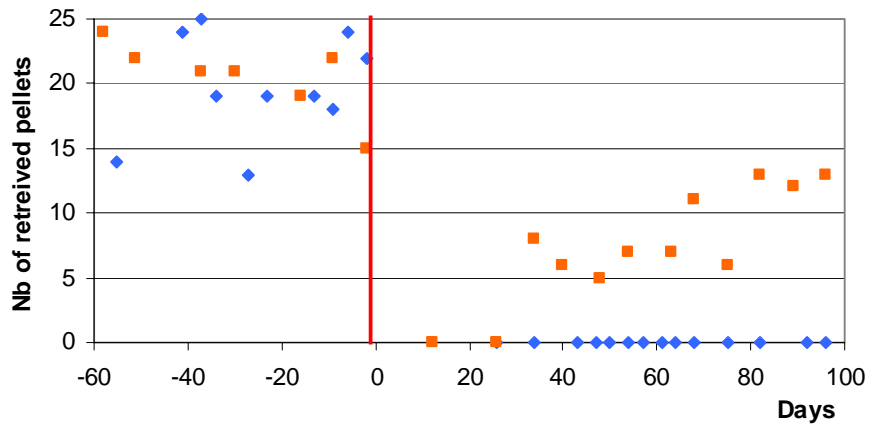


Fig. 5.3: Comparison of precision grip performance in “Pair 2” (monkey Ctrl 2 (blue diamonds) and monkey Treat 1 (orange squares)) for the horizontally oriented slots in the Brinkman board task.

Vertically oriented slots

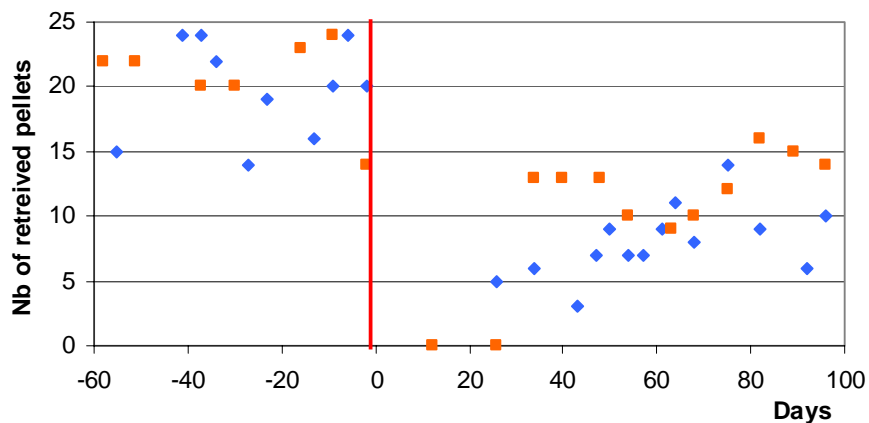


Fig. 5.4: Comparison of precision grip performance in “Pair 2” (monkey Treat 1 (orange squares) versus monkey Ctrl 2 (blue diamonds)), for the vertically oriented slots in the Brinkman board task.

The comparison of Brinkman board scores in “Pair 1” (Ctrl 1 versus Treat 2) revealed no difference for the vertical slots (Table 5.1). For the horizontal slots, Treat 2 performed barely better than Ctrl 1 (Table 5.1), but the recovery was more rapid in Treat 2 (see chapter 3 and VI).

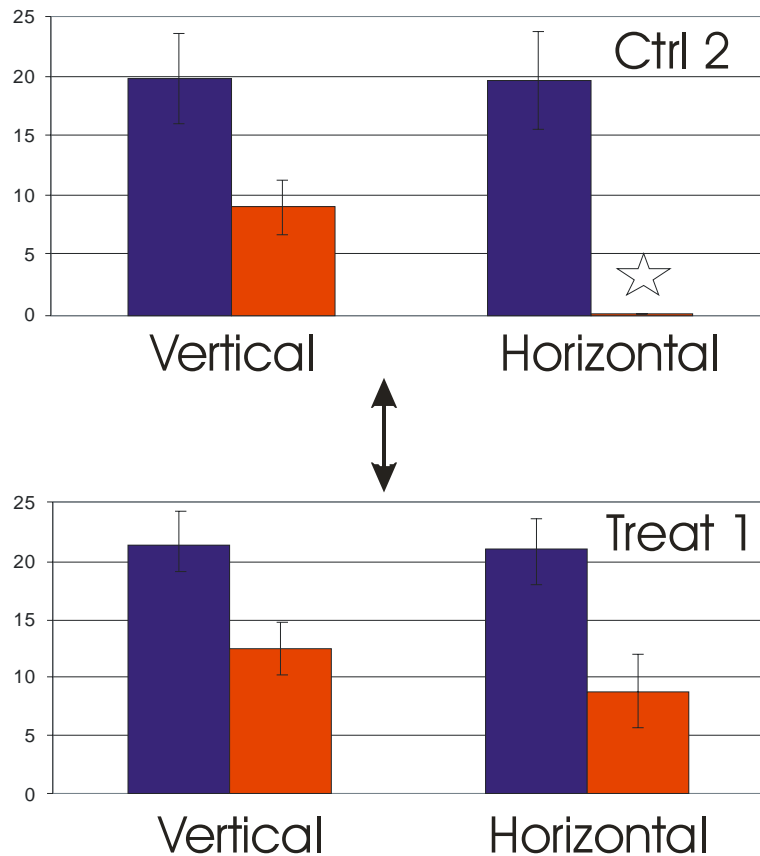


Fig. 5.5: Means of performances, with the standard deviations, pre-lesion and post-lesion (at plateau level) within “Pair 2” (monkey Ctrl 2 on top and Treat 1 on bottom). Left: vertically oriented slots scores pre- (blue) and post-lesion (red). Right: horizontally oriented slots scores pre- (blue) and post-lesion (red). Star: score was equal to 0 (no recovery for horizontal slots in monkey Ctrl 2).

	Pair 1				Pair 2			
	Ctrl 1		Treat 2		Ctrl 2		Treat 1	
Wells orientation	Vert.	Horiz.	Vert.	Horiz.	Vert.	Horiz.	Vert.	Horiz.
Before SCI	100%	100%	100%	100%	100%	100%	100%	100%
3 weeks after SCI	90%	65%	60%	50%	25%	0%	0%	0%
End of recovery period	95%	80%	95%	90%	45%	0%	65%	60%

Table 5.1: Summary of the mean of recovery in the brinkman board task, expressed in % of the pre-lesion score. Three time points have been taken into consideration: the pre-lesion value (100%), the score three weeks post-lesion and the mean at the end of the period of recovery when the animal reached a plateau of performance in the behavioural tasks.

At the end of the period of functional recovery, when a plateau of performances was reached by the lesioned monkeys, we paid attention to the shape of the grip used to perform the Brinkman board task. We observed that the untreated animals had largely changed their motor strategy to adopt a shape of grip optimising their remaining manual dexterity to perform the task. For example, monkey Ctrl 2, handicapped by a flaccid and permanent paresis of the thumb of the left hand, mobilised its index finger to push the food pellet against the dorsal face of the thumb and succeeded to grasp it (Fig. 5.6). This compensatory strategy was successful for the vertically oriented slots of the brinkman board, as the food pellet is located at the bottom of the well. In contrast, in the horizontally oriented slots, although the animal could reach the food pellet with the index finger, he could not maintain it against its thumb, as the requested movement could not be done in case of pronation or supination of the wrist. This observation explains the total lack of recovery to retrieve the food pellets from the horizontally oriented slots of the Brinkman board by the untreated monkey.

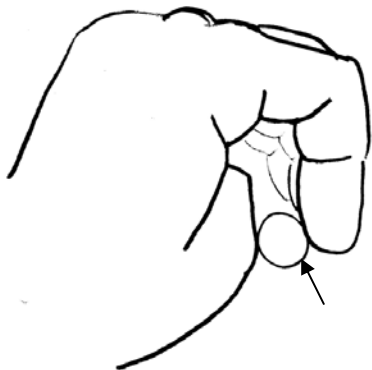


Fig. 5.6: Drawing reproducing the shape of the hand and the fingers of monkey Ctrl 2 at the end of the period of recovery (190 days post-lesion) during a precision grip performance in the Brinkman Board task for a vertically oriented well. The pellet is signified by the black arrow.

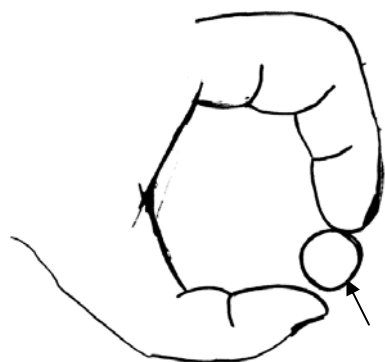


Fig. 5.7: Drawing reproducing the shape of the fingers of monkey Treat 1 when performing the prehension of a food pellet. Same conventions as in Fig. 5.5, 60 days post-lesion. The thumb and the index finger are placed in opposition to perform a nearly normal precision grip.

5.2.2.3: “Drawer” task

In the drawer task, the animal had to fully open a drawer containing a food reward with one hand and to pick it in. After the cervical cord lesion, monkey Ctrl 2 attempted to reach the knob of the drawer, showing a slow movement of the forearm (biceps relaxation and triceps contraction). The movement of the hand and the fingers to grab the knob was performed from the top to the bottom. The strategy developed by the control animal (Ctrl 2) was to place the knob

between the index finger and the middle finger (Fig. 5.8, left column), without performing a precision grip on the knob. But the animal was not able to develop enough force to compensate the resistance of the spring load behind the drawer.

In contrast, monkey Treat 1 was able to perform this task a few weeks post-lesion, with the affected hand (Fig. 5.8, right column). The animal used its index finger and thumb to grab the knob and then to fully open the drawer. The bottom two pictures are representative of the time interval to open the drawer, corresponding to the pulling time (PT, Fig. 5.10). The three time intervals characterizing quantitatively this task, the reaching time (RT), the pulling time (PT) and the picking time (PIT) are represented in Figs. 5.9, 5.10 and 5.11, respectively, for the monkeys Ctrl 2 and Treat 1 of the "Pair 2". Monkey Ctrl 2 was able to reach the knob with the hand, exhibiting a longer reaching time interval (RT) post-lesion (Fig. 5.9, left bins), whereas the monkey Treat 1 was a bit more rapid with less difference pre- versus post-lesion. As the monkey Ctrl 2 was not able to open the drawer post-lesion, its PT interval is represented by a score of 0 (Fig. 5.10, star). In contrast, the monkey Treat 1 recovered enough strength in the precision grip of the left hand to perform this task (Fig. 5.10, right bins), with however an increased PT post-lesion. Fig. 5.11 shows the time intervals needed to pick up the food reward in the drawer (PIT). As monkey Ctrl 2 was not able to open the drawer with the left hand post-lesion, there was no PIT (Fig. 5.11, star). Concerning PIT of Treat 1, it was slightly augmented post-lesion. The intervals RT, PT and PIT for monkey Treat 2 (not shown) were as follows: RT was longer than in Treat 1 and, for PT and PIT, there was less difference pre- versus post-lesion.

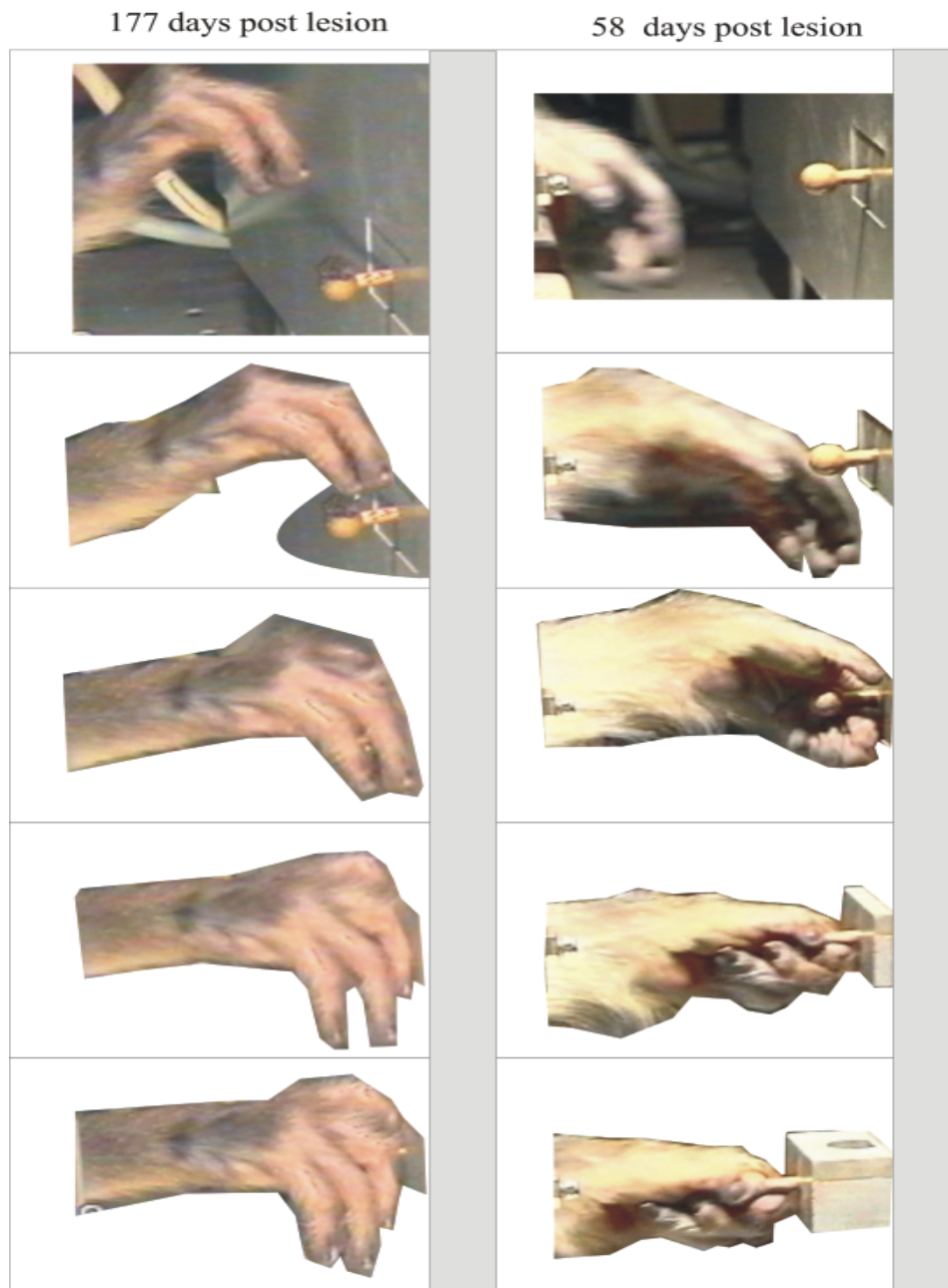


Fig.

5.8: Direct comparison in “Pair 2“, between Ctrl 2 (left column) and Treat 1 (right column). The time delay between each picture is 200 ms. Monkey Ctrl 2 was not able to grasp the knob of the drawer in a precision grip performance with the left hand (left column), whereas monkey Treat 1 grasped the knob between the thumb and the index finger

to fully open the drawer. Note: the period of recovery is shorter in Treat 1 (58 days post-lesion) as compared to Ctrl 2 (177 days post-lesion).

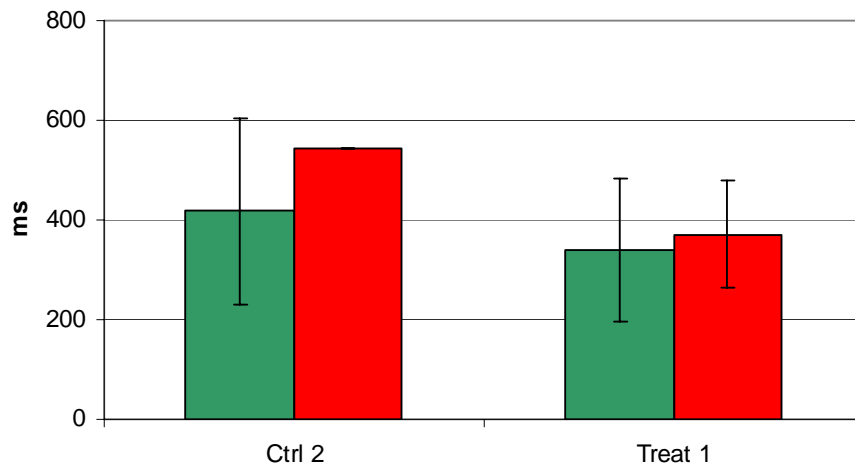


Fig. 5.9: Histogram showing the comparison in “Pair 2” of the reaching time (RT) for the drawer task (monkeys Ctrl 2 and Treat 1). The green bins represent the time intervals pre-lesion and the red bins post-lesion. In monkey Ctrl 2, the red bin is made of only 4 values, that was not sufficient to derive a meaningful standard deviation.

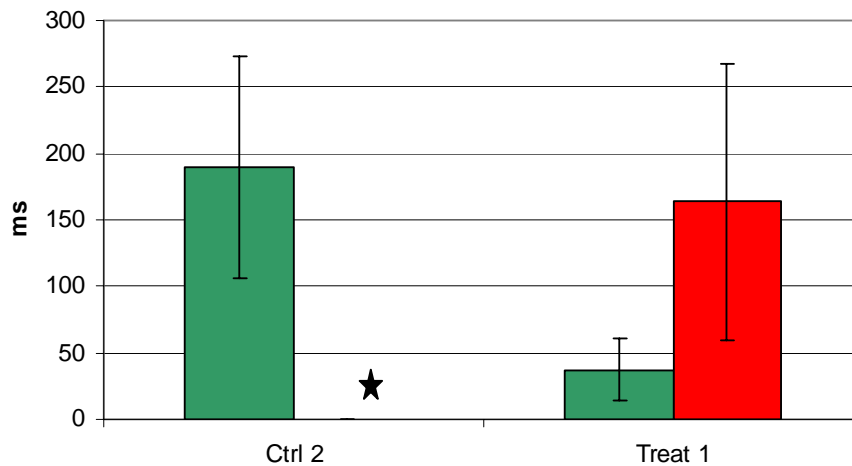


Fig. 5.10: Same as in Fig. 5.9 but for the comparison of the pulling time (PT).

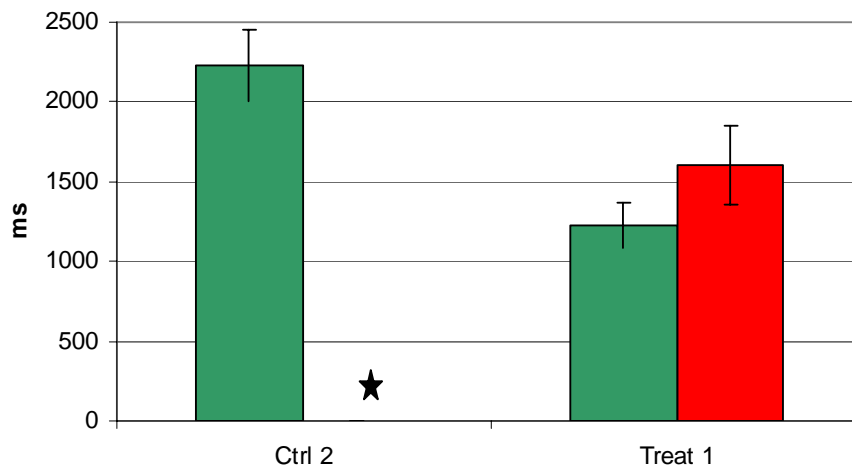


Fig. 5.11: PIT picking time. Star: time interval = ∞ : no picking performance was possible because the drawer could not be open. Same conventions as in Fig. 5.9.

5.2.2.5: Role of the ipsilesional M1 in the recovery of function in Treated monkeys

As expected, the transient inactivation of the hand area of M1 in the right hemisphere, in monkeys Treat 1 and Treat 2 resulted in a complete loss of function of the left hand to perform the Brinkman board test (score = 0, 40 minutes after the cortical micro-infusion of muscimol). Following the transient inactivation of the left M1, the left hand exhibited a slightly decreased score on the Brinkman board test compared to the pre-infusion score. This observation perhaps indicates that the left M1 played a role in the recovery of function of the left hand in the treated animals. In contrast, in the control monkeys, inactivation of the left M1 did not influence the (spontaneous) recovered manual dexterity score.

5.3: Discussion

5.3.1: Mechanisms involved in the improvement of functional recovery

Schwab and collaborators showed in recent studies that rats subjected to unilateral lesion of the CST and treated with the anti-Nogo antibody presented a regeneration of transected fibres: after injection of BDA in the motor cortex, they found caudally to the spinal cord lesion BDA stained fibres that grew through and/or around the lesion over a fairly long distance up to about 10 millimetres (Schnell and Schwab 90; Schnell and Schwab 93; Raineteau et al 99; Brösamle et al 00). In contrast to these results, no fibres located caudally to the cervical lesion have been observed in the present study for the treated monkey Treat 1. Actually, some BDA stained fibres have been observed caudally to the lesion in monkey Treat 2. However, as no reconstruction of the trajectory of these few fibres has been done yet and considering the extent of the cervical lesion in monkey Treat 2, it is now impossible to consider these fibres as regenerated fibres.

Functionally, no recovery was observed in the foot prehension task, in line with an absence of regenerated fibres caudally to the lesion that could re-innervate the motoneurons below the spinal cord lesion down to the lumbar level. However, even if the transected axons would have regenerated, they would probably not been able to reach the lumbar segment if the regeneration would be limited to about 1 cm as in the rat. At the present step, based on our observations, we assume that there is no major regeneration of CS axons after cervical lesion at C7-C8 in our monkeys, even if treated with the anti-Nogo. Therefore, other mechanisms of recovery have to be considered (see below).

5.3.1.1: Compensatory sprouting of the CST projection

Different mechanisms possibly involved in the clear improvement of the functional recovery of the precision grip in the anti-Nogo treated monkeys after the lesion of the dorsolateral funiculus are presented in Figs. 5.12. and 5.13. The lesion at C7-C8 level is represented by a double black arrow tail and interrupts the CST (red) coming from the right hemisphere. The uncrossed CST (blue) originating from the right hemisphere was preserved, as well as the crossed CST (green) originating from the left hemisphere. Pathways possibly exhibiting compensatory sprouting are symbolised by dashed lines, projecting to the motoneurons in the left ventral horn (Rexed lamina IX) of the cervical cord, deprived from CST input as a result of the lesion.

As a result of the lack of CST input to motoneurons at C8 and T1 segments on the left side as a result of the hemi-section, one may speculate about the possibility for the various CST components to give rise to compensatory sprouting, possibly triggered and enhanced by the anti-Nogo treatment. First of all, the crossed CST from the left hemisphere (Ⓜ in Fig.5.12) and the uncrossed CST from the right hemisphere (Ⓝ in Fig. 5.12), not affected by the lesion, are in position to give rise to sprouting, forming axons collaterals, crossing midline at segmental level and thus invading the deprived territory on the other side (④,⑤ and ⑥) in Fig. 5.12). The muscimol data are consistent with the scenarios ⑤ and ⑥, since inactivation of the right hemisphere abolished the post-lesion recovered performance. The scenario ④ is less likely but cannot be completely excluded since muscimol inactivation of the left hemisphere reduced a bit the post-lesion recovered performance in the treated animal Treat 1. One cannot exclude, in addition, that axotomised axons, whose cell bodies survive for most of them (see chapter 3) give rise to axon collaterals by sprouting at higher segments and then invade for instance the grey matter, allowing them to influence either directly or indirectly (via propriospinal system) the deprived motoneurons (Ⓣ in Fig. 5.12). This scenario maybe corresponds to the few obliquely oriented CS axons described above the lesion in chapter 4 (see Fig. 4.2) and, furthermore, is also

supported by the muscimol data in the sense that inactivation of the right hemisphere abolished the post-lesion recovery performance. In summary, based on muscimol data, one is tempted to favour scenarios ⑤, ⑥ and ⑦ in Fig. 5.12, with a possible preference for the scenarios ⑤ and ⑥, which have been demonstrated to play a significant role in the rat (Weidner et al 01).

In another system, such mechanisms of compensatory sprouting in monkeys subjected to lesions have been investigated by Florence and collaborators. HRP staining in the spinal cord in monkeys subjected to thoracic nerve crush or long term forelimb amputation showed sprouting in the dorsal column. They showed that corticocortical sprouting occurred in monkeys subjected to unilateral long standing trauma to forelimb (Florence et al 93; Florence et al 98).

In our study, the anti-Nogo antibody has been ubiquitously found in the brain and the spinal cord. As a consequence, plastic changes enhanced by the treatment can take place not only close to the lesion (corresponding to the site of infusion of the antibody) but also at locations remote from the lesion. Studies investigating the effect of IN-1 on the recovery of function and in anatomical plasticity in adult rats exhibited a strong enhancing effect of the treatment by increasing of the compensatory sprouting. The localisation of this sprouting has been found at different levels such as, in the red nucleus (Z'Graggen et al 98; Raineteau et al 02a) and at spinal level (Thallmair et al 98; Raineteau et al 99; Bareyre et al 02; Raineteau et al 02b).

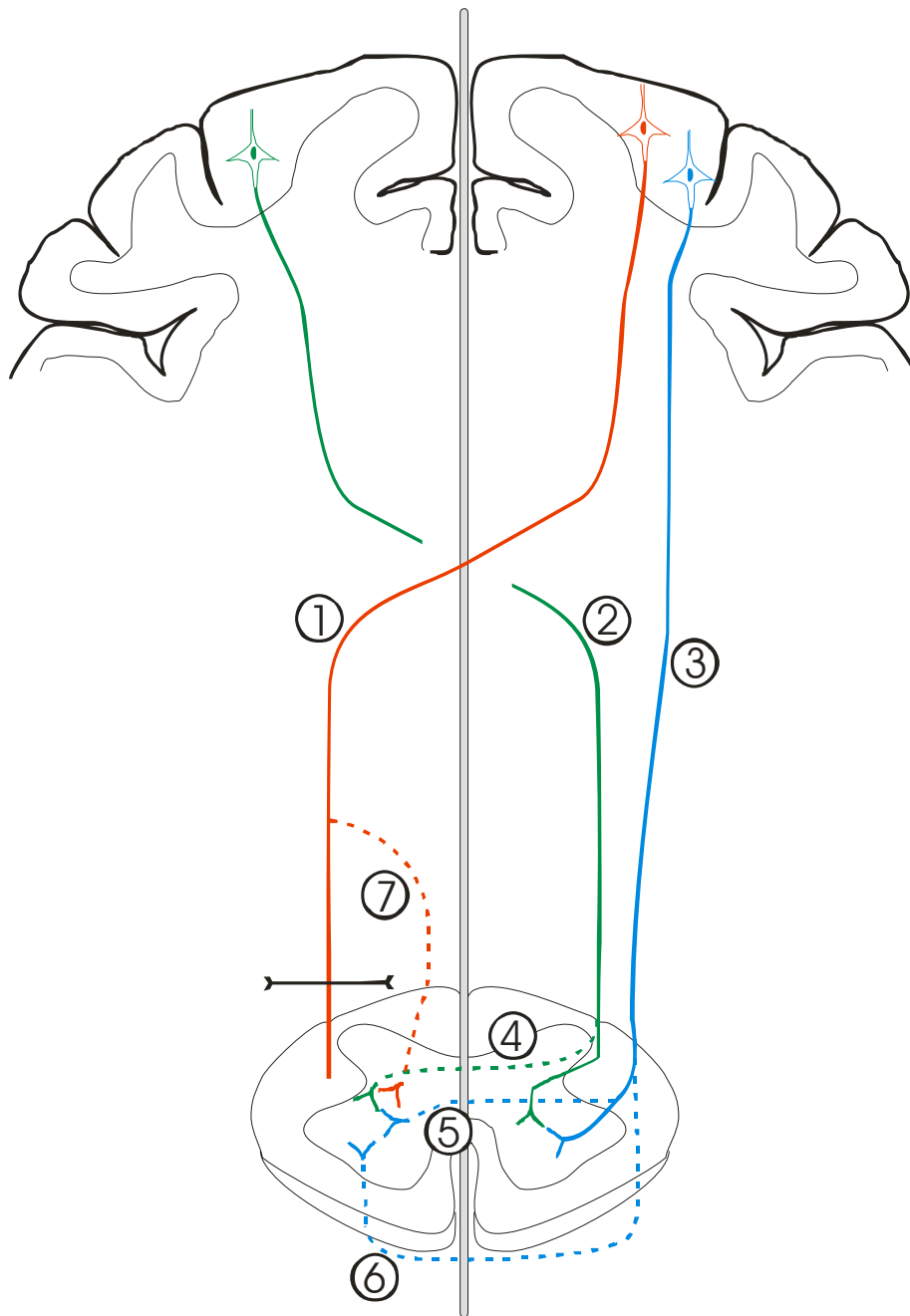


Fig. 5.12: Schematic representation of the possible mechanisms of compensatory sprouting with the respective cortical origin. Grey line: midline; ① crossed CST originating from the right hemisphere and affected by the hemisection (red); ②: crossed CST originating from the left hemisphere (green); ③: right uncrossed CST (blue). ④-⑦: hypothesized locations of compensatory sprouting. The sprouting ④, ⑤ and ⑥, cross (or re-cross) the midline.

Several data in our study support the idea of mechanisms of compensatory sprouting: i) the absence of regeneration caudally to the cervical lesion associated with the improvement of manual dexterity in treated monkeys; ii) the role played by the hand area of the contralesional primary motor cortex in the recovery of function, as assessed by the transient inactivation experiment (Fig. 5.12 ⑤, ⑥ and ⑦); iii) observation of CS axons with unusual trajectories in treated monkeys.

5.3.1.2: Compensatory sprouting involving the red nucleus or the pontine nuclei

In rats subjected to unilateral pyramidal lesion treated with IN-1 antibody, an increased sprouting in the red nucleus was observed using BDA staining. These data also showed an increase of functional recovery of function in the treated animals compared to control group, but considering the level of the unilateral lesion, the rubrospinal tract was not affected and thus could participate to the observed recovery of function (Z'Graggen et al 98).

In the present study, one can speculate that an increased projection by sprouting of the right hemisphere to the red nuclei may contribute to the recovery. In particular, according to the scenario ① and ①' in Fig. 5.13, the rubrospinal projection may come into play in spite of an hemi-section interrupting both the CST and RST on the left side. The scenario ② of Fig. 5.13 would not be possible in case of complete transection of the RST on the left side, but may be considered in case where the CST is lesioned whereas the RST is partly preserved (as in monkeys Ctrl 1 and Treat 2, for instance). The study of Raineteau and collaborators investigated the consequences in rats subjected to bilateral transection of the CST and treated with IN-1 antibody on the organisation of the rubrospinal tract (Raineteau et al 02c). The authors observed that the rubrospinal tract, normally limited in the intermediate layers of the spinal cord, invaded the ventral horn and made close appositions with the motoneurons deafferented by the CST lesion.

Alternatively, or in addition, one can also imagine a re-organisation of the corticobulbar projection to nuclei other than the red nucleus. This would give the possibility to recruit for the recovery for instance the reticulospinal fibres. Evidence in that direction has been provided in an other study based on hemisection of the thoracolumbar spinal cord in rats, the authors focused their attention on the immunoreactive 5-HT fibres. They observed a correlation between the functional recovery of locomotion and the presence of 5-HT fibres crossing the midline to reach the denervated side of the spinal cord (Saruhashi et al 96).

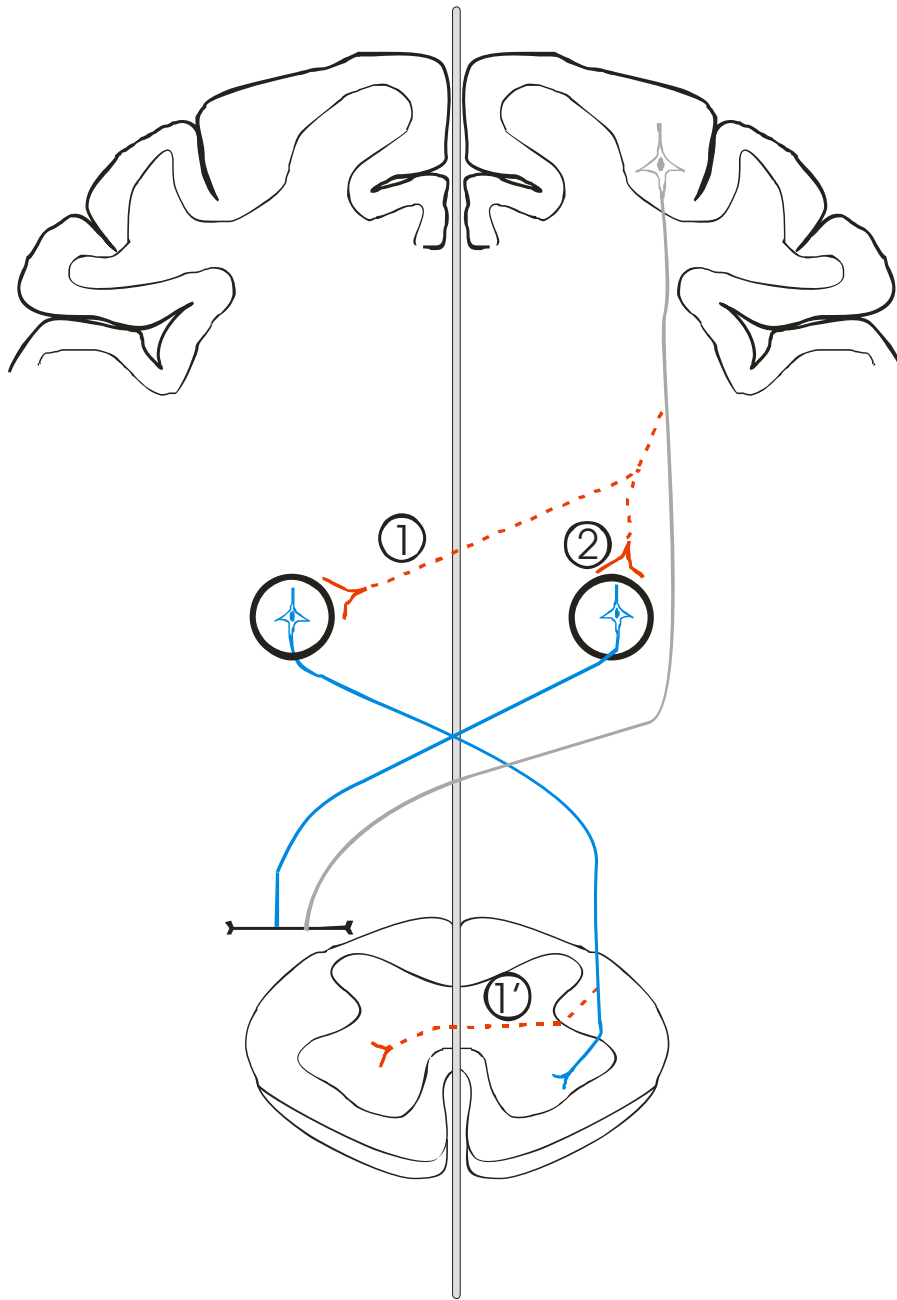


Fig. 5.13: Possible role played by the Rubrospinal tract in the compensatory sprouting mechanisms. The Corticospinal tract affected by the unilateral cervical lesion (arrow) is represented in grey. The Rubrospinal tract is represented in blue. The sprouting, that crosses the midline at the level of the RN (1) or at spinal level (1') is represented in red.

5.3.1.3: Recruitment of intact structures in the spinal cord
Propriospinal tract:

In a study made by Sasaki and collaborators, based on cervical lesion in primate aiming to interrupt the CST and the RST on the left side, the authors observed a rapid recovery of function that they attributed to remaining indirect corticomotoneuronal pathway through the propriospinal system located at C3-C4 (Sasaki et al 04b). Their conclusions are based on the presence of long latency influenced, recorded electrophysiologically, without considering the presence of slow fibres that could explain these long latencies they attributed to disynaptic CM pathway. Bareyre and collaborators investigated the role played by the short and long propriospinal system in the recovery of function in rats subjected to a unilateral section of the CST innervating the motoneurons of the hindlimbs (Bareyre et al 04a). Post-lesion, the authors observed newly formed and permanent contacts (sprouting) between the axotomised CST fibres and the long propriospinal fibres located in the ventromedial part of the grey matter in the spinal cord. They confirmed with electrophysiological methods and behavioural evaluation the function of this system by re-interrupting this pathway. Applied to our study, such scenario of recovery would correspond to the situation depicted in Fig. 5.14.

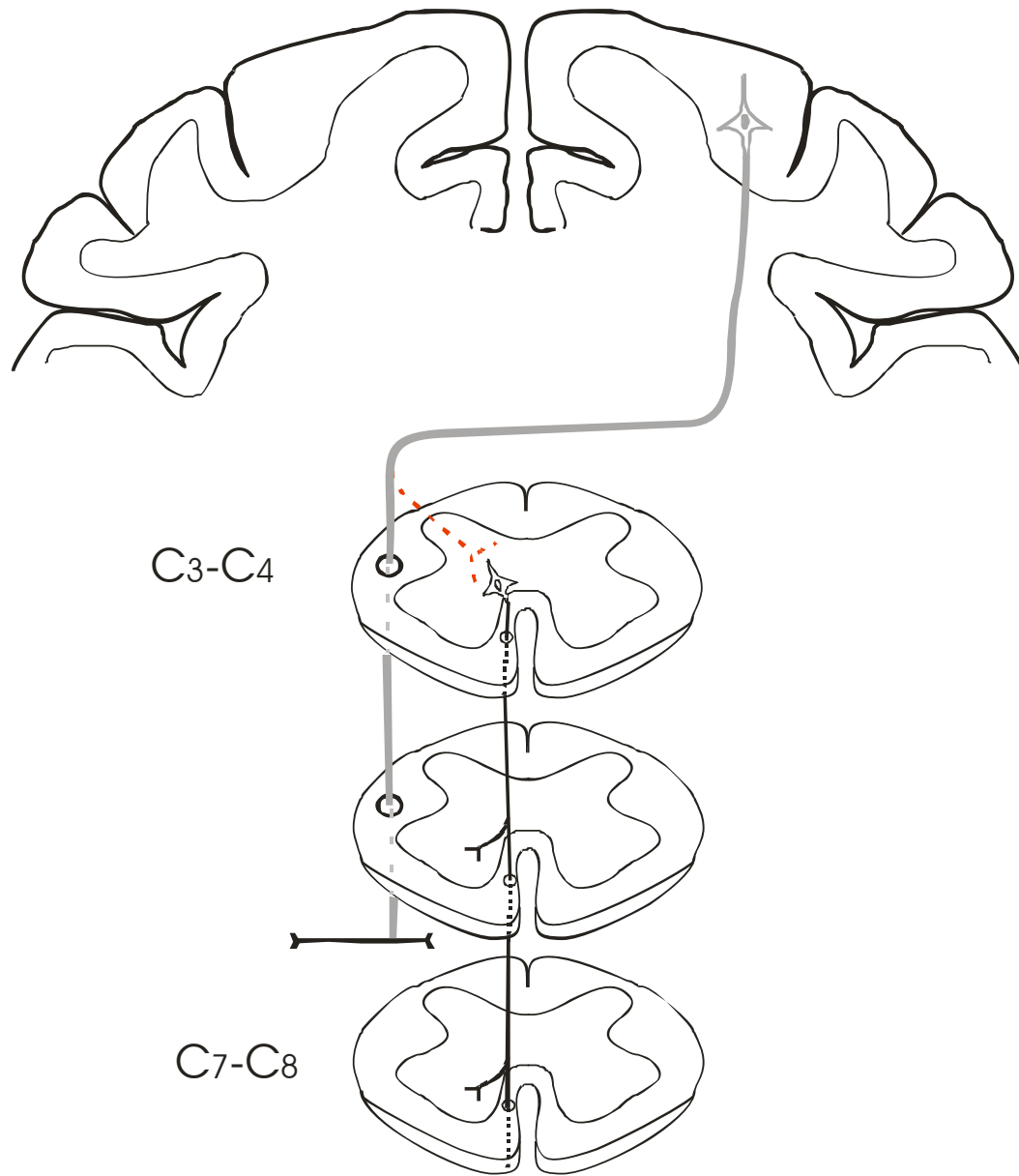


Fig. 5.14: Propriospinal pathway maybe involved in the recovery of function. Grey: axotomised CST fibre. Sprouting to propriospinal system in shown in red.

5.3.2: Conclusions

The recovery of function in the precision grip ability is clearly improved in the treated animals as compared to the control animals in three main aspects.

1. The improvement of precision grip in the Brinkman board test: in the vertically oriented slots in the way that the treated monkeys presented no change of strategy

to perform the task, whereas the recovered score in the control monkeys was due to a change of strategy following the paresis of the thumb and, even more dramatic, the recovery for horizontally oriented slots observed in the treated animal but not in the control animal in “Pair 2”.

2. The control monkey Ctrl 1 was unable to perform the drawer task whereas both treated monkeys Treat 1 and Treat 2 almost completely recovered this ability.
3. The recovery of a symmetric and normal pre-shaping of movement in the left hand in the treated monkeys performing the Ballistic Arm Movement test whereas monkey Ctrl 1 showed a slower movement of catching without pre-shaping by opening the fingers of the left hand to catch the thrown reward.

The treated monkeys Treat 1 and Treat 2 showed a clear improvement of the ability of the forelimb, in particular of the fingers making independent finger movements to perform the precision grip task such as the Brinkman board and the drawer task compared to the control monkeys (considering the extent of the cervical lesion). As no regeneration of descending fibres was observed caudally to the lesion at least in one treated animal, the probable mechanisms behind this functional improvement of recovery are rather involving compensatory sprouting at different levels, and the recruitment of intact local tracts or systems such as the reticulospinal tract or the long Propriospinal system.

Our results are however limited by two important factors. First, because the work with primates such as macaque monkeys needs a lot of investment (time, etc...), the number of animals included in the present study is very small. As a consequence, the present data need to be confirmed on a larger number of monkeys. Second, for ethical reasons, we decided to perform only very small cervical cord lesions, aiming as precisely as possible to the neural pathways (CST) involved in motor control of the fingers. With such restricted lesion, the spontaneous

recovery of the animal (in absence of treatment) is surprisingly good, in line with other studies in monkeys in which hemi-sections of the cervical cord were performed but at higher levels, such as C3-C4 (Galea and Darian-Smith 97a; Galea and Darian-Smith 97b; Sasaki et al 04a). Due to this excellent «spontaneous» recovery, the extent of improvement brought by the treatment is thus limited. For this reason, and this is clearly demonstrated in the present study, it is crucial to develop very well designed challenging behavioural tasks which are strongly perturbed in the control monkeys in spite of the small lesion and substantially improved by the treatment (e.g. horizontal wells in the Brinkman board, drawer task).

Propositions of avenues for future work

Electrophysiology:

An electrophysiological study based on EMG recordings in forelimb and hand muscles associated with spike trigger averaging (facilitation or suppression) or stimulus trigger averaging methods could identify more precisely the pathways used in the control of independent finger movements observed in the treated animals. The measured latencies between stimulation and activity recordings in the EMG would give valuable informations about the pathway or the number of synapses involved (careful however about the quick or slow conducting nerve fibres). The investigation of the functional organisation of the Red Nucleus, associated with stimulation of cells in the magnocellular part could also improve our knowledge on the role played by the red nucleus in the functional recovery.

Anatomy:

Improvement of tracing studies using transneuronal tracers may be a valuable tool to elucidate some mechanisms of re-organisation, as illustrated by a recent study in the rat (Bareyre et al 04b). However, the transposition of such technique using viruses to the monkey model is not trivial. Considering the good recovery of function with small lesions of the cervical cord, a

larger lesion interrupting all the possible pathways involved in a possible spontaneous recovery would increase the motor deficits and emphasize the differences of functional recovery between treated and control animals. In that direction, a research group investigated the effect of olfactory ensheathing glial cells auto implanted in monkeys subjected to complete lumbar section of the cord, and presented their preliminary results in control monkey in the SFN meeting 2003 in New Orleans. The animal were dramatically affected by the complete transection and needed the cares of a veterinary several hours a day, almost placed in an intensive care unit (Garcia-Miguel, M.J. et al., 2003). Clearly, for legal and ethical reasons, such devastating lesions could not be performed in Switzerland. It is also our personal choice to work with monkeys, which underwent limited lesions, and therefore exhibited an acceptable post-lesional health status.

Behaviour:

In our model of spinal cord lesion, restricted to the CST and the RST on the left side, a battery of behavioural tasks focusing on the precision grip had to be developed. Actually, two new tasks have been designed in order to refine the evaluation of the independent finger movements. These two tests are the rotating brinkman board test, consisting of a rotating disc containing 32 slots in two orientations and the “Visual Brinkman board test”, consisting in one board containing 20 slots vertically and horizontally oriented. The animal has no visual feedback to find the slots and thus must retrieve the pellets using tactile feed-back alone.

List of references for chapter 5

1. Bareyre,F.M., Haudenschield,B. & Schwab,M.E. (2002) Long-lasting sprouting and gene expression changes induced by the monoclonal antibody IN-1 in the adult spinal cord. *J.Neurosci.*, **22**, 7097-7110.
2. Bareyre,F.M., Kerschensteiner,M., Raineteau,O., Mettenleiter,T.C., Weinmann,O. & Schwab,M.E. (2004a) The injured spinal cord spontaneously forms a new intraspinal circuit in adult rats. *Nature Neuroscience*, **7**, 269-277.
3. Brösamle,C., Huber,A.B., Fiedler,M., Skerra,A. & Schwab,M.E. (2000) Regeneration of lesioned corticospinal tract fibers in the adult rat induced by a recombinant, humanized IN-1 antibody fragment. *Journal of Neuroscience*, **20**, 8061-8068.
4. Florence,S.L., Garraghty,P.E., Carlson,M. & Kaas,J.H. (1993) Sprouting of peripheral nerve axons in the spinal cord of monkeys. *Brain Res.*, **601**, 343-348.
5. Florence,S.L., Taub,H.B. & Kaas,J.H. (1998) Large-scale sprouting of cortical connections after peripheral injury in adult macaque monkeys. *Science*, **282**, 1117-1121.
6. Galea,M.P. & Darian-Smith,I. (1997a) Corticospinal projection patterns following unilateral section of the cervical spinal cord in the newborn and juvenile macaque monkey. *Journal of Comparative Neurology*, **381**, 282-306.
7. Galea,M.P. & Darian-Smith,I. (1997b) Manual dexterity and corticospinal connectivity following unilateral section of the cervical spinal cord in the macaque monkey. *Journal of Comparative Neurology*, **381**, 307-319.
8. Raineteau,O., Fouad,K., Bareyre,F.M. & Schwab,M.E. (2002a) Reorganization of descending motor tracts in the rat spinal cord. *European Journal of Neuroscience*, **16**, 1761-1771.
9. Raineteau,O., Z'Graggen,W.J., Thallmair,M. & Schwab,M.E. (1999) Sprouting and regeneration after pyramidotomy and blockade of the myelin-associated neurite growth inhibitors NI 35/250 in adult rats. *European Journal of Neuroscience*, **11**, 1486-1490.
10. Saruhashi,Y., Young,W. & Perkins,R. (1996) The recovery of 5-HT immunoreactivity in lumbosacral spinal cord and locomotor function after thoracic hemisection. *Exp.Neurol.*, **139**, 203-213.
11. Sasaki,S., Isa,T., Pettersson,L.G., Alstermark,B., Naito,K., Yoshimura,K., Seki,K. & Ohki,Y. (2004a) Dexterous Finger Movements in Primate without Monosynaptic Corticomotoneuronal Excitation. *Journal of Neurophysiology*.
12. Schnell,L. & Schwab,M.E. (1990) Axonal regeneration in the rat spinal cord produced by an antibody against myelin-associated neurite growth inhibitors. *Nature.*, **343 no 6255**, 269-272.
13. Schnell,L. & Schwab,M.E. (1993) Sprouting and regeneration of lesioned corticospinal tract fibres in the adult rat spinal cord. *European Journal of Neuroscience*, **5**, 1156-1171.

- 14: Thallmair,M., Metz,G.A.S., Z'Graggen,W.J., Raineteau,O., Kartje,G.L. & Schwab,M.E. (1998) Neurite growth inhibitors restrict plasticity and functional recovery following corticospinal tract lesions. *Nature Neurosci.*, **1**, 124-131.
- 15: Weidner,N., Ner,A., Salimi,N. & Tuszynski,M.H. (2001) Spontaneous corticospinal axonal plasticity and functional recovery after adult central nervous system injury. *Proceedings of the National Academy of Sciences of the United States of America*, **98**, 3513-3518.
- 16: Z'Graggen,W.J., Metz,G.A.S., Kartje,G.L., Thallmair,M. & Schwab,M.E. (1998) Functional recovery and enhanced corticofugal plasticity after unilateral pyramidal tract lesion and blockade of myelin-associated neurite growth inhibitors in adult rats. *J.Neurosci.*, **18**, 4744-4757.

Curriculum Vitae

SCHMIDLIN Eric

Date of birth: July 17th 1971

Personal address:

Grand rue 35
1700 Fribourg
Switzerland
Tel: ++41 26 322 16 34

Professional address:

Division of Physiology
Dept. of Medicine
Rue du Musée 5
1700 Fribourg
Tel: ++41 26 300 86 04
E-Mail: e.schmidlin@ion.ucl.ac.uk
Fax: +41-26 300 97 34

Education:

- 2000-2004: PhD in Biological Sciences. Dept. of Medicine, Fribourg Switzerland
Supervisor: Prof. Eric M. ROUILLER.
- 1997-2000: University Diploma in Biological Sciences in Fribourg.
- 1992-1994: Preclinical Diploma in Human Medicine in Fribourg (2 first years of medical school).
- 1987-1991: Swiss Maturity Diploma type B.

Experience:

- 1996 Practical Stage in Neurology and Neurosurgery in University Hospital of Uppsala in Sweden.
- 2000-2003 Teaching assistant in the Department of Physiology for practical lessons to medical students.
- 2001-2002: Teaching assistant in a Cooperation program between Geneva Medical School and Yaoundé I University of biomedical sciences in Cameroon.

List of Publications:

Rouiller E.M., Wannier T., Schmidlin E., Liu Y. :”Reprogramming the motor cortex for functional recovery after neonatal or adult unilateral lesion of the corticospinal system in the macaque monkey.” Chapter in “Reprogramming the cerebral cortex” in **Oxford University Press: In Press** S. Lomber, J. Eggermaont (Eds.)

Wannier T, Schmidlin E, Bloch J, Rouiller E M: “A unilateral section of the corticospinal tract at cervical level in primate does not lead to measurable cell loss in motor cortex.” **Accepted J. of Neurotrauma**

Schmidlin E, Wannier T, Bloch J, Rouiller E M: “Progressive plastic changes in the hand representation of the primary motor cortex parallels incomplete recovery from a unilateral section of the corticospinal tract at cervical level in monkeys” **Brain Research,**

List of Published Abstract

Schmidlin E, Wannier T, Bloch J, Rouiller E M: “Reorganisation of the primary motor cortex (M1) hand region revealed by intracortical microstimulation (ICMS) after a unilateral section of the dorsolateral funiculus in Macaque monkey.” Swiss Society for Neurosciences Meeting **(2000)**

Wannier T, Schmidlin E, , Bloch J, Rouiller E M: “A behavioural and electrophysiological assessment of impairment and incomplete recovery of manual dexterity in a monkey subjected to unilateral section of the dorsolateral funiculus” Functional recovery after spinal cord injury meeting, Ascona **(2001)**

Schmidlin E, Wannier T, Bloch J, Rouiller E M: “Behavioural consequences of a cervical spinal cord hemisection on the manual dexterity in macaque monkeys” Swiss Society for Neurosciences Meeting **(2002)**

Schmidlin E, Wannier T, Wyss, A, Bloch J and Rouiller E M: “In primate, an incomplete spinal cord injury (SCI) induces cell disappearance in supra-spinal structures projecting to the spinal cord. Third Forum of European Neurosciences in Paris, FENS **(2002)**

Jouffrais C., Schmidlin E., Rouiller E. M.: „Single unit activity related to bimanual coordination in the dorsal premotor (PMd) and primary motor (M1) cortices in rhesus monkeys“ Third Forum of European Neurosciences in Paris, FENS **(2002)**

Schmidlin E, Wannier T, Wyss, A, Bloch J and Rouiller E M: ”In primate, a spinal cord hemisection induces cell disappearance in supra-spinal structures projecting to the spinal cord.” Swiss Society for Neurosciences Meeting **(2003)**

Schmidlin E, Wannier T, Bloch J, Schwab M E, Mir A, Rouiller E M: “Functional recovery in macaque monkeys subjected to unilateral spinal lesion effect of anti-Nogo treatment” Society For Neurosciences Meeting in New Orleans **(2003)**